

**The Synthesis, Cytotoxicity, COX inhibitory activity,  
and Anti-angiogenic Activity of Homoisoflavonoid  
Analogues**

Jacob Hiles



Submitted for the Partial Fulfilment of the Degree of Master of  
Science by Research

Dr Sianne Schwikkard and Dr Elizabeth Opara

FACULTY OF SCIENCE, ENGINEERING AND COMPUTING

School of Pharmacy and Chemistry

September 2019

## **Abstract**

Natural products have been used for the treatment of various maladies for thousands of years. Naturally occurring analogues of homoisoflavonoids have shown a range of interesting activities, including anti-inflammatory and anti-cancer activities. Homoisoflavonoids have been primarily isolated from the Hyacinthaceae (Asparagaceae). NSAIDs are a class of drugs widely used. However, due to the numerous side effects due to the poor selectivity (inhibition of both COX-I and COX-II) of the NSAIDs on the cyclooxygenase enzyme (COX), a need for selective COX-II inhibitors has arisen. A series of the sulphur analogues of homoisoflavonoids, 3-benzylidene thiochroman-4-ones, were synthesised and screened for: cytotoxicity via the neutral red assay, selective cytotoxicity towards HREC cells as a measure of potential antiangiogenic activity via the alamarBlue assay, and selective COX activity via the COX screening kit (CAYMAN CHEMICAL). These compounds were evaluated against the cancerous cell line, HeLa (human cervical carcinoma), and non-cancerous cell lines; HREC (human retinal endothelial cells), and ARPE-19 (human retinal pigment epithelial cells). The compound found to be the most cytotoxic against HeLa cells produced an IC<sub>50</sub> of 6.08 µM. The compound found to be the most active with respect to antiproliferation against HREC cells exhibited a GI<sub>50</sub> of 3.07 µM. All compounds demonstrated selectivity with all GI<sub>50</sub> values against ARPE-19 >100 µM. The compound found to be the most active against COX-II produced 22.7 % inhibition at 4.35 nM.

**Keywords:** *Homoisoflavonoid, Synthesis, Anti-proliferative activity, Cytotoxic activity, HeLa, HREC, ARPE-19, COX-II inhibition.*

## **Acknowledgements**

First and foremost, I would like to display my sincere, heartfelt gratitude for the guidance, encouragement, and support from my supervisor Dr Sianne Schwikkard. You have shown me what it is to be a true role model, scientist and mentor and you have pushed me further than I thought possible. This is a great treasure I will cherish, not only in my future academic career but for the whole of my life and I look forward to collaborating with you once again.

I would also like to thank the following people:

My co-supervisor Dr Elizabeth Opara for all the assistance in the bioassay development and help in the biological side of my project. All the staff in the Department of Pharmacy and Chemistry for all the technical support.

All my friends within the Pharmacy and Chemistry department. Thank you for all the help in the lab but especially for the amazing group spirit and all the laughs.

To my friends outside of the lab, you have helped to keep me sane and aided in keeping my life balanced and happy.

Last but definitely not the least, I am greatly indebted to my family. My parents' unconditional love, care, and support have made the hardship of research all worthwhile. Without their assistance I do not think any of this would be possible.

“The time will come when diligent research over long periods will bring to light things which now lie hidden. A single lifetime, even though entirely devoted to the sky, would not be enough for the investigation of so vast a subject... And so this knowledge will be unfolded only through long successive ages. There will come a time when our descendants will be amazed that we did not know things that are so plain to them... Many discoveries are reserved for ages still to come, when memory of us will have been effaced.”

**- Seneca**

# Table of Contents

|   |           |
|---|-----------|
| <b>1. Introduction</b> .....  | <b>15</b> |
| <b>1.1 Homoisoflavonoids</b> .....  | <b>15</b> |
| <b>1.2 Biosynthesis</b> .....   | <b>17</b> |
| 1.2.1 Biosynthesis of homoisoflavonoids.....  | 17        |
| <b>1.3 Methods of Synthesis</b> .....   | <b>19</b> |
| 1.3.1 Synthesis of the chroman-4-one intermediate .....                                       | 20        |
| 1.3.2 Synthesis of 3-benzylidene chroman-4-one.....   | 26        |
| <b>1.4 Bioactivity of homoisoflavonoids</b> .....   | <b>28</b> |
| 1.4.1 Anti-inflammatory .....   | 28        |
| 1.4.2 Anti-Proliferative .....  | 29        |
| 1.4.3 Anti-Angiogenesis .....   | 31        |
| <b>1.5 Cyclooxygenase (COX)</b> .....   | <b>34</b> |
| 1.5.1 Risks associated with selective and non-selective COX inhibitors .....                  | 36        |
| 1.5.2 Upregulation and Overexpression of COX-II .....   | 37        |
| <b>1.6 Aim and Objectives</b> .....   | <b>42</b> |
| <b>2.0 Experimental</b> .....   | <b>43</b> |
| <b>2.1 Synthetic chemistry</b> .....  | <b>43</b> |
| 2.1.1 Instrumentation.....  | 43        |
| 2.1.2 General procedure for the synthesis of substituted phenylsulfanyl propanoic acids ..... | 43        |
| 2.1.3 General procedure for the synthesis of substituted thiochromanones.....                 | 44        |
| 2.1.4 General procedure for the synthesis of the thio-homoisoflavonoids.....                  | 44        |
| <b>2.2 Biological Methods</b> .....   | <b>44</b> |
| 2.2.1 General.....  | 44        |
| 2.2.2 Cell culturing .....  | 44        |
| 2.2.3 Neutral red assay <sup>(47)</sup> .....   | 45        |
| 2.2.4 Cyclooxygenase inhibition assay .....   | 45        |
| 2.2.5 AlamarBlue assay.....   | 46        |
| 2.2.6 Statistical analyses.....   | 46        |
| <b>3.0 Results</b> .....  | <b>47</b> |
| <b>3.1 NMR</b> .....  | <b>47</b> |
| <b>3.2 Biological Results</b> .....   | <b>52</b> |
| 3.2.1 Statistical analysis.....   | 53        |
| <b>4.0 Discussion</b> .....   | <b>54</b> |
| <b>4.1 Chemistry</b> .....  | <b>54</b> |
| 4.1.1 Formation of the phenylsulfanyl propanoic acid.....                                     | 54        |
| 4.1.2 Formation of the thiochromanone .....   | 56        |
| 4.1.3 Formation of the homoisoflavonoid .....   | 60        |
| <b>4.2 Biological discussion</b> .....  | <b>70</b> |
| 4.2.1 Anti-proliferative activity of HRECs and ARPE-19 cells via alamarBlue assay .....       | 70        |
| 4.2.2 Cytotoxicity to HeLa cells via a neutral red assay .....                                | 77        |
| 4.2.3 COX inhibitory activity .....   | 81        |

|                              |           |
|------------------------------|-----------|
| <b>5.0 Conclusion .....</b>  | <b>85</b> |
| <b>6.0 Future works.....</b> | <b>86</b> |
| <b>7.0 References .....</b>  | <b>91</b> |
| <b>A.0 Appendices.....</b>   | <b>98</b> |

## Abbreviations

ACh – Acetylcholine

AChE – Acetylcholine Esterase

AMD – Age-related Macular Degeneration

AMPK – Adenosine Monophosphate Activated Protein Kinase

AOM – Azoxymethane

APC – Adenomatous Polyposis Coli

BCL2 - B-cell Lymphoma 2

BHT – Butylated Hydroxy Toluene

CCR7 – C-C Chemokine Receptor Type 7

COSY - Correlation Spectroscopy

COX – Cyclooxygenase

d – Doublet

dd – Double Doublet

DABCO - (1,4-diazabicyclo[2.2.2]octane)

DEPTQ - Distortionless Enhancement by Polarization Transfer

DMEM – Dulbecco's Modified Eagle Medium

DMSO – Dimethyl Sulphoxide

DPPH – (2,2-diphenyl-1-picrylhydrazyl)

EDTA – Ethylenediaminetetraacetic acid

EWG – Electron Withdrawing Group

FBS – Foetal Bovine Serum

GCMS – Gas Chromatography Mass Spectrometry

GI<sub>50</sub> - Concentration for 50% of Maximal Inhibition of Cell Proliferation

GLUT – Glucose Transporter

HMBC - Heteronuclear Multiple Bond Correlation

HREC – Human Retinal Endothelial Cells

HSQC - Heteronuclear Single Quantum Coherence

HUVEC – Human Umbilical Vein Endothelial Cells

IC<sub>50</sub> – Concentration of an Inhibitor Where the Response is Reduced by Half.

iNOS – Inducible Nitric Oxide Synthase

LASER – Light Amplification by Stimulated Emission of Radiation

LG – Leaving Group

L-NMMA – N<sup>G</sup>-Methyl-L-arginine acetate

LPS – Lipopolysaccharide

MAO – Monoamine Oxidase

MDR – Multi-Drug Resistance

MIC – Minimum Inhibitory Concentration

NBT – Nitroblue Tetrazolium

NCI – National Cancer Institute

NHC – N-Heterocyclic Carbene

NMR – Nuclear Magnetic Resonance

NO – Nitric Oxide

NOESY - Nuclear Overhauser Effect Spectroscopy

NSAID – Non-Steroidal Anti-Inflammatory Drug

OSC – Oesophageal Cancer Cells

OTC – Over the Counter

pAMPK – Phosphorylated Adenosine Monophosphate Activated Protein Kinase

PBS – Phosphate Buffered Saline

PDR – Proliferative Diabetic Retinopathy

PG – Prostaglandin

PGHS – Prostaglandin Endoperoxidase H Synthase

PPA – Polyphosphoric Acid

RIE – Rat Intestinal Epithelial Cells

ROP – Retinopathy of Prematurity

ROS – Reactive Oxygen Species

s – Singlet

SAM – S-Adenosyl Methionine

SAR – Structural Activity Relationship

t – Triplet

TFAA – Trifluoroacetic Acid

TGFβ2 - Transforming Growth Factor, Beta 2

TLC – Thin Layer Chromatography

VEGF – Vascular Endothelial Growth Factor



## List of Figures

**Figure 1.** Structure of a homoisoflavonoid, with two aryl rings (A and B) and a heterocyclic (C ring) in the centre.

**Figure 2.** Structure of an isoflavonoid, with two aryl rings (A and B) and a heterocyclic (C ring) in the centre.

**Figure 3.** Structure of a flavonoid, with two aryl rings (A and B) and a heterocyclic (C ring) in the centre.

**Figure 4.** Structure of a chalcone with two aryl rings (A and B) and a prop-2-ene-1-one bridge connecting the rings.

**Figure 5.** Type I (3-benzyl-4-chromanone).

**Figure 6.** Type II (3-benzylidene-4-chromanone).

**Figure 7.** Type III (3-benzyl-3-hydroxy-4-chromanone).

**Figure 8.** Type IV (Scillascillin).

**Figure 9.** *Eucomin* structure.

**Figure 10.** NO inhibitors isolated from *Ophiopogon japonicas*.

**Figure 11.** Homoisoflavonoids with NO inhibitory effects.

**Figure 12.** Anti-proliferative homoisoflavonoids.

**Figure 13.** Anti-proliferative homoisoflavonoids isolated from *Urginea depressa*.

**Figure 14.** Cremastranone (**20**) and its regioisomer (**21**).

**Figure 15.** Compound **22** containing 3 methoxy groups situated on the A ring.

**Figure 16.** Compound **23** containing the trimethoxy A ring and the adjacent amine and methoxy groups situated on the B ring.

**Figure 17.** Homoisoflavonoids containing acyl groups situated into the B ring. The A ring of the compound is the same as compounds **22** and **23**.

**Figure 18.** Compound **27** with high selectivity and strong anti-proliferative abilities.

**Figure 19.** Structure of flosulide

**Figure 20.** Structure of NS-398

**Figure 21.** Numbered structure of compound **28**

**Figure 22.** Numbered structure of compound **33**.

**Figure 23.** Numbered structure of unsaturated thiochromanone

**Figure 24**  $^1\text{H}$ -NMR spectrum of compound **32U**

**Figure 25.**  $^{13}\text{C}$ -NMR spectrum of compound **32U**

**Figure 26.** Compound **32**

**Figure 27.** Compound **31**

**Figure 28.** Numbered structure for the sulphur analogue compound **34**

**Figure 29.** Numbered structure Compound **35**

**Figure 30.** Numbered structure of compound **36**

**Figure 31.** Numbered structure for homoisoflavonoids **37**, **38**, and **40**

**Figure 32.** Numbered structure of nitro-containing homoisoflavonoids.

**Figure 33.** Compound **39** with numbered structure

**Figure 34.** Numbered structure of compound **41**

**Figure 35.**  $\text{GI}_{50}$  values for synthesised homoisoflavonoids for cell lines HREC and ARPE-19

**Figure 36.** Chromane analogue of homoisoflavonoid

**Figure 37.** Chromanone analogue of chromane homoisoflavonoid

**Figure 38.** Oxygen analogues of homoisoflavonoids and their respective  $\text{GI}_{50}$  values for HREC and ARPE-19

**Figure 39.** Synthesised sulphur analogues of homoisoflavonoids and their respective  $\text{IC}_{50}$  values against HeLa cells

**Figure 40.** Oxygenated homoisoflavonoids and their respective  $\text{IC}_{50}$  values against HeLa cells ( $\text{IC}_{50}$  values in  $\mu\text{M}$ )

**Figure 41.** Homoisoflavonoids with COX inhibitory activity

**Figure 42.** Homoisoflavonoids isolated from three *Rhodocodon* species with COX inhibitory activity

**Figure 43.** Selective COX-II inhibitor NS-398 containing the sulphonamide moiety

## List of Tables

**Table 1.** NMR assignments for compounds **28**, **29**, and **30**.

**Table 2.** NMR assignments for compounds **31**, **32**, and **33**.

**Table 3.** NMR assignments for compounds **34**, **35**, and **36**.

**Table 4.** NMR assignments for compounds **37**, **38** and **40** (\* denotes interchangeable carbons).

**Table 5.** NMR assignments for compounds **39**, **41**, **42**, and **43**.

**Table 6.** Anti-proliferative  $GI_{50}$  values for synthesised compounds against cell lines HREC and ARPE-19 (Mean  $\pm$  SD). Compounds tested at 0.1 nM, 1 nM, 10 nM, 100 nM, 1  $\mu$ M, 10  $\mu$ M, and 100  $\mu$ M concentrations. The results are from 3 independent experiments.

**Table 7.** Cytotoxicity's of homoisoflavonoids against cell line - HeLa.  $IC_{50}$  values given in  $\mu$ M (Mean  $\pm$  SD). Compounds tested at 1  $\mu$ M, 10  $\mu$ M, 30  $\mu$ M, and 100  $\mu$ M and results show the average of 3 independent experiments.

**Table 8.** COX inhibition of each compound tested at two concentrations of 4.35 nM and 2.18 nM as determined by the Cayman Chemicals COX inhibition kit.

## List of Schemes

**Scheme 1.** The mechanistic pathways for the biosynthesis of the chromanone derivatives.

**Scheme 2.** Retrosynthetic analysis of 3-benzylidene chroman-4-one.

**Scheme 3.** Reaction between phenol and 3-chloro propanoic acid catalysed via base to give phenoxy intermediate which is cyclised using PPA to give rise to the chroman-4-one.

**Scheme 4.** Mechanistic scheme for the synthesis of the chroman-4-one skeleton.

**Scheme 5.** Synthesis of thiochromanone from thiophenol and 3-chloro propanoic acid under basic conditions.

**Scheme 6.** Mechanistic scheme for the synthesis of thiochromanone from thiophenol and 3-chloro propanoic acid.

**Scheme 7.** Reaction between resorcinol and 3-chloro propanoic acid under acidic conditions to give intermediate, which is cyclised under basic conditions to give the chroman-4-one.

**Scheme 8.** Reaction between phenol and 3-chloro propanoic acid under acidic conditions to acylate the resorcinol. The next step is the base catalysed intramolecular cyclisation reaction to give the chroman-4-one skeleton.

**Scheme 9.** Formation of chromanone from phenoxynitrile intermediate.

**Scheme 10.** Mechanistic sequence for the synthesis of the chroman-4-one ring from pyrogallol and acrylonitrile

**Scheme 11.** Overall Scheme for the synthesis of the thio derivative of the chroman-4-one known as a thiochroman-4-one.

**Scheme 12.** Overall scheme for the synthesis of the chroman-4-one

**Scheme 13.** The mechanistic scheme for the synthesis of the chromanone.

**Scheme 14.** Condensation between chromanone and benzaldehyde.

**Scheme 15.** Mechanistic scheme for the acid catalysed synthesis of the 3-benzylidene chroman-4-one.

**Scheme 16.** Base catalysed condensation reaction between chromanone and benzaldehyde.

**Scheme 17.** Mechanistic scheme for the base catalysed condensation of chromanone and benzaldehyde

- Scheme 18.** Biosynthesis of PGH<sub>2</sub> from arachidonic acid.
- Scheme 19.** Retrosynthetic analysis of a thio-containing homoisoflavonoid of the sappanin-like structure.
- Scheme 20.** (a) ClCH<sub>2</sub>CH<sub>2</sub>COOH/NaOH/H<sub>2</sub>O/Reflux 3 hrs.
- Scheme 21.** Base catalysed alkylation reaction between thiophenol and 3-chloropropanoic acid.
- Scheme 22.** (a) H<sub>2</sub>SO<sub>4</sub> 16 hr mediated intramolecular cyclisation reaction.
- Scheme 23.** Polyphosphoric acid mediated intramolecular cyclisation.
- Scheme 24.** Polyphosphoric acid mediated intramolecular cyclisation reaction producing a thiochromanone
- Scheme 25.** Piperidine mediated condensation of chromanone with benzaldehyde
- Scheme 26.** Acid catalysed condensation reaction between thiochromanone and benzaldehyde
- Scheme 27.** Acid catalysed condensation reaction between thiochromanone and substituted benzaldehyde producing the homoisoflavonoid derivative
- Scheme 28.** Acid catalysed condensation of thiochromanone and 3-bromobenzaldehyde
- Scheme 29.** Acid catalysed condensation of thiochromanone and protocatechuic aldehyde
- Scheme 30.** Acid catalysed condensation between thiochromanone and 2,4,6-trimethoxybenzaldehyde
- Scheme 31.** Acid catalysed condensation between thiochromanone and 4-nitrobenzaldehyde
- Scheme 32.** Synthetic scheme for the production of homoisoflavonoids containing multiple methoxy groups situated on the A-ring..
- Scheme 33.** Iron catalysed chemoselective reduction of olefinic moiety in the presence of a carbonyl group
- Scheme 34.** Ruthenium catalysed chemoselective reduction of olefinic moiety in the presence of a carbonyl group
- Scheme 35.** Palladium catalysed reduction of  $\alpha$ ,  $\beta$ -unsaturated system
- Scheme 36.** Chemo selective reduction of aromatic nitro group in the presence of  $\alpha$ ,  $\beta$  unsaturated system

# 1. Introduction

## 1.1 Homoisoflavonoids

Homoisoflavonoids are a 16 carbon natural product (**Figure 1**) comprised of a chroman-4-one motif and a benzyl group forming a tricyclic system consisting of two aromatic rings (A and B rings) connected via a heterocyclic C-ring. Homoisoflavonoids are structurally similar to isoflavonoids (**Figure 2**) and flavonoids (**Figure 3**) all containing a tricyclic system. However, homoisoflavonoids bear an additional carbon adjoining the heterocyclic C-ring to the aryl B-ring when compared to the isoflavonoid. When compared to the flavonoid there is the added migration of the benzylic group to the alpha position of the ketone group. Isoflavonoids and flavonoids bear the additional unsaturation of the chroman-4-one motif <sup>(1)</sup>. Homoisoflavonoids are biosynthetically formed via the chalcone intermediate (**Figure 4**).

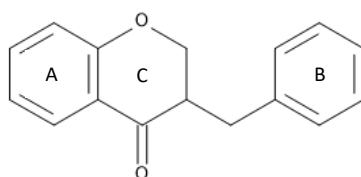


**Figure 1.** Structure of a homoisoflavonoid, with two aryl rings (A and B) and a heterocyclic (C ring) in the centre.

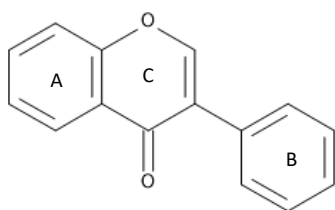


**Figure 2.** Structure of an isoflavonoid, with two aryl rings (A and B) and a heterocyclic (C ring) in the centre.

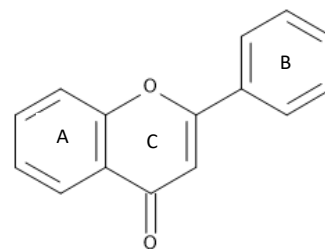


**Figure 3.** Structure of a flavonoid, with two aryl rings (A and B) and a heterocyclic (C ring) in the centre.

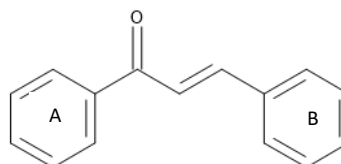


**Figure 4.** Structure of a chalcone with two aryl rings (A and B) and a prop-2-ene-1-one bridge connecting the rings.

The term homoisoflavonoid was first used as a moniker by P. Böhler and C. Tamm in 1967, to identify a new class of natural products <sup>(2)</sup>, which were isolated from the bulbs of *Eucomis bicolor* Bak (*Asparagaceae*). Homoisoflavonoids are a class (approximately 240) <sup>(3)</sup> of naturally occurring compounds that can be primarily extracted and isolated from 6 families: *Asparagaceae*, *Fabaceae*, *Polygonaceae*, *Portulacaceae*, *Orchidaceae* and *Gentianaceae* <sup>(4)</sup>. The homoisoflavonoids can be isolated from many parts of the plant, such as the roots, heartwood, bulbs, leaves and seeds.

An attempt at producing a classification system for homoisoflavonoid-type structures by Du Toit *et al*, postulated that there are four basic structural types of homoisoflavonoid: 3-benzyl-4-chromanones (Type I), 3-benzylidene-4-chromanones (Type II), 3-benzyl-3-hydroxy-4-chromanones (Type III) and scillascillins (Type IV) <sup>(5)</sup> (**Figures 5-8**).

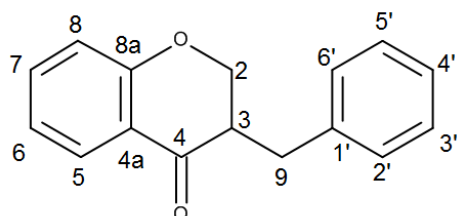


**Figure 5.** Type I (3-benzyl-4-chromanone)

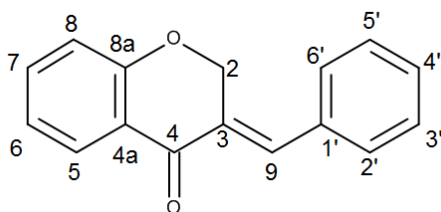


**Figure 6.** Type II (3-benzylidene-4-chromanone)

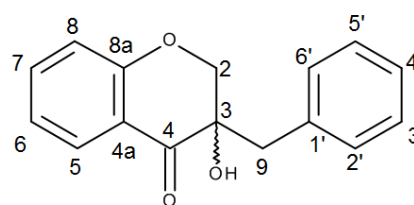


**Figure 7.** Type III (3-benzyl-3-hydroxy-4-chromanone)

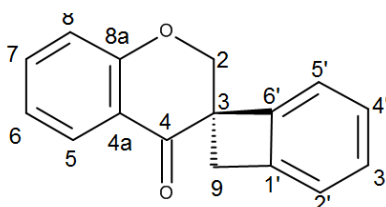


**Figure 8.** Type IV (Scillascillin)



## 1.2 Biosynthesis

The moniker homoisoflavonoid is a misnomer as the compounds that fall under this heading are biogenetically unrelated to isoflavonoids<sup>(6)</sup>. The biosynthesis of the homoisoflavonoid is believed to originate from a chalcone intermediate. Dewick has studied the biosynthesis of homoisoflavonoids and postulates that the carbon-2-stems originate from the  $\alpha$ -methyl of the methionine, with the rest of the skeletal structure originating from cinnamic acid and three acetate units<sup>(7)</sup>.

### 1.2.1 Biosynthesis of homoisoflavonoids

Dewick further proposed a mechanism for the biosynthetic route from the chalcone intermediate via radioactive labelling and feeding. The labelling patterns produced from the phenylalanine precursors in the eucomin (**Figure 9**) skeleton are in fact very similar to that of those demonstrated in the biosynthesis of the flavonoid compounds however a key difference being an extra carbon from methionine in the generation of the heterocyclic ring<sup>(8)</sup>.

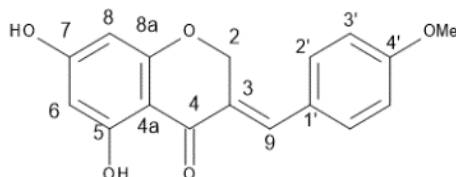
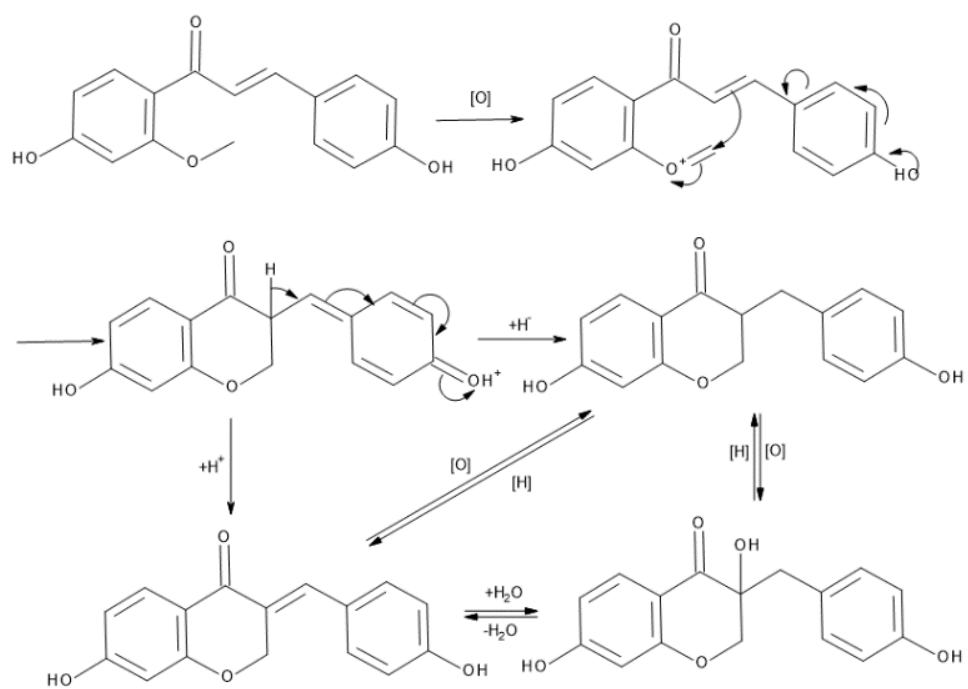


**Figure 9.** *Eucomin* structure

The proposed mechanism initialises with the oxidation of the methoxy group which leads to the flow of electrons originating at the hydroxyl group into the phenolic ring and leading to the attack of the methoxy group via the olefinic moiety present, this intramolecular cyclisation gives the three rings present in the skeleton of the homoisoflavonoid. Loss of a proton or addition of a hydride generates the 3-benzylidene chroman-4-one or the 3-benzylchroman-4-one respectively. Addition of water to the olefinic moiety in the 3-benzylidenechroman-4-one leads to the formation of another derivative known as the 3-benzyl-3-hydroxy chroman-4-one. This derivative can also be generated via oxidation of the 3-benzylchroman-4-one, these derivatives being of the sappanin like structure (**Scheme 1**).

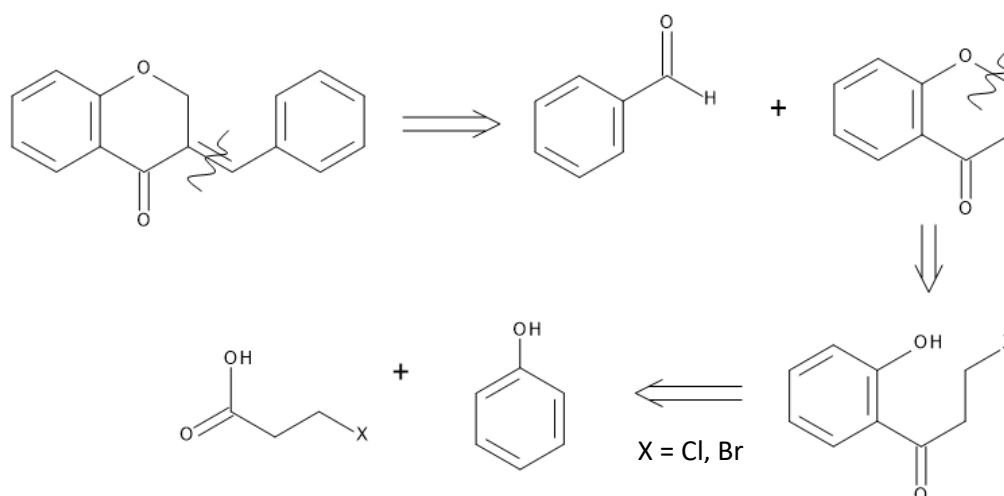


**Scheme 1.** The mechanistic pathways for the biosynthesis of the chromanone derivatives <sup>8</sup>

### 1.3 Methods of Synthesis

In 1968 Parkas *et al* synthesised the 3-benzylidene chroman-4-one utilising a chromanone precursor and condensing this with benzaldehyde in acetic anhydride to give rise to the 3-benzylidene chroman-4-one <sup>(9)</sup>.

A retrosynthetic analysis of the 3-benzylidene chroman-4-one, results in aryl aldehydes, phenols and carboxylic acid synthons (**Scheme 2**).



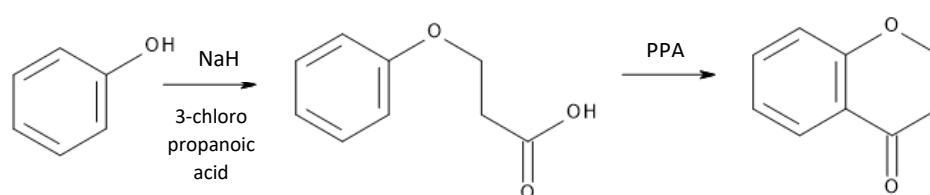
**Scheme 2.** Retrosynthetic analysis of 3-benzylidene chroman-4-one

A possible synthetic route to acquiring 3-benzylidene chroman-4-one is via, Friedel Crafts alkylation of phenol with 3-chloro/3-bromo propanoic acid at the ortho position. Followed by an intramolecular cyclisation reaction resulting in an  $S_N2$  like displacement of the halogen and forming the chromanone ring. The final step is an acid/base catalysed condensation with a substituted benzaldehyde, via exploiting the labile reactivity of the carbonyl moiety and giving rise to the 3-benzylidene chroman-4-one structure. However, there are numerous routes to the production of the chromanone motif, these routes are dependent on the substituents present and also allow for further functionalisation.

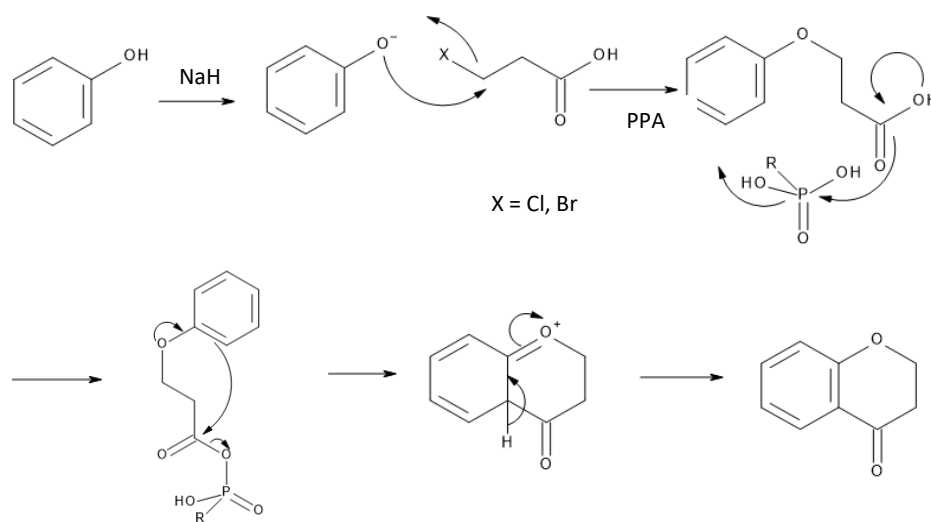
### 1.3.1 Synthesis of the chroman-4-one intermediate

Multiple routes for the production of the chromanone and the sulphur analogues (thiochromanone) have been used.

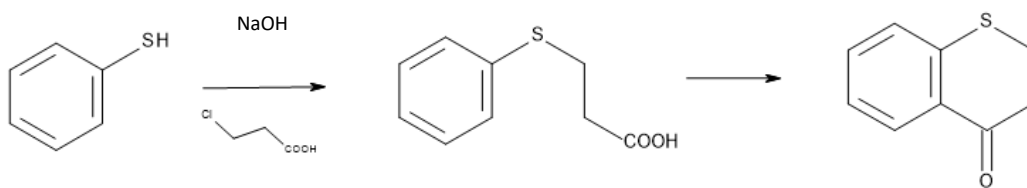
The reaction between a phenol and 3-chloro/3-bromo propanoic acid under basic conditions giving rise to the phenoxy propanoic acid which itself undergoes an acid catalysed (polyphosphoric acid) intramolecular cyclisation producing the chroman-4-one skeleton is commonly used <sup>(10,11)</sup> (**Scheme 3 & Scheme 4**).



**Scheme 3.** Reaction between phenol and 3-chloro propanoic acid catalysed via base to give phenoxy intermediate which is cyclised using PPA to give rise to the chroman-4-one

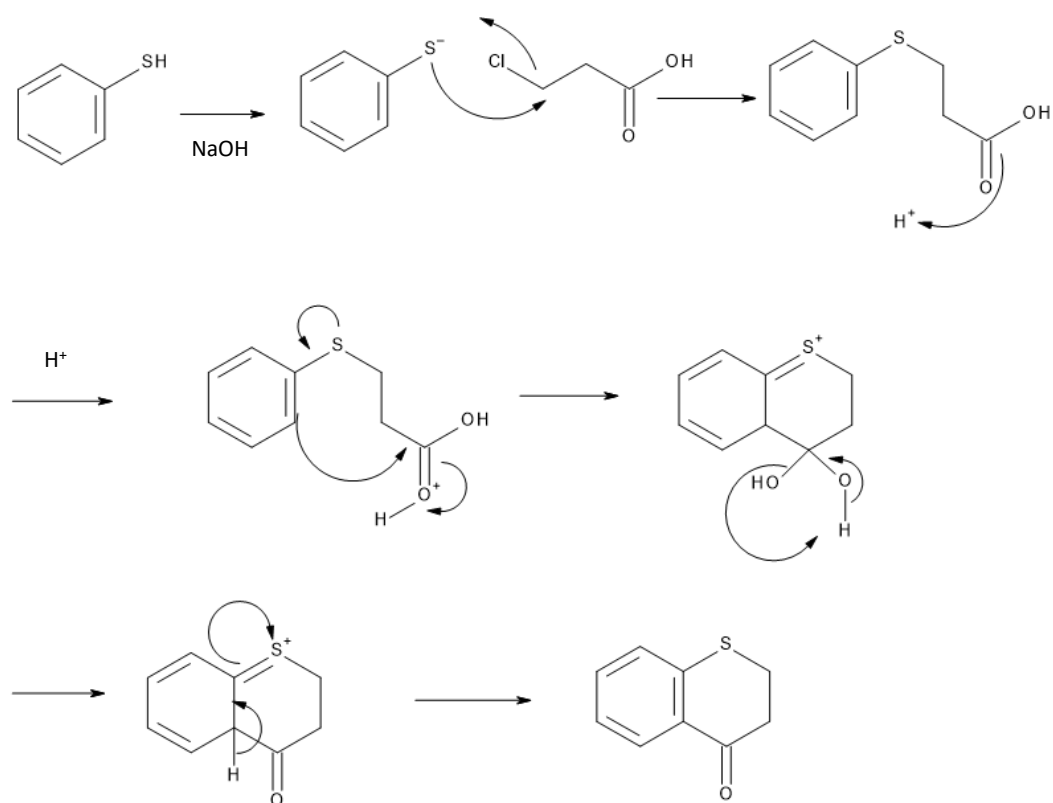


**Scheme 4.** Mechanistic scheme for the synthesis of the chroman-4-one skeleton.



**Scheme 5.** Synthesis of thiochromanone from thiophenol and 3-chloro propanoic acid under basic conditions

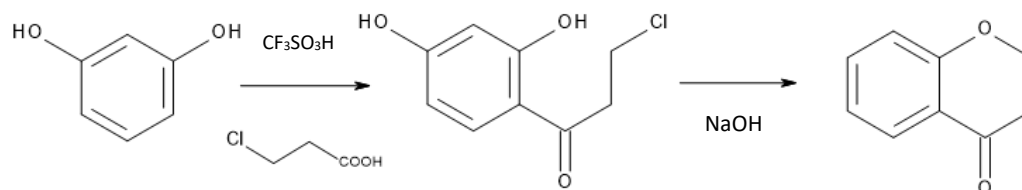
A similar scheme can be utilised when synthesising the sulphur analogue of the chroman-4-one known as a thiochromanone. Rather than starting with phenol as a precursor, thiophenol is utilised. The thiophenol undergoes an  $S_N2$  like reaction with 3-chloro/3-bromo propanoic acid under basic conditions producing a thiophenoxypropanoic acid intermediate. This intermediate undergoes an acid catalysed intramolecular cyclisation reaction, thus giving rise to the thiochromanone<sup>(11)</sup> (**Schemes 5 & 6**).



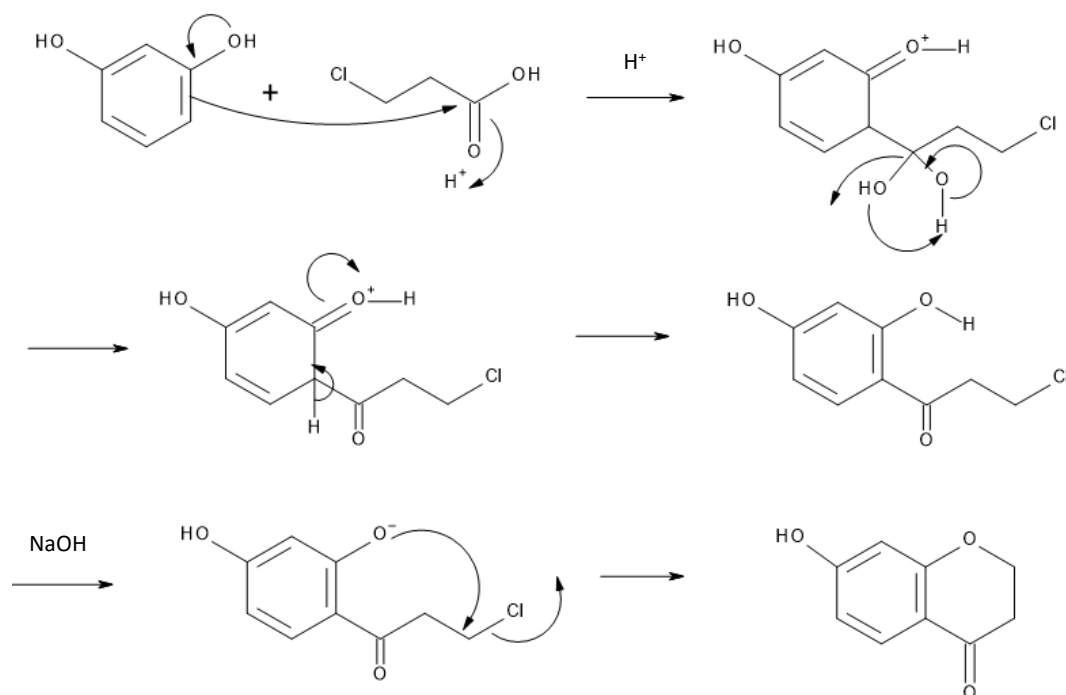
**Scheme 6.** Mechanistic scheme for the synthesis of thiochromanone from thiophenol and 3-chloro propanoic acid

The reaction between resorcinol and 3-chloro/3-bromo propanoic acid under acidic conditions produces an alkyl chloride benzophenone intermediate. This intermediate undergoes a base catalysed intramolecular cyclisation reaction promoted via NaOH to give rise to the chroman-4-one <sup>(12-14)</sup>

(Schemes 7 & 8).

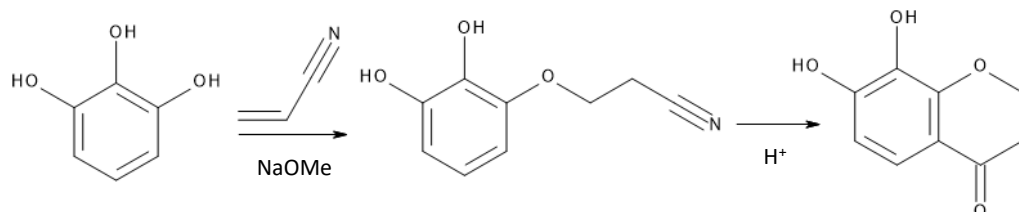


**Scheme 7.** Reaction between resorcinol and 3-chloro propanoic acid under acidic conditions to give intermediate, which is cyclised under basic conditions to give the chroman-4-one



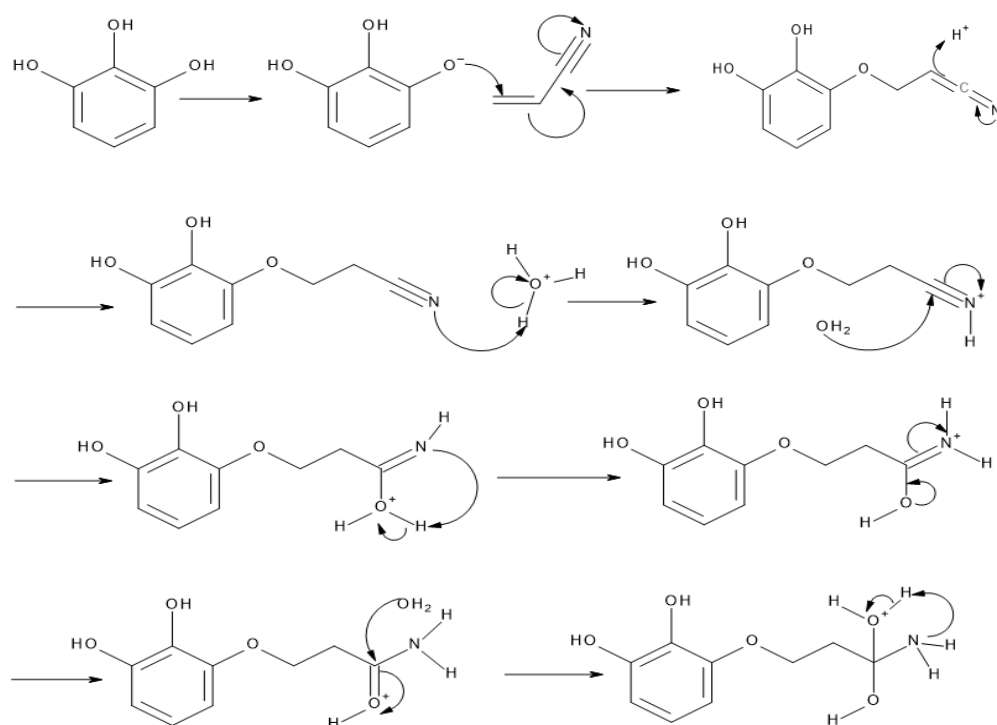
**Scheme 8.** Reaction between phenol and 3-chloro propanoic acid under acidic conditions to acylate the resorcinol. The next step is the base catalysed intramolecular cyclisation reaction to give the chroman-4-one skeleton

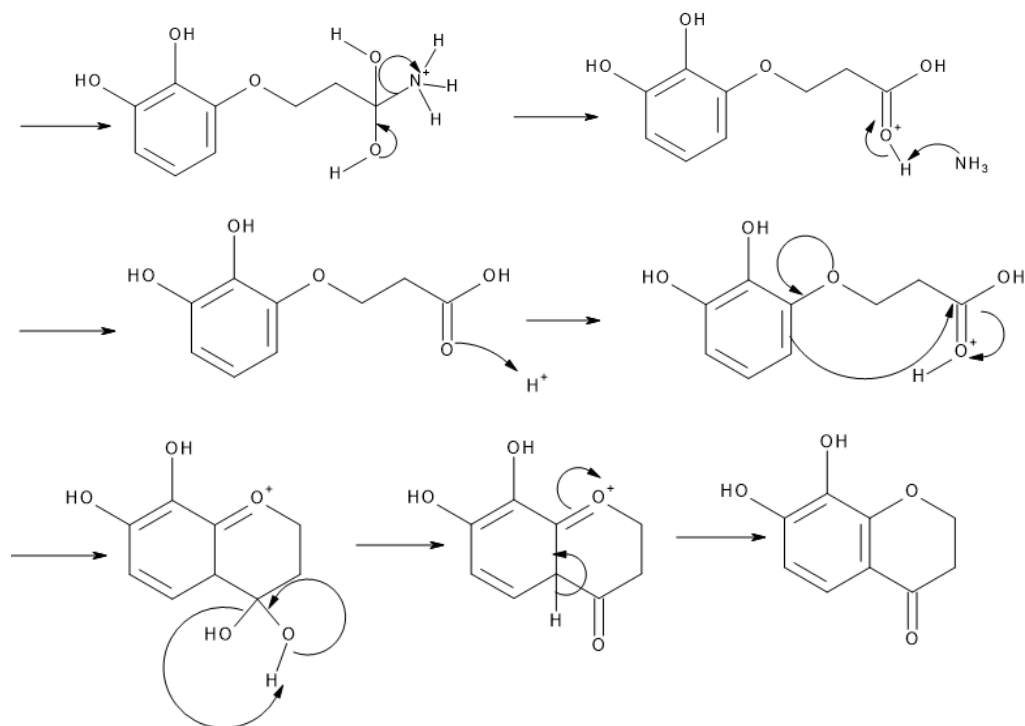
The formation of phenoxynitrile via coupling of pyrogallol with acrylonitrile under basic conditions, followed by subsequent acid catalysed intramolecular cyclisation produces the chroman-4-one skeleton<sup>(15)</sup> (**Scheme 9**).



**Scheme 9.** Formation of chromanone from phenoxynitrile intermediate

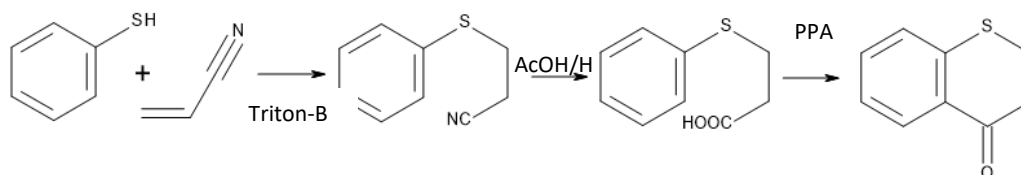
Initially, a proton is abstracted utilising sodium methoxide as the base, forming the phenolate moiety. The nucleophilic oxygen attacks the conjugated alkene, causing rearrangement of the double bond, and forming the phenoxy propionitrile intermediate. The phenoxy propionitrile undergoes an acid mediated reduction of the nitrile group to the subsequent imine, followed by hydrolysis to a carboxylic acid with production of the ammonium salt as a side product. The carboxylic acid is then subjected to acidic conditions catalysing the intramolecular cyclisation, and upon elimination of water the chroman-4-one skeleton is formed (**Scheme 10**).





**Scheme 10.** Mechanistic sequence for the synthesis of the chroman-4-one ring from pyrogallol and acrylonitrile

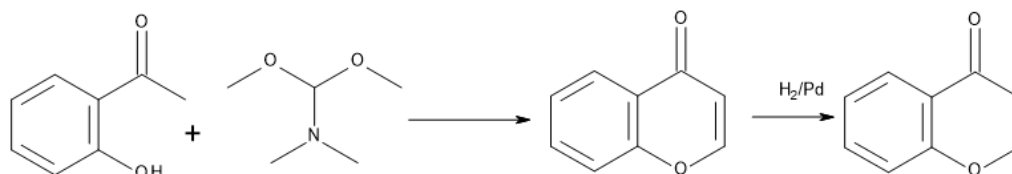
An analogous scheme can be used in order to synthesise a thiochroman-4-one, such as the scheme utilised by Demirayak *et al*<sup>(16)</sup>. In which the phenol is substituted for a thiophenol, and the base used for the abstraction of the proton from the thiol, is Triton-B (trimethylbenzylammonium hydroxide). Once the adduct has formed, the nitrile moiety is hydrolysed to give the corresponding carboxylic acid. This intermediate undergoes an intramolecular cyclisation reaction catalysed by PPA to form the thiochromanone (**Scheme 11**).



**Scheme 11.** Overall Scheme for the synthesis of the thio derivative of the chroman-4-one known as a thiochroman-4-one.

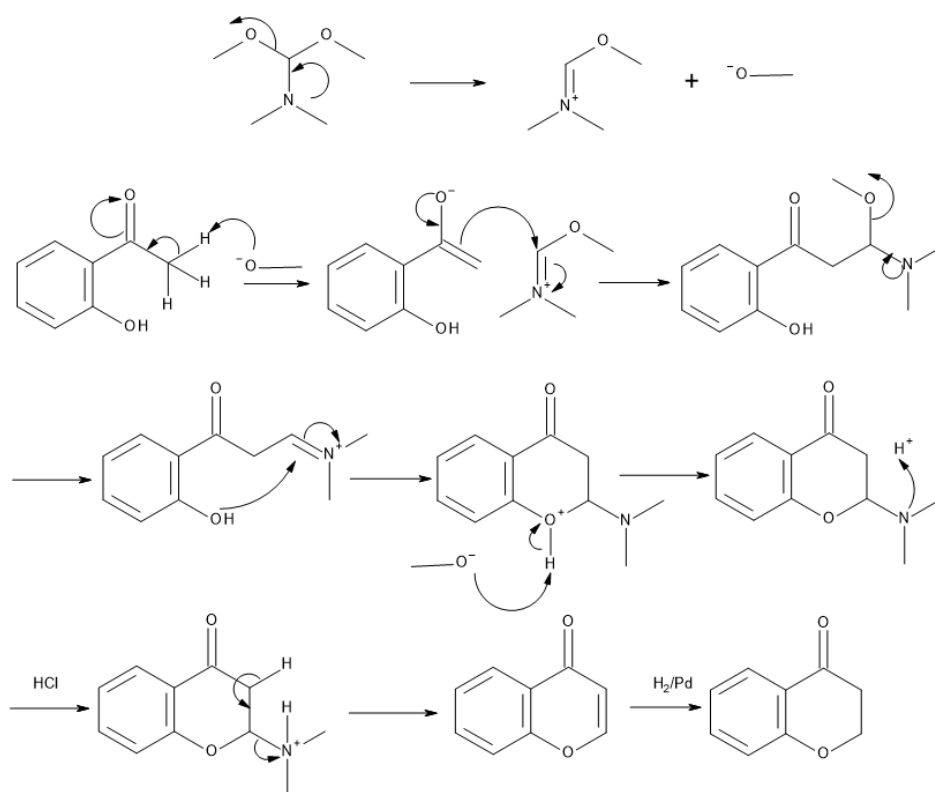


The synthesis of a chromanone via 2-hydroxy acetophenone and N, N- dimethylformamide dimethyl acetal



**Scheme 12.** Overall scheme for the synthesis of the chroman-4-one

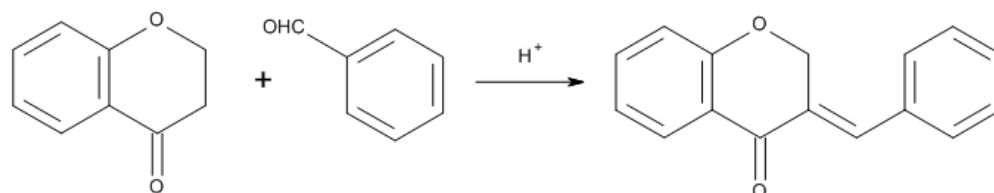
The lone pair of the nitrogen allows the formation of an imine with elimination of a methoxide anion. The methoxide anion abstracts an  $\alpha$ -carbon from the acetophenone forming the enolate which undergoes an addition reaction with the imine with subsequent reformation of the amine. Once again, the lone pair on the nitrogen eliminates the methoxide anion by reforming the imine, which allows the nucleophilic oxygen to attack the electrophilic carbon of the imine via an intramolecular cyclisation reaction. The free methoxide anion abstracts the proton from the positively charged oxygen. Acid workup allows for the elimination of the dimethylamine moiety along with the formation of the unsaturated chromanone, which has the olefinic bond reduced via hydrogenation using palladium to form the chroman-4-one skeleton<sup>(17–19)</sup> (**Schemes 12 & 13**).



**Scheme 13.** The mechanistic scheme for the synthesis of the chromanone.

### 1.3.2 Synthesis of 3-benzylidene chroman-4-one from chroman-4-one

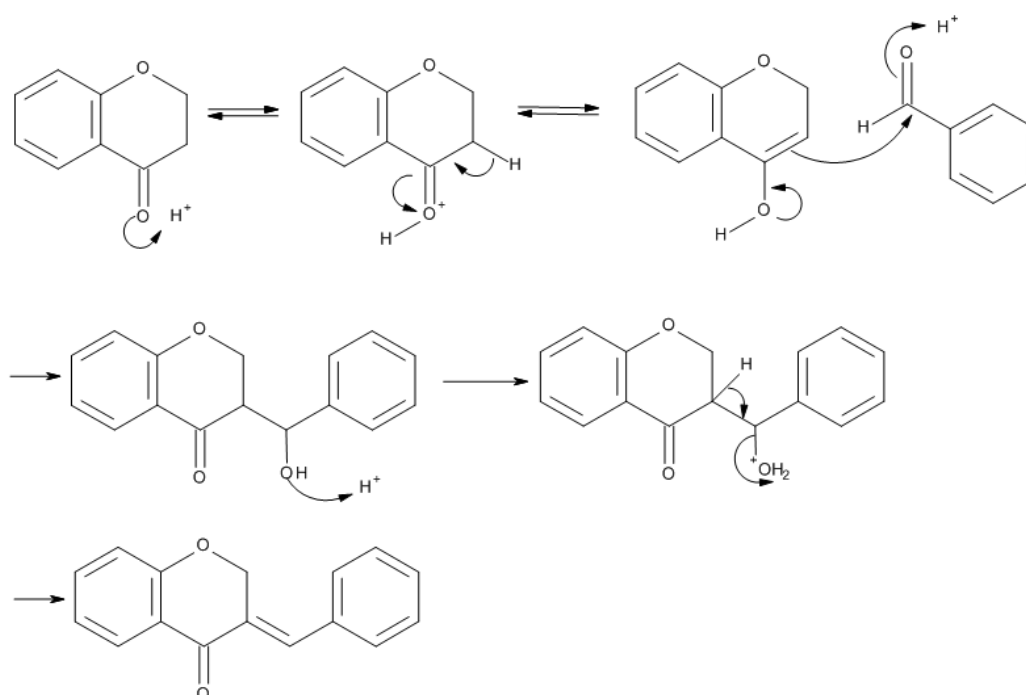
The 3-benzylidene chroman-4-one can be synthesised from either an acid or base catalysed condensation at the 3 position of the chroman-4-one.



**Scheme 14.** Condensation between chromanone and benzaldehyde

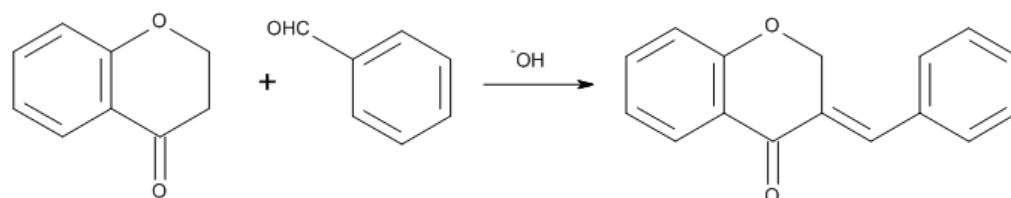
Acid catalysed condensation involves the protonation of the carbonyl group of the chroman-4-one, this induces the formation of an enol. Furthermore, the aldehyde is protonated, thus activating the carbonyl via increasing its electrophilicity therefore increasing the likelihood of nucleophilic attack<sup>(20)</sup>

(Schemes 14 & 15).

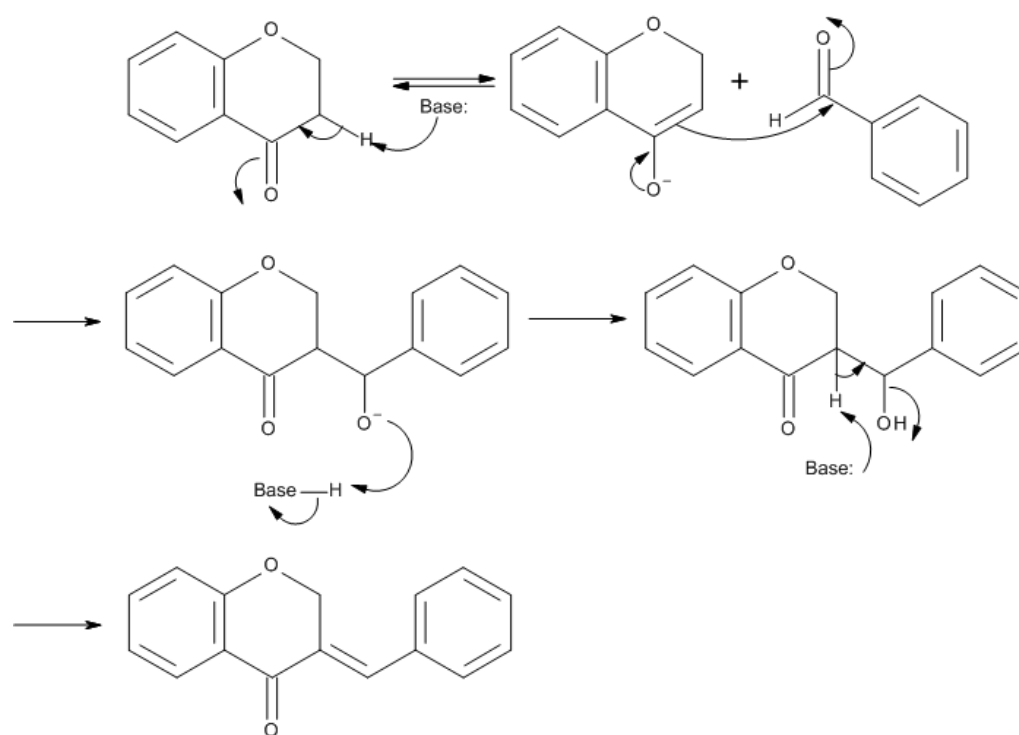


**Scheme 15.** Mechanistic scheme for the acid catalysed synthesis of the 3-benzylidene chroman-4-one

Base catalysed condensation involves the abstraction of the acidic  $\alpha$ -hydrogen, forming the enolate and subsequent nucleophilic addition to the aldehyde, conjoining the two and including the formation of a  $\beta$ -hydroxy ketone. This  $\beta$ -hydroxyl group is eliminated following the abstraction of the  $\alpha$ -hydrogen forming the olefinic moiety of the 3-benzylidene chroman-4-one<sup>(21)</sup> (**Schemes 16 & 17**).



**Scheme 16.** Base catalysed condensation reaction between chromanone and benzaldehyde



**Scheme 17.** Mechanistic scheme for the base catalysed condensation of chromanone and benzaldehyde

Sulphur analogues have been researched substantially less than their oxygen cousins. As such for this project, the *s*-alkylation of thiophenol via the use of 3-chloro/3-bromo propanoic acid under basic conditions, followed by the acid catalysed intramolecular cyclisation was the route chosen due to the cost and availability of reagents as well as due to the facileness/simplicity of the experimental procedures. An acid/base catalysed condensation between the chromanone and substituted benzaldehydes was chosen due to the availability and cost of reagents.

## 1.4 Bioactivity of homoisoflavonoids

Homoisoflavonoids show a wide spectrum of biological activities and as such demonstrate potential to act as various therapeutic agents. A number of these biological activities are outlined in this section.

### 1.4.1 Anti-inflammatory

Proinflammatory cytokines and nitric oxide (NO) are mediators involved in the pathogenesis of injury to tissues. Macrophages are a type of secretory cells that release these mediators. Activated macrophages are a type of macrophage that are able to express inducible nitric oxide synthase (iNOS). iNOS produces NO via the catalysis of oxidative deamination of L-arginine and causes excess production of NO. Excess NO is believed to cause detrimental damage arising from septic shock and inflammatory diseases <sup>(22)</sup>.

A number of homoisoflavonoids isolated from *Ophiopogon Japonicus* by Li *et al* have been investigated in order to determine their anti-inflammatory profile. Due to the implications of NO on inflammatory response, Li *et al* focussed on the production of NO induced by lipopolysaccharide in the murine microglial cell line BV-2 and the inhibitory action of the homoisoflavonoids. Two homoisoflavonoids isolated demonstrated their inhibitory activity due to reduced IC<sub>50</sub> values in comparison to the standard quercetin. Compounds **1** and **2** (**Figure 10**) exhibited IC<sub>50</sub> values of 7.8 μM and 5.1 μM respectively, thus demonstrating their superior activity when compared to quercetin, which had an IC<sub>50</sub> value of 13.9 μM. Therefore, the potential for homoisoflavonoids isolated from *Ophiopogon Japonicus* to act as NO inhibitors and accordingly anti-inflammatory agents has been demonstrated by Li *et al* <sup>(23)</sup>.

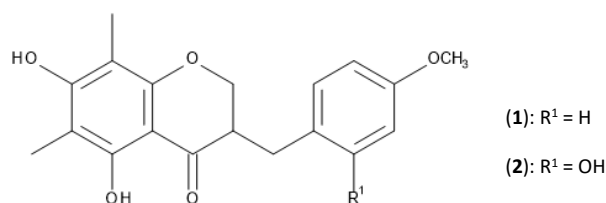


**Figure 10.** NO inhibitors isolated from *Ophiopogon japonicus*

Damodar *et al* also investigated homoisoflavonoids as potential inhibitors of NO production. Multiple homoisoflavonoids synthesised demonstrated their potential after being tested for a concentration dependent inhibitory effect on NO production by RAW264.7 cells. Four homoisoflavonoids (**Figure 11**) displayed their superior activity in comparison to the standard L-NMMA (N-Methylarginine). Homoisoflavonoids **3**, **4**, **5**, and **6** gave IC<sub>50</sub> values of 1.75 μM, 1.26 μM, 2.09 μM, and 2.91 μM respectively, the standard inhibitor used as a positive control was L-NMMA, which gave an IC<sub>50</sub> value of 16.11 μM. Therefore, from these results, it is clear that the synthetic homoisoflavonoids (**3**, **4**, **5**, and **6**) demonstrate superior inhibitory activity against nitric oxide production <sup>(18)</sup>.

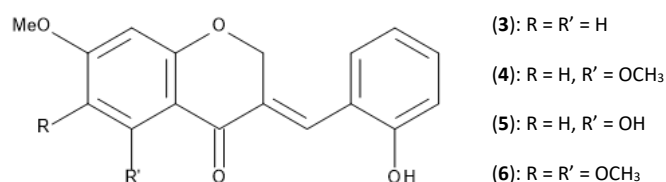


**Figure 11.** Homoisoflavonoids with NO inhibitory effects.

#### 1.4.2 Anti-Proliferative

Homoisoflavonoids have demonstrated anti-proliferative abilities against the growth of cancer cells. Over 30 homoisoflavonoids were synthesised by Demirayak *et al* and 14 were subsequently tested by the National Cancer Institute (NCI). The 14 compounds sent to NCI were screened against 60 tumour cell lines derived from nine cancer diseases at a single micro molar dose (10<sup>-5</sup> M). The results produced are in the form of percent cell growth promotion, and eight of the compounds demonstrated a mean growth percentage lower than 80% against the tumour cells and as such, passed the initial screening and progressed to the subsequent testing. The secondary testing screened the effective compounds at concentrations of 0.01, 0.1, 1, 10, and 100 μM. Compounds **9** and **10** (**Figure 12**) exhibited the greatest anti-proliferative activity with reduction of the growth percentages by 0.10% and 11.63 %. Six of the eight compounds contained a thiochromanone skeleton, which suggests the importance of the thioether moiety of the heterocyclic C-ring <sup>(16)</sup>.

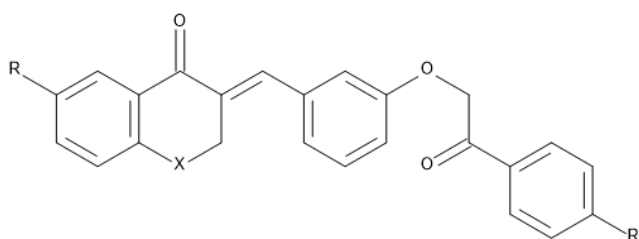


**Figure 12.** Anti-proliferative homoisoflavonoids

(7): X = O, R = R' = H

(8): X = O, R = Me, R' = OMe

(9): X = S, R = H, R' = OMe

(10): X = S, R = H, R' = Cl

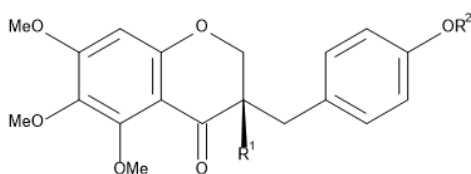
(11): X = S, R = Me, R' = OMe

(12): X = S, R = Me, R' = Cl

(13): X = S, R = Cl, R' = OMe

(14): X = S, R = Cl, R' = Cl

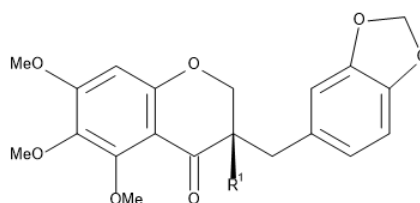
Five homoisoflavonoids (**Figure 13**) isolated from *Urginea depressa* by Dai *et al* have also demonstrated anti-proliferative ability. The five homoisoflavonoids were tested against three cancer cell lines with interesting results. Against the A2780 ovarian cancer cell line, all five homoisoflavonoids (**15 - 19**) demonstrated their anti-proliferative ability with IC<sub>50</sub> values of 0.3 μM, 2.0 μM, 3.4 μM, 1.35 μM, and 0.35 μM, respectively. When the homoisoflavonoids were tested against the A2058 melanoma and the H522-T1 human non-small cell lung cancer cell lines, compound **15** was five times more potent to A2058 and to H522-T1 cell lines than against A2780. Compound **18** was roughly equally as active against all three cell lines. Compounds **16** and **19** were significantly weaker against the A2058 and H522-T1 lines than the A2780 cell line <sup>(24)</sup>.



(15): R<sup>1</sup> = OH, R<sup>2</sup> = Me

(16) R<sup>1</sup> = OH, R<sup>2</sup> = H

(17): R<sup>1</sup> = H, R<sup>2</sup> = Me



(18): R<sup>1</sup> = OH

(19): R<sup>1</sup> = H

**Figure 13.** Anti-proliferative homoisoflavonoids isolated from *Urginea depressa*

### 1.4.3 Anti-Angiogenesis

The formation of new blood vessels from pre-existing ones is a complex physiological process that is mediated by angiogenesis. Angiogenesis typically occurs during development and wound repair processes <sup>(25)</sup>.

Unfortunately, under specific pathological conditions angiogenesis also occurs. New blood vessels abnormally formed in the eye is an example of a pathological event in the occurrence of ocular diseases including: proliferative diabetic retinopathy (PDR), wet age related macular degeneration (wet AMD) and retinopathy of prematurity (ROP) <sup>(17)</sup>. These diseases are a common cause of blindness. Surgical and LASER treatments are a standard treatment however, accumulation of damage to the retinal tissue and partial vision loss is a major drawback. There are a number of anti-angiogenic drugs that are currently used for therapy of these ocular diseases. However, as the target of these drugs is the vascular endothelial growth factor (VEGF), there are a number of side effects that may occur due to VEGF role in maintaining normal blood vessel endothelial cells. Furthermore, circa 35% of AMD patients are resistant to these drugs <sup>(26)</sup>.

Basavarajappa *et al* synthesised a regioisomer of a known anti-angiogenic homoisoflavanone Cremastranone **20** (Figure 14) <sup>(17)</sup>. Whereby one of the hydroxy moieties of the A-ring has been repositioned to where the methoxy group was and the methoxy group repositioned to where the hydroxy group was previously, as shown in (Figure 14). This regioisomer (compound **21**) was tested for its ability to inhibit the HUVEC - (human umbilical vein endothelial cells) with promising results. The GI<sub>50</sub> - 50% growth inhibitory concentration value was that of 18  $\mu$ M thus, demonstrating potential anti-proliferative ability. This compound was then subjected to an anti-proliferative assay on HREC - human retinal endothelial cells, which is a more disease relevant cell line. Compound **21** gave a GI<sub>50</sub> value of 43  $\mu$ M, also suggesting its potential to act as an anti-proliferative agent <sup>(25)</sup>.

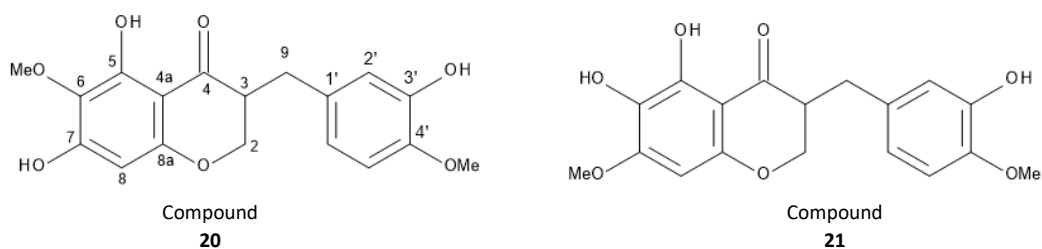
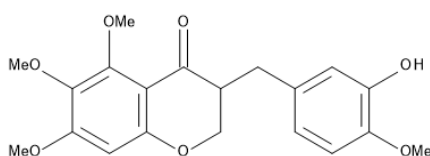


Figure 14. Cremastranone (**20**) and its regioisomer (**21**)

Basavarajappa *et al* <sup>(17)</sup> continued investigating the anti-proliferative effects of homoisoflavonoids (specifically in relation to retinal neovascularisation) by observing the effect of A- and B- ring modifications and therefore the structure activity relationship (SAR). Using cremastranone as a lead structure, A- ring modifications were made first. However, the majority demonstrated weak inhibitory activity against cell proliferation and demonstrated poor selectivity for human microvascular retinal endothelial cells when compared against HUVECs and Human ocular tumour cell lines 92.1 and Y79.

Compound **22** functionalised with 3 methoxy groups situated on the A ring (**Figure 15**) had strong activity against HREC, although not as strong as cremastranone. However, due to the good selectivity for HRECs over HUVECs and the other cell lines, compound **22** was chosen as a starting point where modifications were made to the B-ring next.



**Figure 15.** Compound **22** containing 3 methoxy groups situated on the A ring.

Numerous modifications were made to the B ring, however many did not exhibit strong enough activity against HREC or a strong enough selectivity. Compound **23** with B- ring containing an amine group ortho to a methoxy group (**Figure 16**) demonstrated its strong anti-proliferative activity with  $GI_{50}$  values of 1.1  $\mu$ M -against HREC and 0.51  $\mu$ M against HUVEC, however, also demonstrating its lack of selectivity.

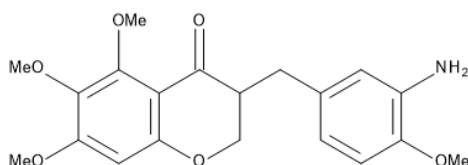


**Figure 16.** Compound **23** containing the trimethoxy A ring and the adjacent amine and methoxy groups situated on the B ring.



When acyl groups such as benzoyl, cinnamoyl and dihydrocinnamoyl were introduced to the B ring, this increased efficacy handsomely with GI<sub>50</sub> values of 0.17-0.65 μM for the HRECs. Additionally, compounds: **24**, **25** and **26** (**Figure 17**) demonstrated good selectivity for HREC inhibition against HUVECs, Y79 and 92.1 cell lines.

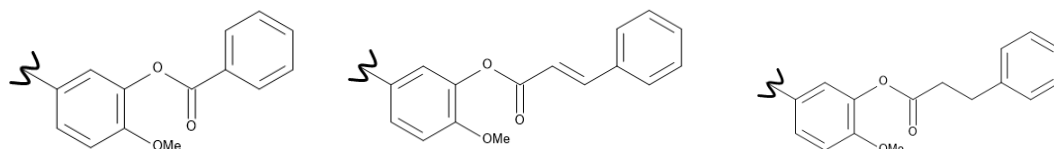


**Figure 17.** Homoisoflavonoids containing acyl groups situated into the B ring. The A ring of the compound is the same as compounds **22** and **23**

Due to the C3' position ostensibly being of importance for the strong selectivity require, further modifications were made, specifically the coupling with N-protected amino acids. This gave rise to compound **27** (**Figure 18**) which demonstrated excellent anti-proliferative activity exhibiting a GI<sub>50</sub> value of 55 nM against HRECs. Additionally, compound **27** demonstrated high selectivity with HREC proliferation inhibition 14x higher than HUVECs and 218x higher than Y79 and over 1000x higher than for 92.1 lines<sup>(17)</sup>.

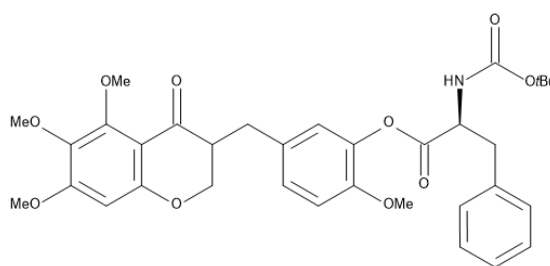


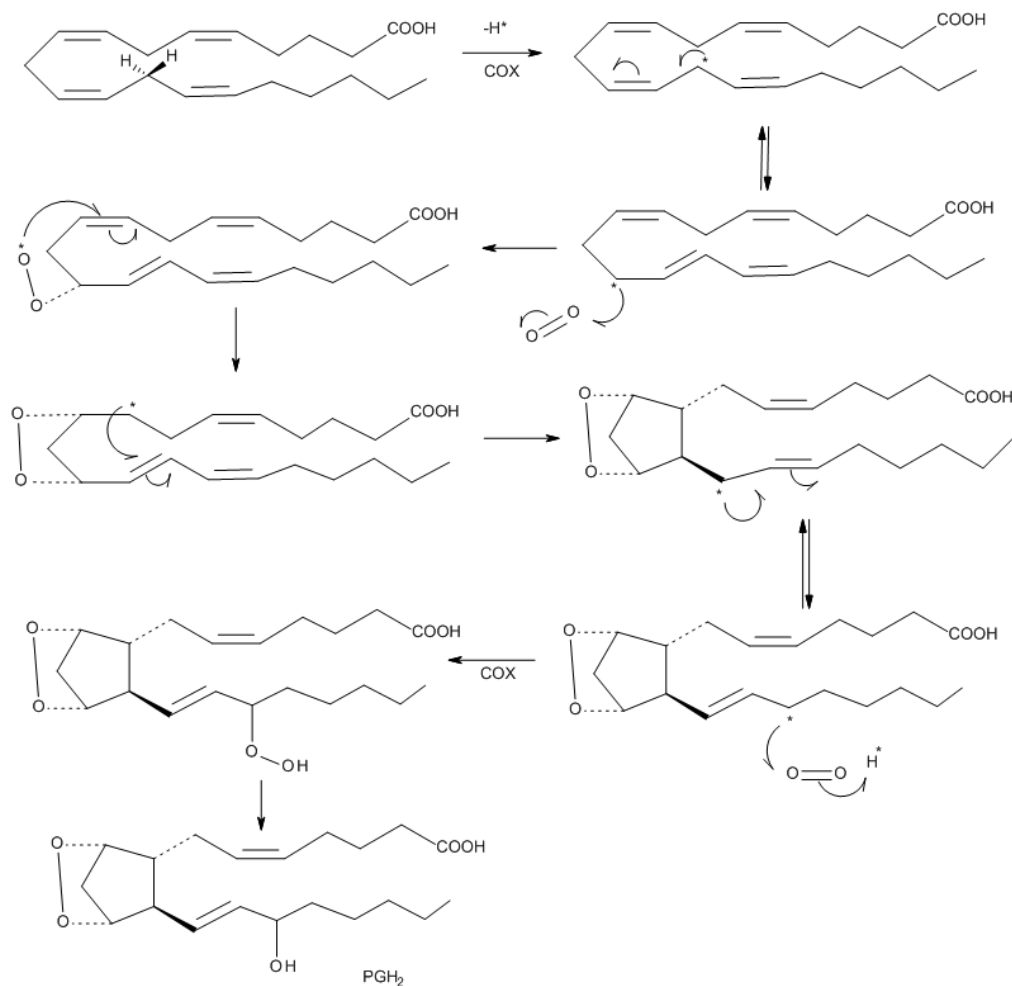
**Figure 18.** Compound **27** with high selectivity and strong anti-proliferative abilities.

## 1.5 Cyclooxygenase (COX)

Cyclooxygenases (COXs), also known as prostaglandin endoperoxidase H synthases (PGHSs)- are endoplasmic reticulum resident proteins, that are anchored to a single face on the endoplasmic reticulum membrane bilayer <sup>(27)</sup>. COX is a key enzyme, responsible for catalysing the rate limiting step of the conversion of free arachidonic acid to prostaglandin H<sub>2</sub> <sup>(28)</sup>.

Cyclooxygenase has two distinguishable isozymes: COX-I and COX-II. COX-I being the more abundant isozyme found in the kidneys, whilst COX-II is found minimally expressed in the kidneys <sup>(29)</sup>. COX-I is constitutively expressed throughout all tissues and is responsible for the cyto-protection of numerous tissues, such as the gastric surface epithelium and vasodilation in the kidney. It is also responsible for platelet production of thromboxane <sup>(28)</sup>. Whereas COX-II is typically induced and can be promoted by inflammatory mediators, including: cytokines, growth factors, and mitogens. Its level in normal tissue is very low <sup>(28)</sup>. COX-II is found to be largely upregulated within many human cancers including, breast, prostate, colorectal and gastric cancers <sup>(30)</sup>.

Non-steroidal anti-inflammatory drugs (NSAIDs) are competitive active site inhibitors of cyclooxygenase and target both isoforms of the enzyme. Despite both COX-I and COX-II existing as homodimers, only one unit is used at a time for the binding of a substrate. Whereby the substrate (i.e. NSAIDs) can bind to and consequently inactivate the COX site of only one of the units of the COX dimer, thus prohibiting the formation of prostanoids, whilst the other unit plays an allosteric-like role <sup>(31)</sup>.



**Scheme 18.** Biosynthesis of PGH<sub>2</sub> from arachidonic acid <sup>(1)</sup>.

Arachidonic acid is converted via a cyclooxygenase (COX) catalysed reaction into prostaglandin H<sub>2</sub>. COX incorporates two molecules of oxygen into arachidonic acid. A free radical intermediate is subsequently formed via a free radical oxidation reaction which occurs due to the methylene motif being located between two olefinic bonds. This intermediate undergoes a concerted cyclisation reaction in which the second molecule of oxygen is incorporated, and an acyclic peroxide group is formed. Lastly via a peroxidase catalysed reaction the peroxide group is cleaved yielding PGH<sub>2</sub> (**Scheme 18**). From PGH<sub>2</sub> other prostaglandins can be formed.

### 1.5.1 Risks associated with selective and non-selective COX inhibitors

Ibuprofen, one of the worlds most commonly used over the counter (OTC) drugs is a non-selective COX inhibitor, known to demonstrate anti-inflammatory activity and is used by all classes of people including pregnant women <sup>(32)</sup>. Around the time of conception and gestation, women who use both selective and non-selective COX inhibitors increase the risk of miscarriage by 80% <sup>(33)</sup> due to the interference of the COX cycle.

In order to investigate the effect of ibuprofen on foetal development, a zebrafish model was employed. When the zebrafish embryos were exposed to 1 µg/L and 5 µg/L of ibuprofen, there was a significant increase in mortality and significant decrease in the swimming activity when compared to both the control and the carrier control. Furthermore, once hatched these exposed groups failed to respond to light stimuli and tactile stimuli. When the zebrafish embryos were exposed to an increased concentration of ibuprofen to 50 µg/L the mortality rate increased by 50%, additionally an increase in the morphological defects affected the organisation of the tail bud, optic vesicle and brain. Not only was hatching delayed but almost 50% of the larvae exhibited cardiac oedema. Lastly when comparing the embryos exposed to 50µg/L to the lower concentrations and the controls there was a significant reduction of body mass, body length and heart rate found in the higher concentration <sup>(32)</sup>.

NSAIDs have been used to treat various health problems including rheumatoid arthritis and lupus. However, the therapeutic use of NSAIDs are limited due to the side effects associated with non-selective inhibition of COX. As COX-I regulates normal physiological processes, including maintenance of the gastric mucosal integrity and platelet aggregation, the side effects associated with the non-selective inhibition negate their clinical use, effects including: gastric irritation, ulceration and bleeding may develop causing potential life-threatening conditions <sup>(34)</sup>.

In 1999, there were three selective COX-II inhibitors known as coxibs, As the compounds were presumed to only target the COX-II isozyme, this would reduce the gastro-intestinal side effects significantly. Gastro-intestinal side effects were reduced, however new complications arose due to the coxibs <sup>(35)</sup>. In a study conducted with 8076 patients all with rheumatoid arthritis, the side effects

of a selective COX inhibitor - rofecoxib and a non-selective NSAID - naproxen were compared. Firstly, both drugs had similar efficacy against rheumatoid arthritis. Secondly, the number of gastrointestinal events were lower (2.1%) in patients treated with rofecoxib compared to naproxen (4.5%). Finally, the incidence of myocardial infarction was lower in the patients treated with naproxen (0.1%) when compared to patients treated with rofecoxib (0.4%) <sup>(36)</sup>.

A second study was conducted to further evaluate the effect of rofecoxib, this time on the incidence of colon cancer. However, adverse thrombotic events were associated with rofecoxib, including cardiac events. In the study, the group treated with rofecoxib had 3.6% of patients experience thrombotic adverse events compared to the placebo group of 2.0%. Of the 3.6%, 2.4% experienced adverse cardiac events and of the 2.0%, 0.9% experienced adverse cardiac events. As such, a recommendation from an external safety monitoring board to terminate the study two months ahead of the completion date due to the risks associated with rofecoxib <sup>(37)</sup>.

The role of COX-II in the production of prostaglandins, makes it an important target of anti-inflammatory activity. Furthermore, due to the various risks highlighted with selective and non-selective COX inhibitors, there is scope to produce selective COX-II inhibitors with reduced side effects.

### 1.5.2 Upregulation and Overexpression of COX-II

Multiple studies have investigated the occurrence of the upregulation and overexpression of COX-II in order to understand its potential role(s) in cancer. In quiescent rat intestinal epithelial (RIE) cells, COX-II is undetectable. However, within 6 hours of treatment with growth factors, it is transiently induced up to ten-fold, allowing the study of overexpression to be performed. In the rat intestinal epithelial cells that over express COX-II there is a greater occurrence of the attachment to the extra cellular matrix than cells that do not express COX-II. Furthermore, these cells were found to express reduced levels of the TGF $\beta$ 2 receptor and E-cadherin, both implicated in formation of tumours. High levels of the protein BCL2 (an anti-apoptotic regulator) were also found within these cells. The occurrence of all of these factors may promote the tumorigenic potential of the intestinal epithelial cells <sup>(38)</sup>.

Increased production of PGE<sub>2</sub> is associated with COX-II overexpression as PGE<sub>2</sub> is a major product of COX-II. PGE<sub>2</sub> is implicated in cell proliferation, cell death and tumour invasion<sup>(39)</sup>. A study conducted by Zimmermann *et al* investigated the functional relevance of PGs produced from COX-II in two oesophageal cancer cell lines: OSC-1 and -2. OSC-2 cells were found to express COX-II but not COX-I. In contrast, OSC-1 cells were found to express COX-I but only expressed very weak levels of COX-II. In the OSC-2 cells, levels of PGE<sub>2</sub> were found to be 600 time higher than in the OSC-1 cells. OSC-2 cells that were treated with selective COX-II inhibitors flosulide (**Figure 19**) and NS-398 (**Figure 20**), reduced PGE<sub>2</sub> production, and cell proliferation, and induced apoptosis. In the OSC-1 cells that were treated with the same inhibitors, no effect was seen. These results suggest that the prostaglandins produced by COX-II demonstrate a consequential role in the mediation of proliferation and apoptosis of the oesophageal cancer cells and that inhibition of COX-II may provide a therapeutic use in the treatment of oesophageal cancer<sup>(40)</sup>.

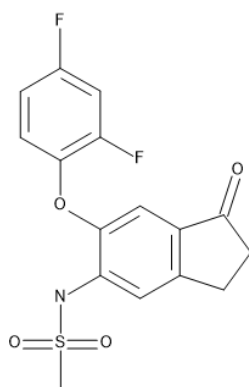


**Figure 19.** Structure of flosulide

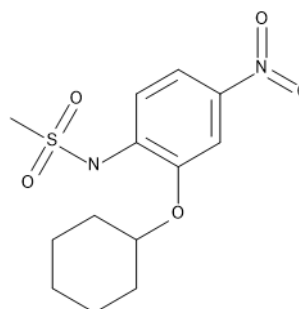


**Figure 20.** Structure of NS-398

COX-II expression was detected in 143 of 145 oesophageal adenocarcinoma specimens *and* was mainly located in the neoplastic cells found in a study conducted by Buskens *et al*. The study found that patients with tumours with a high COX-II expression experienced a more aggressive course of their disease due to the fact that there was an increased likelihood of these patients developing distant metastases and this led to higher mortality rates. The Kaplan-Meier curves produced from this study depicting patient survival, demonstrated a significant difference in the survival of the patients

between patients with a high level of COX-II expression when compared to those with a low level of COX-II expression <sup>(41)</sup>.

A total of 104 gastric carcinoma tissues were resected from patients with locally advanced gastric cancer, of which all showed positive staining with an anti-COX-II antibody. In the majority of the cases, a moderate to high immunoreactive score was recorded. Comparatively, normal gastric mucosa was found not to stain for COX-II. Diffuse staining in the cytoplasm of the tumour cells was shown by the immunoreactivity of COX-II protein and the expression of COX-II occurred in fibroblasts and inflammatory mononuclear cells of the desmoplastic stroma as well as in the smooth muscle cells. A further strong immunoreactive reaction to COX-II was found in epithelial cells that showed intestinal metaplasia and adenoma. A western blot analysis was performed, and the up-regulation of COX-II found in carcinoma tissues compared with normal mucosa was confirmed; the normal mucosa had undetectable levels of COX-II expression <sup>(42)</sup>.

Adenomatous polyposis coli (APC) is a multifunctional tumour suppressing gene (uncontrolled growth of cells that may produce cancerous tumours, are prevented by tumour suppressing genes). Kishimoto *et al* investigated the effects of a selective COX-II inhibitor NS-398 on the expression of the APC gene. Azoxy methane (AOM) - a colon specific carcinogen and NS-398 were administered to a number of rats. The study showed that the rats that were treated with both AOM and NS-398 demonstrated a significant reduction in the amount of pre-neoplastic lesions of colon cancer, in comparison to the rats that were treated with AOM alone. The levels of APC protein were determined by immunohistochemical staining and in the NS-398 treated specimens there was a clear increase in the APC protein expression. Furthermore, the APC mRNA expression for the specimens administered with NS-398 was significantly increased compared to the AOM treated specimen. Myc is a family of regulator genes and proto oncogenes and c-myc is constitutively expressed in cancer. The RNA levels of c-myc were also determined in the treated specimen, where the specimen administered with AOM only were found to have a significantly higher expression of c-myc mRNA than in the group without treatment. Furthermore, the group treated with NS-398 had a significantly lower level of c-myc mRNA expression when compared to the group treated with AOM only <sup>(43)</sup>.

A relationship between the size of tumours in colorectal carcinoma patients and the level of COX-II expression was found by Fujita *et al*, as well as a relationship between those with deeper invasions i.e. more invasive, and levels of COX-II expression. Firstly, in all the carcinoma tissues, both COX-I and -II mRNAs were detected. However, in the normal colorectal mucosa of the patients there was a low level of COX-II still detected. In contrast, significantly higher levels of COX-II were found in the colorectal carcinoma than in the normal colorectal mucosa. Additionally, the ratio of COX-II:COX-I was significantly higher in the larger tumours with respect to the diameter. Finally, the COX-II:COX-I were found to be higher in carcinomas with deeper invasions. Thus, suggesting that tumours with a high level of COX-II expression grow larger; in a more invasive manner<sup>(44)</sup>.

Cancer cells require oxygen and nutrients to facilitate growth. Angiogenesis is the formation of new blood vessels and as such, typically plays a role in the development of tumours. However, an angiogenesis-independent mechanism can occur, in which tumours receive oxygen and nutrients without the use of traditional blood vessels. Epithelial tumour cells manifest vascular channel like systems, allowing obtention of nutrients, without involvement of endothelial cells. This is known as vasculogenic mimicry.

Basu *et al* determined that invasive human breast cancer cells can develop these vascular channels when the breast cancer cells over express COX-II. Conversely, low levels of expressed COX-II found in non-invasive cell lines, did not develop the vascular channels. Furthermore, with high expression of COX-II in high grade invasive ductal carcinomas, the vascular channels were established. Whereas, in low grade breast tumours the tubular network was not identified. As such, the vascular channel regulation by COX-II was investigated. Cells that express high levels of COX-II and that were able to form the tubular networks were required and for these reasons, MDA-MB-231 cells were chosen. The cells were treated with celecoxib - a selective COX-II inhibitor and after treatment, the number of vascular channels formed were significantly reduced when compared to the cells treated only with the vehicle. This further suggests the role of COX-II in the formation of the vascular channels. PGE<sub>2</sub> is a major product of COX-II. Thus, to determine whether PGE<sub>2</sub> production had an effect on the formation of the vascular channels, cells were treated with both celecoxib and exogenous PGE<sub>2</sub>. It was found that after treatment of cells with PGE<sub>2</sub> the formation of the vascular channels was completely



restored, suggesting that the formation of vascular channels was dependent on PGE<sub>2</sub> as mediated by COX-II<sup>(45)</sup>.

CCR7 (C-C chemokine receptor type 7) is a protein involved in the facilitation of the migration of leukocytes and dendritic cells in the direction of the lymphatic endothelial cells. Pan *et al* investigated the relationship between CCR7 and COX-II by comparing metastatic MDA-MB-231 and non-metastatic MCF-7 breast cancer cell lines and their COX-II and CCR7 expression. In the metastatic MDA-MB-231 cells that overexpress COX-II, CCR7 was also highly expressed. Whereas in the non-metastatic MCF-7 cells low levels of COX-II and CCR7 were expressed. PGE<sub>2</sub> was administered to the MCF-7 cells and after treatment, levels of CCR7 mRNA and protein expression were both increased. shRNA was used to knockdown COX-II expression in the MDA-MB-231 cells which have high levels of COX-II expression. Down-regulation of CCR7 expression resulted due to the lack of COX-II expressed. As a result of the relationship between expression of CCR7 and COX-II, Pan *et al* investigated whether the expression affected the migratory capability of the breast cancer cells towards lymphatic endothelial cells. In the MCF-7 cells - which express low levels of COX-II and CCR7, migratory capability was poor. However, after ectopic expression of COX-II, the migratory capability was significantly increased. These results suggest that breast cancer cell migration can be increased due to the up-regulation of CCR7 as mediated by COX-II<sup>(46)</sup>.

Homoisoflavonoids have shown potential as cytotoxic and antiangiogenic compounds. They have shown selectivity in the inhibition of HREC vs cancerous and non-cancerous ocular cell lines. In addition they have shown potential as COX-II inhibitors. The overexpression of COX-II in many cancers as well the importance of identifying novel COX-II inhibitors to treat inflammatory conditions makes this an important drug target. Little work has focused on the sulphur analogues and as such investigating these compounds is of importance.

## 1.6 Aim and Objectives

Natural products have been a source of medicinal products for thousands of years. Homoisoflavonoids are a natural product that have been investigated rigorously for their biological activities. Synthetic sulphur analogues of homoisoflavonoids have been researched substantially less and as such, the aim of this project is to determine the various biological activities associated with multiple synthetic sulphur analogues of homoisoflavonoids and to determine some of the key SARs (structural activity relationships).

The objectives are:

- To synthesise novel sulphur analogues of the homoisoflavonoids containing various functional groups (halogens, nitro and methoxy groups).
- To determine the cytotoxicity of these novel compounds against HeLa cells via the neutral red assay.
- To determine the selective inhibition of HRECs as an indication of antiangiogenic activity of these novel compounds via the alamarBlue assay.
- To determine the selective COX-II inhibitory activity of these novel compounds.

## 2.0 Experimental

### 2.1 Synthetic chemistry

#### 2.1.1 Instrumentation

The NMR spectra were recorded on the Bruker Avance III 400 two channel FT-NMR spectrometer (AV400). Spectra were analysed using Topspin 3.6.1. Low resolution mass spectra of compounds were obtained using Agilent technologies network mass selective detector 5987.

High resolution mass spectra were obtained from the national mass spectrometer facility, Swansea using the Xevo G2-XS QToF Quadrupole Time-of-Flight Mass Spectrometer. Infrared spectra were recorded on Thermo Scientific Nicolet is5 with ATR attachment FTIR spectrometer.

Melting points were recorded using the SANYO Gallenkamp melting point apparatus.

X-ray crystallography: a single crystal of compound **36** was grown from toluene at room temperature. The single crystal data measurements were made using a twin-source SuperNova diffractometer with a micro-focus Cu X-ray beam (50 kV, 0.8 mA), an Atlas (135 mm CCD) detector, the temperature of the sample was controlled using an Oxford Instruments Cryojet5. The data obtained was processed using the CrysAlisPro software package (version 1.171.38.43) and Rigaku Oxford Diffraction.

All chemicals were purchased from Sigma-Aldrich (Poole, Dorset) and used without further purification.

#### 2.1.2 General procedure for the synthesis of substituted phenylsulfanyl propanoic acids

Substituted thiophenol (0.01 mol) and  $\beta$ -chloropropanoic acid (1.30 g, 0.012 mol) were dissolved in a NaOH solution (50 mL, 0.24mol). The system was refluxed for 3 hours under stirred conditions. The reaction was monitored by TLC (1:1 hexane:EtOAc). Once complete, the reaction was cooled to room temperature and the solution was adjusted by dilute HCl (0.1 M) to pH = 1 causing a white solid to precipitate. The solids formed were isolated via vacuum filtration and dried *in vacuo* to yield the desired product.

### 2.1.3 General procedure for the synthesis of substituted thiochromanones

Polyphosphoric acid (20 g, 0.20 mol) was added to a flask containing substituted phenylsulfanyl propanoic acids (4.62 mmol). The reaction mixture was heated at 60 °C for 3 hours under mechanical stirring. The reaction was then quenched with ice and left to stir for further 10 minutes. The mixture was extracted with ethyl acetate (4 x 30 mL). The combined organic layers were washed once with distilled water, followed by a NaOH solution (5%) wash and repeatedly washed with distilled water until a pH = 7 was acquired. The organic layers were washed with brine then dried over MgSO<sub>4</sub>. The reaction mixture was concentrated under reduced pressure yielding a light orange solid.

### 2.1.4 General procedure for the synthesis of the thio-homoisoflavonoids

To a solution of the substituted thiochromanone (2.4 mmol) and substituted benzaldehyde (2.2 mmol) in glacial acetic acid (2mL), concentrated H<sub>2</sub>SO<sub>4</sub> (0.6mL) was added. The reaction was stirred at room temperature for 24 hours. Progress was monitored by TLC (1:1 EtOAc:hexane). Once complete, methanol was added, and solids precipitated. The solids were filtered and dried yielding a fine powder.

## 2.2 Biological Methods

### 2.2.1 General

Dulbecco's modified eagle medium (DMEM), penicillin-streptomycin solution, foetal bovine serum (FBS), trypsin, trypan blue solution, neutral red, doxorubicin, and DMSO were obtained from Sigma Aldrich. T75 mL flasks, 96 well plates, and stripettes were purchased from Fischer Scientific. The plate reader used to read the 96 well plates was the BioTek EPOCH 2 microplate reader.

### 2.2.2 Cell culturing

The HeLa cells were cultured in DMEM supplemented with 1% pen-strep and 10% FBS. The cells were grown in an incubator with 95% humidified air mixed with 5% CO<sub>2</sub> at 37 °C. When the cells had grown to between 80 - 90% confluency, they were sub-cultured. In a laminar flow hood, the media was removed from the cell containing flask to which trypsin (5 mL) was added. The flask was then

incubated for 5 minutes to allow trypsinisation to take place. The cells were viewed under a microscope to determine the level of detachment. The cell suspension was removed and placed into a centrifuge tube, allowing centrifugation to take place. The supernatant was removed from the cell-containing centrifuge tube, to which fresh media (2 mL) was added - resuspending the cells. Cell suspension (1 mL) was then added to a T75 flask containing 20 mL of fresh media. The T75 flask was incubated until reaching 80 - 90% confluency.

### 2.2.3 Neutral red assay<sup>(47)</sup>

DMSO was used to dissolve all homoisoflavonoids to produce stock solutions with concentrations of 10 mM. Serial dilutions of the stock solutions were subsequently prepared (100  $\mu$ M, 30  $\mu$ M, 10  $\mu$ M, and 1  $\mu$ M). Ten thousand cells were seeded per well, with treatments being administered after 24 hours of incubation. After 24 hours of treatment, the media was removed, and the neutral red assay was performed. Addition of neutral red solution (40  $\mu$ g/mL) (100  $\mu$ L) per well was followed by an incubation period of 2 hours. After this incubation period, the plates were washed with PBS (100  $\mu$ L per well), followed by addition of a de-stain solution (50% ethanol, 49% dH<sub>2</sub>O, and 1% glacial acetic acid). The plates were shaken rapidly for 20 minutes allowing dissolution of the neutral red uptake from the cells. The plates were then read by the plate reader at 540 nm at 25 °C.

### 2.2.4 Cyclooxygenase inhibition assay

The inhibition of cyclooxygenase was determined via the COX (ovine/human) Inhibitor Screening Assay Kit Item № 560131 (Cayman Chemical company, Ann Arbor, MI, USA). COX inhibition was assayed using the Cayman COX (ovine/human) Inhibitor Screening Assay Kit guidelines via the direct measurement of PGF<sub>2 $\alpha$</sub>  by the reduction of COX derived PGH<sub>2</sub> by SnCl<sub>2</sub>. To a series of supplied reaction buffer solutions (0.1 M Tris-HCl, pH = 8, containing 5 mM EDTA and 2 mM phenol) with heme, either COX-I or COX-II enzyme and two concentrations (4.35 nM and 2.18 nM) of inhibitor samples (homoisoflavonoids synthesised in this study) were added. The solutions were subsequently incubated at 37 °C for 5 minutes. After 5 minutes, the substrate arachidonic acid was added. After a further 2 minutes, saturated stannous chloride solution was added in order to stop the reaction. The COX inhibition assay is based upon the competition between PGs and a PG tracer (PG-acetylcholinesterase conjugate) for a limited amount of PG antiserum. Due to the concentration of

the PG tracer being constant whilst the concentration of the PG varies, the amount of PG tracer able to bind to the PG antiserum is inversely proportional to the concentration of PG in the well. The plates were washed to remove any unbound reagents in the wells. Subsequent addition of Ellman's reagent, containing the substrate to acetylcholine esterase allowed for a distinctive yellow colour to appear. This yellow colour is generated due to the enzymatic reaction product. To determine the intensity of the yellow colour, an ELISA plate reader (BioTek EPOCH 2 microplate reader) was utilised at wavelength of 405 nm. As the colour is proportional to the amount of PG tracer bound to the well, which is inversely proportional to the amount of PGs present in the well, this allows for the determination of percent inhibition via the use of multiple control incubations.

### 2.2.5 AlamarBlue assay

The antiproliferative activities of the synthesised homoisoflavonoids were monitored by the alamarBlue fluorescence assay described in previous literature<sup>(53)</sup> and performed by Dr Kamakshi Sishtla at the Glick eye institute, University of Indiana.

### 2.2.6 Statistical analyses

Statistical testing was performed using GraphPad PRISM version 8. Firstly, all the data from the cytotoxicity testing, anti-proliferative testing and COX inhibitory testing were subjected to normality testing via the Shapiro-Wilks test to determine whether the results are normally distributed. If P values were found to be > 0.05 the results were found to be normally distributed. Once normal distribution was established, the data from the cytotoxicity and anti-proliferative testing was then subjected to the one way ANOVA to determine the significance of the data when compared to the negative control. The one way ANOVA was performed comparing the means to the negative control with subsequent Dunnett's multiple comparison *post-hoc* test (P values <0.05 are considered significant). For the COX inhibitory testing a two sample t-test was used to compare the % inhibition of the two concentrations of each compound respectively i.e. for compound 34, the percent inhibition for COX-I at concentration 4.35 nM compared against the percent inhibition for COX-I at concentration 2.18 nM.

### 3.0 Results

The synthesised compounds in this project, including the homoisoflavonoids and the intermediates were subjected to NMR analysis, the characterisation can be found within **tables 1-5** (further experimental data including IR, GCMS, HRESMS and NMR can be found in the Appendices). The biological evaluation pertaining to the anti-proliferative, cytotoxic and COX inhibition can be found in herein (**tables 5-8**) (further experimental data including IC<sub>50</sub> and GI<sub>50</sub> curves can be found in the Appendices).

#### 3.1 NMR

**Table 1.** NMR assignments for compounds **28**, **29**, and **30**

|                  | <b>28</b>             |                      |         |       | <b>29</b>             |                      |         |       | <b>30</b>              |                      |         |       |
|------------------|-----------------------|----------------------|---------|-------|-----------------------|----------------------|---------|-------|------------------------|----------------------|---------|-------|
|                  |                       |                      |         |       |                       |                      |         |       |                        |                      |         |       |
| Position         | $\delta_c$            | $\delta_H$ (J in Hz) | HMBC    | COSY  | $\delta_c$            | $\delta_H$ (J in Hz) | HMBC    | COSY  | $\delta_c$             | $\delta_H$ (J in Hz) | HMBC    | COSY  |
| 2                | 29.1, CH <sub>2</sub> | 3.07, t, (7.2)       | 3, 4, 8 | 2 → 3 | 28.9, CH <sub>2</sub> | 3.07, t, (7.2)       | 3, 4, 8 | 2 → 3 | 30.8, CH <sub>2</sub>  | 2.96, t, (7.0)       | 3, 4, 8 | 2 → 3 |
| 3                | 34.0, CH <sub>2</sub> | 2.59, t, (7.2)       | 2, 4    | 3 → 2 | 33.9, CH <sub>2</sub> | 2.60, t, (7.20)      | 2, 4    | 3 → 2 | 34.3, CH <sub>2</sub>  | 2.53, t, (7.0)       | 2, 8    | 3 → 2 |
| 4                | 177.3, C              |                      |         |       | 177.2, C              |                      |         |       | 177.7, CH <sub>2</sub> |                      |         |       |
| 5                | 131.8, CH             | 7.24, d, (8.9)       |         | 5 → 6 | 132.2, CH             | 7.20, d, (8.6)       |         | 5 → 6 | 134.5, CH              | 7.32, d, (8.7)       | 6, 7    | 5 → 6 |
| 6                | 129.3, CH             | 7.20, d, (8.9)       |         | 6 → 5 | 131.8, CH             | 7.40, d, (8.6)       |         | 6 → 5 | 114.7, CH              | 6.78, d, (8.7)       | 5, 7, 8 | 6 → 5 |
| 7                | 132.9, C              |                      |         |       | 120.8, C              |                      |         |       | 159.5, CH              |                      |         |       |
| 8                | 133.0, C              |                      |         |       | 134.1, C              |                      |         |       | 124.8, C               |                      |         |       |
| OCH <sub>3</sub> |                       |                      |         |       |                       |                      |         |       | 55.4, CH <sub>3</sub>  | 3.73, s              | 7       |       |

Table 2. NMR assignments for compounds **31**, **32**, and **33**

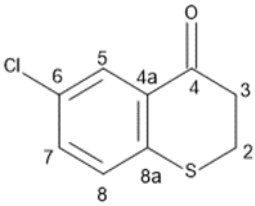
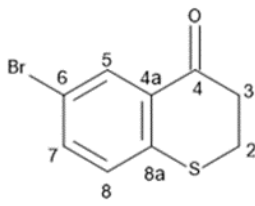
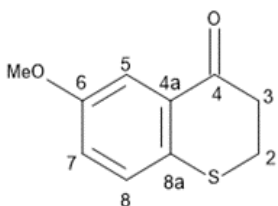
|                  | <b>31</b>   |                      |           |          | <b>32</b>   |                      |          |          | <b>33</b>   |                      |         |          |
|------------------|---|----------------------|-----------|----------|---|----------------------|----------|----------|---|----------------------|---------|----------|
|                  |  |                      |           |          |  |                      |          |          |  |                      |         |          |
| Position         | $\delta_c$  | $\delta_H$ (J in Hz) | HMBC      | COSY     | $\delta_c$  | $\delta_H$ (J in Hz) | HMBC     | COSY     | $\delta_c$  | $\delta_H$ (J in Hz) | HMBC    | COSY     |
| 2                | 26.9, CH <sub>2</sub>   | 3.17, m              | 3, 4, 8a  | 2 → 3    | 34.4, CH <sub>2</sub>   | 3.26, m              | 3, 4, 4a | 2 → 3    | 40.7, CH <sub>2</sub>   | 3.12, m              | 4,4a    | 2 → 3    |
| 3                | 39.3, CH <sub>2</sub>   | 2.90, m              | 2,4       | 3 → 2    | 39.1, CH <sub>2</sub>   | 2.99, m              | 2, 4     | 3 → 2    | 27.6, CH <sub>2</sub>   | 2.88, m              | 4       | 3 → 2    |
| 4                | 192.9, C  |                      |           |          | 192.9, C  |                      |          |          | 194.2, C  |                      |         |          |
| 4a               | 131.9, C  |                      |           |          | 141.18, C   |                      |          |          | 131.6, C  |                      |         |          |
| 5                | 128.8, CH   | 8.00, d, (2.5)       | 4, 4a, 8a | 5 → 7    | 131.5, CH   | 8.24, d, (2.1)       | 7        | 5 → 7    | 111.6, CH   | 7.53, d, (3.0)       | 4, 6, 8 | 5 → 7    |
| 6                | 131.2, C  |                      |           |          | 119.0, C  |                      |          |          | 157.5, C  |                      |         |          |
| 7                | 133.4, CH   | 7.26, dd, (2.5, 8.6) | 5, 6, 8a  | 7 → 5, 8 | 136.1, CH   | 7.50, dd, (2.1, 7.7) | 5, 8     | 7 → 5, 8 | 122.1, CH   | 6.92, dd, (3.0, 8.8) | 6, 8a   | 7 → 5, 8 |
| 8                | 129.1, CH   | 7.15, d, (8.6)       | 4a        | 8 → 7    | 129.4, CH   | 7.18, d, (7.7)       | 7        | 8 → 7    | 129.6, CH   | 7.09, d, (8.8)       | 6       | 8 → 7    |
| 8a               | 140.4, C  |                      |           |          | 132.0, C  |                      |          |          | 133.6, C  |                      |         |          |
| OCH <sub>3</sub> |   |                      |           |          |   |                      |          |          | 55.5, CH <sub>3</sub>   | 3.74, s              | 6       |          |



Table 3. NMR assignments for compounds 34, 35, and 36

| Position         | 34                    |                                      |          |           |        | 35                    |                                     |             |         |          | 36                    |                                      |             |         |       |
|------------------|-----------------------|--------------------------------------|----------|-----------|--------|-----------------------|-------------------------------------|-------------|---------|----------|-----------------------|--------------------------------------|-------------|---------|-------|
|                  | $\delta_c$            | $\delta_H$ (J in Hz)                 | HMBC     | COSY      | NOESY  | $\delta_c$            | $\delta_H$ (J in Hz)                | HMBC        | COSY    | NOESY    | $\delta_c$            | $\delta_H$ (J in Hz)                 | HMBC        | COSY    | NOESY |
| 2                | 29.1, CH <sub>2</sub> | 3.99, d, (1.0)                       | 3,9,4,8a | 2 → 9     | 2'     | 29.1, CH <sub>2</sub> | 3.97, d, (1.3)                      | 3, 4, 4a    | 2 → 9   | 2'       | 29.4, CH <sub>2</sub> | 3.96, d, (1.0)                       | 9,4         | 2 → 9   | 2'    |
| 3                | 132.5, C              |                                      |          |           |        | 132.6, C              |                                     |             |         |          | 132.4, C              |                                      |             |         |       |
| 4                | 184.5, C              |                                      |          |           |        | 184.6, C              |                                     |             |         |          | 185.6, C              |                                      |             |         |       |
| 4a               | 133.5, C              |                                      |          |           |        | 132.2, C              |                                     |             |         |          | 133.7, C              |                                      |             |         |       |
| 5                | 133.3, CH             | 8.23, d, (2.2)                       | 7,4,6,8a | 5 → 7     |        | 130.0, CH             | 8.08, d, (2.3)                      | 4, 4a, 6    | 5 → 7   |          | 112.8, CH             | 7.62, d, (3.0)                       | 4, 4a, 6, 7 | 5 → 7   |       |
| 6                | 119.7, C              |                                      |          |           |        | 133.6                 |                                     |             |         |          | 158.1, C              |                                      |             |         |       |
| 7                | 136.0, CH             | 7.44, dd, (2.2, 8.2)                 | 5,8a     | 7 → 5,8   |        | 133.1, CH             | 7.29, dd, (2.3, 8.2)                |             | 7 → 5,8 |          | 122.2, CH             | 6.95, dd, (3.0, 8.8)                 | 5,8         | 7 → 5,8 | 8     |
| 8                | 129.5, CH             | 7.12, d, (8.2)                       | 6,4a,4   | 8 → 7     |        | 129.4, CH             | 7.19, d, (8.2)                      | 6           | 8 → 7   |          | 129.1, CH             | 7.14, d, (8.8)                       | 5, 6, 7, 8  | 8 → 7   | 7     |
| 8a               | 139.9, C              |                                      |          |           |        | 139.3                 |                                     |             |         |          | 133.1, C              |                                      |             |         |       |
| 9                | 137.2, CH             | 7.62, brs, (w <sub>1/2</sub> = 2.70) | 3,2,4,1' | 9 → 2,2'  | 2'     | 137.2, CH             | 7.62, brs, (w <sub>1/2</sub> = 3.2) | 2, 3, 4, 4a | 9 → 2'  | 2'       | 136.3, CH             | 7.60, brs, (w <sub>1/2</sub> = 2.70) | 2,2',4      | 9 → 2   |       |
| 1'               | 133.6, C              |                                      |          |           |        |                       |                                     |             |         |          | 123.2, C              |                                      |             |         |       |
| 2'               | 131.0, CH             | 7.19, d, (8.4)                       | 4',3',9  | 2' → 3',9 | 2,9,3' | 131.0, CH             | 7.19, d, (7.9)                      | 4'          | 2' → 3' | 2' → 2,9 | 131.3, CH             | 7.19, d, (8.2)                       | 9, 3'       | 2' → 3' | 3',2  |
| 3'               | 132.2, CH             | 7.51, d, (8.4)                       | 4',1',2' | 3' → 2'   | 2'     | 132.1, CH             | 7.51, d, (7.9)                      | 4'          | 3' → 2' | 3' → 2'  | 132.0, CH             | 7.49, d, (8.2)                       | 1', 2'      | 3' → 2' | 2'    |
| 4'               | 123.5, C              |                                      |          |           |        | 132.3, C              |                                     |             |         |          | 133.9, C              |                                      |             |         |       |
| OCH <sub>3</sub> |                       |                                      |          |           |        |                       |                                     |             |         |          | 55.9, CH <sub>3</sub> | 3.79, s                              | 6           |         |       |

**Table 4.** NMR assignments for compounds **37**, **38** and **40** (\* denotes interchangeable carbons).

|                  | <b>37</b>             |                                      |          |          | <b>38</b>             |                      |                  |             | <b>40</b>             |                      |                    |       |
|------------------|-----------------------|--------------------------------------|----------|----------|-----------------------|----------------------|------------------|-------------|-----------------------|----------------------|--------------------|-------|
|                  |                       |                                      |          |          |                       |                      |                  |             |                       |                      |                    |       |
| Position         | $\delta_c$            | $\delta_H$ (J in Hz)                 | HMBC     | COSY     | $\delta_c$            | $\delta_H$ (J in Hz) | HMBC             | COSY        | $\delta_c$            | $\delta_H$ (J in Hz) | HMBC               | COSY  |
| 2                | 28.9, CH <sub>2</sub> | 3.99, d, (1.2)                       | 3, 4, 8a | 2 → 9    | 29.8, CH <sub>2</sub> | 3.99, d, (1.1)       | 3, 4, 4a, 8a, 1' | 2 → 9       | 29.3, CH <sub>2</sub> | 3.97, d, (1.1)       | 4, 4a, 8a, 9       | 2 → 9 |
| 3                | 136.4, C              |                                      |          |          | 133.2, C              |                      |                  |             | 132.4, C              |                      |                    |       |
| 4                | 184.6, C              |                                      |          |          | 184.4, C              |                      |                  |             | 185.7, C              |                      |                    |       |
| 4a               | 133.6, C              |                                      |          |          | 133.2, C              |                      |                  |             | 121.8, C              |                      |                    |       |
| 5                | 133.0, CH             | 8.23, d, (2.1)                       | 2, 6, 8a | 5 → 7    | 130.1, CH             | 8.07, d, (2.4)       | 4, 4a, 6, 8a     | 5 → 7       | 112.6, CH             | 7.62, d, (2.9)       | 4, 4a, 6, 7, 8, 8a | 5 → 7 |
| 6                | 119.6, C              |                                      |          |          | 132.1, C              |                      |                  |             | 158.4, C              |                      |                    |       |
| 7                | 132.0, CH             | 7.44, dd (2.1, 8.6)                  | 8a       | 7 → 5, 8 | 133.1, CH             | 7.29, dd, (2.4, 8.5) | 5, 6, 8a         | 7 → 5, 8    | 122.0, CH             | 6.96, dd, (2.9, 8.7) | 5, 6, 8, 8a        | 5, 8  |
| 8                | 129.55, CH            | 7.13, d, (8.6)                       |          | 8 → 7    | 129.2, CH             | 7.19, d, (8.5)       | 6                | 8 → 7       | 129.5, C              | 7.15, d, (8.7)       | 6, 7, 8a           | 8 → 7 |
| 8a               | 139.8, C              |                                      |          |          | 139.8, C              |                      | 8a               |             | 133.0, C              |                      |                    |       |
| 9                | 136.8, CH             | 7.62, brs, (w <sub>1/2</sub> = 2.70) | 4        | 9 → 2    | 136.7, CH             | 7.62, brs, (2.5)     |                  | 9 → 2       | 135.2, CH             | 7.61, s              | 2                  | 9 → 2 |
| 1'               |                       |                                      |          |          | 136.8, C              |                      |                  |             | 137.2, C              |                      |                    |       |
| 2'               | 132.2, CH             | 7.45, d, (1.8)                       | 3        | 2' → 6'  | *130.0, CH            | 7.45, m              |                  | 2' → 6'     | *131.8, CH            | 7.45, m              | 6'                 |       |
| 3'               | 122.9, C              |                                      |          |          | 122.9, C              |                      |                  |             | 134.4, C              |                      |                    |       |
| 4'               | 130.1, CH             | 7.25, m                              | 3'       | 4' → 5'  | *132.0, CH            | 7.24, m              |                  | 4' → 5'     | *130.2, CH            | 7.24, m              | 5'                 |       |
| 5'               | 135.8, CH             | 7.25, m                              |          |          | *132.4, CH            | 7.24, m              |                  | 5' → 4', 6' | *127.9, CH            | 7.24, m              | 4', 6'             |       |
| 6'               | 127.9, CH             | 7.45, m                              | 3'       | 6' → 5'  | *127.9, CH            | 7.45, m              |                  | 6' → 5'     | *132.1, CH            | 7.45, m              | 5'                 |       |
| OCH <sub>3</sub> |                       |                                      |          |          |                       |                      |                  |             | 55.6, CH <sub>3</sub> | 3.79, s              | 5, 8, 7            |       |

Table 5. NMR assignments for compounds 39, 41, 42, and 43

|                  | 39                    |                         |              |         |       | 41                    |                         |              |         |       | 42                    |                         |           |         |       | 43                    |                         |           |         |                  |
|------------------|-----------------------|-------------------------|--------------|---------|-------|-----------------------|-------------------------|--------------|---------|-------|-----------------------|-------------------------|-----------|---------|-------|-----------------------|-------------------------|-----------|---------|------------------|
|                  |                       |                         |              |         |       |                       |                         |              |         |       |                       |                         |           |         |       |                       |                         |           |         |                  |
| Position         | $\delta_c$            | $\delta_H$ (J in Hz)    | HMBC         | COSY    | NOESY | $\delta_c$ (J in Hz)  | $\delta_H$ (J in Hz)    | HMBC         | COSY    | NOESY | $\delta_c$            | $\delta_H$ (J in Hz)    | HMBC      | COSY    | NOESY | $\delta_c$            | $\delta_H$ (J in Hz)    | HMBC      | COSY    | NOESY            |
| 2                | 29.1, CH <sub>2</sub> | 3.99, d, (1.0)          | 9, 4, 8a, 1' | 2 → 9   | 2',3' | 29.1, CH <sub>2</sub> | 4.10, d, (1.0)          | 4, 8a, 9, 1' | 2 → 9   | 2'    | 28.5, CH <sub>2</sub> | 4.27, s                 | 4, 8a, 1' | 2 → 9   | 3'    | 29.3, CH <sub>2</sub> | 3.94, d, (1.1)          | 9, 4, 8a  | 2 → 9   |                  |
| 3                | 133.1, C              |                         |              |         |       | 130.9, C              |                         |              |         |       | 141.4, C              |                         |           |         |       | 132.3                 |                         |           |         |                  |
| 4                | 184.3, C              |                         |              |         |       | 184.6, C              |                         |              |         |       | 184.5, C              |                         |           |         |       | 185.3, C              |                         |           |         |                  |
| 4a               | 133.5, C              |                         |              |         |       | 133.5, C              |                         |              |         |       | 133.5, C              |                         |           |         |       | 132.8, C              |                         |           |         |                  |
| 5                | 133.0, CH             | 8.23, d, (2.2)          | 4, 6, 8a, 4a | 5 → 7   |       | 133.2, CH             | 8.32, d, (2.3)          | 7, 8a        | 5 → 7   | 8     | 132.1, CH             | 8.13, d, (2.4)          | 3         | 5 → 7   |       | 112.8, CH             | 7.62, d, (3.0)          | 4, 7, 8a  | 5 → 7   | OCH <sub>3</sub> |
| 6                | 119.6, C              |                         |              |         |       | 119.6, C              |                         |              |         |       | 118.7, C              |                         |           |         |       | 158.2, C              |                         |           |         |                  |
| 7                | 136.0, CH             | 7.44, dd, (2.2, 8.5)    | 5, 8a        | 7 → 5,8 | 8     | 135.8, CH             | 7.43, dd, (2.3, 8.5)    | 4a, 8a       | 7 → 5,8 | 5,8   | 136.5, CH             | 7.73, dd, (2.4, 8.4)    |           | 7 → 5,8 | 8     | 122.3, CH             | 6.98, dd, (3.0, 8.8)    | 6, 8a     | 7 → 5,8 | OCH <sub>3</sub> |
| 8                | 129.5, CH             | 7.13, d, (8.5)          | 5, 4a        | 8 → 7   | 7     | 129.4, CH             | 7.22, d, (8.5)          | 4a, 6        | 8 → 7   | 7     | 130.5, CH             | 7.44, d, (8.4)          | 4a, 6     | 8 → 7   | 7     | 129.4, CH             | 7.16, d, (8.8)          | 4a, 6, 7  | 8 → 7   |                  |
| 8a               | 139.9, C              |                         |              |         |       | 139.9, C              |                         |              |         |       | 135.5, C              |                         |           |         |       | 136.1, C              |                         |           |         |                  |
| 9                | 137.2, CH             | 7.65, brs, (w1/2 = 2.5) | 2,3',4       | 9 → 2   |       | 137.4, CH             | 7.77, brs, (w1/2 = 3.0) | 2, 2', 4, 1' | 9 → 2   |       | 135.3, CH             | 7.72, brs, (w1/2 = 1.8) | 3, 3'     | 9 → 2   |       | 134.6, CH             | 7.67, brs, (w1/2 = 3.2) | 2', 3', 4 | 9 → 2   |                  |
| 1'               | 132.5, C              |                         |              |         |       | 131.8, C              |                         |              |         |       | 140.8, C              |                         |           |         |       | 141.7, C              |                         |           |         |                  |
| 2'               | 129.2, CH             | 7.35, d, (8.4)          | 3',4',1'     | 2' → 3' | 2     | 131.4, CH             | 7.41, dd, (5.3, 8.5)    | 3',9, 1', 4' | 2' → 3' | 2     | 123.9, CH             | 8.32, d, (8.7)          | 3, 3'     | 2' → 3' | 3'    | 124.0, CH             | 8.23, d, (8.6)          | 3',1',4'  | 2' → 3' | 3'               |
| 3'               | 130.9, CH             | 7.25, d, (8.4)          | 2',4'        | 3' → 2' | 2'    | 116.2, CH, d (21.8)   | 7.14, t, (8.5)          | 2', 1', 4'   | 3' → 2' |       | 131.1, C              | 7.81, d, (8.7)          | 2', 4'    | 3' → 2' | 2, 2' | 130.3, CH             | 7.48, d, (8.6)          | 2',4'     | 3' → 2' | 2',2             |
| 4'               | 135.2, C              |                         |              |         |       | 164.2, C, d, (244.9)  |                         |              |         |       | 147.7, C              |                         |           |         |       | 147.7, C              |                         |           |         |                  |
| OCH <sub>3</sub> |                       |                         |              |         |       |                       |                         |              |         |       |                       |                         |           |         |       | 55.7, CH <sub>3</sub> | 3.79, s                 | 6         |         | 5,7              |

## 3.2 Biological Results

**Table 6.** Anti-proliferative GI<sub>50</sub> values for synthesised compounds against cell lines HREC and ARPE-19 (Mean ± SD). Compounds tested at 0.1 nM, 1 nM, 10 nM, 100 nM, 1 μM, 10 μM, and 100 μM concentrations. The results are from 3 independent experiments.

| Compound  | HREC GI <sub>50</sub> (μM) | ARPE-19 GI <sub>50</sub> (μM) |
|-----------|----------------------------|-------------------------------|
| <b>34</b> | 17.8 ± 12.4                | > 100                         |
| <b>35</b> | 11.2 ± 3.12                | > 100                         |
| <b>36</b> | 4.06 ± 0.53                | > 100                         |
| <b>37</b> | 10.0 ± 2.70                | > 100                         |
| <b>38</b> | 4.11 ± 0.52                | > 100                         |
| <b>39</b> | 15.7 ± 2.22                | > 100                         |
| <b>40</b> | 3.07 ± 0.38                | > 100                         |
| <b>41</b> | 3.65 ± 0.17                | > 100                         |
| <b>42</b> | > 100                      | > 100                         |
| <b>43</b> | 33.7 ± 19.4                | > 100                         |

**Table 7.** Cytotoxicity's of homoisoflavonoids against cell line - HeLa. IC<sub>50</sub> values given in μM (Mean ± SD). Compounds tested at 1 μM, 10 μM, 30 μM, and 100 μM and results show the average of 3 independent experiments

| Compound  | HeLa IC <sub>50</sub> (μM) |
|-----------|----------------------------|
| <b>34</b> | 22.03 ± 1.5                |
| <b>35</b> | 22.69 ± 0.54               |
| <b>36</b> | 17.33 ± 0.66               |
| <b>37</b> | 18.93 ± 1.90               |
| <b>38</b> | 19.73 ± 0.76               |
| <b>39</b> | 30.32 ± 2.56               |
| <b>40</b> | 12.65 ± 0.89               |
| <b>41</b> | 6.08 ± 2.03                |
| <b>42</b> | > 100                      |
| <b>43</b> | 59.46 ± 22.7               |

**Table 8.** COX inhibition of each compound tested at two concentrations of 4.35 nM and 2.18 nM as determined by the Cayman Chemicals COX inhibition kit

| Compound  | COX-I Inhibition (%) |             | COX-II Inhibition (%) |             |
|-----------|----------------------|-------------|-----------------------|-------------|
|           | 4.35 nM              | 2.18 nM     | 4.35 nM               | 2.18 nM     |
| <b>34</b> | 26.2 ± 3.96          | 9.42 ± 2.21 | 5.60 ± 1.15           | 0           |
| <b>35</b> | 34.3 ± 3.68          | 3.48 ± 2.63 | 3.89 ± 1.51           | 0           |
| <b>36</b> | 28.7 ± 4.95          | 7.83 ± 4.90 | 13.5 ± 2.55           | 0           |
| <b>37</b> | 31.3 ± 2.86          | 5.65 ± 2.26 | 22.7 ± 1.78           | 6.61 ± 1.54 |
| <b>38</b> | 27.5 ± 4.27          | 14.8 ± 4.86 | 0                     | 0           |
| <b>40</b> | 24.3 ± 2.35          | 9.67 ± 1.12 | 0                     | 0           |

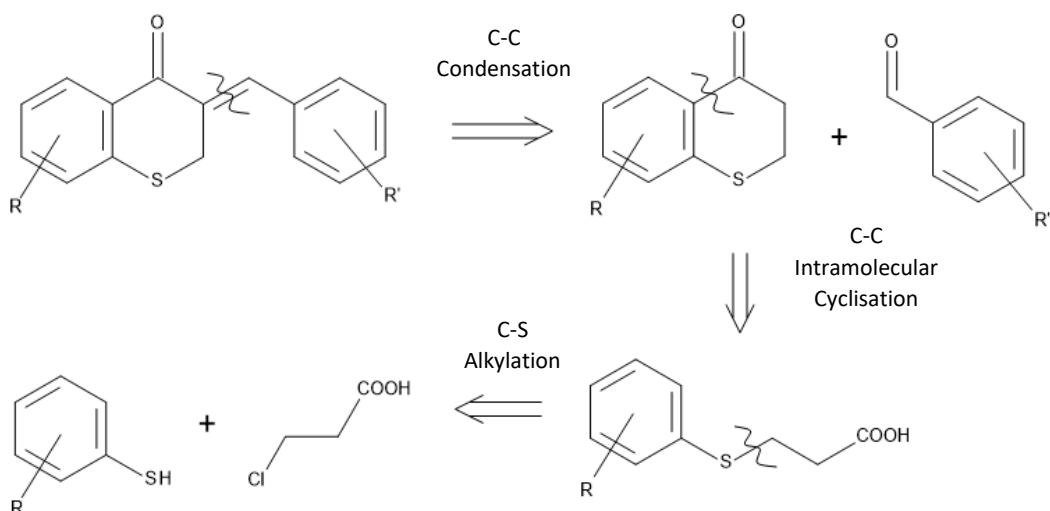
### 3.2.1 Statistical analysis

For the HeLa cell cytotoxicity testing, all compounds at all concentrations (excluding the 1 and 10  $\mu$ M concentration for compound **42**) the P value was found to be <0.05, thus determined as significantly different. For the anti-proliferative activity of the homoisoflavonoids against HREC cells, significance was found for all compounds at concentrations of 10 and 100  $\mu$ M (excluding compound **42** where significance was found only at a concentration of 100  $\mu$ M) due to P values <0.001. For the COX inhibitory testing compounds **34**, **35**, **37**, and **40** exhibited statistically significant differences between the two concentrations for COX-I with P values < 0.05. Compounds **34**, **36**, **37**, and **40** exhibited statistically significant differences between the two concentrations for COX-II with P values <0.05.

## 4.0 Discussion

### 4.1 Chemistry

This chapter highlights the synthetic details of the different steps involved in the synthesis of the sulphur analogues of homoisoflavonoids, each section begins with a brief review of literature pertaining to each step. Finally, the results for each synthetic step are discussed. The retrosynthetic scheme is displayed below (**Scheme 19**).

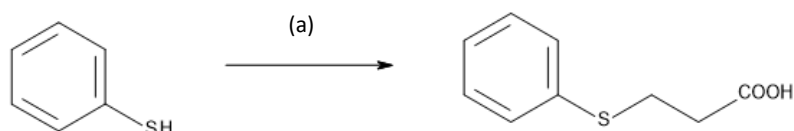


**Scheme 19.** Retrosynthetic analysis of a thio-containing homoisoflavonoid of the sappanin-like structure.

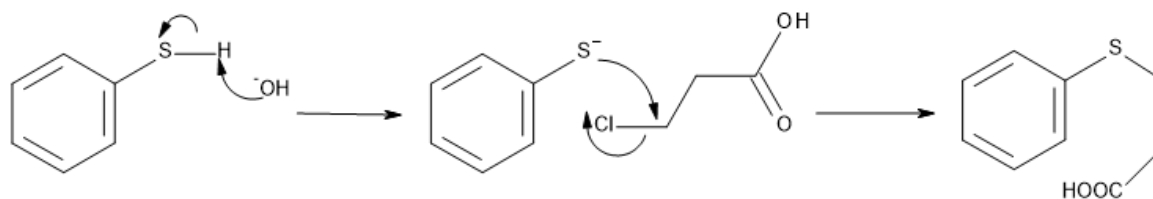
Following the retrosynthetic scheme as shown above in (**Scheme 19**) it was decided that the substituted thiophenol would be an appropriate starting point due to availability and price.

#### 4.1.1 Formation of the phenylsulfanyl propanoic acid

The initial step would be the formation of the phenylsulfanyl propanoic acid via the alkylation of thiophenol <sup>(11)</sup> (**Schemes 20 & 21**).



**Scheme 20.** (a) ClCH<sub>2</sub>CH<sub>2</sub>COOH/NaOH/H<sub>2</sub>O/Reflux 3 hrs.



**Scheme 21.** Base catalysed alkylation reaction between thiophenol and 3-chloropropanoic acid

The alkylation of thiophenol takes place under basic conditions with 3-chloro propanoic acid whilst refluxing for 3 hours. Song *et al*<sup>(11)</sup> achieved a yield of 92-97%. Therefore, following the literature precedent, 4-chloro-thiophenol was refluxed with 3-chloropropanoic acid under basic conditions. After 3 hours the reaction was quenched, producing a white solid – compound **28**, with a yield of 65%. The solids formed, were subjected to NMR spectral analysis, which confirmed the alkylation of the thiophenol via the appearance of two triplets located at  $\delta_{\text{H}}$  3.07 ppm and  $\delta_{\text{H}}$  2.59 ppm (representative of H-2 and H-3 respectively) in the <sup>1</sup>H-NMR spectrum (**A.1.1.1**). The use of HSQC coupled these protons to their respective carbons located at  $\delta_{\text{C}}$  29.1 ppm and  $\delta_{\text{C}}$  34.0 ppm respectively (**A.1.1.4**) and the use of DEPTQ (**A.1.1.2**) confirmed that these protons were indeed CH<sub>2</sub>. These resonances were seen to be coupled in the COSY spectrum (**A.1.1.3**).

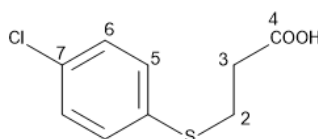
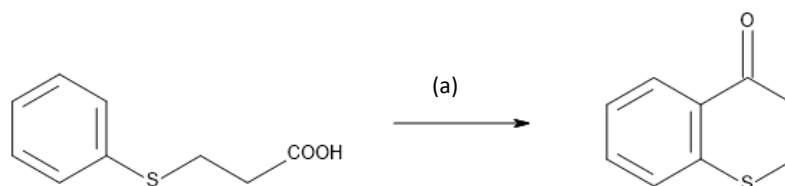


**Figure 21.** Numbered structure of compound **28**

As the reaction proceeded cleanly, the next attempts utilised other substituted thiophenols, namely 4-bromothiophenol and 4-methoxythiophenol. White solids were formed as previously and yields of 91.9% and 97.4% were produced for compounds **29** and **30**. NMR spectral analysis was conducted to ascertain the structural identity of the products and as with the previous product the two triplets (H-2,  $\delta_{\text{H}}$  3.07 ppm and H-3,  $\delta_{\text{H}}$  2.60 ppm for compound **29** (**A.2.1.1**), and H-3,  $\delta_{\text{H}}$  2.53 ppm and H-2,  $\delta_{\text{H}}$  2.96 ppm for compound **30** (**A.3.1.2**)) which are representative of the two CH<sub>2</sub> groups, were located and coupled to their respective carbons in the HSQC spectrum (**A.2.1.4**) (H-2,  $\delta_{\text{H}}$  3.07 ppm coupled to C-2,  $\delta_{\text{C}}$  28.9 ppm and H-3,  $\delta_{\text{H}}$  2.60 ppm coupled to C-3,  $\delta_{\text{C}}$  33.9 ppm) (H-2,  $\delta_{\text{H}}$  2.96 ppm coupled the C-2,  $\delta_{\text{C}}$  30.8 ppm and H-3,  $\delta_{\text{H}}$  2.53 ppm coupled to C-3,  $\delta_{\text{C}}$  34.3 ppm for compound **30**) (**A.3.1.4**). In each case H-2 was coupled to H-3 in the COSY spectrum (**A.2.1.3** & **A.3.1.3**).

#### 4.1.2 Formation of the thiochromanone

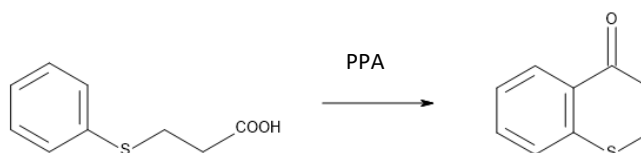
The next step is the formation of the thiochromanone via an intramolecular cyclisation reaction. Following the previous literature by Song *et al*, this reaction can be mediated via sulphuric acid <sup>(11)</sup> (Scheme 22).



Scheme 22. (a) H<sub>2</sub>SO<sub>4</sub> 16 hr mediated intramolecular cyclisation reaction.<sup>10</sup>

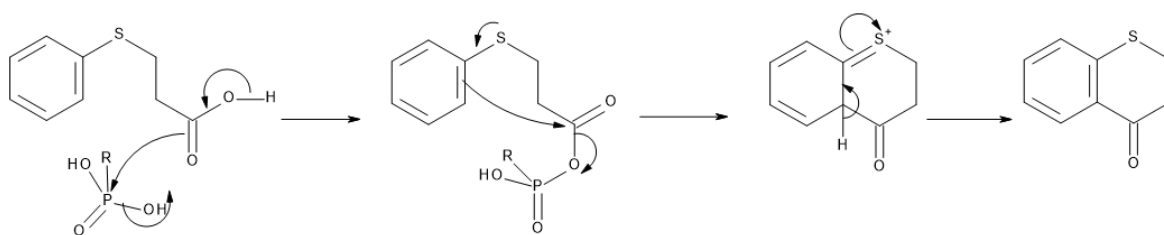
The reaction was quenched after 16 hours and a large amount of white precipitate was expected. However, no solids were produced and analysis via TLC indicated that no products were formed. The reaction was attempted again, however instead of using compound **28**, compound **29** was utilised. Furthermore, the reaction time was increased from 16 hours to 24 hours to allow the reagents more time to react. Again, no precipitate formed. Thus, in an attempt to ascertain whether the electron-withdrawing groups were a reason for the reaction to fail, compound **30** was used. The reaction time was kept at 24 hours. After 24 hours the reaction was worked up and still no product formed.

After the sulphuric acid route seemed to fail for all substrates used, an alternative route was required. Upon searching the literature, a polyphosphoric acid mediated intramolecular cyclisation was found <sup>(48)</sup> (Schemes 23 & 24).



Scheme 23. Polyphosphoric acid mediated intramolecular cyclisation.





**Scheme 24.** Polyphosphoric acid mediated intramolecular cyclisation reaction producing a thiochromanone

Thus, this acid mediated cyclisation was then utilised, initially using compound **30** and after 1 hour, the reaction was quenched and worked up. However, after the removal of solvent under pressure, the reaction yielded 1 % of product. Compound **33** (**Figure 22**) was confirmed via NMR spectral analysis (**A.6.1**), the formation of the heterocyclic ring was established due to the observance of a pair of multiplets (located at  $\delta_{\text{H}}$  2.88 ppm and  $\delta_{\text{H}}$  3.12 ppm representative of H-3 and H-2 respectively) and the loss of the triplets (previously found at  $\delta_{\text{H}}$  2.53 ppm and  $\delta_{\text{H}}$  2.96 ppm) confirmed that the intramolecular cyclisation had been successful. Due to the strained structure, the protons in the heterocyclic ring are found to not be in the same chemical environment and as such, rather than producing the pair of triplets as previously, this produces a multiplet splitting pattern. Furthermore, the intramolecular cyclisation reaction concludes with the loss of a proton from the aromatic ring; which changes the substitution pattern from a symmetrical para splitting to a 1,3,6-trisubstituted arrangement. Thus, resulting in a doublet located at  $\delta_{\text{H}}$  7.09 ppm (H-8, coupled to H-7), a double doublet located at  $\delta_{\text{H}}$  6.92 ppm (H-7, coupled to H-8 and H-5) and a doublet located at  $\delta_{\text{H}}$  7.53 ppm (H-5, coupled to H-7). GCMS was utilised in order to confirm the presence of impurities, by-product or starting materials. The chromatogram (**A.6.3**) of compound **33** provided a single peak that is representative of the product - the methoxy-substituted thiochromanone. The mass spectrum of this compound provided a  $m/z$  ratio of 194 for the  $M^+$  ion, which supports the previous data.

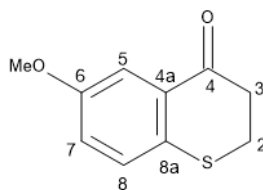


**Figure 22.** Numbered structure of compound **33**.

In an attempt to increase the yield, the reaction was performed again. This time tripling the reaction time to 3 hours produced a yield of 38.7%, effectively tripling the yield. As such, the next attempt utilised compound **29** and the reaction time was increased to 10 hours. Upon NMR spectral analysis, the lack of the characteristic triplets in the aliphatic region suggested that the intramolecular cyclisation had occurred, however, the lack of a multiplet in the aliphatic region further suggested that the unsaturated thiochromanone may have formed. The rest of the  $^1\text{H-NMR}$  (**Figure 24**) is indicative of the occurrence of the intramolecular cyclisation, due to the splitting pattern, lacking the symmetrical appearance of the substituted phenyl sulfanyl propanoic acid instead showing a 1,3,6-trisubstituted splitting pattern. The A - ring, consists of a doublet at  $\delta_{\text{H}}$  8.62 ppm (H-5 coupled to H-7), a double doublet at  $\delta_{\text{H}}$  7.65 ppm (H-7 coupled to H-5 and to H-8), and a doublet at  $\delta_{\text{H}}$  7.43 ppm (H-8 coupled to H-5). The appearance of an extra pair of doublets located at  $\delta_{\text{H}}$  6.97 ppm and  $\delta_{\text{H}}$  7.78 ppm (H-3 and H-2 respectively), alongside the lack of aliphatic signals, further suggests the formation of the unsaturated thiochromanone. The DEPTQ experiment (**Figure 25**) suggests that carbons C-2 and C-3 are only bonded to 1 proton each (H-2 and H-3 respectively) due to the orientation of the peaks associated, also corroborating with the suggestion of the unsaturated thiochromanone (**Figure 23**).

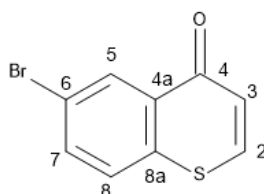


**Figure 23.** Numbered structure of unsaturated thiochromanone **32U**

The increased reaction time compared to the literature precedent from 3 hours to 10 hours could account for this observation.

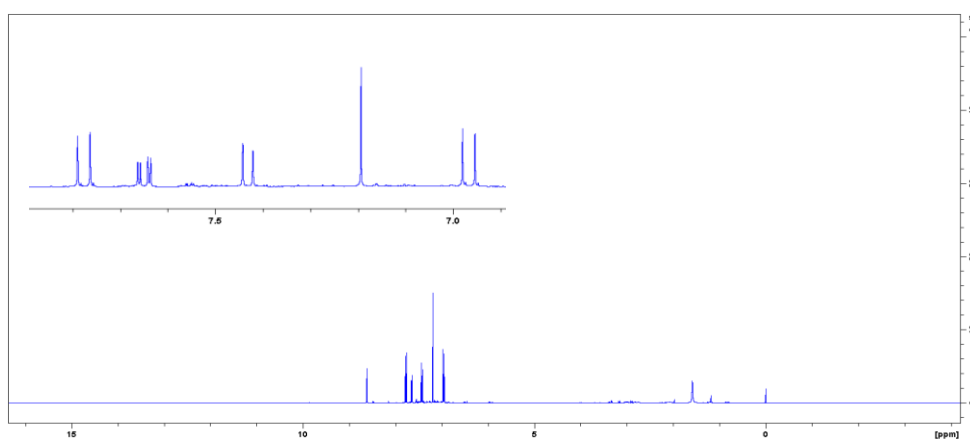


**Figure 24**  $^1\text{H-NMR}$  spectrum of **32U**

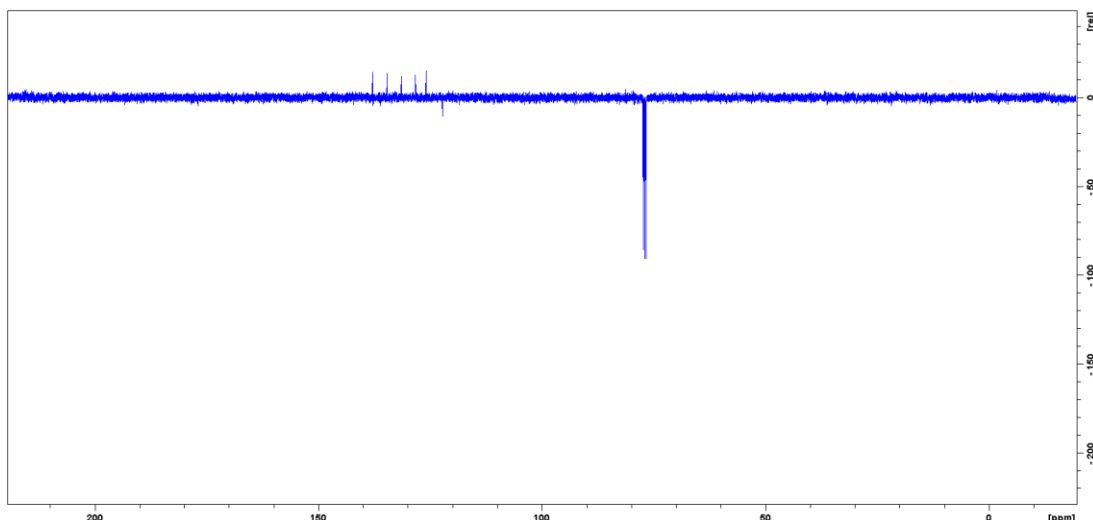


**Figure 25.**  $^{13}\text{C}$ -NMR spectrum of **32U**

As such, the next attempt which utilised compound bromo-**29**, had its reaction time reduced from 10 hours to 3 hours, which was used previously. After 3 hours, the reaction was quenched and a 49.7% crude yield of compound **32** obtained. The product was subjected to  $^1\text{H}$ -NMR spectral analysis (**A.5.1**) and due to the observance of a pair of multiplets (located at  $\delta_{\text{H}}$  2.99 ppm and  $\delta_{\text{H}}$  3.26 ppm representative of H-3 and H-2 respectively and the change in aromatic splitting pattern (from a symmetrical para splitting) to a 1,3,6-trisubstituted pattern thus, resulting in a doublet (H-8, coupled to H-7), a double doublet (H-7, coupled to H-8 and H-5) and a doublet (H-5, coupled to H-7). GCMS analysis of compound **3B** gave two peaks in the chromatogram (**A.5.3**). One of the peaks is representative of compound **32** which shows the isotopic effect of bromine via two peaks of similar height with  $m/z$  ratios of 242 and 244 in the mass spec. The other peak in the chromatogram is representative of a small amount of the unsaturated bromo-substituted thiochromanone as the  $M^+$  peak produced in the mass spec has an  $m/z$  value of 242 factoring the loss of the two protons. Isotopic effects can also be seen in this mass spec via the two peaks of similar height with  $m/z$  values of 240 and 242. The formation of the unsaturated form of compound **32** was unexpected, due to the time differences of the reaction and the amount of product formed, it seems that there is a time dependent competing reaction in which over increased durations of time the **32U** predominates. However this observation was found only when using the bromo substituted thiophenol.

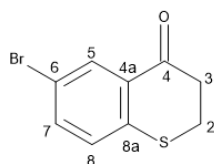


**Figure 26.** Compound **32**

The same procedure was then utilised for compound **28** and a yield of 50.3% was obtained. The product was confirmed via NMR spectral analysis (**A.4.1**), with the same observations found: observance of a pair of multiplets ( $\delta_{\text{H}}$  2.90 ppm and  $\delta_{\text{H}}$  3.17 ppm, representative of H-3 and H-2), the loss of the triplets (previously located at  $\delta_{\text{H}}$  2.59 ppm and  $\delta_{\text{H}}$  3.07 ppm), and the change in aromatic splitting pattern (from the symmetrical para splitting to the 1,3,6-trisubstituted splitting pattern). Thus, resulting in a doublet (H-8, coupled to H-7), a double doublet (H-7, coupled to H-8 and H-5) and a doublet (H-5, coupled to H-7). GCMS analysis of compound 3A gave a chromatogram (**A.4.3**) (with a very large peak and also with a very small peak. The  $M^+$  for the large peak came out at  $m/z$  198 which is what is expected from the target compound. The small peak is representative of the starting material that had not been consumed.

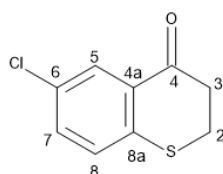
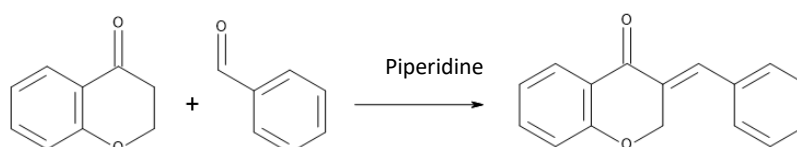


**Figure 27.** Compound **31**

#### 4.1.3 Formation of the homoisoflavonoid

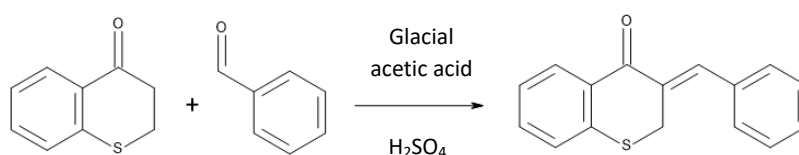
The final step for the formation of the homoisoflavonoid derivative was the condensation of the thiochromanone with a substituted benzaldehyde. From previous literature piperidine has been used as a base to mediate a condensation reaction between a chromanone and a benzaldehyde <sup>(10)</sup> (**Scheme 25**).



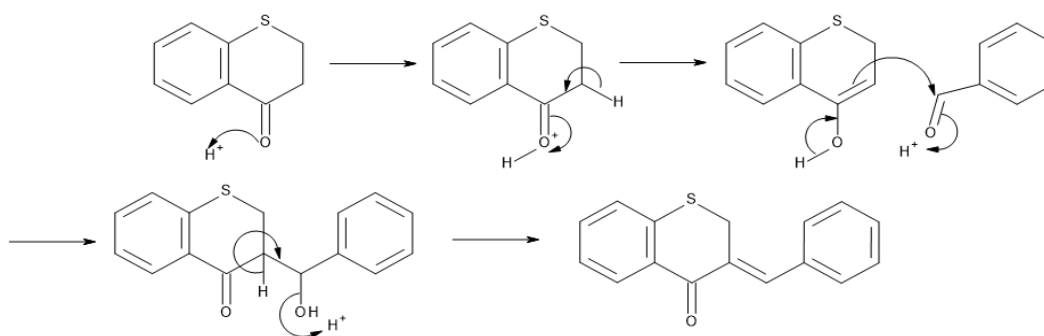
**Scheme 25.** Piperidine mediated condensation of chromanone with benzaldehyde

Due to the similarity of the chromanone and the thiochromanone, it was believed that this reaction should proceed as it would for a chromanone. Thus, the chloro-substituted thiochromanone was used alongside 4-bromobenzaldehyde, the reaction was left for 48 hours as stipulated by the literature<sup>(3)</sup>. However, upon analysis of TLC, there seemed to be no product forming. Thus, after the 48 hours, the reaction was worked up and no product had formed.

Upon returning to the literature, an alternative acid catalysed scheme was found. The procedure reported the use of a mix of sulphuric acid and glacial acetic acid<sup>(49)</sup> (**Schemes 26 & 27**).



**Scheme 26.** Acid catalysed condensation reaction between thiochromanone and benzaldehyde



**Scheme 27.** Acid catalysed condensation reaction between thiochromanone and substituted benzaldehyde producing the homoisoflavonoid derivative

The first of the thiochromanones utilised was compound **32**, and the benzaldehyde used was the 4-bromobenzaldehyde. After 24 hours, a precipitate was expected to form, it did not. However, the procedure instructs to perform a recrystallisation using methanol, therefore, an aliquot of the acidic solution was taken, to which methanol was added. Upon the addition of methanol, fine yellow solids started to appear. NMR spectral analysis (**A.7.1**) confirmed that the condensation reaction had succeeded and the desired product (**Figure 28**) had formed, firstly due to the observation of a broad singlet at  $\delta_{\text{H}}$  7.62 ppm which is representative of H-9. Furthermore, the multiplets that were observed in the previous product (located at  $\delta_{\text{H}}$  2.90 ppm and  $\delta_{\text{H}}$  3.17 ppm) cease to be visible as the protons

which were located at the  $\alpha$ -position had been removed and the carbon at the  $\alpha$ -position is now connected to the aromatic B ring via an olefinic bond. As such, the protons located adjacent to the sulphur, 2H-2 now give rise to a doublet (located at  $\delta_{\text{H}}$  3.99 ppm) with a coupling constant of 1.0 Hz due to long range coupling with H-9. The use of NOESY (A.7.1.6) confirmed the *Z* conformation of the olefinic bond conjoining the heterocyclic C-ring to the aromatic B-ring. Correlations could be seen between 2H-2 and H-2', rather than between 2H-2 and H-9, as would be expected for the *E* conformation. Furthermore, the previous coupling pattern caused by the protons located on the A-ring, namely H-5, H-7, and H-8 was still seen, with a doublet (H-5,  $\delta_{\text{H}}$  8.23 ppm coupled to H-7,  $\delta_{\text{H}}$  7.44 ppm), a double doublet (H-7,  $\delta_{\text{H}}$  7.44 ppm, coupled to H-5,  $\delta_{\text{H}}$  8.23 ppm and to H-8,  $\delta_{\text{H}}$  7.12 ppm), and a doublet (H-8,  $\delta_{\text{H}}$  7.12 ppm, coupled to H-7  $\delta_{\text{H}}$  7.44 ppm). The coupling pattern of the B-ring, agreed with the structure of the product with a pair of doublets representative of H-2' and H-3' located at  $\delta_{\text{H}}$  7.19 ppm and  $\delta_{\text{H}}$  7.51 ppm respectively, consistent with the symmetrical para splitting. The  $^{13}\text{C}$ -NMR spectra (A.7.1.2) agreed with the structure, firstly with the quaternary carbonyl peak C-4 located at  $\delta_{\text{C}}$  184.5 ppm, characteristic of the ketone environment and the C-2 (CH<sub>2</sub> group) located at  $\delta_{\text{C}}$  29.1 ppm. Secondly, the number of carbon environments observed matches with the predicted number of carbon environments of compound **34** as shown in (A.7.1.2). That is: 7 quaternary carbons, 6 CH environments, and 1 CH<sub>2</sub> environment.

The chromatogram produced from GCMS analysis of compound **34** gave rise to one large peak (A.7.2.1). The sole peak gave an M<sup>+</sup> of  $m/z$  410, which coincides with the predicted mass of the target compound. The compound was also subjected to high resolution mass spectrometry (A.7.3) and found an  $m/z$  of 408.8895 with the calculated  $m/z$  of 408.8897, thus agreeing with all other data.

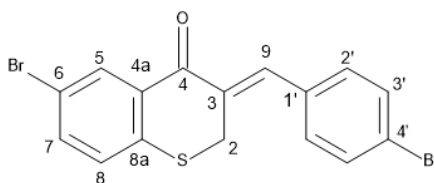


**Figure 28.** Numbered structure for the sulphur analogue compound **34**

The next thiochromanone utilised was compound **31** and the reaction was repeated as above using the 4-bromobenzaldehyde and the product precipitated. The formation of this homoisoflavonoid derivative (**Figure 29**) was confirmed via NMR spectral analysis (**A.8.1**) with similar observations as with the previous homoisoflavonoid. <sup>1</sup>H-NMR spectral analysis afforded a broad singlet located at  $\delta_{\text{H}}$  7.62 ppm, representative of H-9, which is an important observation with regards to the formation of the product as it is a new chemical environment. Furthermore, the disappearance of the pair of multiplets (previously located at  $\delta_{\text{H}}$  2.90 ppm and  $\delta_{\text{H}}$  3.17 ppm), indicates the reaction took place at the predicted location. With the appearance of the doublet represented by the 2H-2 located  $\delta_{\text{H}}$  3.97 ppm as the previous protons adjacent (H-3) have been removed. The splitting pattern of the A-ring (as with compound **34**) remains unchanged with a doublet (H-5 coupled to H-7), a double doublet (H-7 coupled to H-5 and H-8) and a doublet (H-8 coupled to H-7). The splitting pattern of the B-ring is analogous to compound **34**, represented by the pair of doublets of H-2' and H-3' representative of the para splitting pattern. The <sup>13</sup>C-NMR spectra (**A.8.1.2**) also support the structural analysis, with the quaternary carbonyl peak located at  $\delta_{\text{C}}$  184.6 ppm. As well as the correct number of C, CH, and CH<sub>2</sub> environments, respectively (7, 6, and 1). The use of NOESY (**A.8.1.6**) confirmed the Z conformation of the homoisoflavonoid, with correlations seen between the proton located at the H-2 position with the proton located at the 2' position. Furthermore, as single crystal XRD (data located at **A.8.5**) was performed on this compound, this resulted in a definitive structure of this compound and further corroborated the Z conformation desired, GCMS analysis (**A.8.2**) afforded a single peak in the chromatogram. The single peak gave rise to an M<sup>+</sup> of *m/z* 366, which matches the predicted mass of the target compound. Notable fragments being the loss of the bromide ion giving a peak at 285, another notable loss is that of the chloride ion at 250. Another notable peak is the loss of the chloro-substituted thiochromanone leaving the brominated benzylic group and giving rise to a peak at *m/z* 170. The compound was also subjected to high res mass spec (**A.8.3**) and found an *m/z* of 364.9399 with the calculated *m/z* of 364.9043, thus agreeing with all other data.

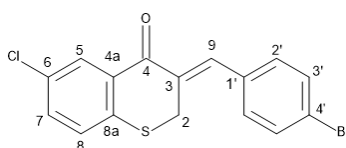


**Figure 29.** Numbered structure Compound **35**

Compound **33** was the next thiochromanone to be used with the 4-bromobenzaldehyde and again the formation of the homoisoflavonoid compound **36** (**Figure 30**) was confirmed via NMR spectral analysis (**A.9.1**). The same previous observations were made i.e. appearance of the broad singlet located at  $\delta_{\text{H}}$  7.60 ppm, characteristic of H-9 of the olefinic bond present. Disappearance of the pair of multiplets (previously located at  $\delta_{\text{H}}$  2.88 ppm and  $\delta_{\text{H}}$  3.12 ppm). The appearance of the doublet represented by 2H-2 found adjacent to the sulphur located at  $\delta_{\text{H}}$  3.96. The A-ring splitting pattern is consistent with the previous two homoisoflavonoids (compounds **34** and **35**) with a doublet (H-5 coupled to H-7), a double doublet (H-7 coupled to H-5 and H-8), and a doublet (H-8 coupled to H-7). The B-ring splitting pattern is also consistent with the previous two homoisoflavonoids (Compounds **34** and **35**) with a pair of doublets, H-2' and H-3' located at  $\delta_{\text{H}}$  7.19 ppm and  $\delta_{\text{H}}$  7.49 ppm respectively. The  $^{13}\text{C}$ -NMR spectra (**A.9.1.2**) also coincided with the previous two homoisoflavonoids, namely the number of carbon environments (7C, 6CH and 1 CH<sub>2</sub>). With the carbonyl peak located at  $\delta_{\text{C}}$  185.6 and the C-2 (CH<sub>2</sub> group) located at  $\delta_{\text{C}}$  29.4. The use of NOESY (**A.9.1.6**) allowed for the Z conformation to be determined due to the correlations seen between the proton located at H-2 and the proton located at the 2' position. The GCMS analysis (**A.9.2**) of compound **36** gave rise to a single peak in the chromatogram. The M<sup>+</sup> peak was  $m/z$  362, which matches the predicted mass of the target compound. Furthermore, another notable peak being the loss of the bromide ion giving an  $m/z$  of 281. The compound was further subjected to high res mass spec (**A.9.3**) and found an  $m/z$  of 360.9896 with the calculated  $m/z$  of 360.9898, thus agreeing with previous data.

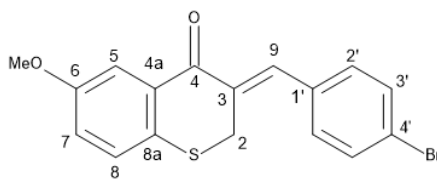
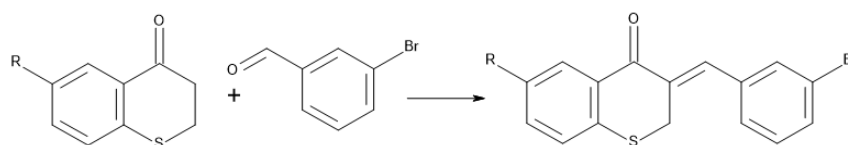


**Figure 30.** Numbered structure of compound **36**



All three thiochromanones were then reacted respectively with a regioisomer of the 4-bromobenzaldehyde, namely the 3-bromobenzaldehyde (**Scheme 28**).



**Scheme 28.** Acid catalysed condensation of thiochromanone and 3-bromobenzaldehyde

The reaction was successful for these three reactions, and the products – compounds **37**, **38**, and **40** (**Figure 31**) were confirmed via NMR spectral analysis (**A. 10.1** for compound **37**, **A.11.1** for compound **38**, and **A.13.1** for compound **40**).  $^1\text{H-NMR}$  analysis gave rise to significant peaks, namely the broad singlets located at  $\delta_{\text{H}}$  7.62 ppm, 7.62 ppm, 7.61 ppm, demonstrating the H-9 proton of compounds **37**, **38**, and **40** respectively. Another important change from the intermediate reactant was the disappearance of the pair of multiplets found in the aromatic regions of each compound, previously located at  $\delta_{\text{H}}$  2.90 ppm and 3.17 ppm,  $\delta_{\text{H}}$  2.90 ppm and 3.17 ppm,  $\delta_{\text{H}}$  2.88 ppm and 3.12 ppm, for the substituted thiochromanones used as the intermediates. These multiplets were replaced with a doublet in each case indicative of H-2 and located at  $\delta_{\text{H}}$  3.99 ppm,  $\delta_{\text{H}}$  3.99 ppm,  $\delta_{\text{H}}$  3.97 ppm for compounds **37**, **38**, and **40** respectively. The A-ring splitting pattern consisted of a doublet (H-5 coupled to H-7), a double doublet (H-7 coupled to H-5 and H-8), and a doublet (H-8 coupled to H-7). Due to overlapping signals from protons in the B-ring, it is difficult to assign specific signals to their corresponding protons, as such the multiplets produced are indicative of multiple environments. The integration also demonstrates the fact that the multiplets consist of multiple overlapping proton environments. From the HSQC, the multiplets can be afforded to multiple carbon signals further corroborating the overlapping signals and their respective carbons. The  $^{13}\text{C-NMR}$  data concurred with the rest of the spectral data. However, due to the overlapping signals from the proton spectra, there was difficulty in assigning some carbon environments as such they are marked as interchangeable as the carbon peaks could be respective of multiple positions around the B-ring. Other notable carbon environments include the C of the carbonyl (C-4) were located at:  $\delta_{\text{C}}$  184.6 ppm,  $\delta_{\text{C}}$  184.4 ppm, and  $\delta_{\text{C}}$  184.7 ppm for compounds **37**, **38**, and **40** respectively. With the  $\text{CH}_2$  group of H-2 being found at:  $\delta_{\text{C}}$  28.9 ppm,  $\delta_{\text{C}}$  29.8 ppm, and  $\delta_{\text{C}}$  29.3 ppm for compounds

**37**, **38**, and **40** respectively. GCMS analysis of each of these three compounds gave rise to single peaks in each of their chromatograms. Furthermore, the  $M^+$  for each of these peaks came out at  $m/z$  410, 366 and 362 for compounds **37** (**A.10.2**), **38** (**A.11.2**), and **40** (**A.13.2**) respectively. Each of these masses matches the predicted mass for the target compounds. All three compounds were subjected to HRESMS which found  $m/z$  values of 408.8896, 364.9400, and 360.9897 for compounds **37** (**A.10.3**), **38** (**A.11.3**), and **40** (**A.13.3**) respectively, with calculated  $m/z$  values of 408.8897, 364.9403, and 360.9898 respectively. The HRESMS supports the previous data regarding the characterisation of these compounds.

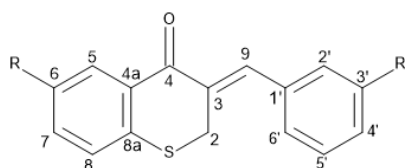
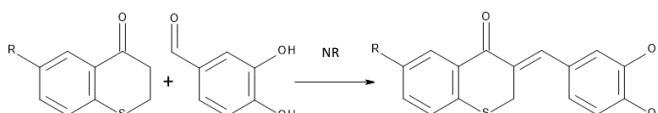


**Figure 31.** Numbered structure for homoisoflavonoids **37**, **38**, and **40**  
**(37)** R = R' = Br  
**(38)** R = Cl, R' = Br  
**(40)** R = OMe, R' = Br

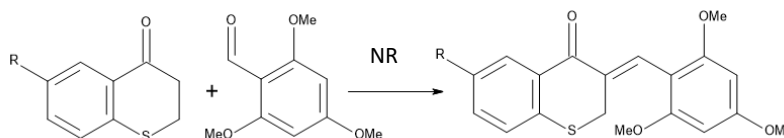
The next benzaldehyde to be employed was the protocatechuic aldehyde, which rather than being an electron-withdrawing substituent (as is the case with the bromo-group); is instead an electron donating substituent and also more closely resembles the natural product like homoisoflavonoids.



**Scheme 29.** Acid catalysed condensation of thiochromanone and protocatechuic aldehyde. NR = No reaction  
The reaction (**Scheme 29**) was performed as the previous reactions were. However, no product was formed for any of the three thiochromanones. A potential reason could be the effect of the electronic differences between the electron withdrawing groups used previously and the electron donating hydroxyl groups used here. As the electron donating groups may reduce the electrophilicity of the carbonyl group of the benzaldehyde and as such, reduce the likelihood of a successful reaction. A potential development could be the use of a Lewis acid catalyst which may aid in activating the carbonyl for nucleophilic attack. An alternative attempt at improving the reaction could be via the use of the base mediated condensation reaction in which piperidine is used, this reaction proceeds via the

enamine intermediate rather than the enol intermediate and as such this may improve the success of the nucleophilic attack on the carbonyl.

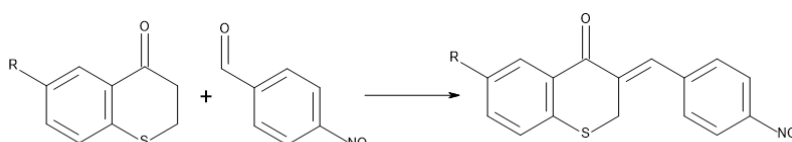
Thus, a weaker electron donating group was utilised in the form of a differing benzaldehyde, namely the 2,4,6-trimethoxybenzaldehyde.



**Scheme 30.** Acid catalysed condensation between thiochromanone and 2,4,6-trimethoxybenzaldehyde. NR = No reaction

The reactions (**Scheme 30**) were performed for all of the three thiochromanones and as with the protocatechuic aldehyde, no products were formed. The acidic reaction conditions used again did not seem to be compatible with the electron-donating groups located on the benzaldehyde, thus alternative routes to assist the condensation reaction are required. As mentioned previously, the use of a Lewis acid catalyst or the route of the enolate intermediate via base catalysis may be preferable.

As such, the next benzaldehyde applied was the 4-nitrobenzaldehyde. Only the methoxy-thiochromanone and the bromo-thiochromanone were attempted due to a lack of materials. The reactions (**Scheme 31**) were performed as previously and both homoisoflavonoids were produced in the form of yellow solids.



**Scheme 31.** Acid catalysed condensation between thiochromanone and 4-nitrobenzaldehyde

**(42)** R = Br  
**(43)** R = OMe

The nitro group is a particularly strong electron-withdrawing group and within twenty minutes of reaction time the product had already precipitated without the need for the addition of methanol. This corroborates with the suggestion that the reaction conditions favour electron-withdrawing substituents. The two homoisoflavonoids – compounds **42** and **43** (**Figure 32**) were confirmed due to NMR spectral analysis (**A.15.1** for compound **42** & **A.16.1** for compound **43**). As previously the significant indicators being the appearance of the singlet representative of H-9 found on the olefinic

bond with chemical shifts of  $\delta_{\text{H}}$  7.72 ppm and  $\delta_{\text{H}}$  7.67 ppm for compounds **42** and **43** respectively. The disappearance of the pair of multiplets due to the removal of the alpha protons (previously located at  $\delta_{\text{H}}$  2.90 ppm, 3.17 ppm and  $\delta_{\text{H}}$  2.88 ppm, 3.12 ppm for compounds **42** and **43** respectively). The appearance of a doublet representative of H-2 adjacent to the sulphur (located at  $\delta_{\text{H}}$  4.27 ppm and 3.94 ppm for compounds **42** and **43** respectively). The A-ring splitting pattern was consistent with compounds **34**, **35**, and **36**, with a doublet (H-5 coupled to H-7) a double doublet (H-7 coupled to H-5 and H-8) and a doublet (H-8 coupled to H-7). The B-ring splitting pattern also coincides with compounds **34**, **35**, and **36** with the symmetrical para splitting caused by protons H-2' and H-3' located at  $\delta_{\text{H}}$  8.32 ppm and  $\delta_{\text{H}}$  7.81 ppm for compound **42** and  $\delta_{\text{H}}$  8.23 ppm and  $\delta_{\text{H}}$  7.48 ppm for compound **43**. Both **42** (**A.15.3**) and **43** (**A.16.3**) were subjected to HRESMS, which found  $m/z$  values of 375.9640 and 328.0644 respectively, with calculated  $m/z$  values of 375.9643 and 328.0644.

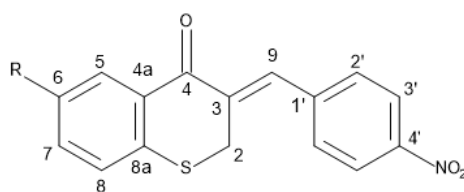


**Figure 32.** Numbered structure of nitro-containing homoisoflavonoids.  
**(42)** R = Br  
**(43)** R = OMe

The last two attempts both utilised the compound **32**, along with 4-fluorobenzaldehyde and 4-chlorobenzaldehyde. The reactions were repeated as previously. Compound **39** (**Figure 33**), when subjected to NMR analysis (**A.12.1**), gave similar results to the other para-substituted benzaldehydes (**34**, **35**, **36**, **42**, and **43**), with the broad singlet representative of H-9 located on the olefinic bond found at  $\delta_{\text{H}}$  7.65 ppm. Furthermore, the disappearance of the two multiplets (previously located at  $\delta_{\text{H}}$  2.90 ppm and  $\delta_{\text{H}}$  3.17 ppm). The appearance of the doublet at  $\delta_{\text{H}}$  3.99 ppm; representative of H-2 adjacent to the sulphur. The A-ring splitting pattern is also consistent with compounds **34**, **35**, and **36**, with the observation of a doublet (H-5 coupled to H-7), a double doublet (H-7 coupled to H-5 and H-8), and a doublet (H-8 coupled to H-7). The B-ring splitting corroborated with the splitting pattern of **34**, **35**, and **36**, with a pair of doublets (H-2' and H-3' located at  $\delta_{\text{H}}$  7.35 ppm and 7.25 ppm respectively). The  $^{13}\text{C}$ -NMR further coincided with the spectral characterisation, namely due to the number of corresponding peaks. Such as, the carbonyl of C-4 located at  $\delta_{\text{C}}$  184.3 ppm and the  $\text{CH}_2$

group of H-2 located at  $\delta_c$  29.1 ppm. GCMS analysis (**A.12.2**) of compound **39** gave rise to one peak in the chromatogram. The  $M^+$  ion was found at  $m/z$  366, which matches the predicted mass of the target compound. Compound **39** was subjected to HRESMS (**A.12.3**) which found an  $m/z$  value of 364.9398 with a calculated  $m/z$  value of 364.9403 thus, supporting other data with respect to the formation of compound **39**.

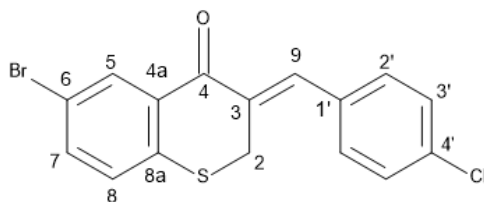


**Figure 33.** Compound **39** with numbered structure

Compound **41** (**Figure 34**) also gave similar spectroscopic (**A.14.1**) results to the previous para-substituted homoisoflavonoids (compounds **34**, **35**, **36**, **39**, **42**, and **43**), with the broad singlet of H-9 (located at  $\delta_H$  7.77 ppm), the disappearance of the multiplets (previously located at  $\delta_H$  2.90 ppm and 3.17 ppm) and appearance of the doublet representative of H-2 located at  $\delta_H$  4.10.

The A-ring produced analogous results to the previous para-substituted homoisoflavonoids (compounds **34**, **35**, **36**, **39**, **42**, and **43**), with a doublet (H-5 coupled to H-7), a double doublet (H-7 coupled to H-5 and H-8), and a doublet (H-8 couple to H-5). However, one key difference observed in the B-ring was due to the fluorine atom possessing a nuclear spin of  $\frac{1}{2}$ , it acts in a similar fashion to a proton - which also possesses a nuclear spin of  $\frac{1}{2}$ . As such, this causes the splitting pattern of the aromatic B ring to differ from the previous homoisoflavonoids and produces a triplet located at  $\delta_H$  7.16 ppm representative of H-3', as well as a double doublet located at  $\delta_H$  7.41 ppm representative of H-2'. The  $^{13}C$ -NMR further aided in the elucidation of the structural identity of **41** with the C-4 carbonyl peak located  $\delta_c$  184.6 ppm and the  $CH_2$  group of C-2 located at  $\delta_c$  29.1 ppm. Due to the presence of the fluorinated B-ring, there is also coupling between the C-4' and the fluorine observed in the  $^{13}C$ -NMR spectra (located **A.14.1.2**) and located at  $\delta_c$  164.2 ppm ( $J = 244.9$  Hz) and further coupling between the C-3' and the fluorine located at  $\delta_c$  116.2 ppm ( $J = 21.8$  Hz).

GCMS analysis (**A.14.2**) of compound **41** gave rise to a single peak in the gas chromatogram suggestive of a single compound. The  $M^+$  ion produced was  $m/z$  350 which matches the predicted mass of the target compound. Compound **41** was also subjected to HRESMS (**A.14.3**) in which an  $m/z$  value of

348.9695 and a calculated value of 348.9698, thus supporting previous data on the formation of the product.

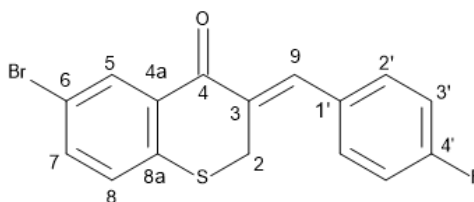


**Figure 34.** Numbered structure of compound **41**

## 4.2 Biological discussion

### 4.2.1 Anti-proliferative activity of HRECs and ARPE-19 cells via alamarBlue assay

The anti-proliferative testing was performed at the Glick Eye Institute, University of Indiana by Timothy Corson's research group. Initially all compounds were tested against the human retinal endothelial cell line (HREC) to determine the anti-angiogenic activities via the anti-proliferative effects of the synthesised compounds. Retinal vasculature functions are controlled by Müller cells, microglia, endothelial cells and the balance of positive and negative factors of regulation. When this balance is altered this can produce various angiogenesis associated eye diseases, including diabetic retinopathy, and age-related macular degeneration <sup>(50)</sup>. Environmental signals received from the angiogenic endothelial cells allow for the proliferation, migration, and the avoidance of apoptosis <sup>(51)</sup>.

All compounds were tested at concentrations of 0.1 nM, 1nM, 0.01  $\mu$ M, 0.1  $\mu$ M, 1  $\mu$ M, 100  $\mu$ M. Compounds **35** and **38** are regioisomers of one another. Both contain the chloride moiety located at the C6 position of the A ring, whilst differing with the location of the bromide motif on the B ring. In compound **35** the bromide is located at the 4' position and in compound **38** the bromide is located at the 3' position. This singular change (from the 4' to the 3') reduces the GI<sub>50</sub> by almost three-fold (from 11.2  $\mu$ M to 4.22  $\mu$ M) (GI<sub>50</sub> curve for compound **35** found at **A.8.5.2.2**, GI<sub>50</sub> curve for compound **38** found at **A.11.5.2.2**). Thus, initial observation suggests the 3' position potentially being significant with respect to the anti-proliferative activity on the HREC cell line.

Compound **34** is analogous to compound **35** with the exception of **34** bearing a bromide group situated on the A-ring rather than the chloride group found in **35**. Compound **37** is analogous with **38**, again with the exception of **37** bearing a bromide group on the A-ring rather than the chloride group. As such, **34** and **37** are regioisomers of one another. The slight structural difference between **34** and **37** bears a more significant difference between the GI<sub>50</sub> values for both compounds. With **34** bearing a GI<sub>50</sub> value of 17.8 μM (GI<sub>50</sub> curve located at **A.7.5.2.2**), whilst **37** bore a GI<sub>50</sub> value of 10.3 μM (GI<sub>50</sub> curve located at **A.10.5.2.2**). The potentiation of the activity of compound **37** compared with **34** further suggests the significance of the 3' position with regards to anti-proliferative activity. Furthermore, the modification of the A-ring to bear the chloride substituent was found to increase the activity when compared to when the A-ring bears the bromide substituent demonstrated by the GI<sub>50</sub> values of the above compounds.

Compound **36** and **40** bear the same A-ring (methoxy located at the C-6 position) and bear a regioisomeric relationship with regards to the bromide substituent located on the B-ring, namely the 4' position and the 3' position. In compound **36** where the bromide moiety resides at the 4' position, this resulted in a GI<sub>50</sub> value of 4.06 μM (GI<sub>50</sub> curve located at **A.9.5.2.2**) compared to a GI<sub>50</sub> value of 3.07 μM of compound **40** (GI<sub>50</sub> curve located at **A.13.5.2.2**), where the bromide resides at the 3' position. As with the above compounds, the positional change of the substituents from the 4' position to the 3' position resulted in a more active effect demonstrated by the reduction of the GI<sub>50</sub> value.

The compounds which bear a methoxy moiety located on the A-ring at the C6 position were found to be more active than the compounds bearing the halogenated substituents on the A-ring, thus suggesting the relationship of OMe > Cl > Br with respect to the anti-proliferative activity.

Compounds **42** and **43** bore nitrated B-rings located at the 4' position. The difference between these two compounds being that **42** contains a bromide group at the C-6 position and **43** contains a methoxy group located at the C6 position. The change in substituent here had a noteworthy change in the activity of the compound. **42** bore a GI<sub>50</sub> value > 100 μM (GI<sub>50</sub> curve located at **A.15.5.2.2**), whilst **43** bore a GI<sub>50</sub> value of 33.70 μM (GI<sub>50</sub> curve located at **A.16.5.2.2**). This suggests a potential improvement

that the methoxy group located at the C-6 position provides. Furthermore, the nitro containing B-ring compounds **42** and **43** resulted in the least active anti-proliferative effect of all the homoisoflavonoids described in this study.

Compounds **39** and **41** differ only in that, at the 4' position **39** contains a chloride group, whereas in **41** there is a fluoride group located at this position. This change in halogen causes a pronounced difference in activity, with **41** bearing a GI<sub>50</sub> value of 3.65 μM (GI<sub>50</sub> curve located at **A.14.5.2.2**) and **39** bearing a GI<sub>50</sub> value of 15.70 μM (GI<sub>50</sub> located at **A.12.5.2.2**). In order to ascertain whether the increase in activity is caused by the change in halogen, further fluorinated analogues are required, preferably one containing the methoxy group situated at the C6 position and the fluoride group situated at the 3' position.

In order to ascertain whether the synthesised compounds acted specifically against HREC cells, the homoisoflavonoids were also tested against normal cell types, the compounds were also tested against the human retinal pigment epithelial cell line (ARPE-19), a non-target ocular cell type. These cells have multiple functions, they are responsible for the development and maintenance of adjacent photoreceptors, as well as being involved in the transportation of nutrients, and formation of the blood-retinal barrier<sup>(52)</sup>. This cell line was tested to determine the selectivity of the synthesised compounds as activity against the HREC cell type is highly desirable, with activity against normal cell types being undesirable. All compounds were tested at concentrations of 0.1 nM, 1nM, 0.01 μM, 0.1 μM, 1 μM, 100 μM. All the compounds tested afforded a lack of anti-proliferative activity against this cell line at concentrations up to 100 μM (all compounds GI<sub>50</sub> > 100 μM with GI<sub>50</sub> curves for compounds **34**, **35**, **36**, **37**, **38**, **39**, **40**, **41**, **42** and **43** located at **A.7.5.2.4**, **A.8.5.2.4**, **A.9.5.2.4**, **A.10.5.2.4**, **A.11.5.2.4**, **A.12.5.2.4**, **A.13.5.2.4**, **A.14.5.2.4**, **A.15.5.2.4**, **A.16.5.2.4** respectively). This lack of activity against ARPE-19 demonstrated the selectivity of the sulphur analogues of homoisoflavonoids with respect to their anti-proliferative activity.



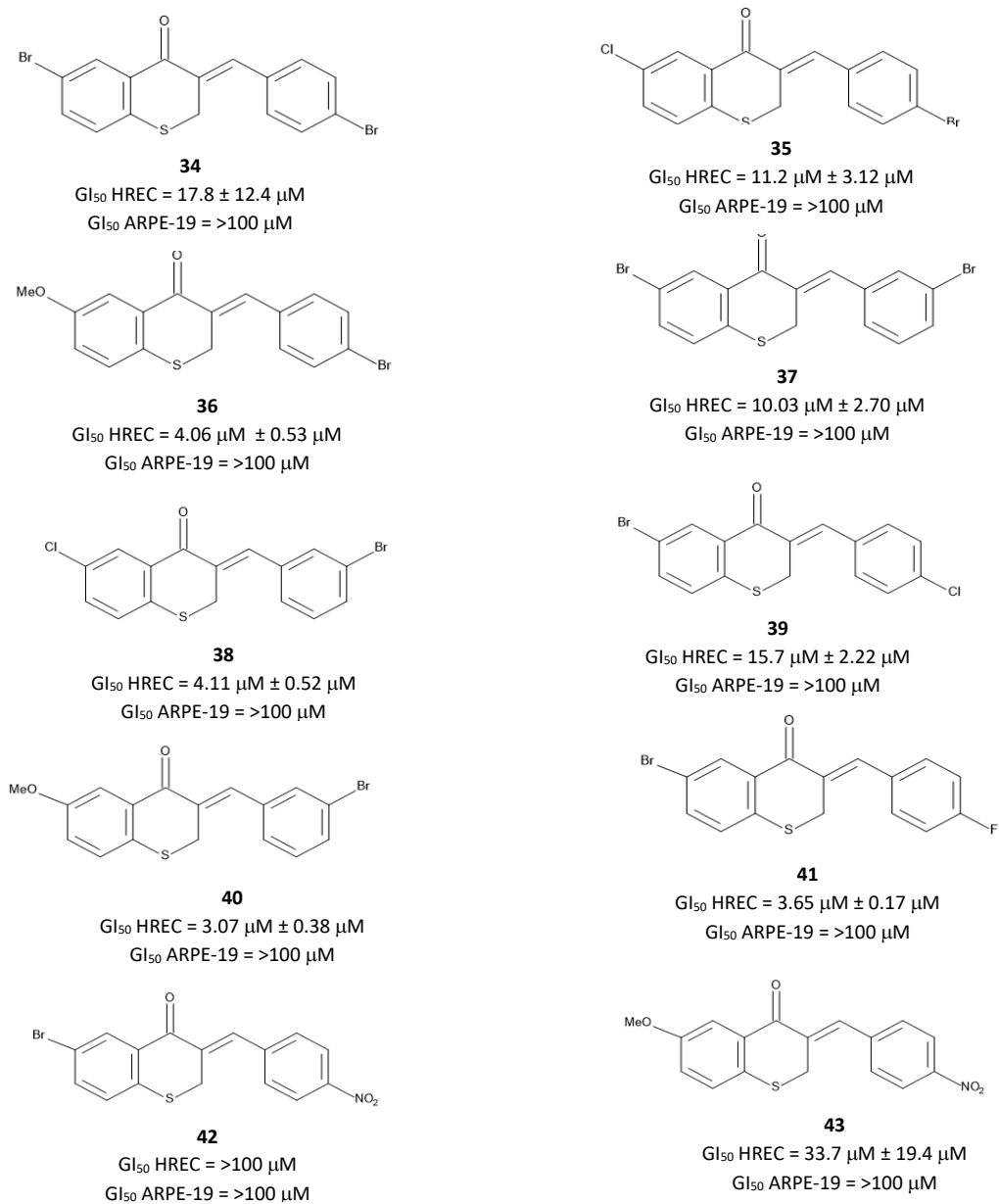


**Figure 35.** GI<sub>50</sub> values for synthesised homoisoflavonoids for cell lines HREC and ARPE-19

Previous studies investigating the anti-angiogenic activity of natural and synthetic oxygenated homoisoflavonoid analogues provide comparable activity against the HREC cell line <sup>(53)</sup>. The homoisoflavonoid analogues investigated by Schwikkard *et al*, gave a range of GI<sub>50</sub> activities between  $2.3 \times 10^{-4}$   $\mu\text{M}$  and  $>100$   $\mu\text{M}$ . The most active homoisoflavonoid analogue (the chromane depicted in **Figure 36**) bore a GI<sub>50</sub> of  $2.3 \times 10^{-4}$   $\mu\text{M}$ , demonstrating very strong anti-proliferative activity against the HREC cell type. However, this compound also demonstrated strong anti-proliferative activity against the non-target ocular cell type ARPE-19, with a GI<sub>50</sub> value of  $3.4 \times 10^{-4}$   $\mu\text{M}$ . Due to the activity afforded with this compound, it lacks the highly desirable selectivity aspect.

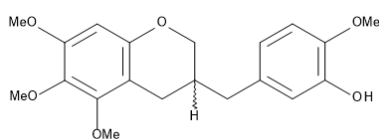


**Figure 36.** Chromane analogue of homoisoflavonoid

However, the chromanone analogue of this compound (**Figure 37**) bore a GI<sub>50</sub> value of 0.035  $\mu\text{M}$  against the HREC cell type, with a GI<sub>50</sub> value of  $>100$   $\mu\text{M}$  against ARPE-19, thus demonstrative strong anti-proliferative activity and a high selectivity against the HREC.

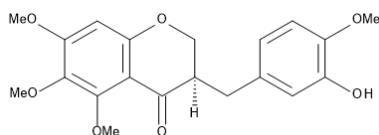


**Figure 37.** Chromanone analogue of chromane homoisoflavonoid

Other homoisoflavonoid analogues and their GI<sub>50</sub> values for both HREC and ARPE-19 are depicted in **Figure 38**. From the activities against HREC it seems to be that, increasing the number of methoxy groups in the A-ring from two to three also increases the anti-proliferative activity. Thus, from the results of investigation into the sulphur analogues of the homoisoflavonoids where it appears that the methoxy containing A-ring provided improved activity against HREC, cells it is possible that increasing the number of methoxy substituents on the A-ring could also potentiate their activity against the HREC cell type.

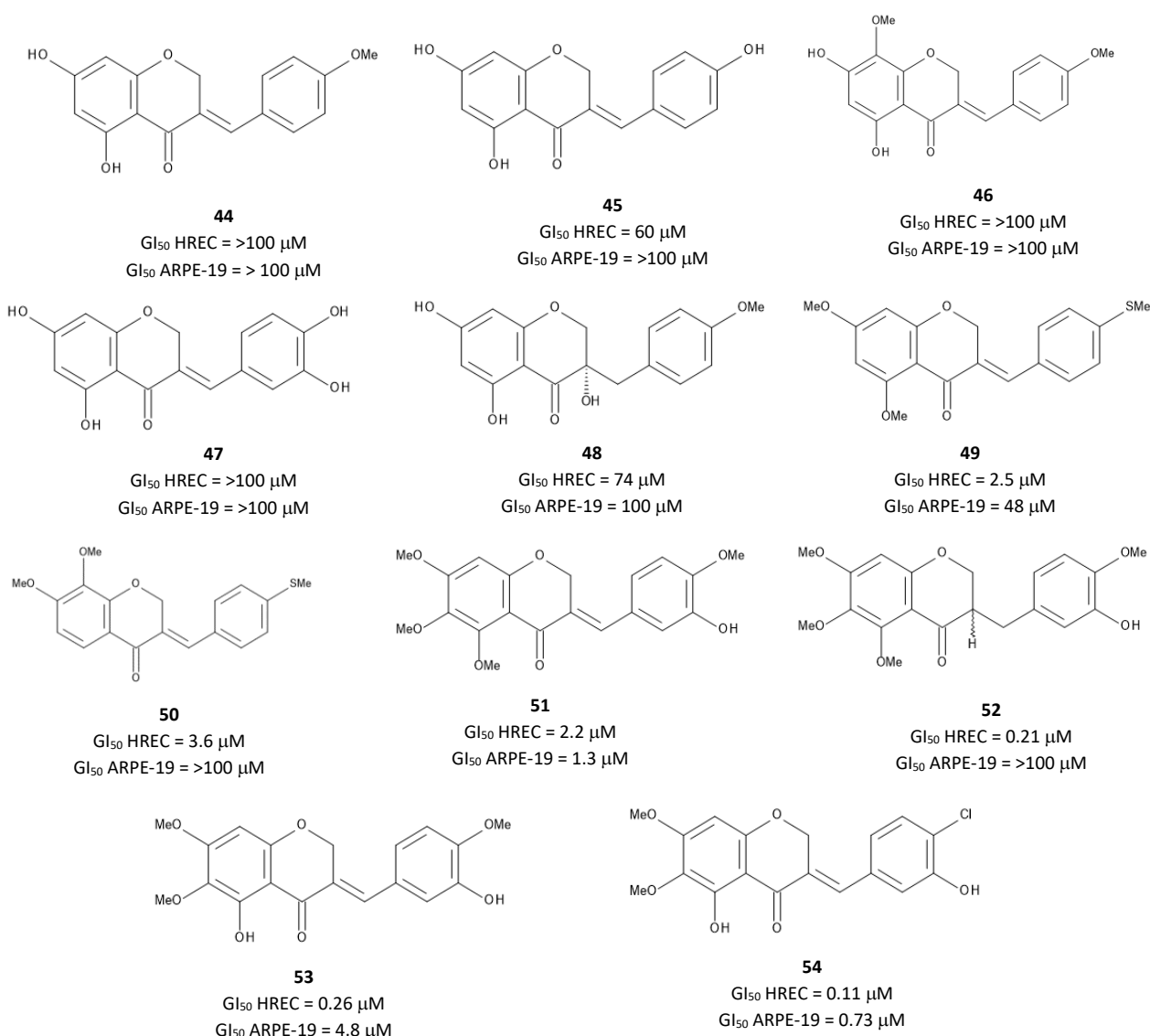


**Figure 38.** Oxygen analogues of homoisoflavonoids and their respective GI<sub>50</sub> values for HREC and ARPE-19

The compounds with their A-ring bearing multiple methoxy groups (compounds **49**, **50**, **51**, **52**, **53**, and **54**) demonstrated strong activity. When a hydroxyl group is substituted for the methoxy group located at the 5 position (in compounds **53** and **54**), the activity is increased slightly. However many of the multiply methoxy-substituted homoisoflavonoids lacked specificity for the HREC cells. However, when comparing two homoisoflavonoids containing identical A and B-rings (compounds **51** and **52**) (**Figure 38**), there is a vast change in the selectivity, which can only be attributable to the singular change in the compound structure i.e. the reduction of the olefinic moiety that connects the B-ring to the C-ring. This change in structure produces a profound effect, via the change in activity for the ARPE-19 cells, from a  $GI_{50}$  value of 4.8  $\mu\text{M}$  to  $>100 \mu\text{M}$ .

Furthermore, when comparing the two homoisoflavonoids with identical B-rings, the difference in activity can be observed due to the positioning of the A-ring substituents, producing a significant increase in selectivity via a reduction in activity against the ARPE-19 cells with a  $GI_{50}$  value changing from 48  $\mu\text{M}$  to  $>100 \mu\text{M}$ .

#### 4.2.2 Cytotoxicity to HeLa cells via a neutral red assay

The cytotoxicity of the synthesised compounds was measured via the neutral red assay against cervical cancer cell line - HeLa, a non-ocular cancerous cell type. All compounds were tested at concentrations of 100  $\mu\text{M}$ , 30  $\mu\text{M}$ , 10  $\mu\text{M}$ , and 1  $\mu\text{M}$ .

Compounds **35** and **38** are regioisomers of one another, both bearing the chloride moiety located at the C-6 position of the A-ring. The B-ring of these two compounds differ with the located of the bromide motif. In **35**, the bromide atom is located at the 4' position, and in **38** the bromide atom is located at the 3' position. The change in position from 4' to 3' resulted in a reduction of  $\text{IC}_{50}$  from 22.69 ( $\text{IC}_{50}$  curve located at **A.8.5.1.2**) to 19.73  $\mu\text{M}$  ( $\text{IC}_{50}$  curve located at **A.11.5.1.2**). As with the anti-proliferative activities, the change in position from 4' to 3', produces an increase in activity, thus suggesting the 3' position is important for activity, both cytotoxic and anti-proliferative.

Compound **34** is analogous with compound **35** with the difference being that in **34** there is a bromide located on the A-ring rather than the chloride group found in **35**. Similarly, **37** is analogous to **38**, with the difference being that there is a bromide group located on the A-ring rather than the chloride group found previously. The change of location of the bromide group from 4' to 3' produced similar results to the change of location of the bromide species previously shown. The repositioning from 4' to 3' reduced the  $\text{IC}_{50}$  from 22.03  $\mu\text{M}$  ( $\text{IC}_{50}$  curve located at **A.7.5.1.2**) to 18.93  $\mu\text{M}$  ( $\text{IC}_{50}$  curve located at **A.10.5.1.2**), further suggesting the importance of the 3' position with respect to activity. As seen with the anti-proliferative activity, the change of halogen from bromide to chloride also potentiated the activity.

Compounds **36** and **40** both bear the methoxy substituted A-ring at the C-6 position and bear a regioisomeric relationship regarding the bromide substituent located on the B-ring i.e. the 4' position and the 3' position. The change of position of the bromide group from the 4' position to the 3' position reduced the  $\text{IC}_{50}$  from 17.33  $\mu\text{M}$  ( $\text{IC}_{50}$  curve located at **A.9.5.1.2**) to 12.65  $\mu\text{M}$  ( $\text{IC}_{50}$  curve located at **A.13.5.1.2**). As with the previous two pairs of compounds, the change in position from the 4' to the 3' potentiates the cytotoxic abilities of the compounds.

Compounds **42** and **43**, contain a nitrated B-ring, the nitro group is located at the 4' position in each case. The difference between the two compounds being the A-ring substituent (position C-6), a methoxy group in the case of compound **43** and a bromide group in the case of compound **42**. The change in A-ring substituent resulted in a prominent difference with regards to cytotoxic effects. In the bromide bearing A-ring of the homoisoflavonoid **42** the IC<sub>50</sub> value was >100 μM (IC<sub>50</sub> located at **A.15.5.1.2**). In the methoxy bearing A-ring of compound **43**, the IC<sub>50</sub> value was 59.46 μM (IC<sub>50</sub> located at **A.16.5.1.2**). This change from bromide to methoxy almost produces a two-fold increase with regards to cytotoxic effect.

Compounds **39** and **41** differ only in the B-ring substituent. In compound **39** the B-ring bears a bromide group located at the 4' position, and in compound **41** the substituent at the same position is the fluoride group. The change of halogen species (from bromide to fluoride) resulted in an evident increase of activity with **39** affording an IC<sub>50</sub> of 30.32 μM (IC<sub>50</sub> curve located at **A.12.5.1.2**) and **41** affording an IC<sub>50</sub> of 6.08 μM (IC<sub>50</sub> located at **A.14.5.1.2**). In order to ascertain the effect of the modification of halogenated species, further fluorinated compounds are required to be synthesised and tested.

From the cytotoxicity studies conducted here, there seems to be a similar relationship between A-ring substituents and the biological activities. In methoxy bearing A-ring compounds there was a noticeable increase in activity when compared to the chlorine and bromine bearing A-ring compounds. Thus, a potential relationship with regards to cytotoxic abilities is suggested of OMe > Cl > Br. Furthermore, due to the increase in activity observed from the change in position of the B-ring substituent, there also appears a relationship with regards to the position of the B-ring substituent and the cytotoxic ability, namely the 3' > 4'.

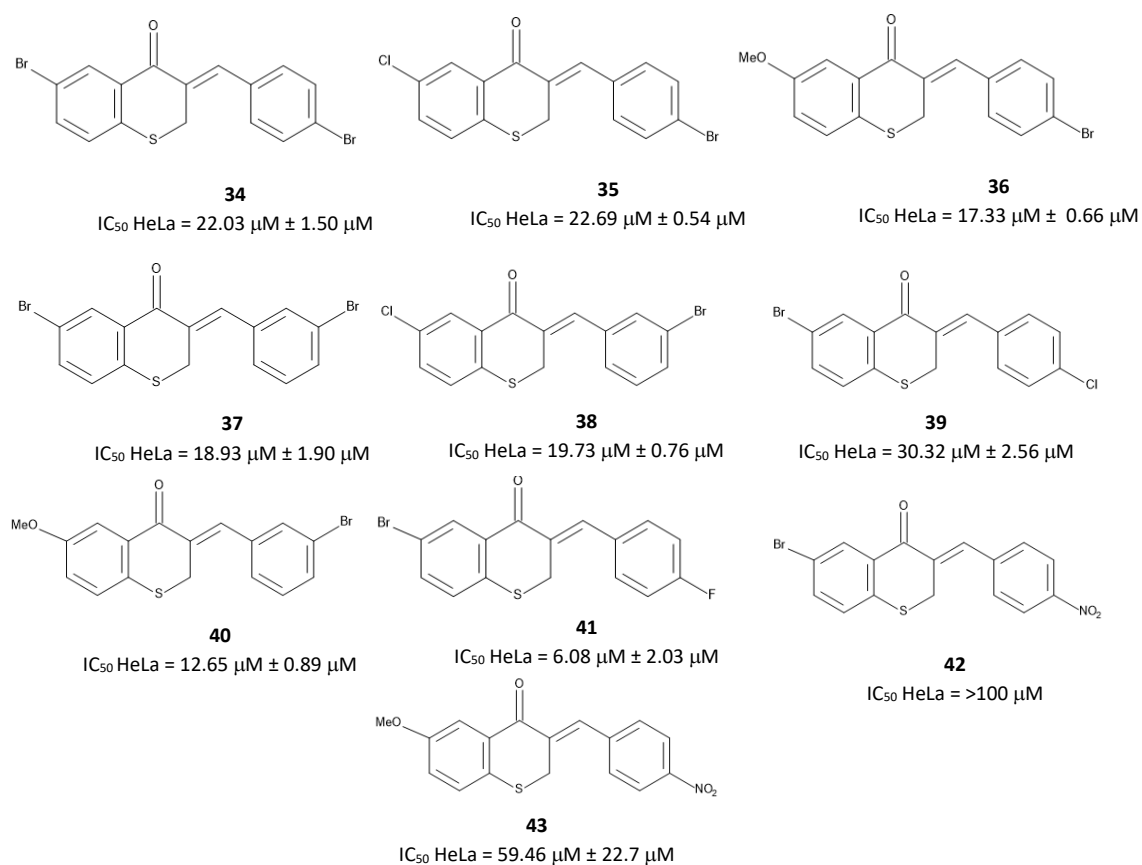


**Figure 39.** Synthesised sulphur analogues of homoisoflavonoids and their respective IC<sub>50</sub> values against Hela cells.

A similar study conducted by Simon *et al* <sup>(54)</sup>, various oxygenated analogues of homoisoflavonoids were synthesised and tested for their cytotoxic abilities against HeLa cells. This resulted in comparable IC<sub>50</sub> values to the IC<sub>50</sub> values produced in this study. 15 homoisoflavonoids were synthesised with IC<sub>50</sub> values ranging between 20.45 μM to >100 μM.

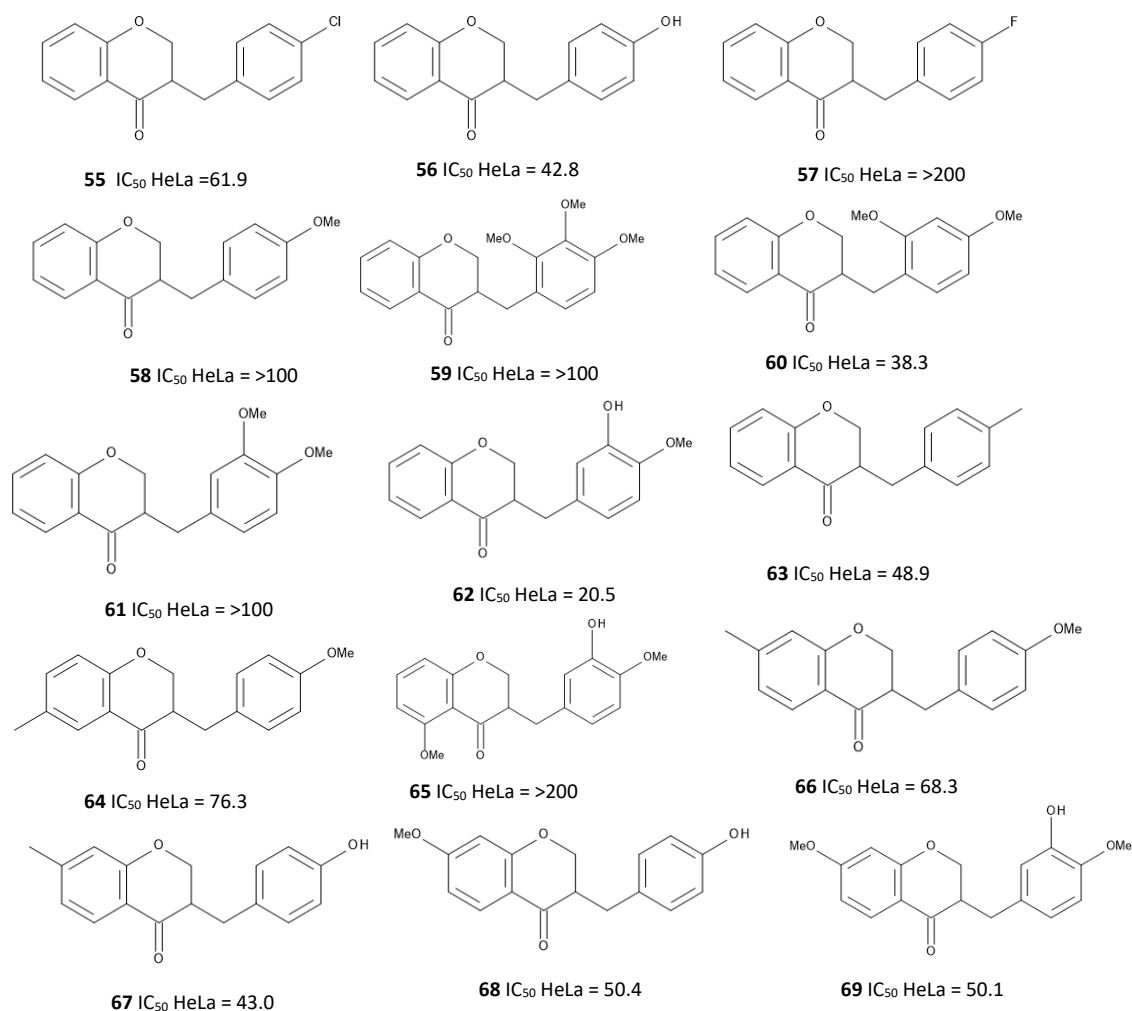


**Figure 40.** Oxygenated homoisoflavonoids and their respective IC<sub>50</sub> values against HeLa cells (IC<sub>50</sub> values in μM)

The study above looked primarily at modifying the B-ring. Compound **57** bears similarities to the compound **41** with identical B-rings. These two compounds differ in that in the A-ring of **41** also contains a bromide motif, compound **41** also contains an olefinic bond conjoining the B-ring to the heterocyclic C-ring, and the heterocyclic C-ring bears a sulphur atom rather than an oxygen atom. In compound **57**, the IC<sub>50</sub> value was reported as >200 μM. Whereas **41** bears an IC<sub>50</sub> of 6.6 μM. Compound **55** from the study above reported an IC<sub>50</sub> value of 61.9 μM. Compound **39** bears similarities



to compound **55**; both bearing the same B-ring whilst differing with the olefinic bond found in **39** and the A-ring bromide substituent found in **39**, as well as the presence of a sulphur atom in the heterocyclic C-ring. These modifications lead to an increase in cytotoxic activity from the reported IC50 value of 61.9  $\mu$ M to 29.8  $\mu$ M.

#### 4.2.3 COX inhibitory activity

Initially, all synthesised homoisoflavonoids were tested for their inhibitory activity against the COX enzyme. The six most promising candidates from the preliminary testing were then subsequently repeated for an N = 2. All compounds tested demonstrated stronger inhibitory activity against COX-I, rather than COX-II. Compounds **38** and **40** displayed the greatest selectivity for COX-I, with percent inhibitions of 27.5% and 24.3% respectively at a concentration of 4.35 nM. These two compounds exhibited zero activity against COX-II at the two concentrations tested. Compound **37** demonstrated the greatest COX-II inhibitory activity at the two concentrations tested. At 4.35 nM the percent inhibition was 22.7% and at the lower concentration of 2.18 nM, the percent inhibition produced was 6.61%. However, this compound lacked selectivity due to also inhibiting COX-I. At the two concentrations tested, 4.35 nM and 2.18 nM, COX-I was inhibited by compound **37** by 31.3% and 5.65% respectively. At a concentration of 4.35 nM the next three homoisoflavonoids tested: **34**, **35**, and **36** gave percent inhibitions of 26.2%, 34.3 %, and 28.7% respectively against COX-I. These compounds also exhibited weak COX-II inhibitory activity with percent inhibitions of 9.41%, 3.48%, and 7.84% respectively.

Compounds **37**, **38**, and **40** show differences in their structures of the substitution found in the A-ring. In compound **37** the A-ring contains the bromide moiety, in compound **38**, the A-ring contains the chloride moiety and in compound **40**, the A-ring contains the methoxy moiety. The change of substituent of the A-ring produces a strong difference in the percent inhibition of COX-II, with compounds **38** and **40** displaying zero activity at the two concentrations tested. Compound **37** (containing the bromide motif located on the A-ring) demonstrated COX-II inhibition suggesting the importance of the A-ring substituent with regards to inhibitory activity. Compounds **34** and **37** are

regioisomers of one another, differing with the location of the B-ring substituent from the 4' position (in compound **34**) to the 3' position (in compound **37**). This change in position of the substituent shows no clear improvement or deterioration with regards to COX-I inhibitory activity. However, the change in position of substituent (to the 3' position) produces an increased COX-II inhibitory effect, suggesting an importance of this position for COX-II inhibitory activity. Likewise, compounds **35** and **38** are also regioisomers of one another, with the difference being the location of the bromide substituent on the B-ring. In compound **35** the bromide substituent is located at the 4' position and in compound **38** the bromide substituent is located at the 3' position. This change in position produces no clear improvement or deterioration with regards to COX-I inhibitory activity. However, the change of location of the substituent (to the 3') position produces a stronger COX-II inhibitory effect, thus contradicting the statement found with the change of position and its effect mentioned above in the case of compounds **34** and **37**. This suggests, that there is more involved than just the position of the substituents. As such, further studies are required to determine the IC<sub>50</sub> of each homoisoflavonoid produced, which provides a better comparison of the compounds rather than the inhibitory activity found at a single concentration. This would be produced via repeating the previous testing but rather than testing at two concentrations, a minimum of four concentrations should be tested. This will allow for a dose-response curve to be produced and IC<sub>50</sub> values to be calculated.

A previous study <sup>(55)</sup> conducted investigating the COX inhibitory activity of homoisoflavonoids (containing the oxygen heterocyclic C-ring analogue) have shown the compounds to be moderately active at 10 μM. Compound **70** (**Figure 41**) demonstrated the strongest activity with regards to COX-II inhibitory activity with 100% inhibition. Furthermore, this compound also demonstrated strong selectivity with COX-I being inhibited by only 26.2%. Other homoisoflavonoids (**Figure 41**) investigated in this study, produced stronger COX-I inhibition than COX-II inhibition. Compounds **71** and **72** exhibited 100% inhibitory activity against COX-II and displayed 43% and 46% inhibition of COX-I respectively, at a concentration of 10 μM. Compound **73** is structurally similar to compound **72**, with the key difference being the substituent modification of the B-ring. In compound **72** the B-ring contains the catecholic moiety, and in compound **73** the hydroxy group located at the 3' position has

been substituted for a hydrogen atom. This B-ring modification produces a strong change in the activity of the compound. Specifically, the alteration causes a decrease in inhibitory activity against COX-II, with a percent inhibition of 26.8%. Furthermore, the compound lacks any activity against COX-I therefore increasing selectivity. As seen with these examples, small structural modifications produce large variations in the activity of the compound as well as the selectivity of the compound.

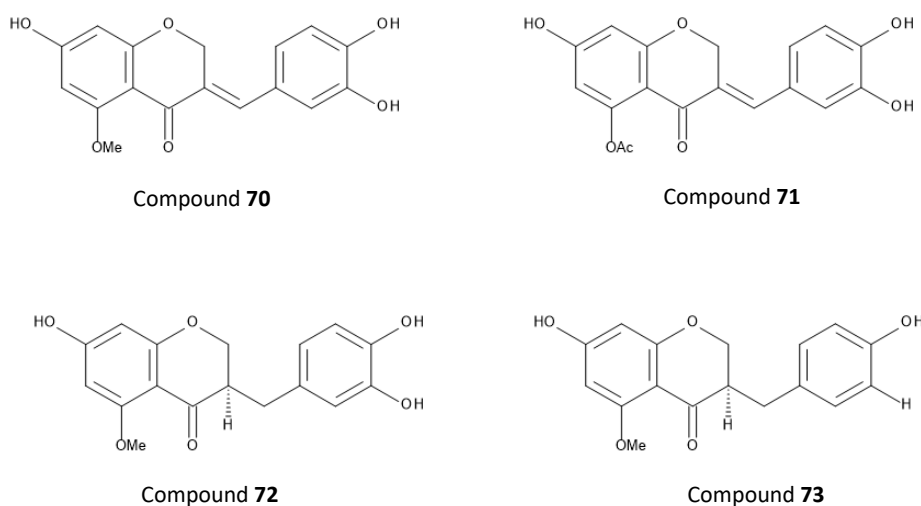
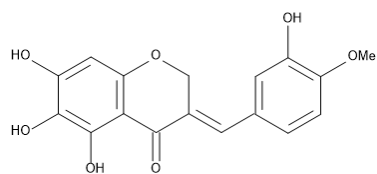
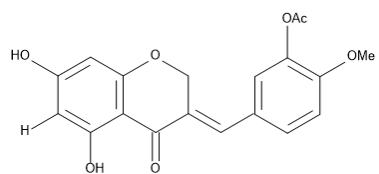


**Figure 41.** Homoisoflavonoids with COX inhibitory activity

A similar study <sup>(56)</sup> which the COX-II inhibitory activity of homoisoflavonoids (oxygen analogues) isolated from three *Rhodocodon* species was investigated, produced active species. Two homoisoflavonoids (**Figure 42**) were tested for their COX-II inhibitory activity at a concentration of 12.5  $\mu$ M. Compounds **74** and **75** from the study exhibited COX-II percent inhibition of 20% and 11% respectively. These compounds provide comparable activity to the compounds **36** and **37** analysed in this project, 13.5% and 22.7% respectively. Compounds **36** and **37** provide slightly greater activity compared to the two homoisoflavonoids investigated by Schwikkard *et al* <sup>(56)</sup>, with a major difference being the concentrations tested. Compounds **36** and **37** were tested at a concentration of 4.35 nM, nevertheless providing COX-II inhibitory activity akin to the study above, at a lower concentration.



Compound **74**



Compound **75**

**Figure 42.** Homoisoflavonoids isolated from three *Rhodocodon* species with COX inhibitory activity

From the results of the COX inhibitory assay, it is clear that the compounds synthesised in this project produce COX inhibitory effects, however they lack the specificity desired. Thus, in order to determine what structural changes of the sulphur homoisoflavonoids may produce an increase in activity and selectivity, further investigation is required. This investigation may proceed via further analysis of other sulphur containing homoisoflavonoids to determine whether a specific position or moiety may aid in producing the desired effect of inhibition the preferred enzyme selectively, as well as potentiating the inhibitory ability.

## 5.0 Conclusion

A total of ten sulphur analogues of homoisoflavonoids were synthesised and characterised. All ten were tested for their anti-proliferative effects against two cells lines of HREC and ARPE-19. Against the HREC cells, nine of the ten homoisoflavonoids demonstrated moderate anti-proliferative abilities ( $P < 0.001$  relative to negative control) with compound **40** demonstrating the strongest anti-proliferative effect with a  $GI_{50}$  of  $3.07 \mu\text{M}$ . Against the ARPE-19 cells all the homoisoflavonoids exhibited  $GI_{50}$  values  $>100 \mu\text{M}$  thus demonstrating the strong selectivity of the sulphur analogues of homoisoflavonoids for the HREC over the ARPE-19 cells. All ten compounds were tested for their cytotoxic effects against the HeLa cell line. Nine of the ten homoisoflavonoids demonstrated weak to moderate cytotoxic effects ( $P < 0.001$  relative to negative control) with compound **41** demonstrating the strongest cytotoxic effects, with an  $IC_{50}$  of  $6.08 \mu\text{M}$ . Five of the ten homoisoflavonoids were tested for their selective COX activity ( $N = 2$ ), with compound **37** demonstrating the strongest COX-II inhibitory effect with 22.7 percent inhibition at a concentration of  $4.35 \text{ nM}$ . Compound **35** demonstrated the strongest COX-I inhibitory effect with 34.3 percent inhibition at a concentration of  $4.35 \text{ nM}$ . All five homoisoflavonoids screened for their COX inhibitory activity lacked the preferential selectivity of COX-II inhibition due to COX-I inhibition occurring simultaneously.

The results of this project highlight the potential of the sulphur analogues of homoisoflavonoids to act as anti-angiogenic agents due to their moderate anti-proliferative effects as well as the strong selectivity demonstrated. Furthermore, the project highlights the potential of the sulphur analogues to act as anti-cancer agents due to the weak to moderate cytotoxic effects against human cervical carcinoma cells. However to be sure of such potential, their cytotoxicity against non-cancer cell lines needs to be determined (although their lack of an anti-proliferative effect against the ARPE cell line suggests they may be selectively cytotoxic to cancer cells. Finally, this project demonstrate the COX inhibitory activity of the sulphur analogues of the homoisoflavonoids, however, a lack of selectivity of COX-II inhibition was observed and as such reduces the therapeutic use of these compounds to act as anti-inflammatory agents.

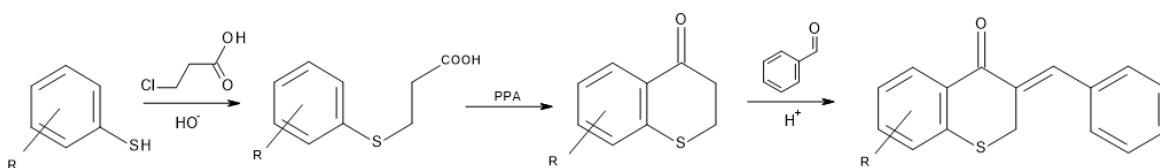
Further investigation is required in order to optimise and improve the biological effects of the sulphur analogues of the homoisoflavonoids.

## 6.0 Future works

There are numerous ways to further investigate the sulphur analogues of homoisoflavonoids. Firstly, via the production of multiple analogues of the compounds previously made, including regioisomers of compounds that have previously shown to be active with respect to the biological activities studied in this project, as well as incorporating similar motifs that have shown to be active in previous studies. Secondly, via further investigation into the biological activities (cytotoxic and anti-proliferative effects) exhibited by the sulphur analogues of the homoisoflavonoids, specifically the cell lines/types on which the homoisoflavonoids are to be tested on, this may include HUVECs (human umbilical vein endothelial cells) which would allow contrast between the HREC and HUVEc cells to determine the specificity of the homoisoflavonoids against different endothelial cells. Furthermore due to the possible anti-angiogenic effects of the homoisoflavonoids on ocular cells and their implication in eye related diseases including wet AMD <sup>(17)</sup> it is logical to test these compounds against eye cell lines such as 92-1 and Y-79. 92-1 is a human uveal melanoma cell type and Y-79 is a line of human retinoblastoma cells. Both of these cell types are cancerous forms and due to the cytotoxic effects of the homoisoflavonoids against HeLa cells (cervical cancer cells) and due to the anti-proliferative effects against the HREC cells it is possible for the homoisoflavonoids to show cytotoxic and anti-proliferative effects against the two eye cancer cell lines. Additional investigation into antiangiogenic activity may be explored by use of in vivo matrigel plug angiogenesis assay, which may allow for the inhibition of neovascularisation to be determined.

Further exploration into inhibition of cyclooxygenase would also be beneficial to the continued investigation of the homoisoflavonoids. This may proceed via testing all the homoisoflavonoids made for their COX inhibition activity, as well as testing at a minimum of 4 concentrations to allow for dose-response curves to be formed and IC<sub>50</sub> values to be calculated. This would allow the comparison of the homoisoflavonoids to other known COX inhibitors to understand their relative activity. Also investigating the homoisoflavonoids effect on COX within cell lines known to express COX-I and COX-II via western blotting would provide further insight into their therapeutic potential.

Further structural modifications and analogues will allow additional information with regards to structural activity relationships of the homoisoflavonoids and their biological activities. There are various ways to incorporate structural modifications and analogues of the previously synthesised homoisoflavonoids, one being via the use of alternative starting materials namely; alternative thiophenols. There are many different thiophenols available, meaning that this would allow a vast collection of analogues to be produced via these means. Previous studies investigating the anti-proliferative abilities of the oxygen analogue of homoisoflavonoids have shown that multiple methoxy groups in the A-ring increases the activity with respect to anti-proliferation<sup>(53)</sup>. The results of this project also suggest that homoisoflavonoids with A-rings containing a methoxy group are more active when compared to the halogenated analogues (chloride/bromide). Thus, one major structural modification would be in the incorporation of a 3,4-dimethoxythiophenol or a 2,5-dimethoxythiophenol as a starting material. This would produce homoisoflavonoids (**Scheme 32**) with multiple methoxy groups in the A-ring and could potentiate the anti-proliferative effects.

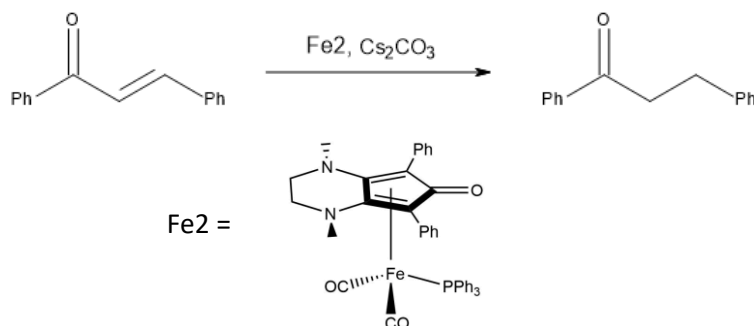


**Scheme 32.** Synthetic scheme for the production of homoisoflavonoids containing multiple methoxy groups situated on the A-ring. Where R = 3,4-dimethoxy/2,5-dimethoxy.

Another way to incorporate structural modifications would be via the condensation step with benzaldehyde. This step allows for functionality due to the functional groups situated on the aromatic ring of the benzaldehyde analogues. From the data reported in this project, incorporation of the fluoro-containing B-ring is advantageous over its halogenated sisters and as such, producing regioisomers of the fluorinated B-ring would produce analogues that may have increased activity and in turn provide more information about the structural activity relationship with regards to the anti-proliferative effects. This may allow a deeper understanding into the importance of specific regions of the homoisoflavonoids and how this affects their anti-proliferative effects. Regioisomers of the 4-fluoro benzaldehyde i.e. the 3-fluorobenzaldehyde or the 2-fluorobenzaldehyde will aid in ascertaining positional importance. Another possibility would be via the use of 4-(trifluoromethyl)-

benzaldehyde which is an analogue of benzaldehyde containing 3-fluoro groups connected to a single carbon attached to the aromatic ring. The trifluoromethyl motif is found in various medicinal compounds <sup>(57)</sup>, most notably found in celecoxib - a non-steroidal anti-inflammatory drug known to be a COX inhibitor. This motif also provides increased lipophilicity and due to its highly electronegative behaviour it has a much more dramatic effect on the electronic characteristics of the aromatic ring.

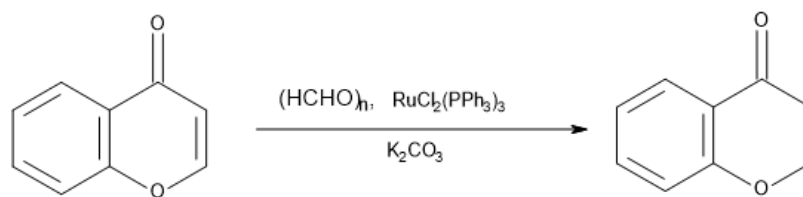
Another, structural modification would be via the reduction of functional groups of the homoisoflavonoid. Specifically the olefinic moiety connecting the B-ring to the C-ring. This can be done chemoselectively, i.e. reducing one of the substituents preferentially over the other, or both motifs can be reduced. Reducing the olefinic moiety would give rise to compounds of the 3-benzyl-4-thiochromanone like homoisoflavonoids. The oxygen analogues of this type of homoisoflavonoid have also demonstrated anti-proliferative abilities <sup>(53)</sup>, thus in order to ascertain whether this would have a significant effect on the sulphur analogues various compounds containing the reduced olefin are required. There are various ways to chemoselectively reduce the olefinic moiety, one being via the use of an iron catalyst <sup>(58)</sup> (**Scheme 33**). This reduction allows for a moderate yield of 51%.



**Scheme 33.** Iron catalysed chemoselective reduction of olefinic moiety in the presence of a carbonyl group

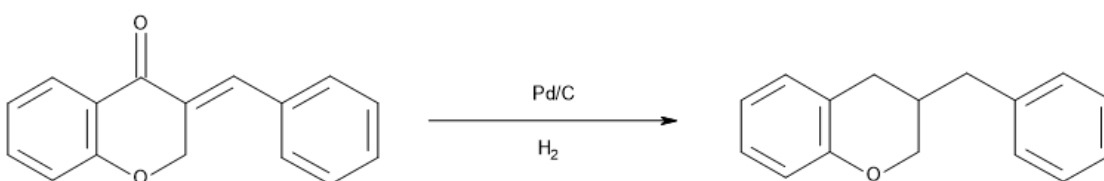
An alternative method <sup>(59)</sup> of the chemoselective reduction of the olefin of an  $\alpha$ ,  $\beta$ -unsaturated carbonyl would be via the use of  $\text{RuCl}_2(\text{PPh}_3)_3$  as a catalyst (**Scheme 34**). The use of this catalyst allows for a very high percentage conversion, and in the case of this study, a 91% conversion was observed.





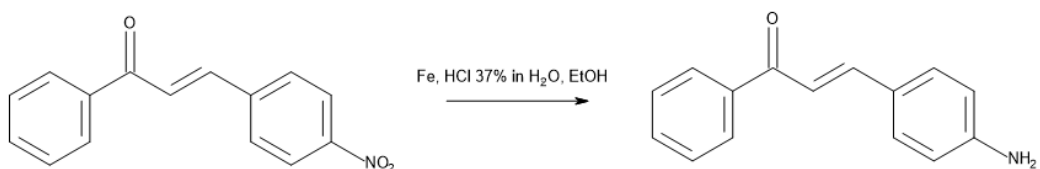
**Scheme 34.** Ruthenium catalysed chemoselective reduction of olefinic moiety in the presence of a carbonyl group

It is also possible to reduce both the carbonyl and the olefin of the  $\alpha,\beta$ -unsaturated system, to produce a thiochromane motif. The oxygen analogues of the chromane have demonstrated strong anti-proliferative abilities as seen in the study conducted by Schwikkard *et al* <sup>(53)</sup>. Thus, in order to determine whether this analogous reduction of the homoisoflavonoid would provide an improvement with regards to anti-proliferative effects, the total reduction would be desired. This reduction has been performed on the oxygen analogues previously <sup>(53)</sup> (**Scheme 35**), using Pd/C and due to the analogous structure of the sulphur analogous one may surmise that this method can be used here.



**Scheme 35.** Palladium catalysed reduction of  $\alpha, \beta$ -unsaturated system

As all the compounds synthesised in this project contain electron withdrawing substituents located on the B-ring, one way to introduce an electron donating group would be via the reduction of the nitro containing homoisoflavonoids. This would convert the nitro group to an amine group thus producing the electron donating substituent of the B-ring, whilst also allowing further modifications to be made. One way of chemoselectively reducing the aromatic nitro group could potentially be done via the use of iron with HCl whilst refluxing in ethanol <sup>(60)</sup> (**Scheme 36**). Thus, could be suitable for the reduction of the aromatic nitro containing homoisoflavonoids.



**Scheme 36.** Chemo selective reduction of aromatic nitro group in the presence of  $\alpha, \beta$  unsaturated system

Once reduced to the amine, this would allow the further modifications to be made subsequently. Potential modifications could be via the formation of amides or imines. An inspiration for the formation of the sulphonamide motif is due to the highly active and selective COX-II inhibitor known as NS-398 (**Figure 43**)<sup>(61)</sup>. As NS-398 is extremely active and selective, it is plausible to investigate whether the sulphonamide motif could potentiate the homoisoflavonoids synthesised in this project.

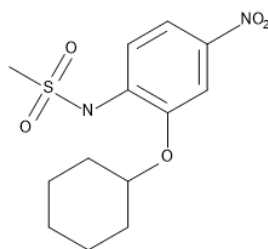


**Figure 43.** Selective COX-II inhibitor NS-398 containing the sulphonamide moiety

## 7.0 References

1. Dewick P. Medicinal Natural Products. 3rd ed. 2009. 60 p. Chichester: Wiley & Sons
2. Böhler P, Tamm C. The homo-isoflavones, a new class of natural product. Isolation and structure of eucomin and eucomol. *Tetrahedron Lett.* 1967 Jan;8(36):3479–83.
3. Yu Y-C, Zhu S, Lu X-W, Wu Y, Liu B. Enantioselective Synthesis of Four Natural Homoisoflavonoids. *European J Org Chem.* 2015 Aug;2015(22):4964–72.
4. Lin L-G, Liu Q-Y, Ye Y. Naturally Occurring Homoisoflavonoids and Their Pharmacological Activities. *Planta Med.* 2014 Aug 25;80(13):1053–66.
5. du Toit K, Drewes SE, Bodenstein J. The chemical structures, plant origins, ethnobotany and biological activities of homoisoflavanones. *Nat Prod Res.* 2010 Mar 20;24(5):457–90.
6. Grisebach H. The flavonoids, advances in research since 1980. *Trends Biochem Sci.* 1989 Jun;14(6):242.
7. Dewick PM. Biosynthesis of the 3-benzylchroman-4-one eucomin. *J Chem Soc Chem Commun.* 1973;(13):438.
8. Dewick PM. Biosynthesis of the 3-benzylchroman-4-one eucomin in *Eucomis bicolor*. *Phytochemistry.* 1975 Apr;14(4):983–8.
9. Parkas L, Gottsegen A, Nógrádi M. The synthesis of eucomin and (±)-eucomol. *Tetrahedron.* 1970 Jan;26(11):2787–90.
10. Shaikh MM, Kruger HG, Bodenstein J, Smith P, du Toit K. Anti-inflammatory activities of selected synthetic homoisoflavanones. *Nat Prod Res.* 2012 Aug;26(16):1473–82.
11. Song Y-L, Wu F, Zhang C-C, Liang G-C, Zhou G, Yu J-J. Ionic liquid catalyzed synthesis of 2-(indole-3-yl)-thiochroman-4-ones and their novel antifungal activities. *Bioorg Med Chem Lett.* 2015 Jan;25(2):259–61.
12. Takao K, Yamashita M, Yashiro A, Sugita Y. Synthesis and Biological Evaluation of 3-Benzylidene-4-chromanone Derivatives as Free Radical Scavengers and  $\alpha$ -Glucosidase

- Inhibitors. *Chem Pharm Bull* (Tokyo). 2016;64(8):1203–7.
13. Foroumadi A, Samzadeh-Kermani A, Emami S, Dehghan G, Sorkhi M, Arabsorkhi F, et al. Synthesis and antioxidant properties of substituted 3-benzylidene-7-alkoxychroman-4-ones. *Bioorg Med Chem Lett*. 2007 Dec;17(24):6764–9.
  14. Asadipour A, Pourshojaei Y, Eskandari K, Foroumadi A. A short synthesis of 7-amino alkoxy homoisoflavonoides. *RSC Adv*. 2017;7(71):44680–7.
  15. Siddaiah V, Maheswara M, Venkata Rao C, Venkateswarlu S, Subbaraju G V. Synthesis, structural revision, and antioxidant activities of antimutagenic homoisoflavonoids from *Hoffmanosseggia intricata*. *Bioorg Med Chem Lett*. 2007 Mar;17(5):1288–90.
  16. Demirayak S, Yurttas L, Gundogdu-Karaburun N, Karaburun AC, Kayagil I. New chroman-4-one/thiochroman-4-one derivatives as potential anticancer agents. *Saudi Pharm J*. 2017 Nov;25(7):1063–72.
  17. Basavarajappa HD, Lee B, Lee H, Sulaiman RS, An H, Magaña C, et al. Synthesis and Biological Evaluation of Novel Homoisoflavonoids for Retinal Neovascularization. *J Med Chem*. 2015 Jun 25;58(12):5015–27.
  18. Damodar K, Lee JT, Kim J-K, Jun J-G. Synthesis and in vitro evaluation of homoisoflavonoids as potent inhibitors of nitric oxide production in RAW-264.7 cells. *Bioorg Med Chem Lett*. 2018 Jun;28(11):2098–102.
  19. Lee H, Yuan Y, Rhee I, Corson T, Seo S-Y. Synthesis of Natural Homoisoflavonoids Having Either 5,7-Dihydroxy-6-methoxy or 7-Hydroxy-5,6-dimethoxy Groups. *Molecules*. 2016 Aug 13;21(8):1058.
  20. Pourshojaei Y, Gouranourimi A, Hekmat S, Asadipour A, Rahmani-Nezhad S, Moradi A, et al. Design, synthesis and anticholinesterase activity of novel benzylidenechroman-4-ones bearing cyclic amine side chain. *Eur J Med Chem*. 2015;97:181–9.
  21. Liu Q-H, Wu J-J, Li F, Cai P, Yang X-L, Kong L-Y, et al. Synthesis and pharmacological evaluation of multi-functional homoisoflavonoid derivatives as potent inhibitors of

monoamine oxidase B and cholinesterase for the treatment of Alzheimer's disease.

*Medchemcomm*. 2017;8(7):1459–67.

22. Min BS, Cuong TD, Hung TM, Min BK, Shin BS, Woo MH. Compounds from the heartwood of *Caesalpinia sappan* and their anti-inflammatory activity. *Bioorg Med Chem Lett*. 2012 Dec;22(24):7436–9.
23. Li N, Zhang J-Y, Zeng K-W, Zhang L, Che Y-Y, Tu P-F. Anti-inflammatory homoisoflavonoids from the tuberous roots of *Ophiopogon japonicus*. *Fitoterapia*. 2012 Sep;83(6):1042–5.
24. Dai Y, Harinantenaina L, Brodie PJ, Goetz M, Shen Y, TenDyke K, et al. Antiproliferative Homoisoflavonoids and Bufatrienolides from *Urginea depressa*. *J Nat Prod*. 2013 May 24;76(5):865–72.
25. Basavarajappa HD, Lee B, Fei X, Lim D, Callaghan B, Mund JA, et al. Synthesis and Mechanistic Studies of a Novel Homoisoflavanone Inhibitor of Endothelial Cell Growth. Leung YF, editor. *PLoS One*. 2014 Apr 21;9(4):e95694.
26. Lux A, Llacer H, Heussen FMA, Jousseaume AM. Non-responders to bevacizumab (Avastin) therapy of choroidal neovascular lesions. *Br J Ophthalmol*. 2007 Oct 1;91(10):1318–22.
27. Sidhu RS, Lee JY, Yuan C, Smith WL. Comparison of Cyclooxygenase-1 Crystal Structures: Cross-Talk between Monomers Comprising Cyclooxygenase-1 Homodimers. *Biochemistry*. 2010 Aug 24;49(33):7069–79.
28. Ti Y, Yu L, Tang Y, Jin T, Yang M, Wang R, et al. A hypoxia-activated near infrared fluorescent probe for cyclooxygenase-2 and in vivo imaging for tumor and inflammation. *Sensors Actuators B Chem*. 2018 Jul;265:582–90.
29. Honma S, Takahashi N, Shinohara M, Nakamura K, Mitazaki S, Abe S, et al. Amelioration of cisplatin-induced mouse renal lesions by a cyclooxygenase (COX)-2 selective inhibitor. *Eur J Pharmacol*. 2013 Sep;715(1–3):181–8.
30. Chen H, Cai W, Chu ESH, Tang J, Wong C-C, Wong SH, et al. Hepatic cyclooxygenase-2 overexpression induced spontaneous hepatocellular carcinoma formation in mice.

- Oncogene*. 2017 Aug 27;36(31):4415–26.
31. Ricciotti E, FitzGerald GA. Prostaglandins and Inflammation. *Arterioscler Thromb Vasc Biol*. 2011 May;31(5):986–1000.
  32. David A, Pancharatna K. Developmental anomalies induced by a non-selective COX inhibitor (ibuprofen) in zebrafish (*Danio rerio*). *Environ Toxicol Pharmacol*. 2009 May;27(3):390–5.
  33. Li, D.-K. Liu, L. Odouli R. Exposure to non-steroidal anti-inflammatory drugs during pregnancy and risk of miscarriage: population based cohort study. *BMJ*. 2003 Aug 16;327(7411):368–0.
  34. Karaman R, Mecca G, Jumaa S. X-ray Crystal Structure of COX-2 Enzyme as a Tool to Predict Active Sites of Bitter Taste Receptors. *Br J Pharm Res*. 2016 Jan 10;12(5):1–5.
  35. Cairns JA. The coxibs and traditional nonsteroidal anti-inflammatory drugs: A current perspective on cardiovascular risks. *Can J Cardiol*. 2007 Feb;23(2):125–31.
  36. Bombardier C, Laine L, Reicin A, Shapiro D, Burgos-Vargas R, Davis B, et al. Comparison of Upper Gastrointestinal Toxicity of Rofecoxib and Naproxen in Patients with Rheumatoid Arthritis. *N Engl J Med*. 2000 Nov 23;343(21):1520–8.
  37. Bresalier RS, Sandler RS, Quan H, Bolognese JA, Oxenius B, Horgan K, et al. Cardiovascular Events Associated with Rofecoxib in a Colorectal Adenoma Chemoprevention Trial. *N Engl J Med*. 2005 Mar 17;352(11):1092–102.
  38. Tsujii M, DuBois RN. Alterations in cellular adhesion and apoptosis in epithelial cells overexpressing prostaglandin endoperoxide synthase 2. *Cell*. 1995 Nov;83(3):493–501.
  39. Sobolewski C, Cerella C, Dicato M, Ghibelli L, Diederich M. The Role of Cyclooxygenase-2 in Cell Proliferation and Cell Death in Human Malignancies. *Int J Cell Biol*. 2010;2010:1–21.
  40. Zimmermann KC, Sarbia M, Weber AA, Borchard F, Gabbert HE, Schrör K. Cyclooxygenase-2 expression in human esophageal carcinoma. *Cancer Res*. 1999 Jan 1;59(1):198–204.
  41. Buskens CJ, van Rees BP, Sivula A, Reitsma JB, Haglund C, Bosma PJ, et al. Prognostic significance of elevated cyclooxygenase 2 expression in patients with adenocarcinoma of the

- esophagus. *Gastroenterology*. 2002 Jun;122(7):1800–7.
42. Lim HY, Joo HJ, Choi JH, Yi JW, Yang MS, Cho DY, et al. Increased expression of cyclooxygenase-2 protein in human gastric carcinoma. *Clin Cancer Res*. 2000 Feb;6(2):519–25.
  43. Kishimoto Y, Yashima K, Morisawa T, Shiota G, Kawasaki H, Hasegawa J. Effects of cyclooxygenase-2 inhibitor NS-398 on APC and c-myc expression in rat colon carcinogenesis induced by azoxymethane. *J Gastroenterol*. 2002;37(3):186–93.
  44. Fujita T, Matsui M, Takaku K, Uetake H, Ichikawa W, Taketo MM, et al. Size- and invasion-dependent increase in cyclooxygenase 2 levels in human colorectal carcinomas. *Cancer Res*. 1998 Nov 1;58(21):4823–6.
  45. Basu GD, Liang WS, Stephan DA, Wegener LT, Conley CR, Pockaj BA, et al. A novel role for cyclooxygenase-2 in regulating vascular channel formation by human breast cancer cells. *Breast Cancer Res*. 2006 Dec 11;8(6):R69.
  46. Pan M-R, Hou M-F, Chang H-C, Hung W-C. Cyclooxygenase-2 Up-regulates CCR7 via EP2/EP4 Receptor Signaling Pathways to Enhance Lymphatic Invasion of Breast Cancer Cells. *J Biol Chem*. 2008 Apr 25;283(17):11155–63.
  47. Repetto G, del Peso A, Zurita JL. Neutral red uptake assay for the estimation of cell viability/cytotoxicity. *Nat Protoc*. 2008;3(7):1125–31.
  48. Song J, Jones LM, Kumar GDK, Conner ES, Bayeh L, Chavarria GE, et al. Synthesis and Biochemical Evaluation of Thiochromanone Thiosemicarbazone Analogues as Inhibitors of Cathepsin L. *ACS Med Chem Lett*. 2012 Jun 14;3(6):450–3.
  49. Hammam, A. Fahmy, A. Amr, A. Mohamed A. Synthesis of Novel Tricyclic Heterocyclic Compounds as Potential Anticancer Agents Using Chromanone and Thiochromanone as Synthons. *Indian J Chem*. 2003;34(47):1985–93.
  50. Bharadwaj AS, Appukuttan B, Wilmarth PA, Pan Y, Stempel AJ, Chipps TJ, et al. Role of the retinal vascular endothelial cell in ocular disease. *Prog Retin Eye Res*. 2013 Jan;32:102–80.

51. Muñoz-Chápuli R, Quesada AR, Medina MÁ. Angiogenesis and signal transduction in endothelial cells. *Cell Mol Life Sci*. 2004 Aug;61(17):2224–43.
52. Dunn KC, Aotaki-Keen AE, Putkey FR, Hjelmeland LM. ARPE-19, A Human Retinal Pigment Epithelial Cell Line with Differentiated Properties. *Exp Eye Res*. 1996 Feb;62(2):155–70.
53. Schwikkard S, Whitmore H, Sischtla K, Sulaiman RS, Shetty T, Basavarajappa HD, et al. The Antiangiogenic Activity of Naturally Occurring and Synthetic Homoisoflavonoids from the *Hyacinthaceae* (sensu APGII). *J Nat Prod*. 2019 May 24;82(5):1227–39.
54. Simon L, Abdul Salam AA, Madan Kumar S, Shilpa T, Srinivasan KK, Byrappa K. Synthesis, anticancer, structural, and computational docking studies of 3-benzylchroman-4-one derivatives. *Bioorg Med Chem Lett*. 2017 Dec;27(23):5284–90.
55. Waller CP, Thumser AE, Langat MK, Crouch NR, Mulholland DA. COX-2 inhibitory activity of homoisoflavanones and xanthenes from the bulbs of the Southern African *Ledebouria socialis* and *Ledebouria ovatifolia* (Hyacinthaceae: Hyacinthoideae). *Phytochemistry*. 2013 Nov;95:284–90.
56. Schwikkard S, Alqahtani A, Knirsch W, Wetschnig W, Jaksevicius A, Opara EI, et al. Phytochemical Investigations of Three *Rhodocodon* (Hyacinthaceae Sensu APG II) Species. *J Nat Prod*. 2017 Jan 27;80(1):30–7.
57. Yale HL. The Trifluoromethyl Group in Medical Chemistry. *J Med Pharm Chem*. 1959 Apr;1(2):121–33.
58. Lator A, Gaillard S, Poater A, Renaud J-L. Iron-Catalyzed Chemoselective Reduction of  $\alpha,\beta$ -Unsaturated Ketones. *Chem - A Eur J*. 2018 Apr 17;24(22):5770–4.
59. Li W, Wu X-F. Ruthenium-Catalyzed Conjugate Hydrogenation of  $\alpha,\beta$ -Enones by in situ Generated Dihydrogen from Paraformaldehyde and Water. *European J Org Chem*. 2015 Jan;2015(2):331–5.
60. Romagnoli R, Baraldi PG, Carrion MD, Cruz-Lopez O, Cara CL, Balzarini J, et al. Hybrid  $\alpha$ -bromoacryloylamido chalcones. Design, synthesis and biological evaluation. *Bioorg Med*



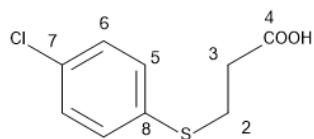
*Chem Lett.* 2009 Apr;19(7):2022–8.

61. Futaki N, Takahashi S, Yokoyama M, Arai I, Higuchi S, Otomo S. NS-398, a new anti-inflammatory agent, selectively inhibits prostaglandin G/H synthase/cyclooxygenase (COX-2) activity in vitro. *Prostaglandins.* 1994 Jan;47(1):55–9.

## A.0 Appendix

### A.1 Compound 28

#### 3-[(4-chlorophenyl)sulfanyl]propanoic acid (28)



White solid, 1.41 g, 65.1 %, 93.7 - 93.9 °C, IR  $\nu_{\max}$  ( $\text{cm}^{-1}$ ): 2561 (O-H, carboxylic acid), 1696 (C=O), 1477

(Aromatic C=C), 1092 (C-O), 813 (C-Cl), 659 (C-S),  $^1\text{H-NMR}$  (400 MHz,  $\text{CDCl}_3$ ):  $\delta$  = 7.24 (2H, d,  $J$  = 8.9 Hz,

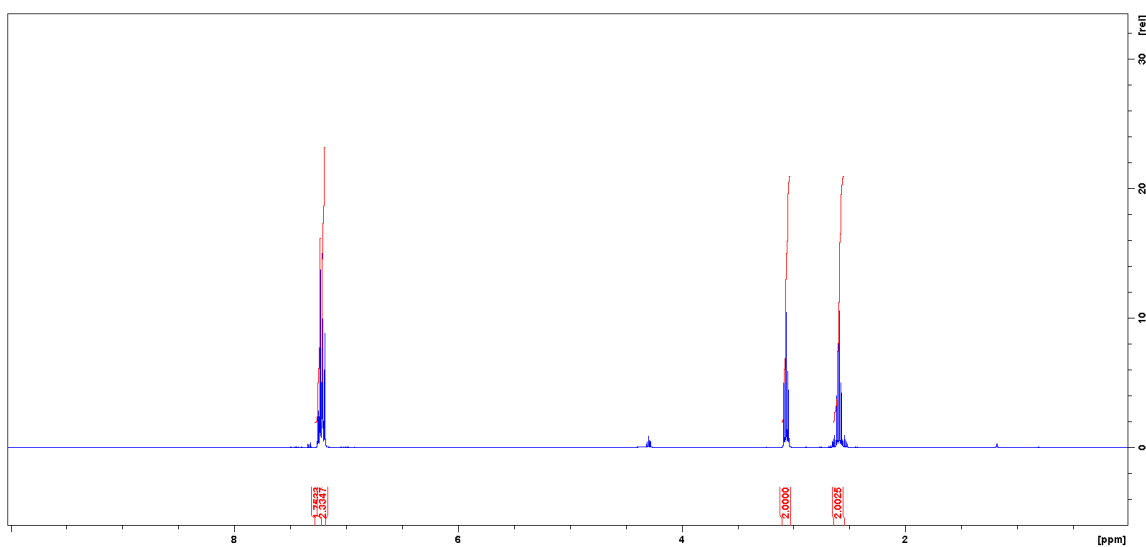
2 x H-5), 7.20 (2H, d,  $J$  = 8.9 Hz, 2 x H-6), 3.07 (2H, t,  $J$  = 7.2 Hz, H-2), 2.59 (2H, t,  $J$  = 7.2 Hz, H-3);  $^{13}\text{C-}$

NMR (100 MHz,  $\text{CDCl}_3$ ):  $\delta$  = 177.3 (C-4), 133.0 (C-8), 132.9 (C-7), 131.8 (C-5), 129.3 (C-6), 34.0 (C-3),

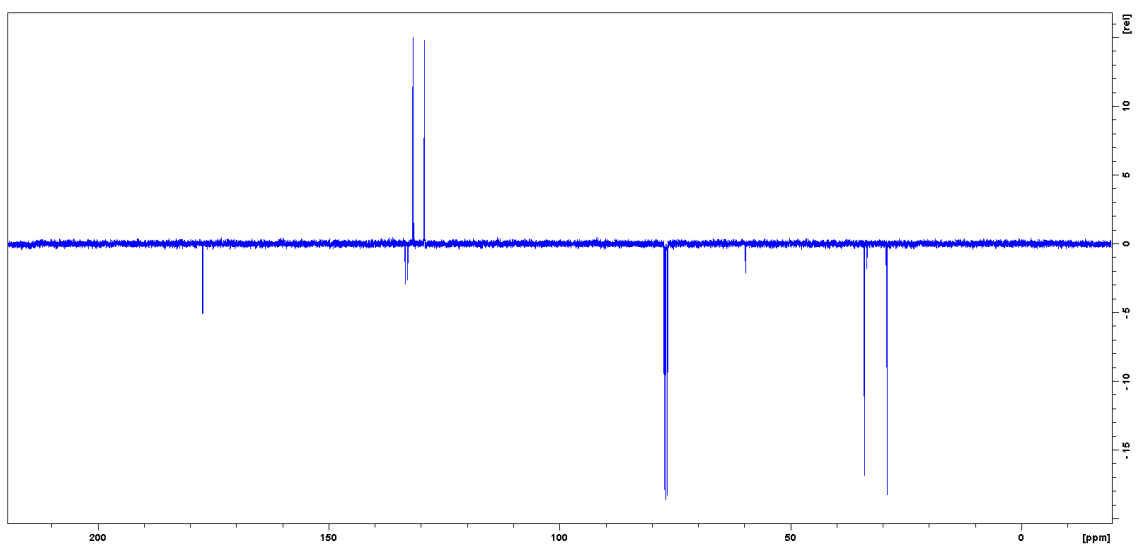
29.1(C-2),  $R_f$  = 0.68 (1:1 EtOAc:hexane)

#### A.1.1 NMR data

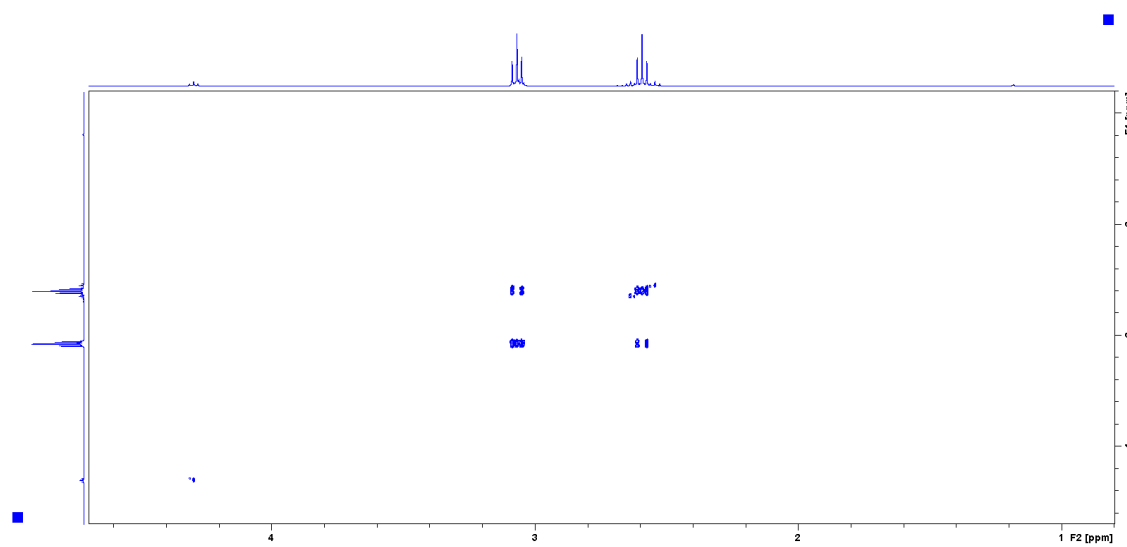
##### A.1.1.1 $^1\text{H-NMR}$



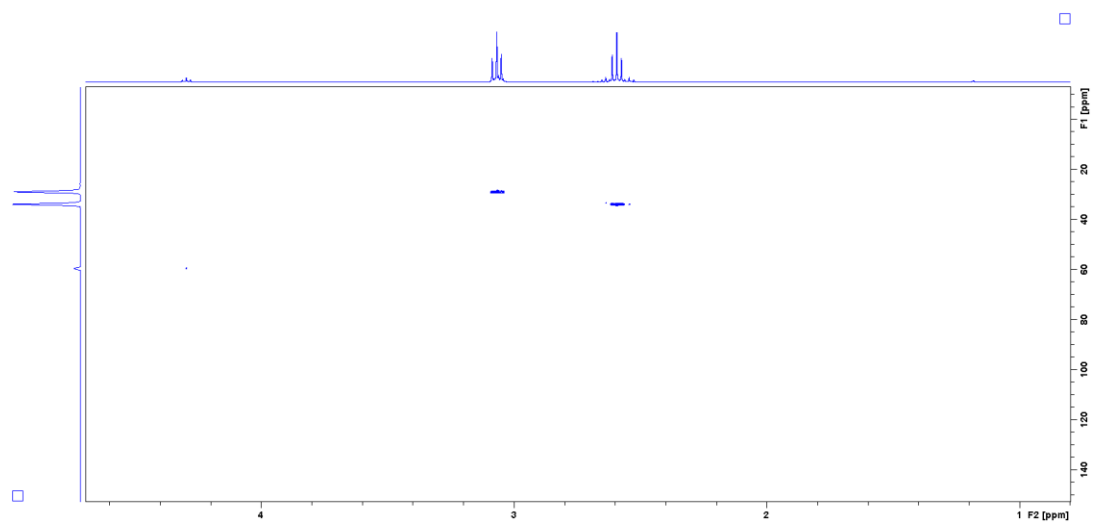
### A.1.1.2 $^{13}\text{C}$ -NMR



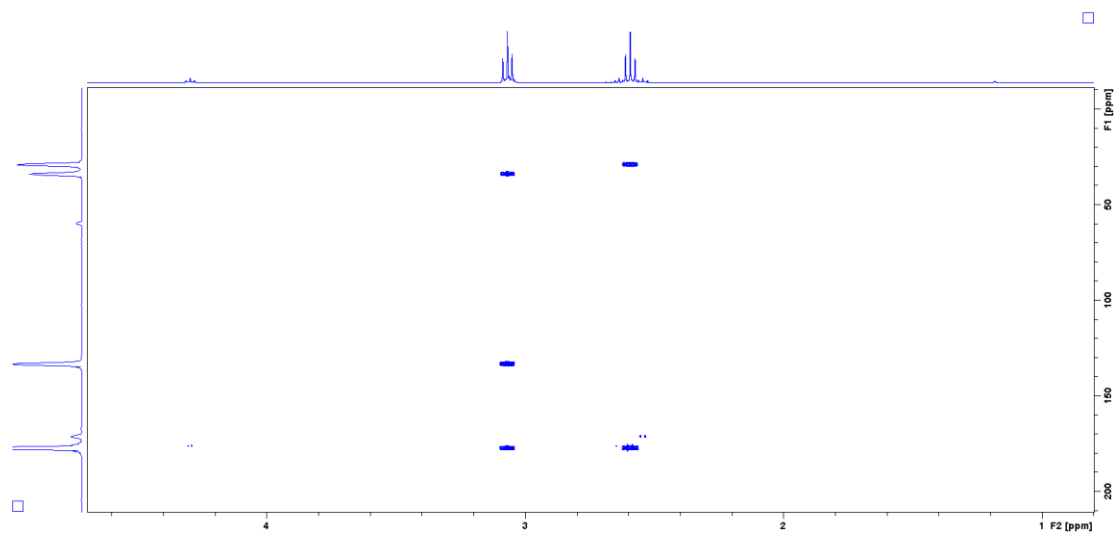
### A.1.1.3 COSY



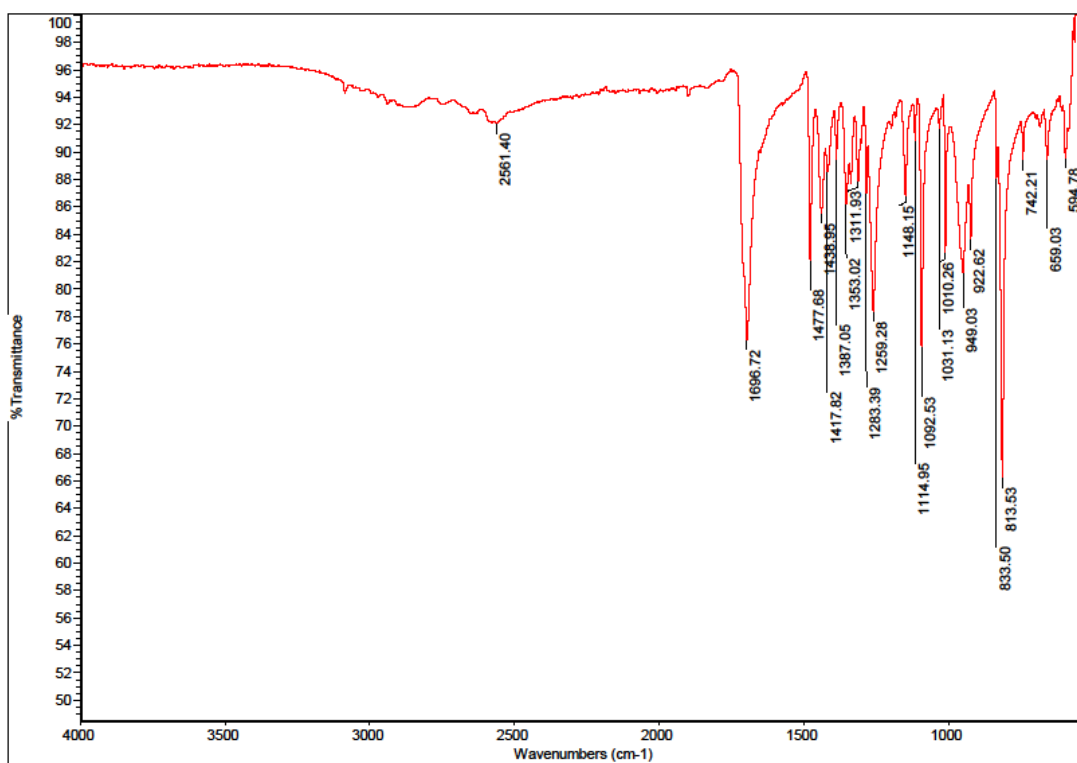
#### A.1.1.4 HSQC



#### A.1.1.5 HMBC

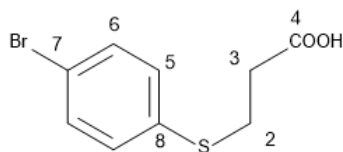


### A.1.2 IR Data



## A.2 Compound 29

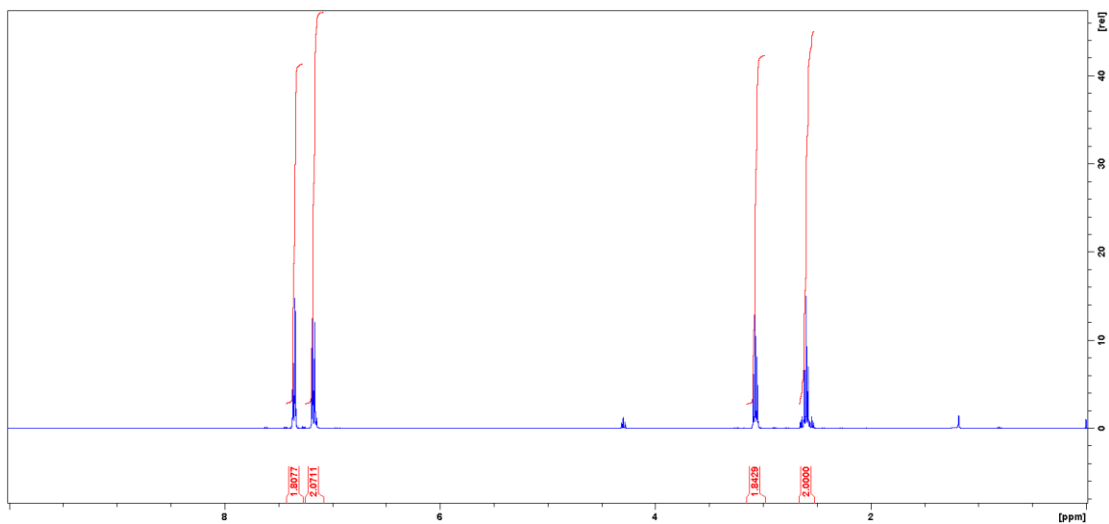
### 3-[(4-bromophenyl)sulfanyl]propanoic acid (29)



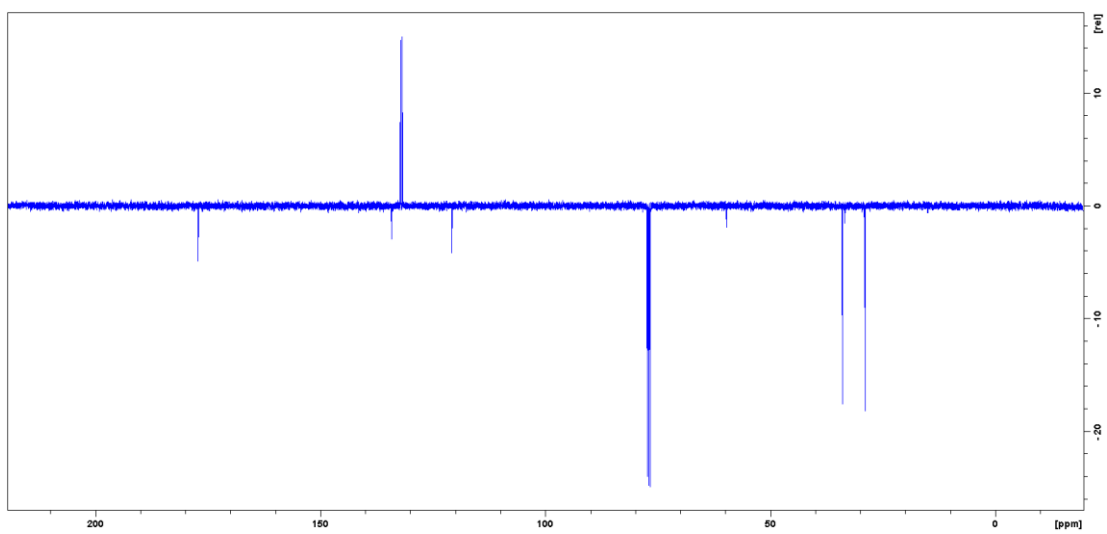
White solid, 2.41 g, 91.9 %, 120.3 - 121.0 °C, IR  $\nu_{\max}$  (cm<sup>-1</sup>): 2561 (O-H), 1697 (C=O), 1474 (Aromatic C=C), 1006 (C-O), 809 (C-Br), 657 (C-S), <sup>1</sup>H-NMR (400 MHz, CDCl<sub>3</sub>):  $\delta$  = 7.40 (2H, d, J = 8.6 Hz, 2 x H-6), 7.20 (2H, d, J = 8.6 Hz, 2 x H-5), 3.07 (2H, t, J = 7.2 Hz, H-2), 2.60 (2H, t, J = 7.2 Hz, H-3); <sup>13</sup>C-NMR (100 MHz, CDCl<sub>3</sub>):  $\delta$  = 177.2 (C-4), 134.1 (C-8) 132.2 (C-5), 131.8 (C-6), 120.8 (C-7), 33.9 (C-3), 28.9 (C-2), R<sub>f</sub> = 0.70 (1:1 EtOAc:hexane).

### A.2.1 NMR

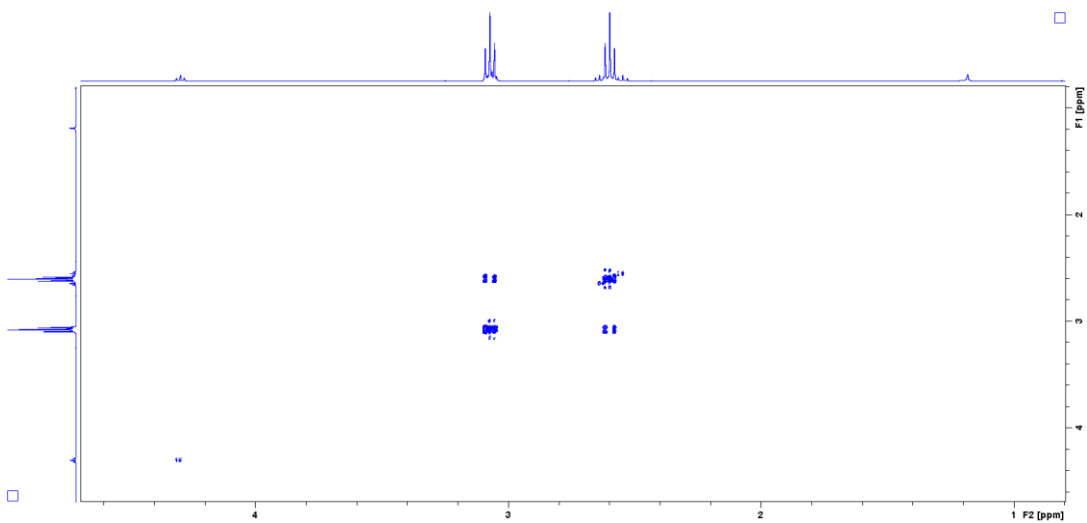
#### A.2.1.1 <sup>1</sup>H-NMR



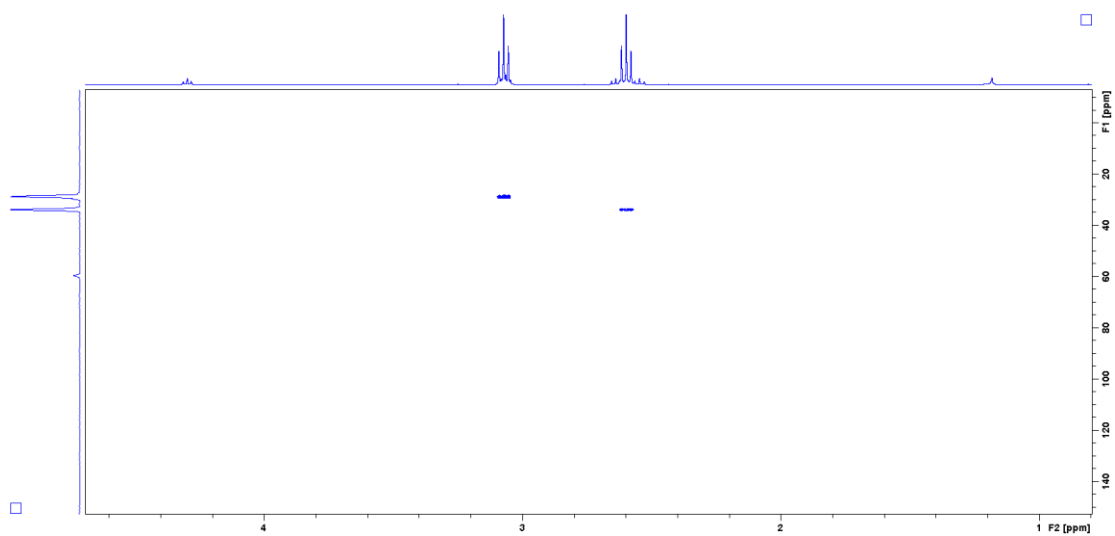
### A.2.1.2 $^{13}\text{C}$ -NMR



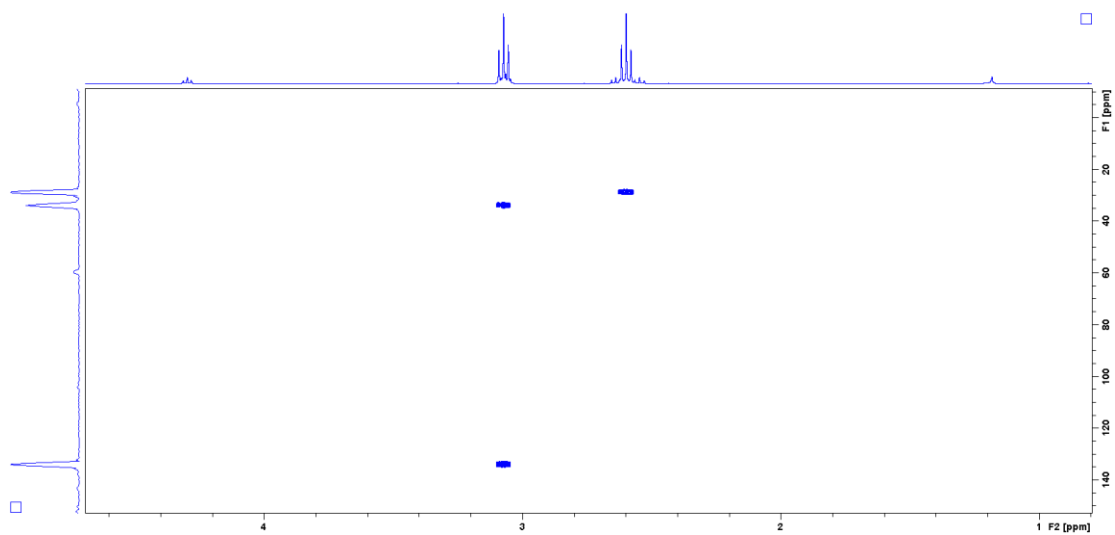
### A.2.1.3 COSY



#### A.2.1.4 HSQC

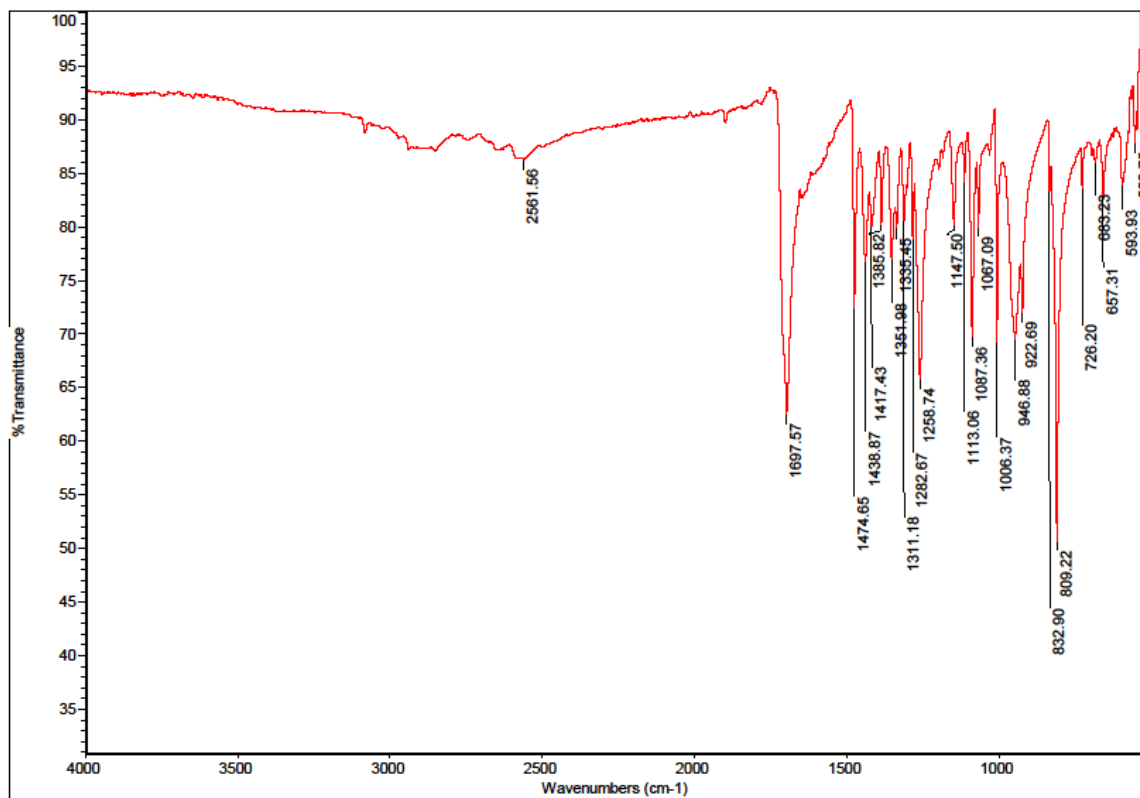


#### A.2.1.5 HMBC



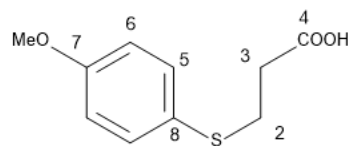


## A.2.2 IR Data



### A.3 Compound 30

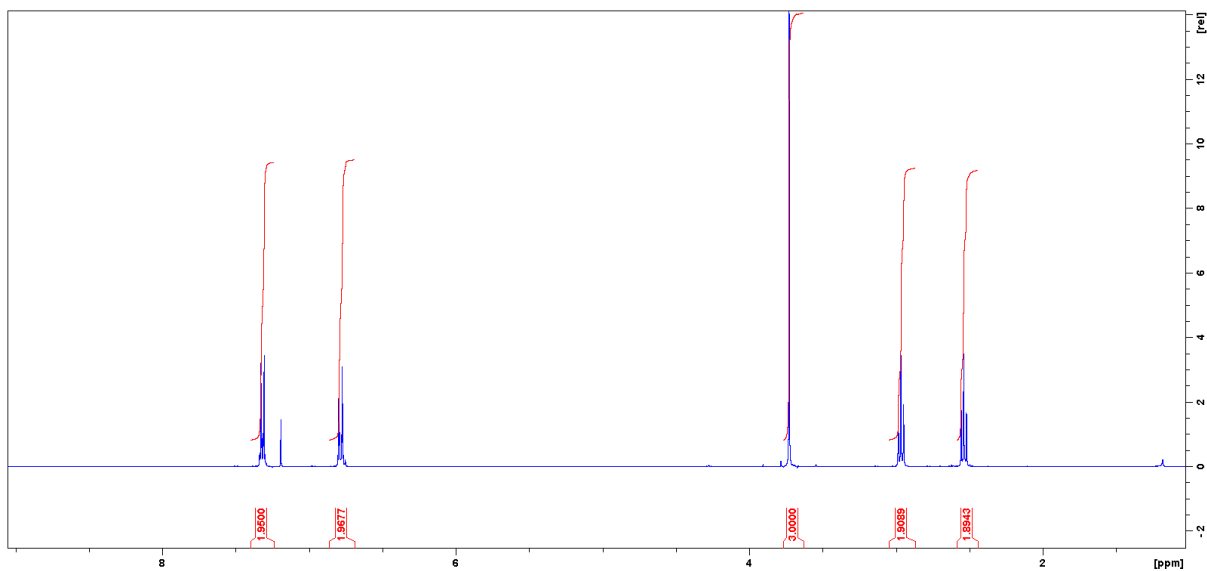
#### 3-[(4-methoxyphenyl)sulfanyl]propanoic acid (30)



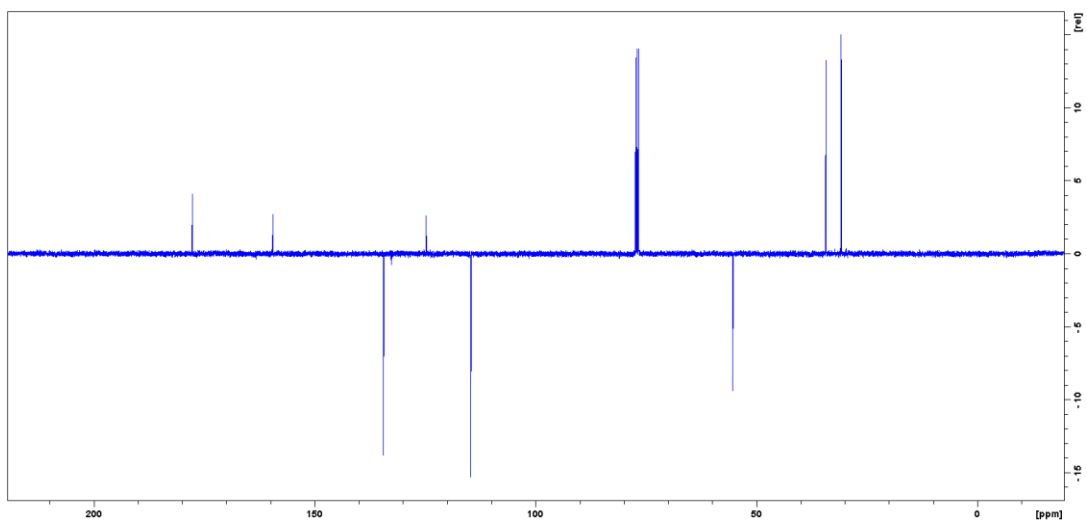
White solid, 2.08 g, 97.4 %, 85.2 - 85.7 °C, IR  $\nu_{\max}$  (cm<sup>-1</sup>): 2958 (Ar-H), 2591 (O-H), 1694 (C=O), 1492 (CH<sub>3</sub> bend), 1469 (Aromatic C=C), 1027 (C-O), 664 (C-S), <sup>1</sup>H-NMR (400 MHz, CDCl<sub>3</sub>):  $\delta$  = 7.32 (2H, d, J = 8.7 Hz, 2 x H-6), 6.78 (2H, d, J = 8.7, 2 x H-5), 3.73 (3H, s, OCH<sub>3</sub>), 2.96 (2H, t, J = 7.0 Hz, H-2), 2.53 (2H, t, J = 7.0, H-3); <sup>13</sup>C-NMR (100 MHz, CDCl<sub>3</sub>):  $\delta$  = 177.7 (C-4), 159.5 (C-7), 134.5 (C-5), 124.8 (C-8), 114.7 (C-6), 55.4 (OCH<sub>3</sub>), 34.3 (C-3), 30.8 (C-2), R<sub>f</sub> = 0.73 (1:1 EtOAc:hexane).

#### A.3.1 NMR

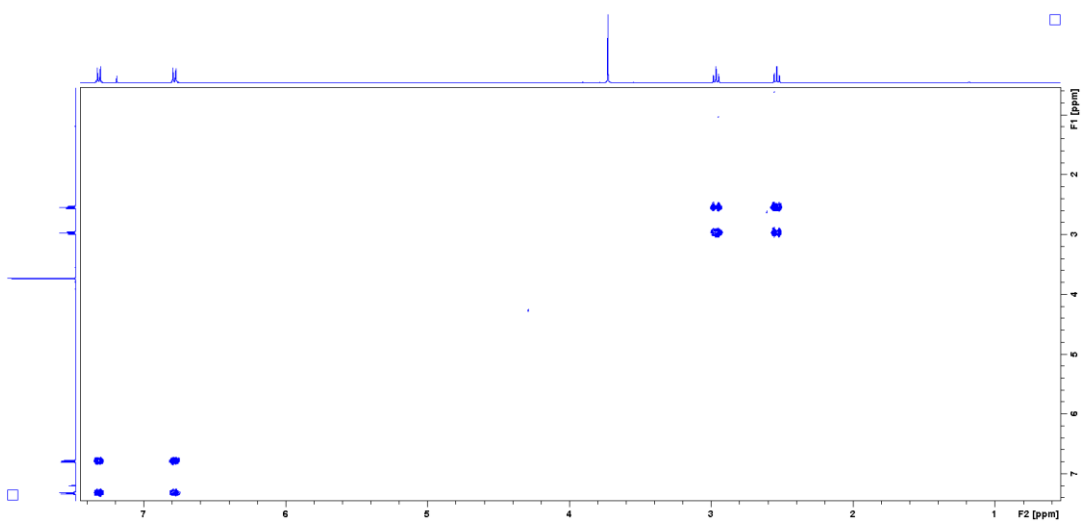
##### A.3.1.1 <sup>1</sup>H-NMR



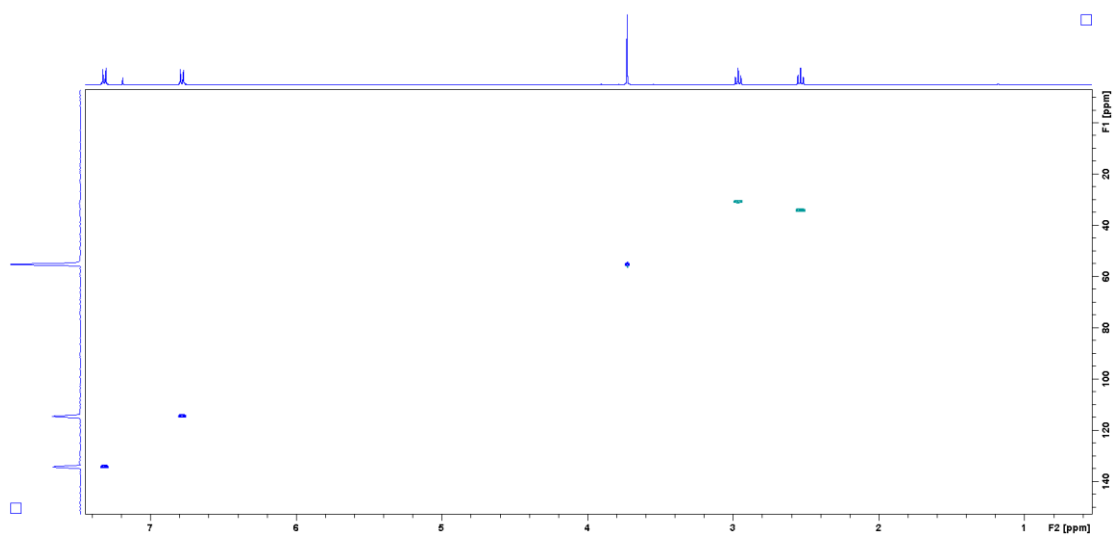
### A.3.1.2 $^{13}\text{C}$ -NMR



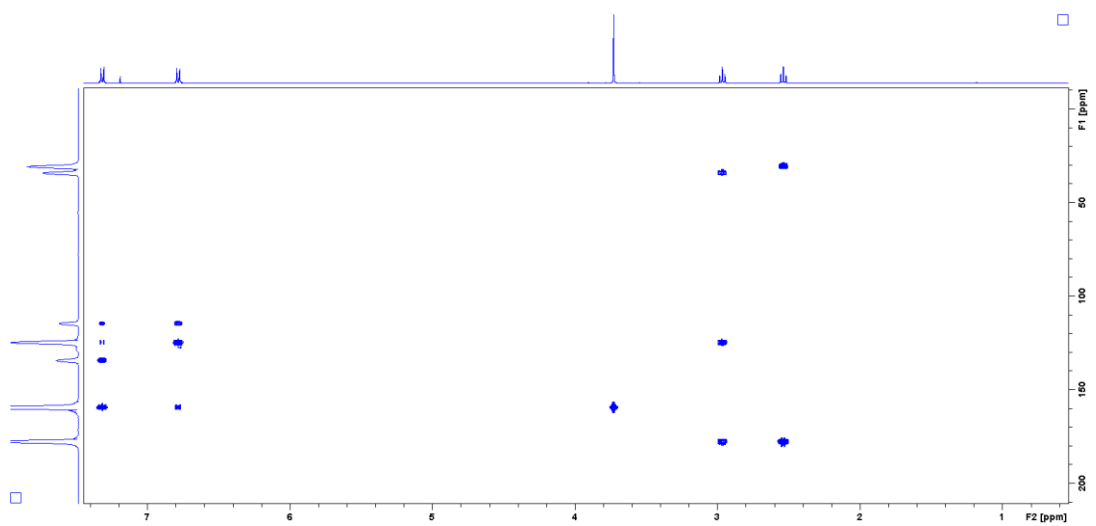
### A.3.1.3 COSY



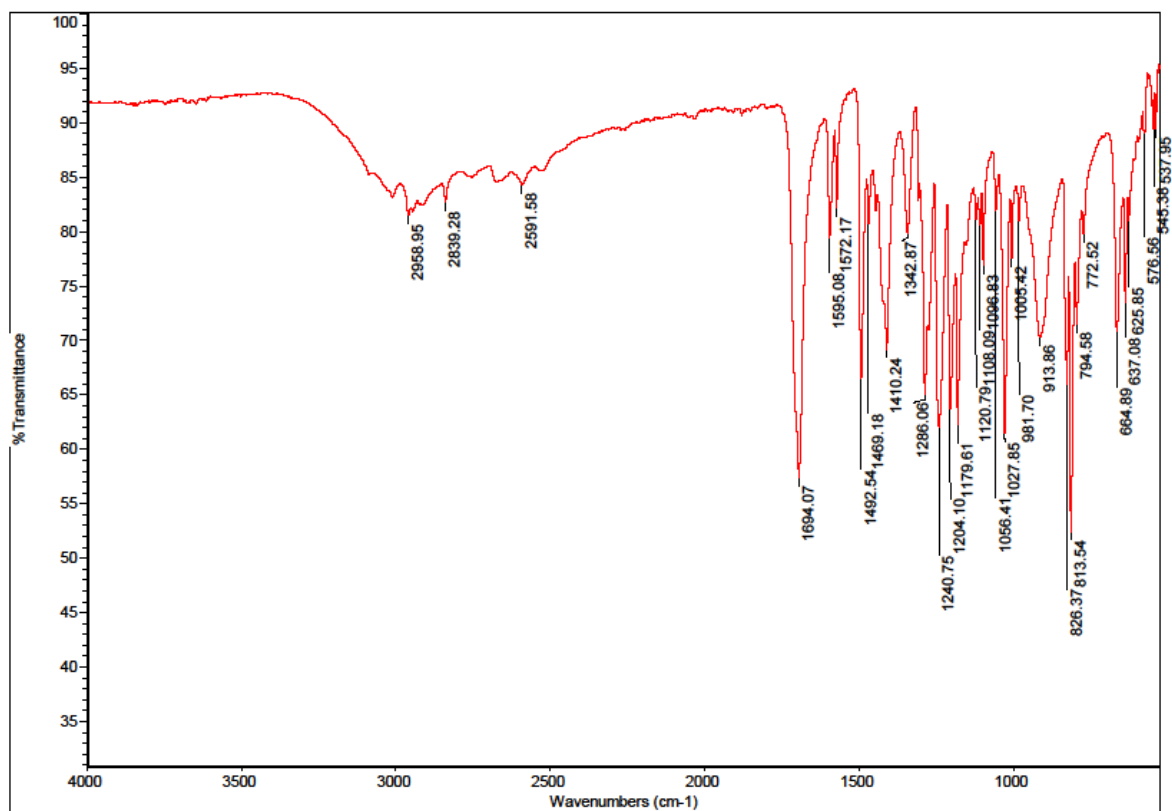
### A.3.1.4 HQSC



### A.3.1.5 HMBC

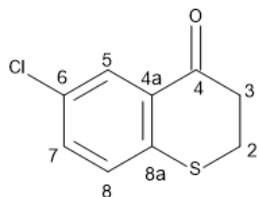


### A.3.2 IR Data



## A.4 Compound 31

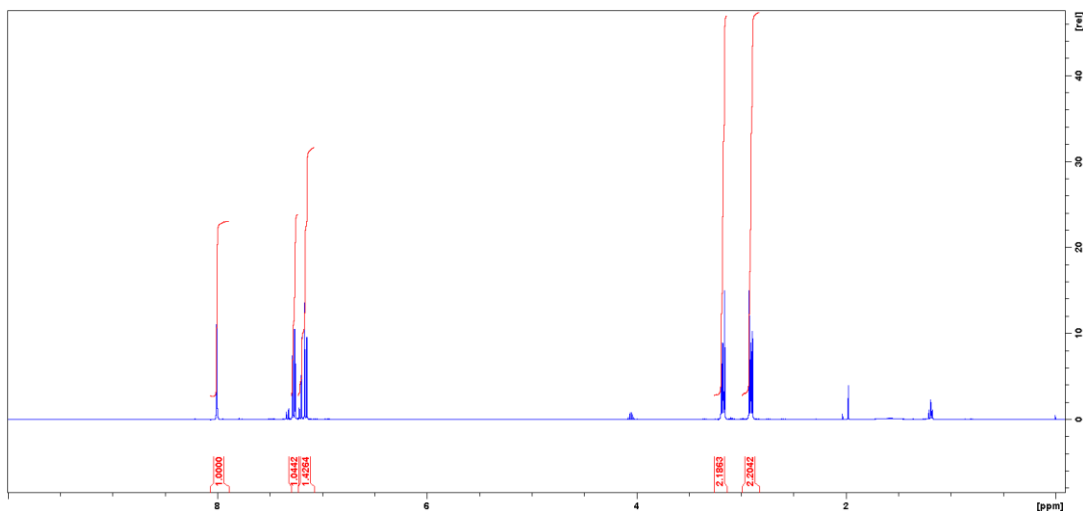
### 6-chloro-2,3-dihydro-4H-1-benzothiopyran-4-one (31)



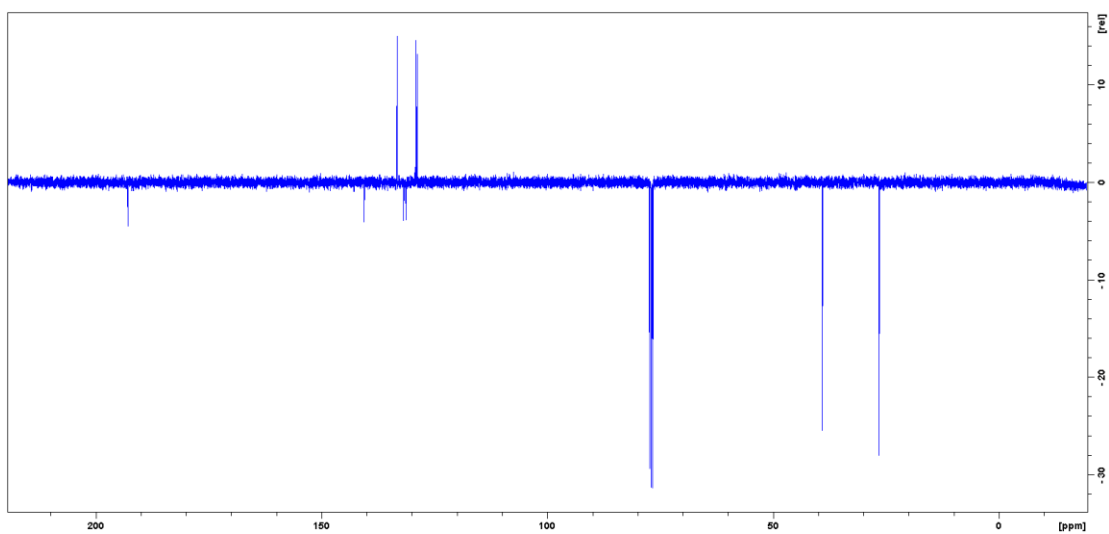
Light orange solid, 0.46 g, 50.3 %, 78.8 - 79.3 °C, IR  $\nu_{\max}$  (cm<sup>-1</sup>): 3047 (Ar-H), 2939 (Aliphatic C-H), 1666 (C=O), 1472 (Aromatic C=C), 815 (C-Cl), 655 (C-S), <sup>1</sup>H-NMR (400 MHz, CDCl<sub>3</sub>):  $\delta$  = 8.00 (1H, d, J = 2.5 Hz, H-5), 7.26 (1H, dd, J = 2.5 Hz, 8.6 Hz, H-7), 7.15 (1H, d, J = 8.6 Hz, H-8), 3.17 (2H, m, H-2), 2.90 (2H, m, H-3); <sup>13</sup>C-NMR (100 MHz, CDCl<sub>3</sub>):  $\delta$  = 192.9 (C-4), 140.5 (C-8a), 133.4 (C-7), 131.9 (C-4a), 131.2 (C-6), 129.1 (C-8), 128.8 (C-5), 39.3 (C3), 26.9 (C-2), R<sub>f</sub> = 0.49 (1:1 EtOAc:hexane).

#### A.4.1 NMR

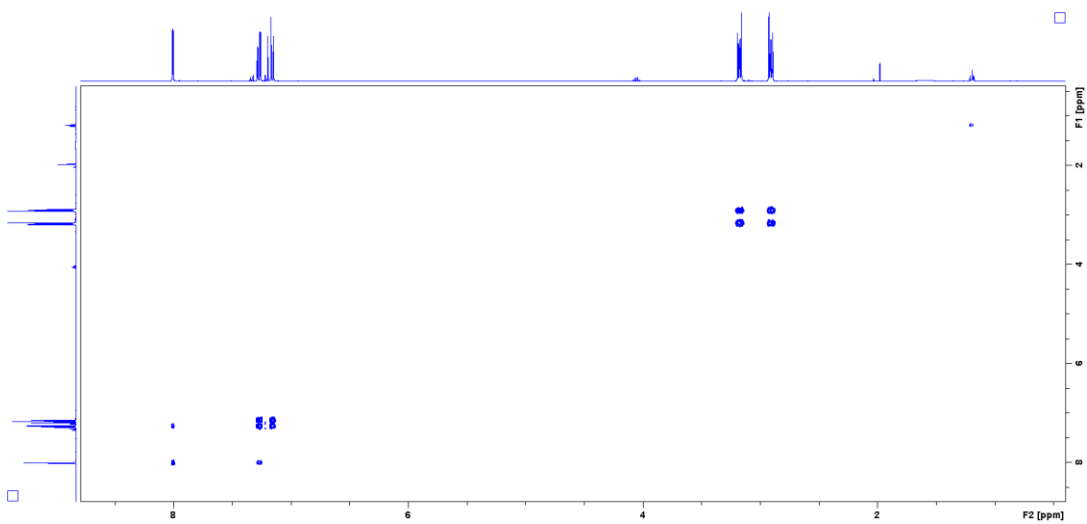
##### A.4.1.1 <sup>1</sup>H-NMR



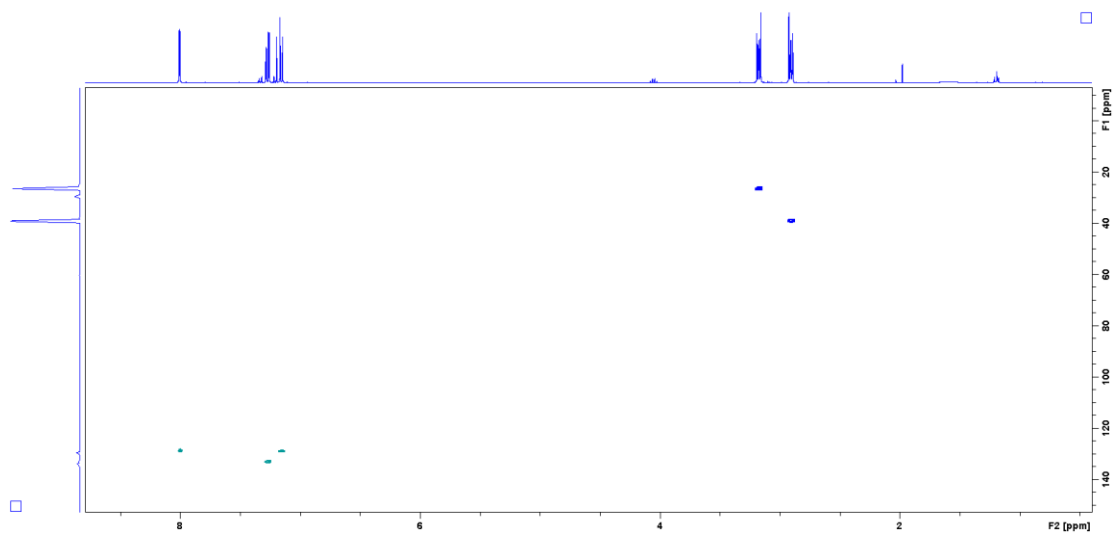
### A.4.1.2 $^{13}\text{C}$ -NMR



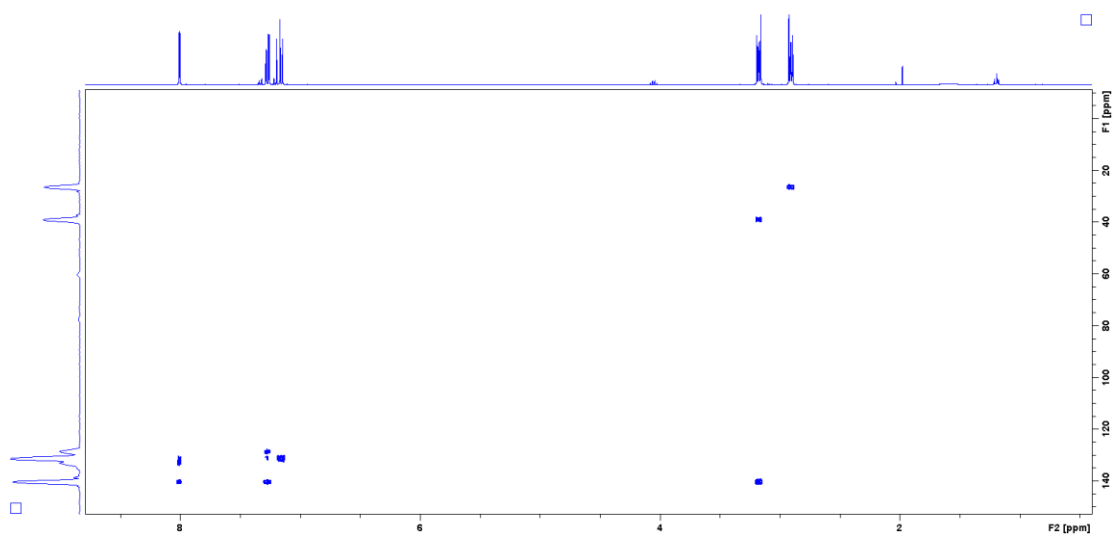
### A.4.1.3 COSY



#### A.4.1.4 HSQC

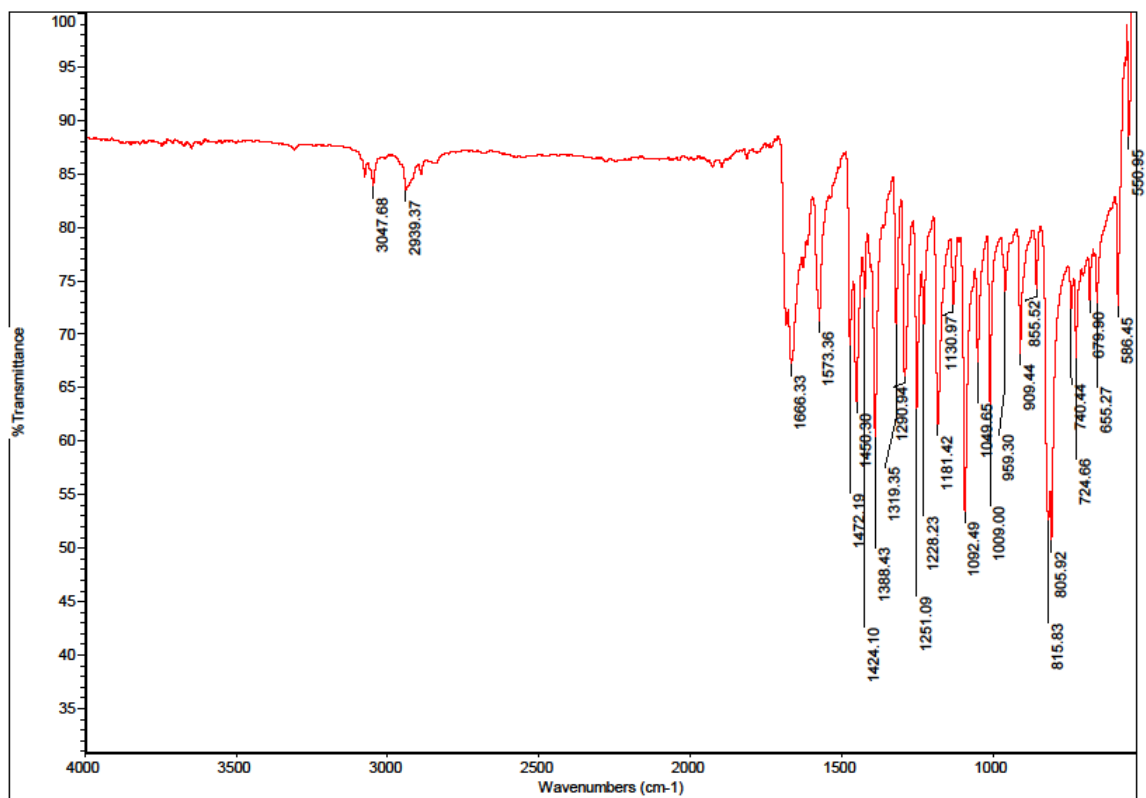


#### A.4.1.5 HMBC

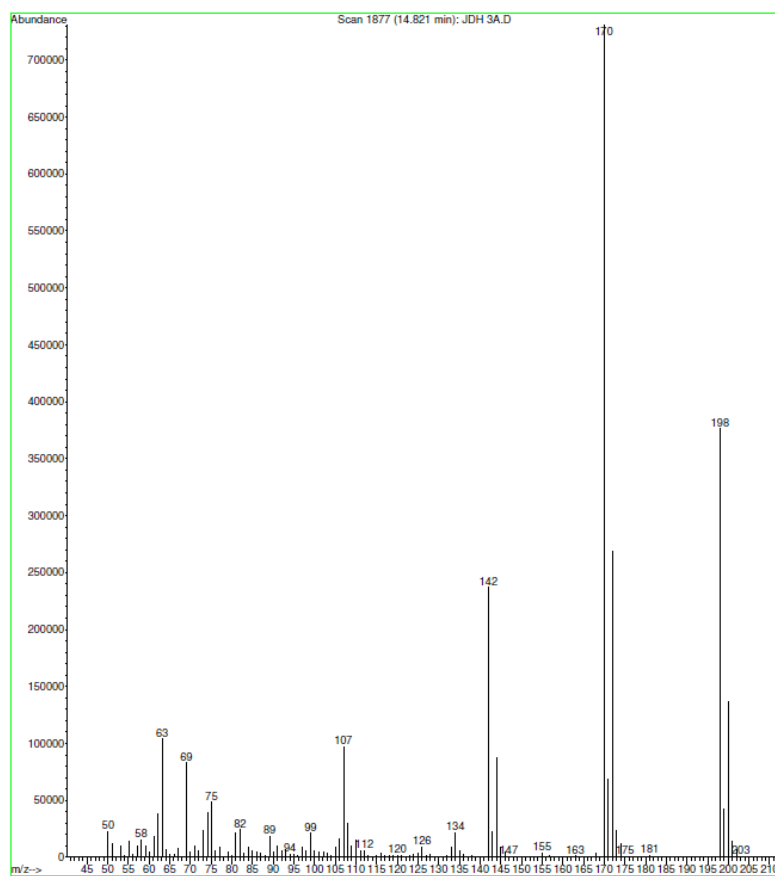
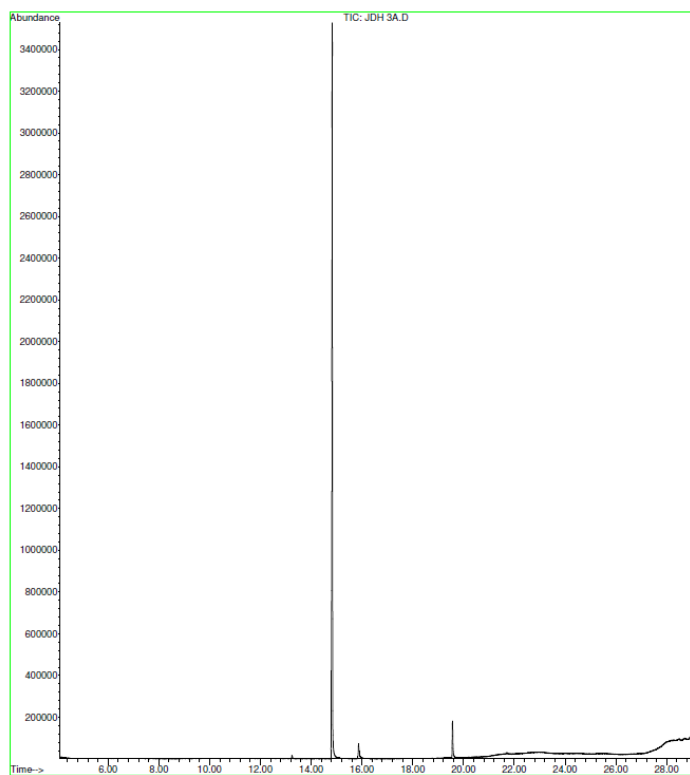




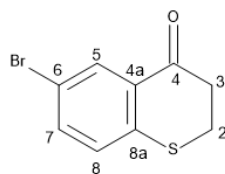
### A.4.2 IR Data



### A.4.3 GCMS



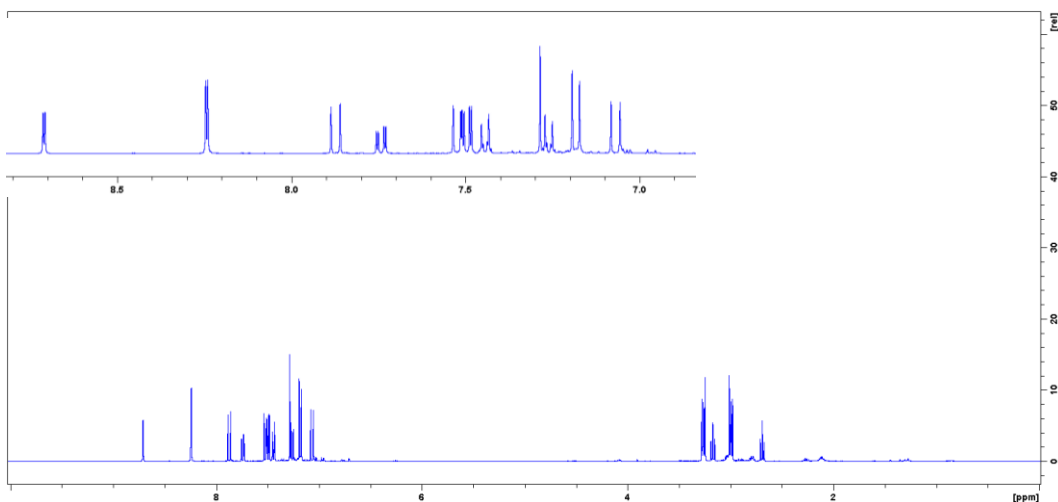
## A.5 Compound 32



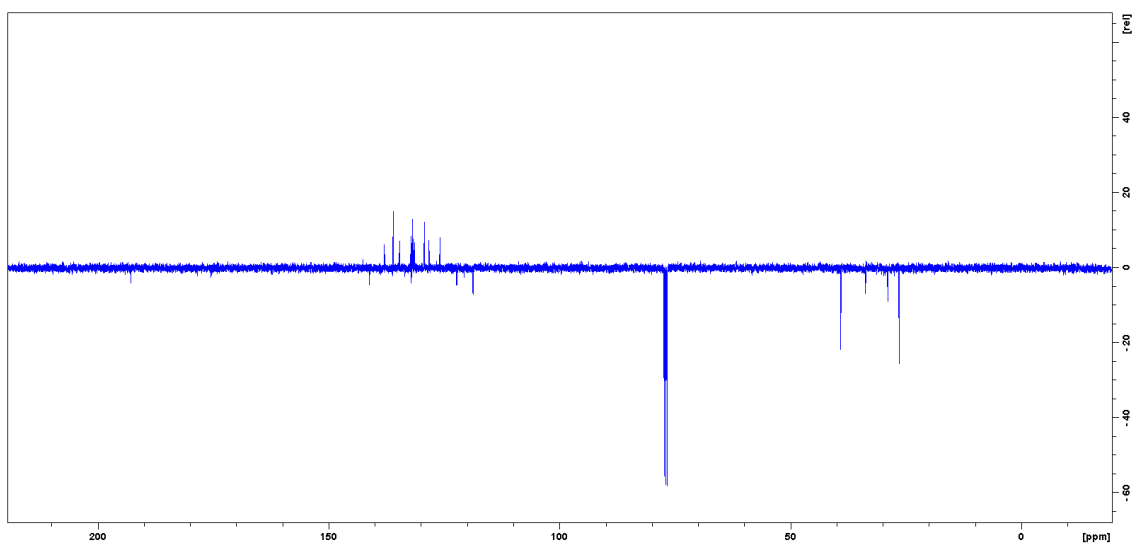
Light orange solid, 0.47 g, 49.7 %, 120.3 - 121.0 °C, IR  $\nu_{\max}$  (cm<sup>-1</sup>): 2930 (Ar-H), 1667 (C=O), 1447 (Aromatic C=C), 809 (C-Br), 657 (C-S), <sup>1</sup>H-NMR (400 MHz, CDCl<sub>3</sub>):  $\delta$  = 8.24 (1H, d, J = 2.1 Hz, H-5), 7.50 (1H, dd, J = 2.1 Hz, 7.7 Hz, H-7), 7.18(1H, d, J = 8.5 Hz, H-8), 3.26 (2H, m, H-2), 2.99 (2H, m, H-3); <sup>13</sup>C-NMR (100 MHz, CDCl<sub>3</sub>):  $\delta$  = 192.9 (C-4), 141.2 (C-4a), 136.1 (C-7), 132.0 (C-8a), 131.5 (C-5), 129.4 (C-8), 119.0 (C-6), 39.1 (C-3), 34.4 (C-2), Rf = 0.46 (1:1 EtOAc:hexane).

### A.5.1 NMR

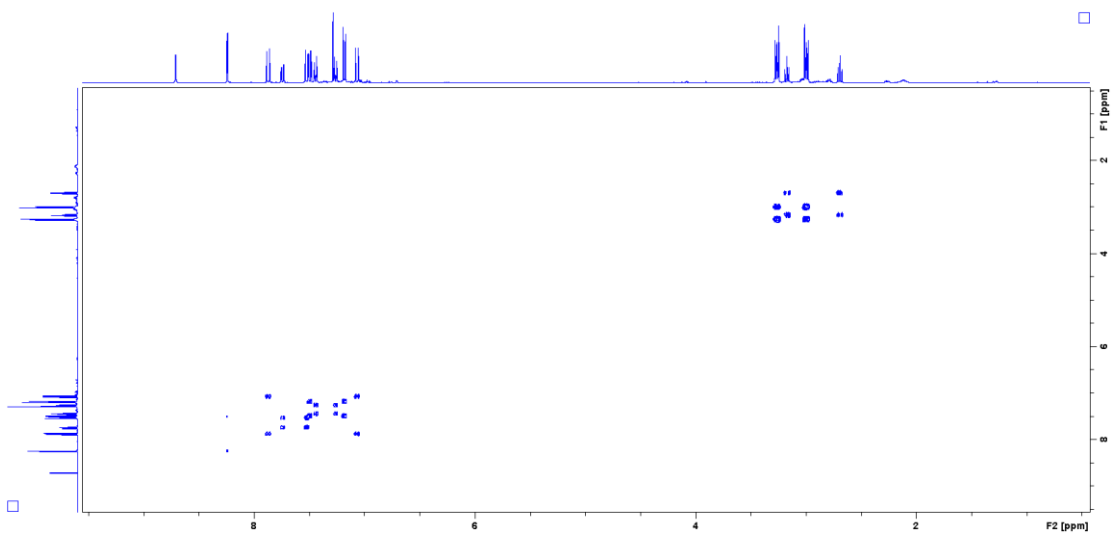
#### A.5.1.1 <sup>1</sup>H-NMR



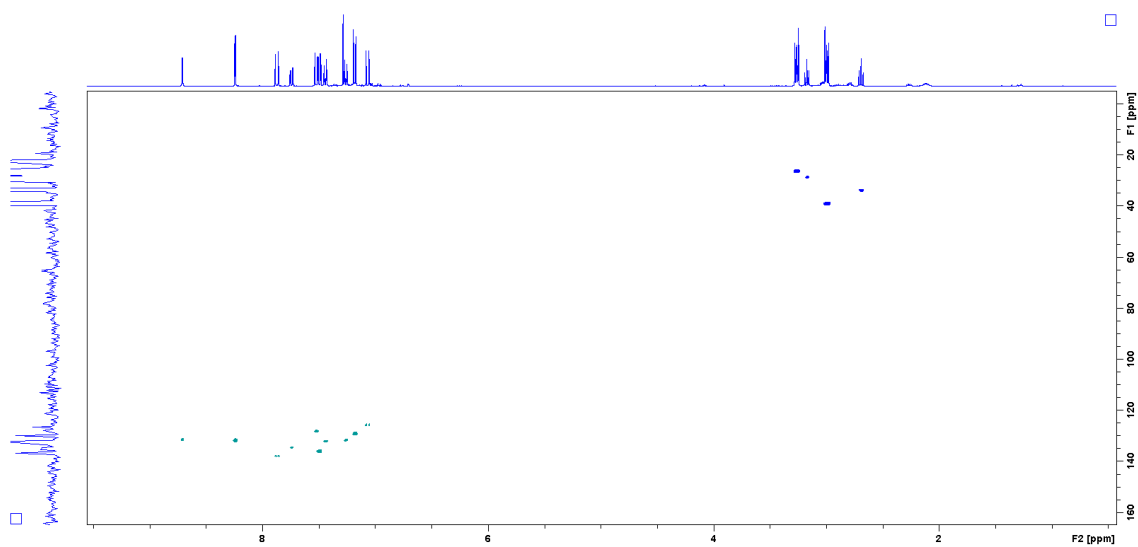
### A.5.1.2 <sup>13</sup>C-NMR



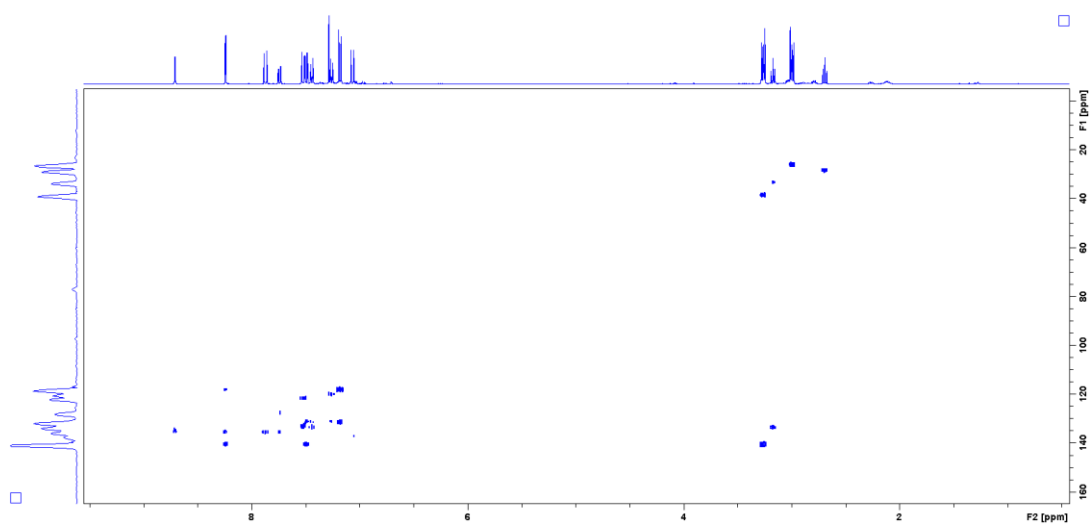
### A.5.1.3 COSY



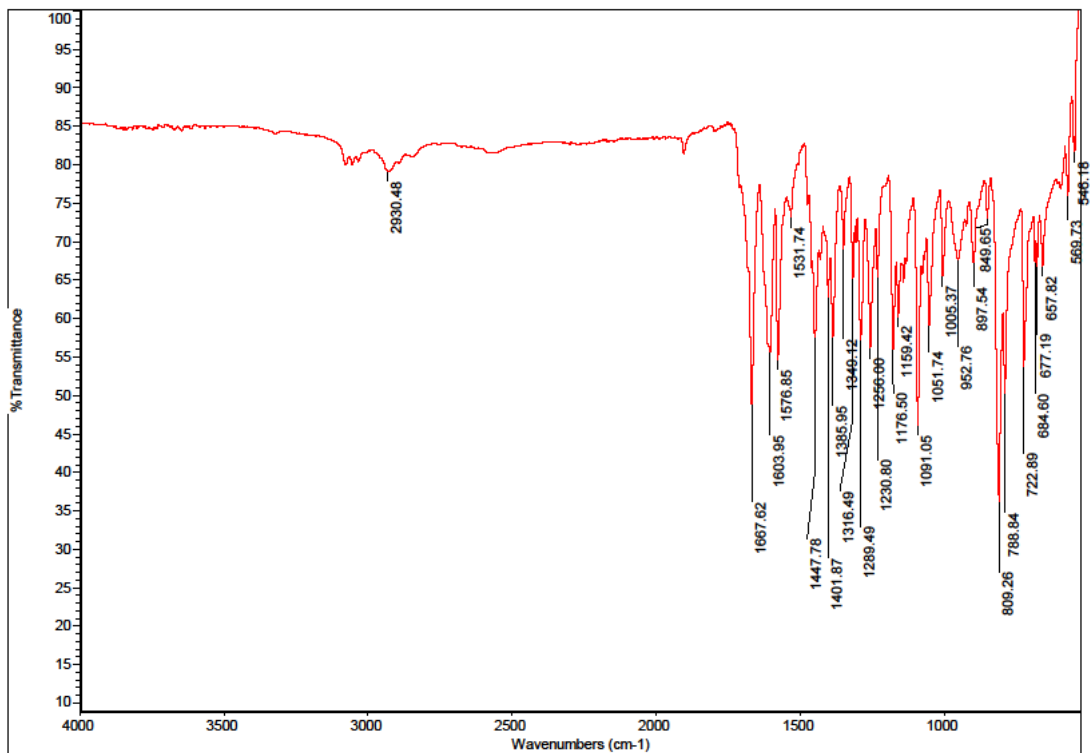
### A.5.1.4 HSQC



### A.5.1.5 HMBC

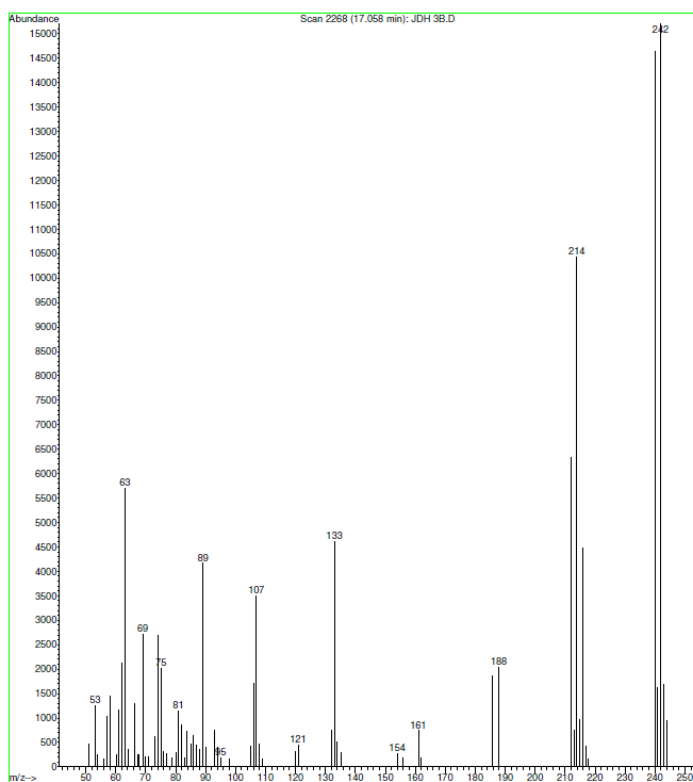
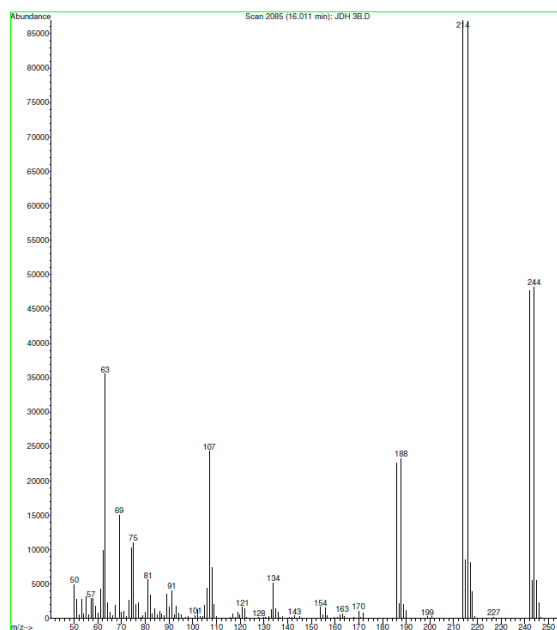
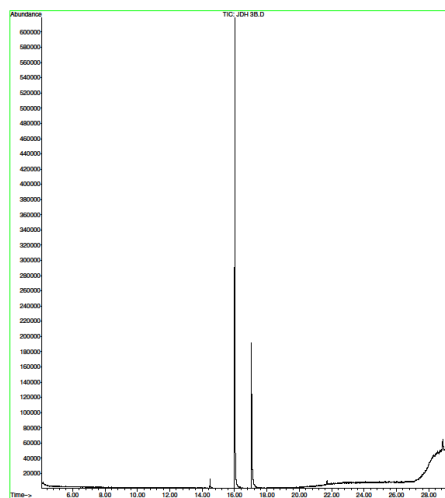


## A.5.2 IR Data



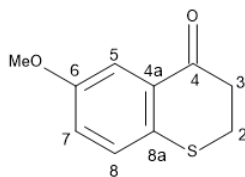
### A.5.3 GCMS

File : E:\DATA\JDH 38.D  
 Operator :  
 Acquired : 8 May 2019 17:41 using AcqMethod DEFAULTAUTO.M  
 Instrument : GC MS 1  
 Sample Name : JDH 38  
 Mass Info :  
 Vial Number : 29



## A.6 Compound 33

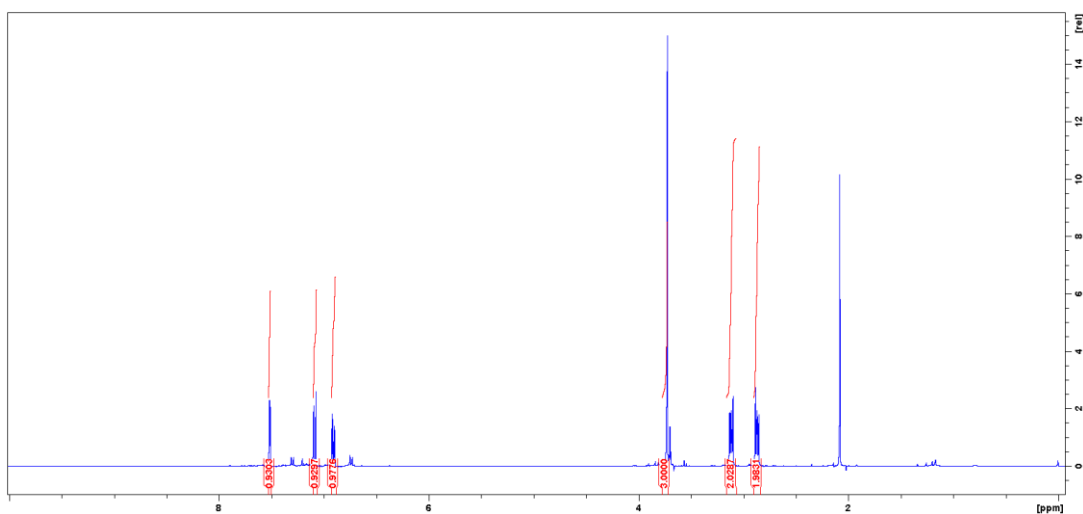
### 6-methoxy-2,3-dihydro-4H-1-benzothiopyran-4-one (33)



Light orange solid, 0.35 g, 38.6 %, 85.2 - 85.7 °C, IR  $\nu_{\max}$  ( $\text{cm}^{-1}$ ): 3022 (Ar-H), 1598 (C=O), 1473 (Aromatic C=C), 1359 ( $\text{CH}_3$  bend), 1046 (C-O), 637 (C-S),  $^1\text{H-NMR}$  (400 MHz,  $\text{CDCl}_3$ ):  $\delta$  = 7.53 (1H, d,  $J$  = 3.0 Hz, H-5), 7.09 (1H, d,  $J$  = 8.8 Hz, H-8), 6.92 (1H, dd,  $J$  = 3.0 Hz, 8.8 Hz, H-7), 3.74 (3H, s,  $\text{OCH}_3$ ), 3.12 (2H, m, H-2), 2.88 (2H, m, H-3);  $^{13}\text{C-NMR}$  (100 MHz,  $\text{CDCl}_3$ ):  $\delta$  = 194.2 (C-4), 157.5 (C-6), 133.6 (C-8), 131.6 (C-4a), 129.6 (C-8), 122.1 (C-7), 111.6 (C-5), 55.5 ( $\text{OCH}_3$ ), 40.7 (C-3), 27.6 (C-2),  $R_f$  = 0.43 (1:1 EtOAc:hexane).

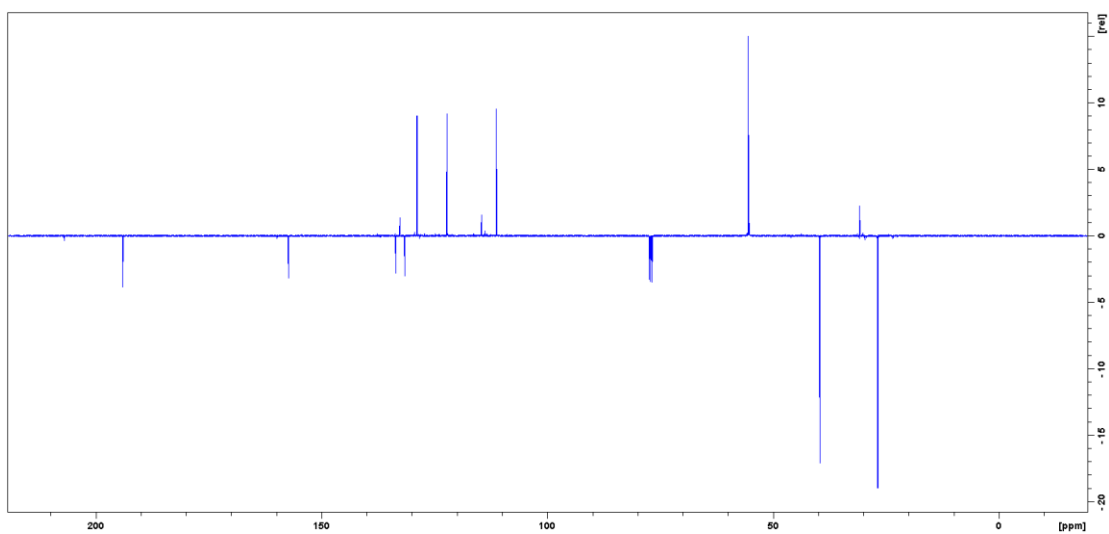
## A.6.1 NMR

### A.6.1.1 $^1\text{H-NMR}$

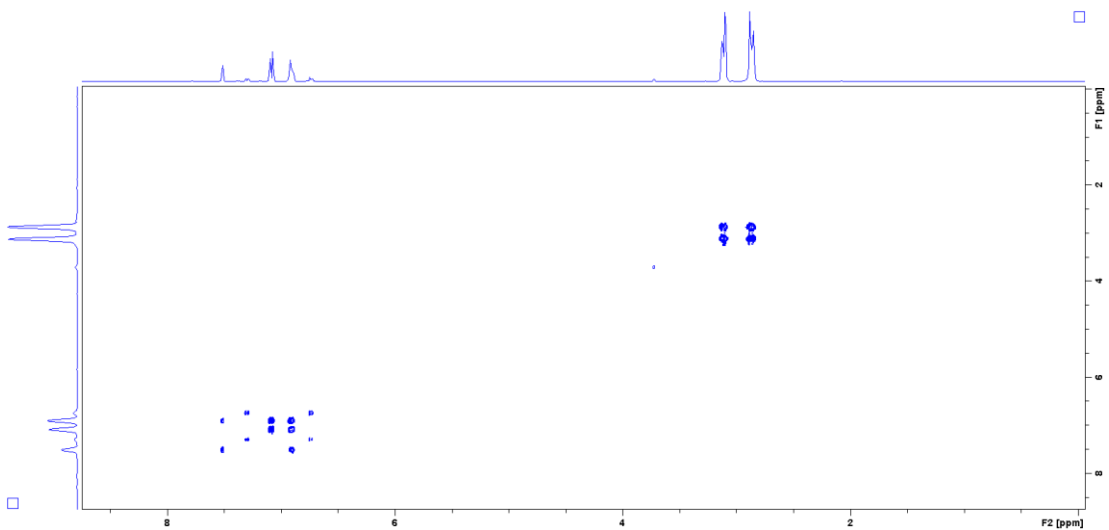




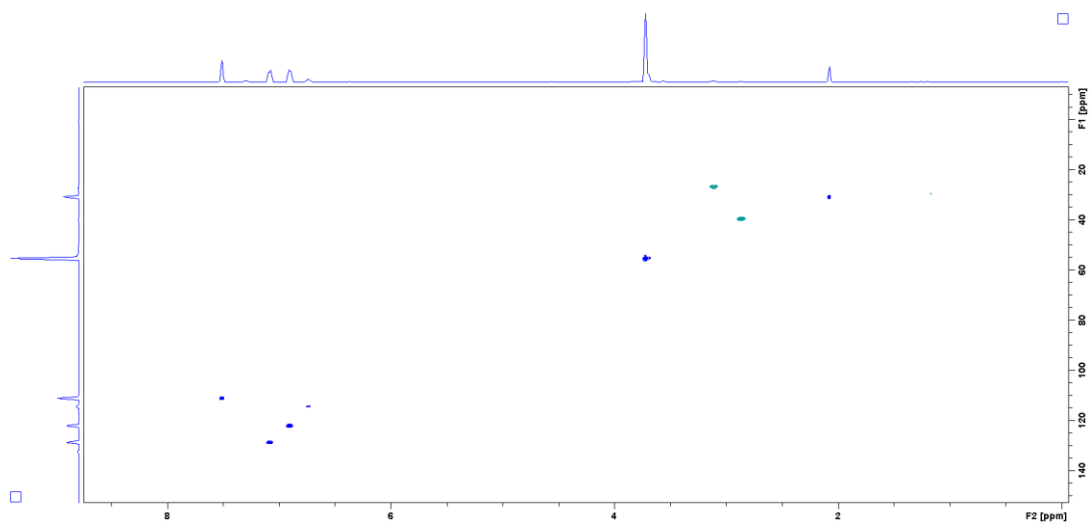
### A.6.1.2 <sup>13</sup>C-NMR



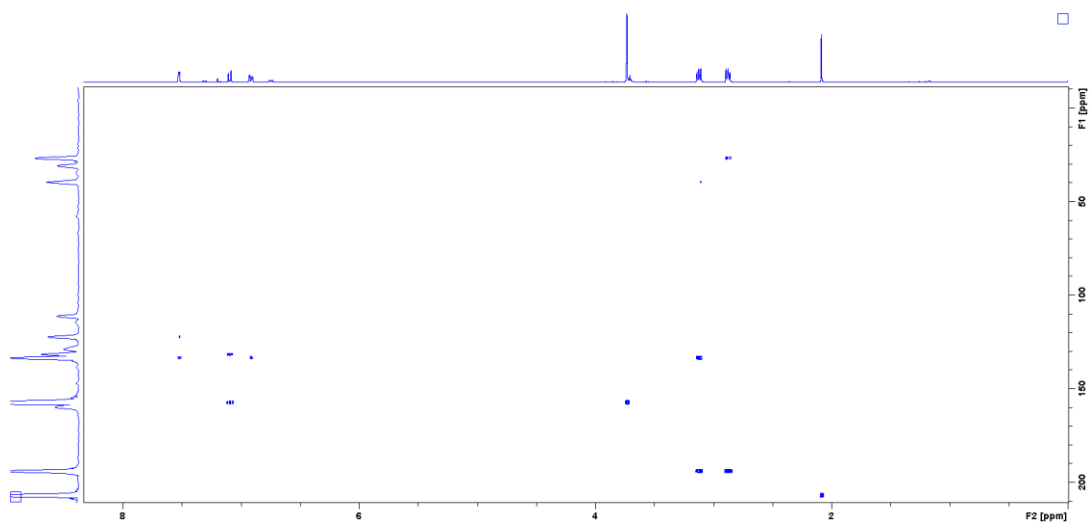
### A.6.1.3 COSY



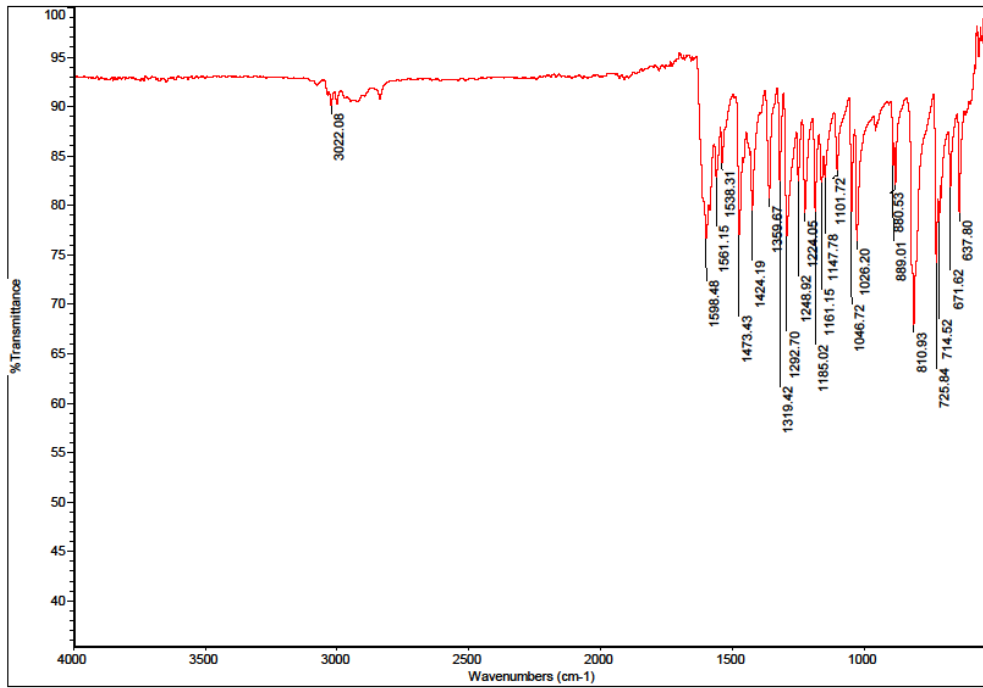
#### A.6.1.4 HSQC



#### A.6.1.5 HMBC



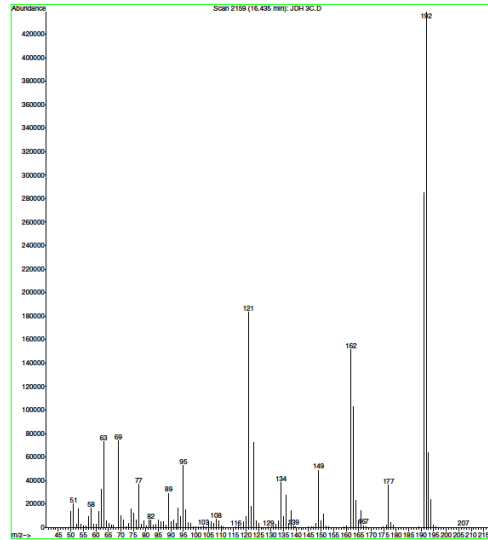
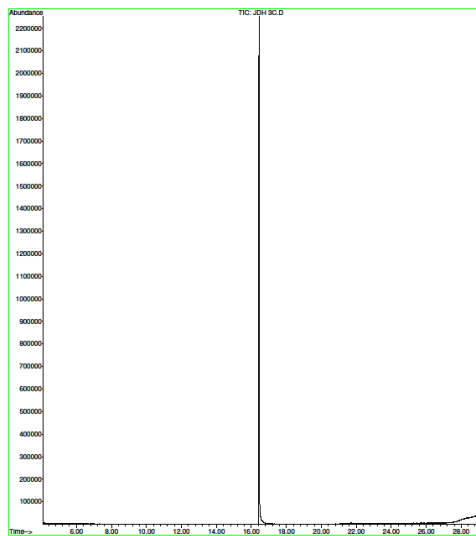
#### A.6.2 IR Data



### A.6.3 GCMS

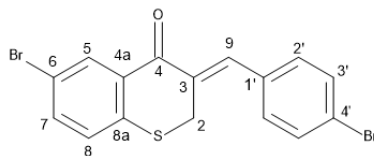
File : E:\DATA\JDR 3C.D  
 Operator :  
 Acquired : 8 May 2019 18:17 using AcqMethod DEFAULTAUTO.M  
 Instrument : GC MS 1  
 Sample Name : JDR 3C  
 Misc Info :  
 Vial Number: 30

File : E:\DATA\JDR 3C.D  
 Operator :  
 Acquired : 8 May 2019 18:17 using AcqMethod DEFAULTAUTO.M  
 Instrument : GC MS 1  
 Sample Name : JDR 3C  
 Misc Info :  
 Vial Number: 30



## A.7 Compound 34

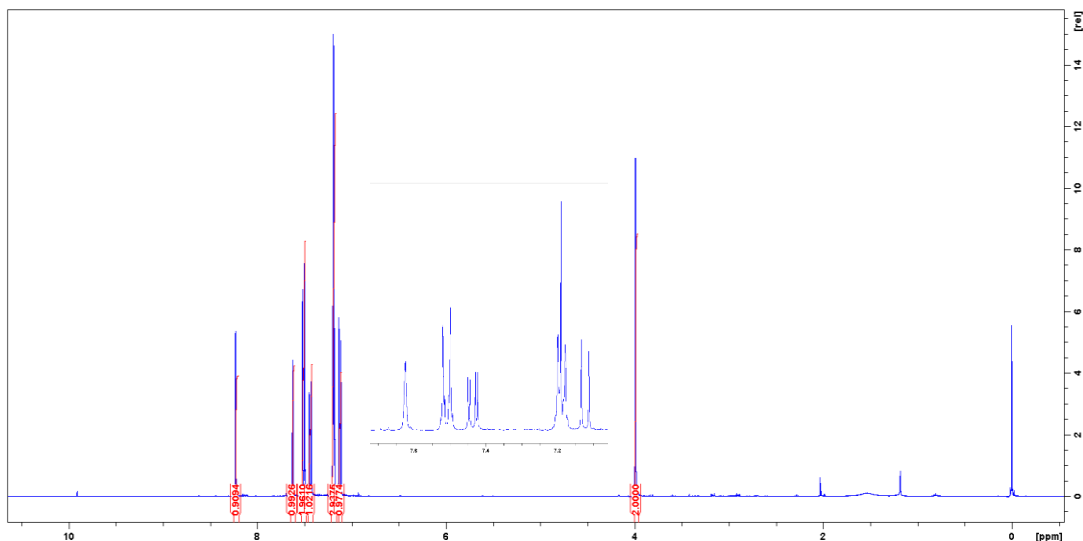
### (3Z)-6-bromo-3-[(4-bromophenyl)methylidene]-2,3-dihydro-4H-1-benzothiopyran-4-one (34)



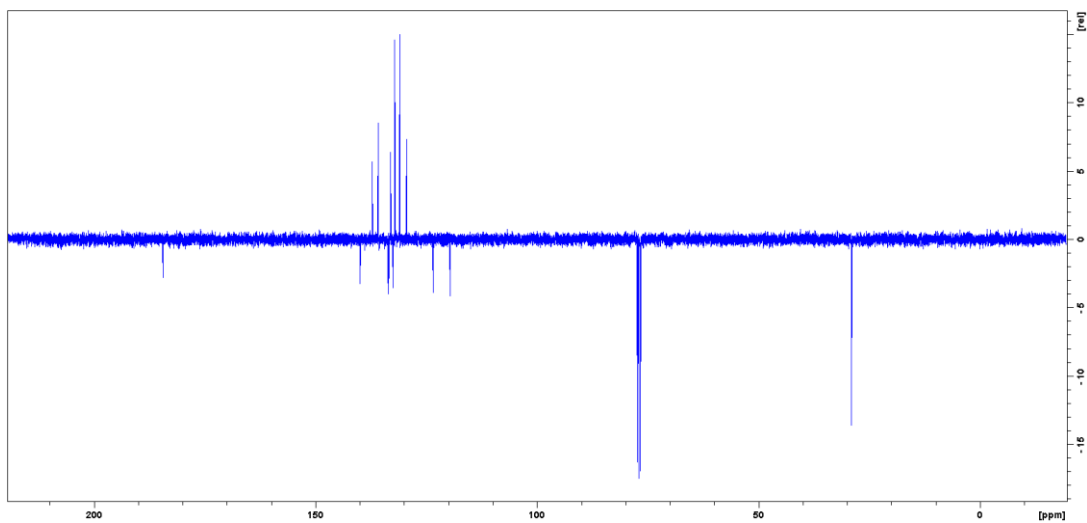
Light yellow solid, 244 mg, 28.3 %, 186.2 - 186.7 °C, IR  $\nu_{\max}$  (cm<sup>-1</sup>): 1647 (C=O), 1568 (Aliphatic C=C), 1485 (Aromatic C=C), 812 (C-Br), 664 (C-S), <sup>1</sup>H-NMR (400 MHz, CDCl<sub>3</sub>):  $\delta$  = 8.23 (1H, d, J = 2.2 Hz, H-5), 7.62 (1H, brs,  $w_{1/2}$  = 2.65 Hz, H-9), 7.51 (2H, d, J = 8.4 Hz, H-3'), 7.44 (1H, dd, J = 2.2 Hz, 8.2 Hz, H-7), 7.19 (2H, d, 8.4 Hz, H-2'), 7.12 (1H, d, J = 8.2 Hz, H-8), 3.99 (2H, d, J = 1.0 Hz, H-2); <sup>13</sup>C-NMR (100 MHz, CDCl<sub>3</sub>):  $\delta$  = 184.5 (C-4), 133.9 (C-8a), 137.2 (C-9), 136.0 (C-7), 133.6 (C-1'), 133.5 (C-4a), 133.3 (C-5), 132.5 (C-3), 132.2 (C-3'), 131.0 (C-2'), 129.5 (C-8), 123.5 (C-4'), 119.7 (C-6), 29.1 (C-2), R<sub>f</sub> = 0.75 (1:1 EtOAc:hexane). HRESMS (ASAP)  $m/z$  408.8895 [M]<sup>+</sup> (calcd for [C<sub>16</sub>H<sub>11</sub>OSBr<sub>2</sub>], 408.8897).

## A.7.1 NMR

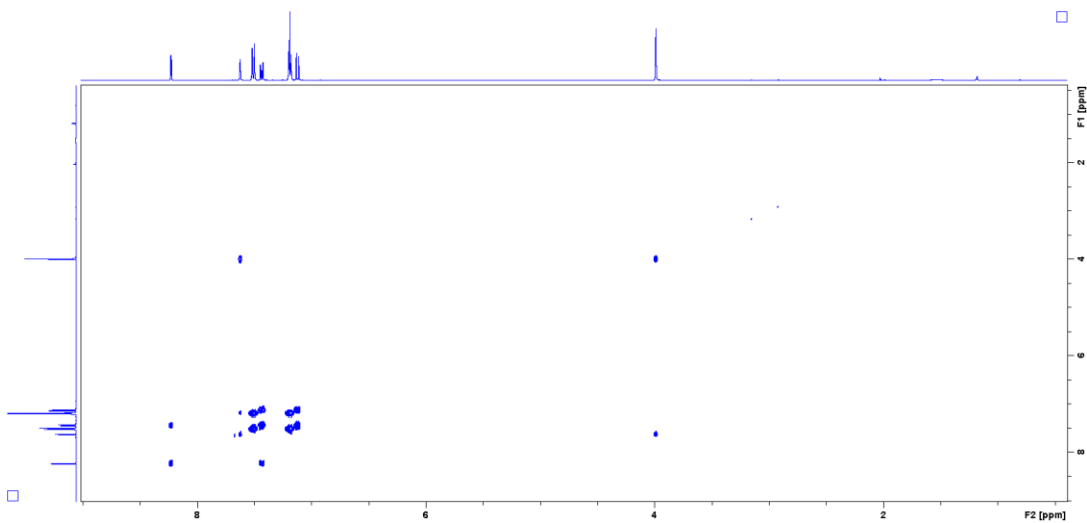
### A.7.1.1 <sup>1</sup>H-NMR



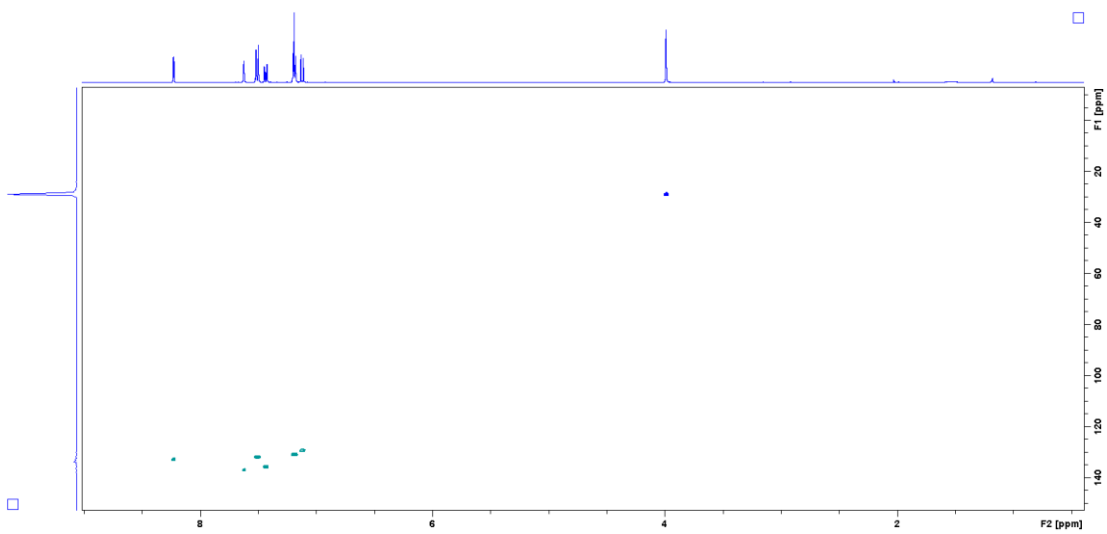
### A.7.1.2 <sup>13</sup>C-NMR



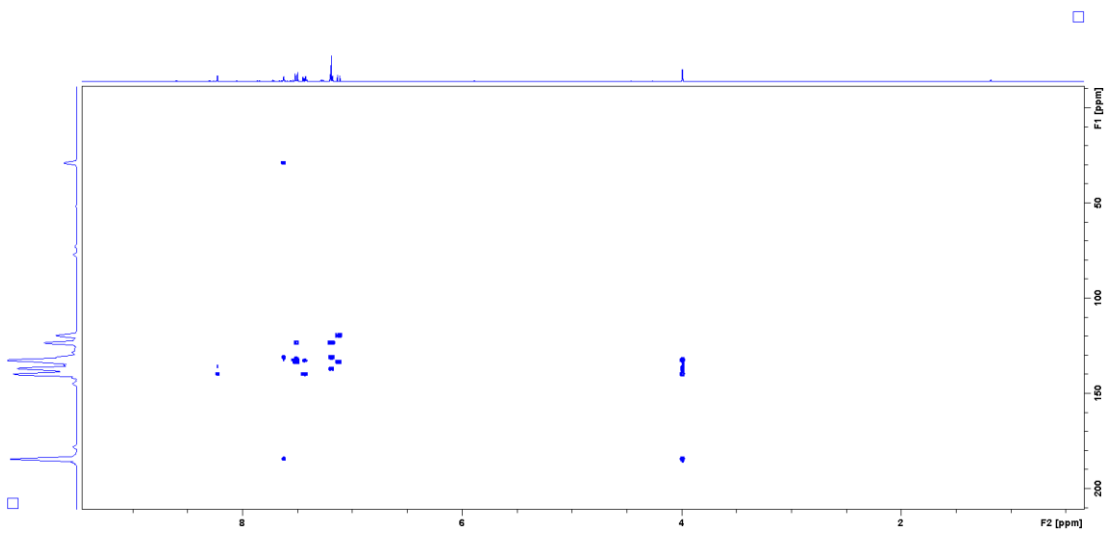
### A.7.1.3 COSY



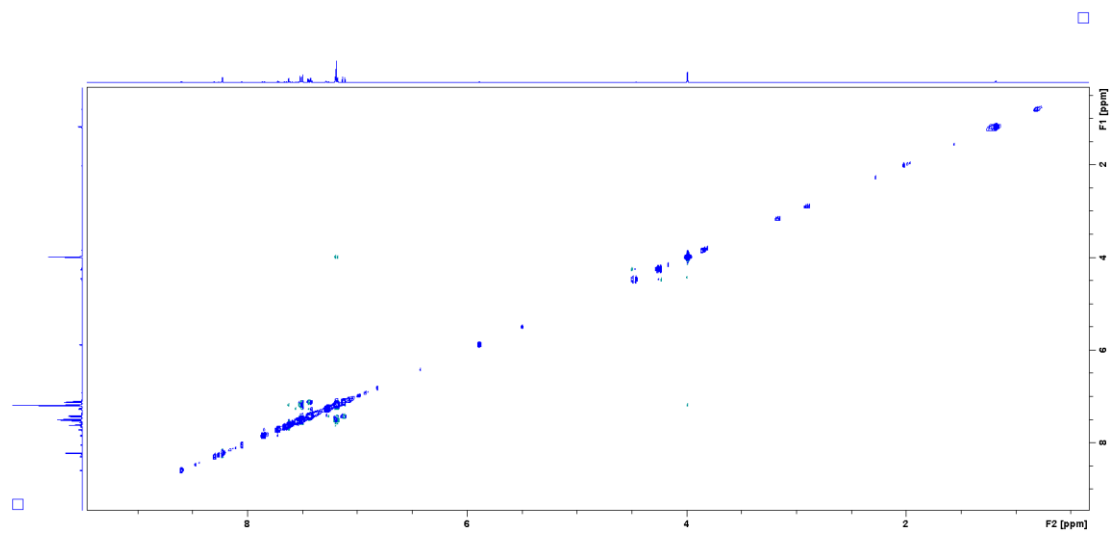
#### A.7.1.4 HSQC



#### A.7.1.5 HMBC



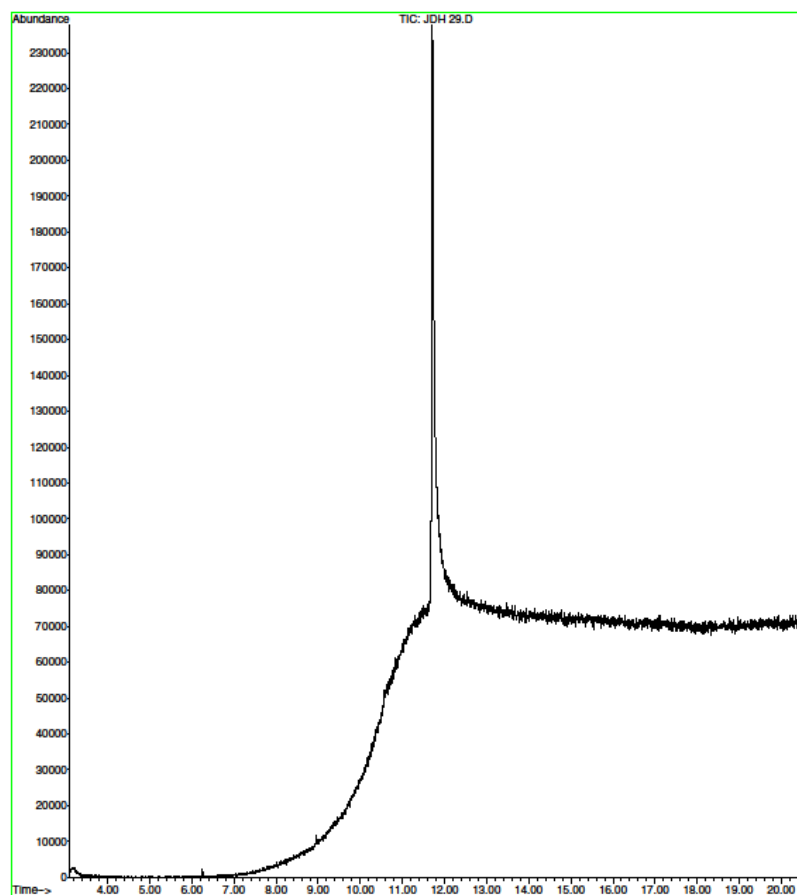
### A.7.1.6 NOESY



## A.7.2 GCMS

### A.7.2.1 CHROMATOGRAM

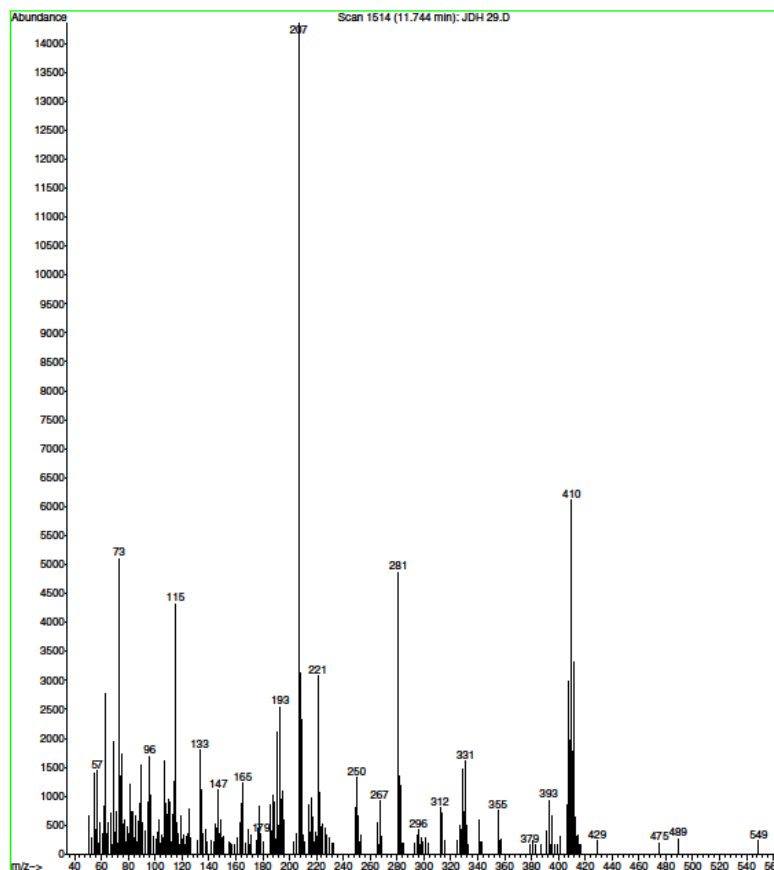
File : E:\DATA\JDH 29.D  
Operator :  
Acquired : 8 May 2019 18:52 using AcqMethod HIGHTEMPAUTO.M  
Instrument : GC MS 1  
Sample Name: JDH 29  
Misc Info :  
Vial Number: 31



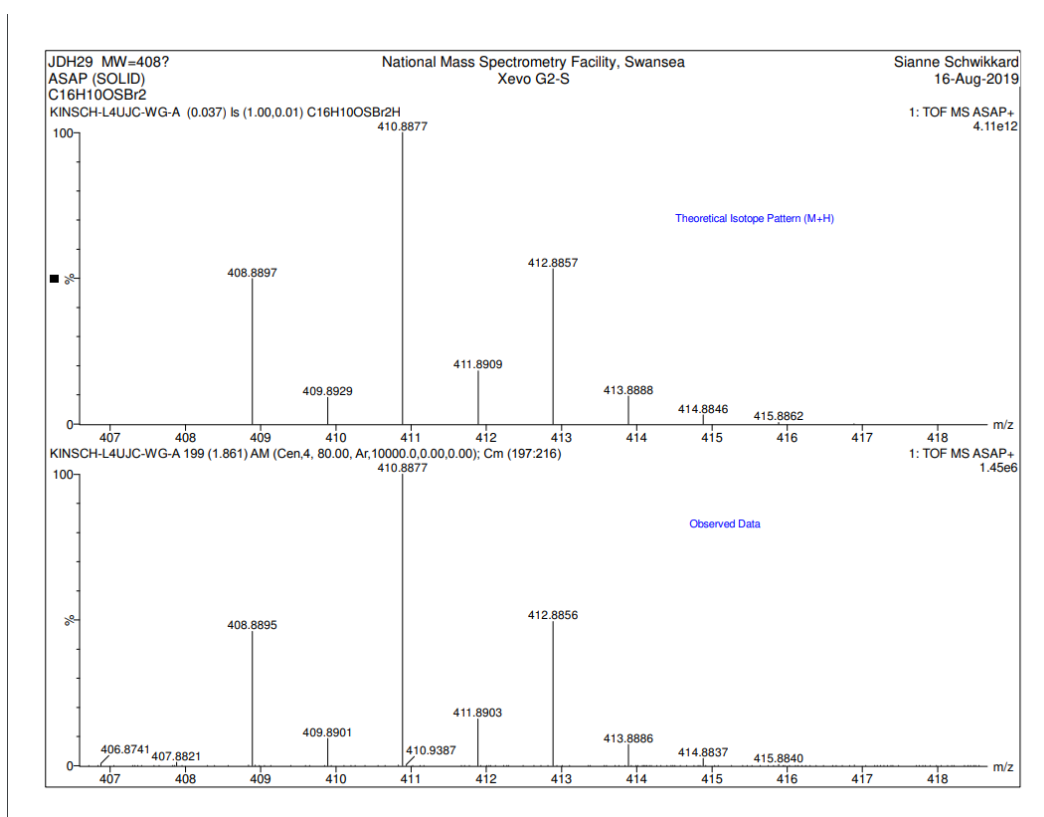
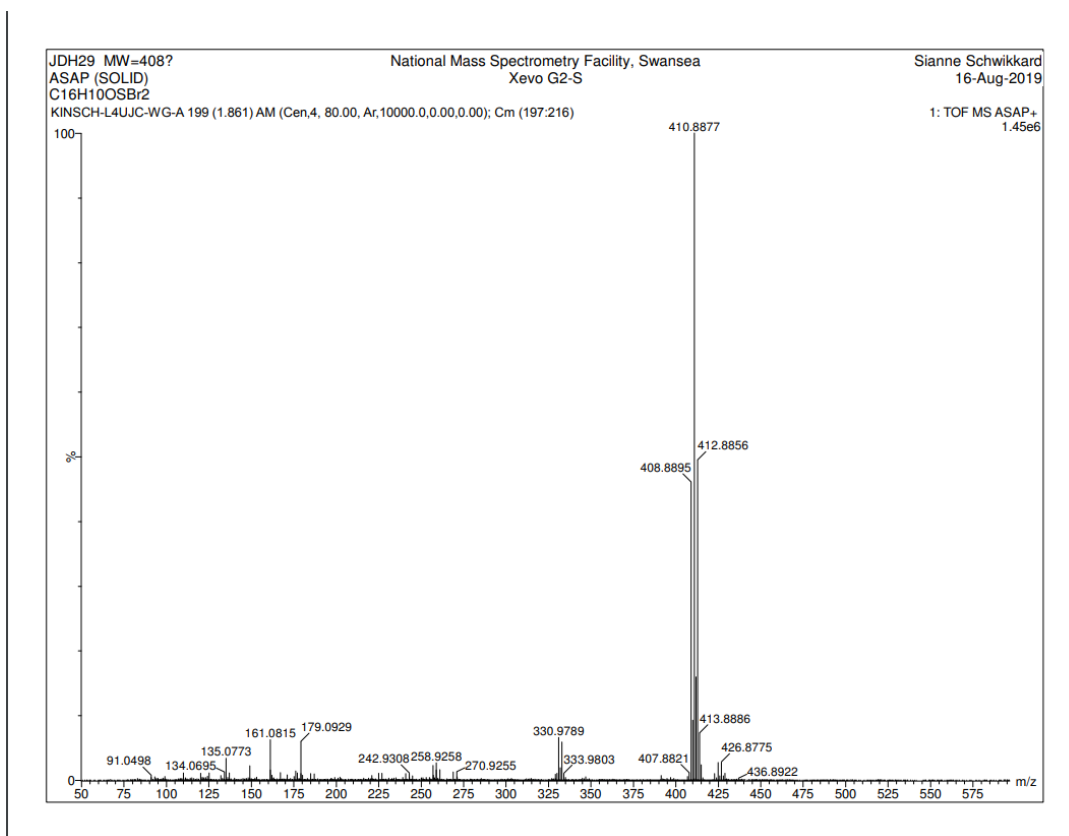


### A.7.2.2 MASS SPEC

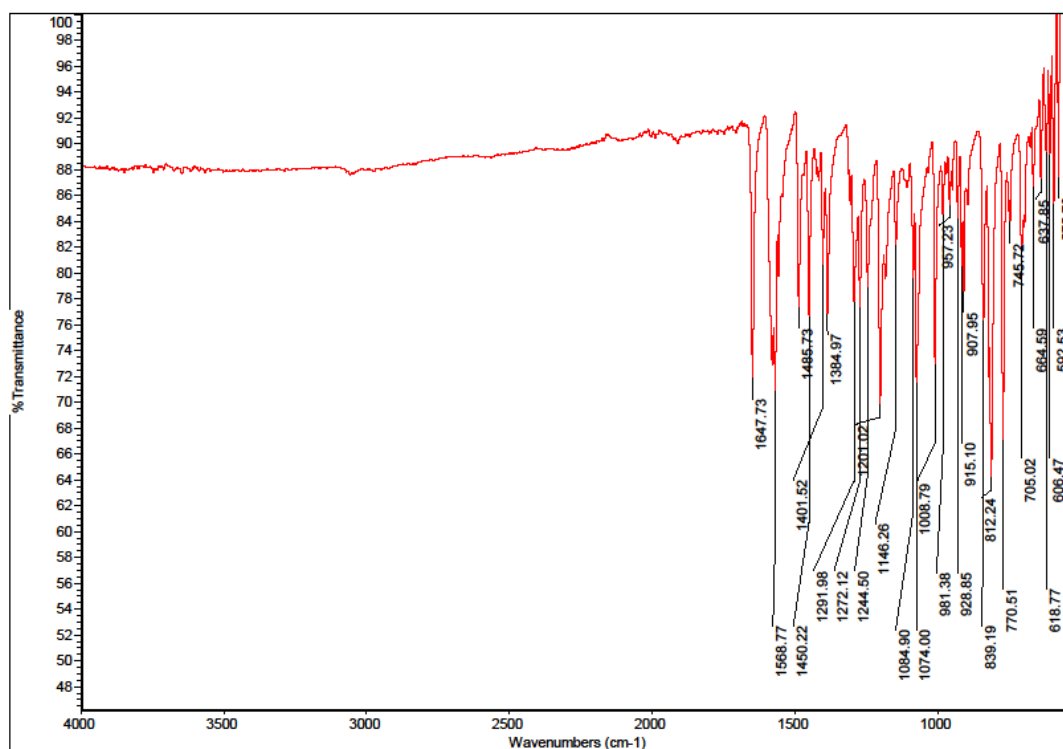
File : E:\DATA\JDH 29.D  
Operator :  
Acquired : 8 May 2019 18:52 using AcqMethod HIGHTEMPAUTO.M  
Instrument : GC MS 1  
Sample Name : JDH 29  
Misc Info :  
Vial Number : 31



### A.7.3 HIGH RES MASS SPEC



## A.7.4 IR DATA



## A.7.5 BIOLOGICAL DATA

### A.7.5.1 CYTOTOXICITY (HeLa)

#### A.7.5.1.1 CYTOTOXICITY PER CONCENTRATION

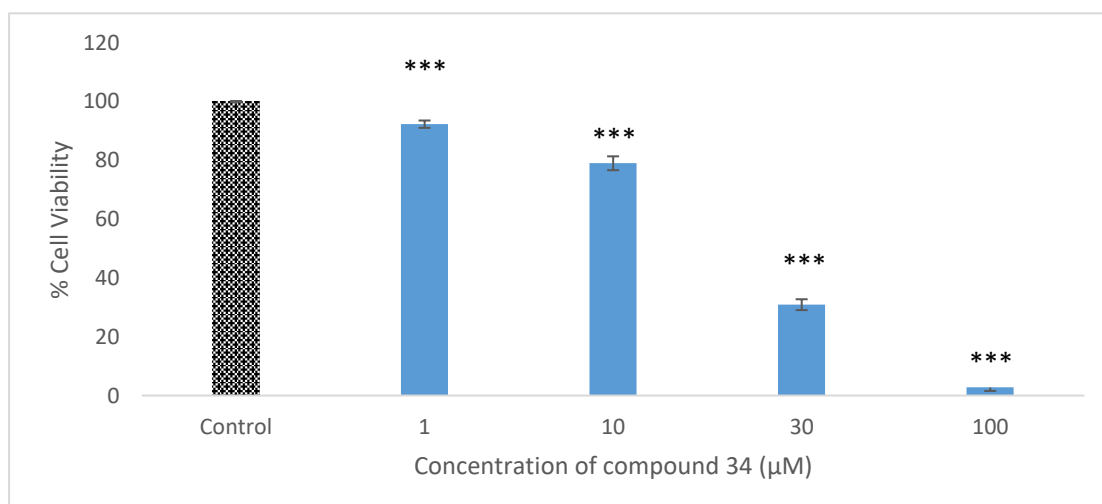
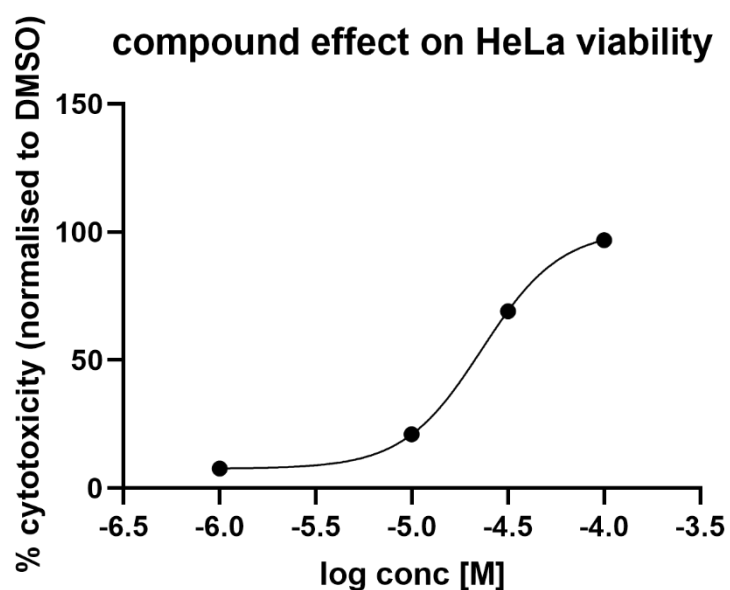


**Figure A.7.5.1.1.** Viability of HeLa cells exposed to different concentrations of compound 34 after 24 h incubation period. Cytotoxicity was determined via neutral red assay. The data is expressed as the percentage of inhibition compared with negative control in which the cell viability was assumed 100 % (means  $\pm$  SD, N=3). All concentrations tested showed significant cytotoxic effect compared to negative control (one way ANOVA with Dunnett's *posthoc* test, \*\*\*P <0.001)

#### A.7.5.1.2 IC<sub>50</sub>



#### A.7.5.2 ANTI-PROLIFERATIVE DATA

##### A.7.5.2.1 ANTI-PROLIFERATION PER CONCENTRATION (HREC)

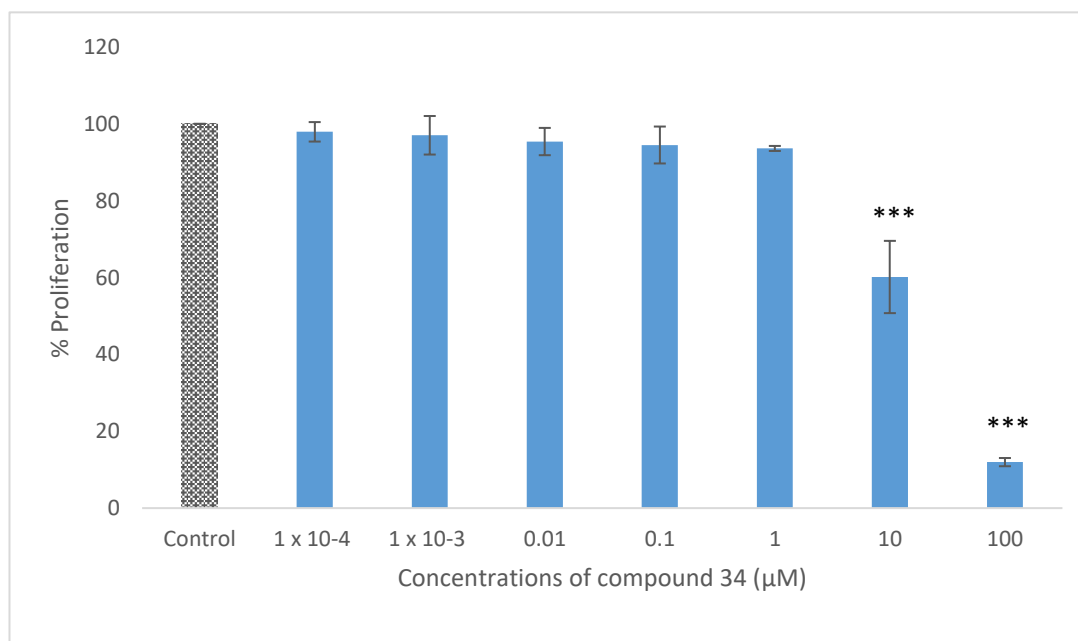
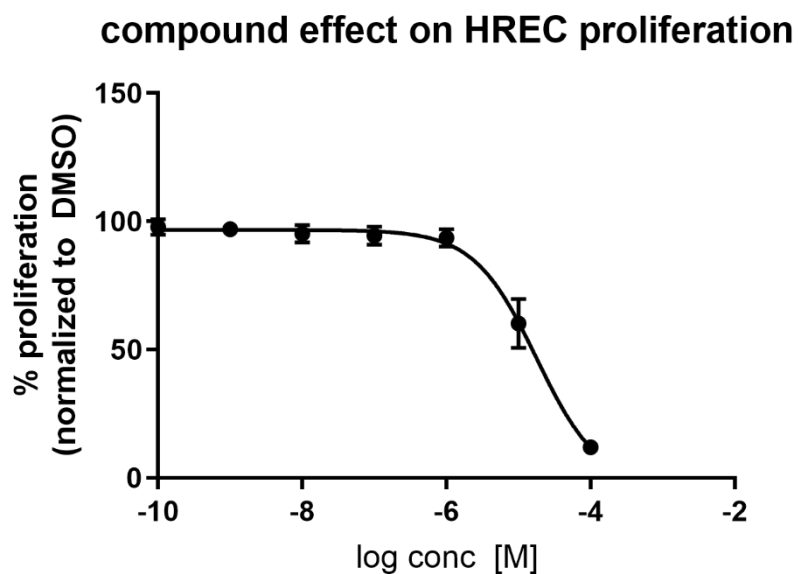


**Figure A.7.5.2.1.** Cell proliferation of HREC cells exposed to different concentrations of compound 34 after 24 hr incubation period. Cell proliferation was determined via the alamarBlue assay. The data is expressed as the percent proliferation compared with negative control in which the cell proliferation was assumed 100% (means  $\pm$  SD, N =3). Concentrations of 10  $\mu$ M and 100  $\mu$ M showed significant anti-proliferative effects compared to negative control (one way ANOVA with Dunnett's *posthoc* test, \*\*\*P <0.001)

#### A.7.5.2.2 GI<sub>50</sub> (HREC)



#### A.7.5.2.3 ANTI-PROLIFERATION PER CONCENTRATION (ARPE-19)

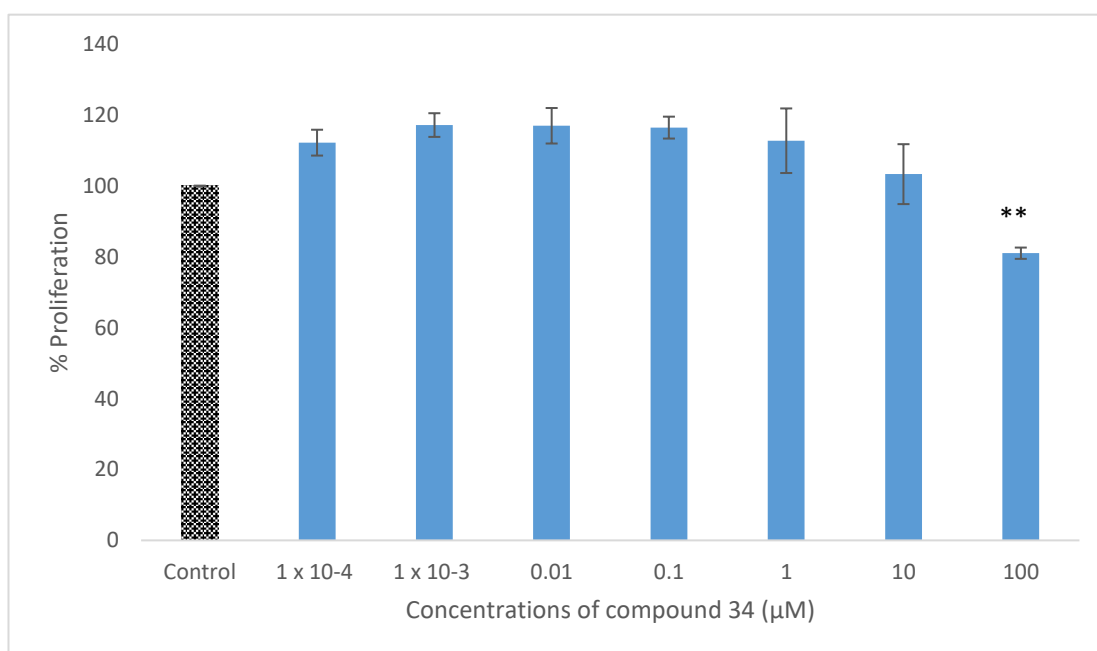
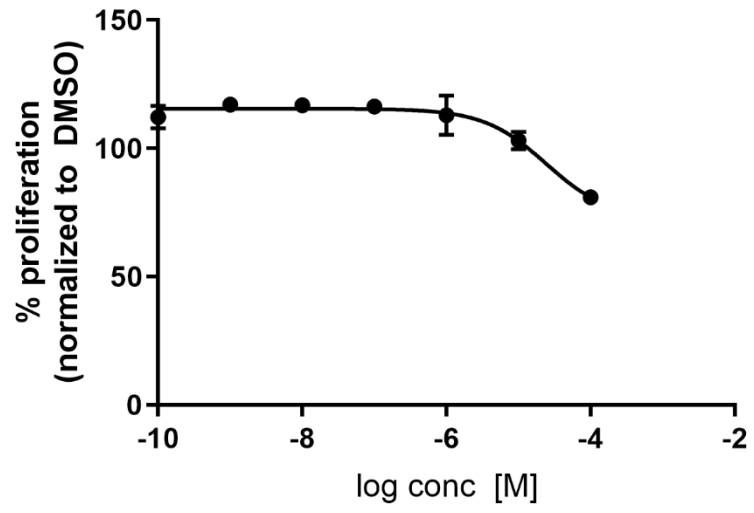


**Figure A.7.5.2.3.** Cell proliferation of ARPE-19 cells exposed to different concentrations of compound 34 after 24 hr incubation period. Cell proliferation was determined via the alamarBlue assay. The data is expressed as the percent proliferation compared with negative control in which the cell proliferation was assumed 100% (means  $\pm$  SD, N=3). Concentration 100  $\mu$ M showed significant anti-proliferative effects compared to negative control (one way ANOVA with Dunnett's *posthoc* test, \*\*P < 0.01).

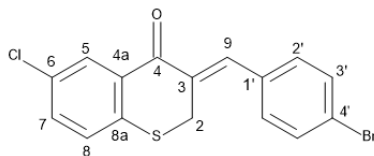
A.7.5.2.4 GI<sub>50</sub> (ARPE-19)

compound effect on ARPE-19 proliferation



## A.8 Compound 35

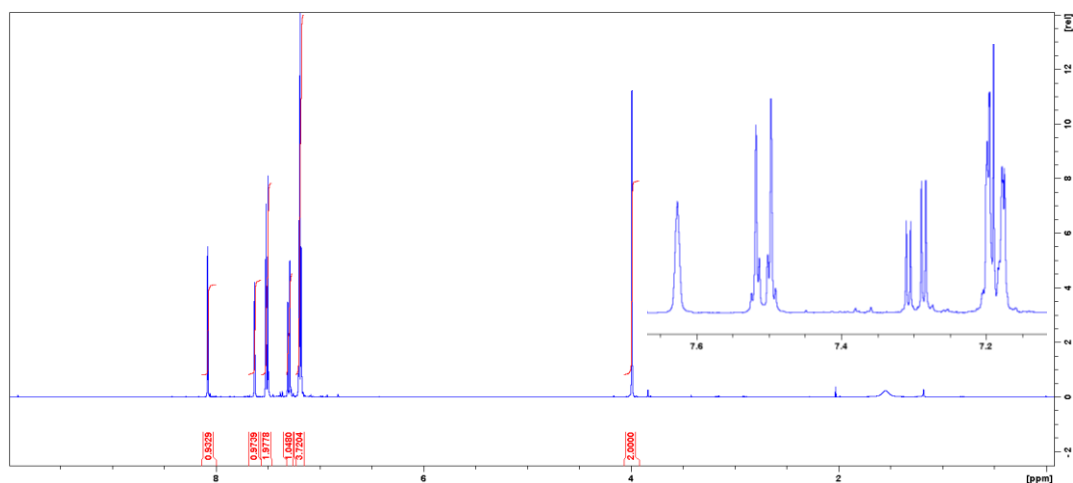
### (3Z)-3-[(4-bromophenyl)methylidene]-6-chloro-2,3-dihydro-4H-1-benzothiopyran-4-one (35)



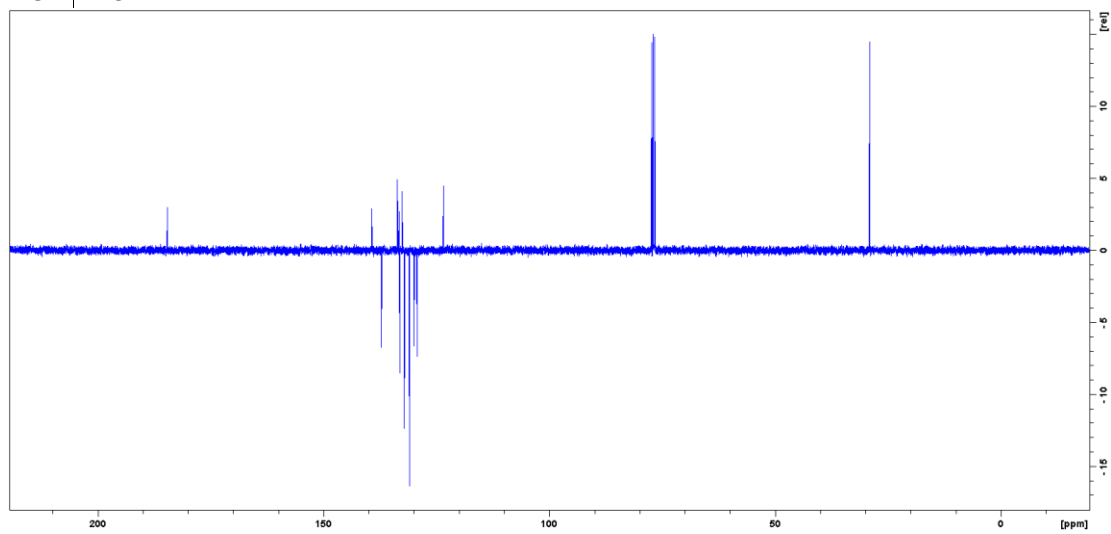
Light yellow solid, 742 mg, 92.3 %, 171.2 - 171.8°C, IR  $\nu_{\max}$  ( $\text{cm}^{-1}$ ): 3375 (Ar-H), 1659 (C=O), 1595 (Aliphatic C=C), 1487 (Aromatic C=C), 814 (C-Cl), 803 (C-Br), 665 (C-S).  $^1\text{H-NMR}$  (400 MHz,  $\text{CDCl}_3$ ):  $\delta$  = 8.08 (1H, d,  $J$  = 2.3 Hz, H-5), 7.62 (1H, brs,  $w_{1/2}$  = 3.2 Hz, H-9), 7.51 (1H, d,  $J$  = 7.9 Hz, H-3'), 7.29 (1H, dd,  $J$  = 2.3, 8.2 Hz, H-7), 7.19 (1H, d,  $J$  = 7.9 Hz, H-2'), 7.19 (1H, d,  $J$  = 8.2 Hz, H-8), 3.97 (2H, d,  $J$  = 1.3 Hz, H-2);  $^{13}\text{C-NMR}$  (100 MHz,  $\text{CDCl}_3$ ):  $\delta$  = 184.6 (C-4), 139.3 (C-8a), 137.2 (C-9), 133.6 (C-6), 133.1 (C-7), 132.6 (C-3), 132.3 (C-4'), 132.2 (C-4a), 132.1 (C-3'), 131.0 (C-2'), 130.0 (C-5), 129.4 (C-8), 29.1 (C-2),  $R_f$  = 0.78 (1:1 EtOAc:hexane). HRESMS (ASAP)  $m/z$  364.9399  $[\text{M}]^+$  (calcd  $[\text{C}_{16}\text{H}_{11}\text{OSClBr}]$ , 364.9043).

## A.8.1 NMR

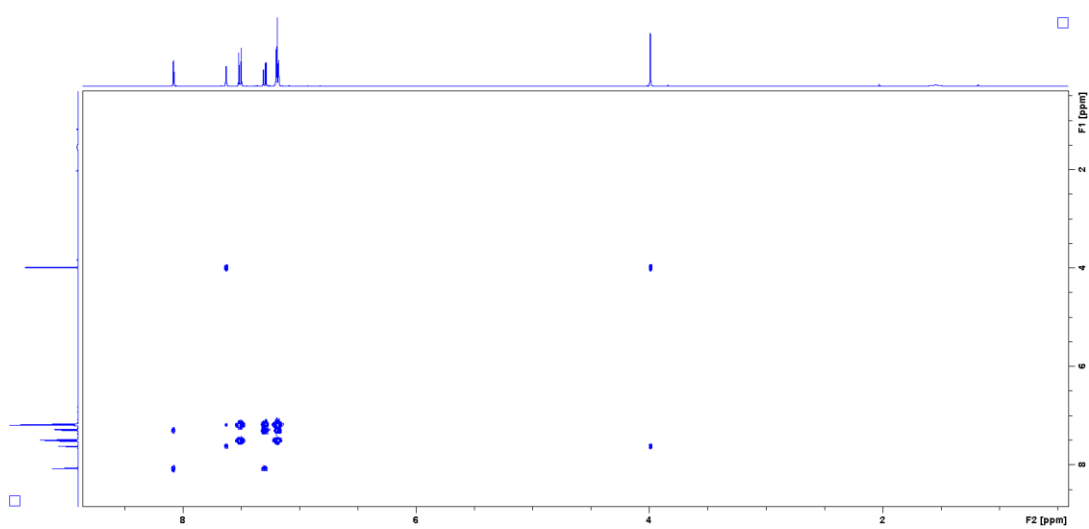
### A.8.1.1 $^1\text{H-NMR}$



### A.8.1.2 $^{13}\text{C}$ -NMR

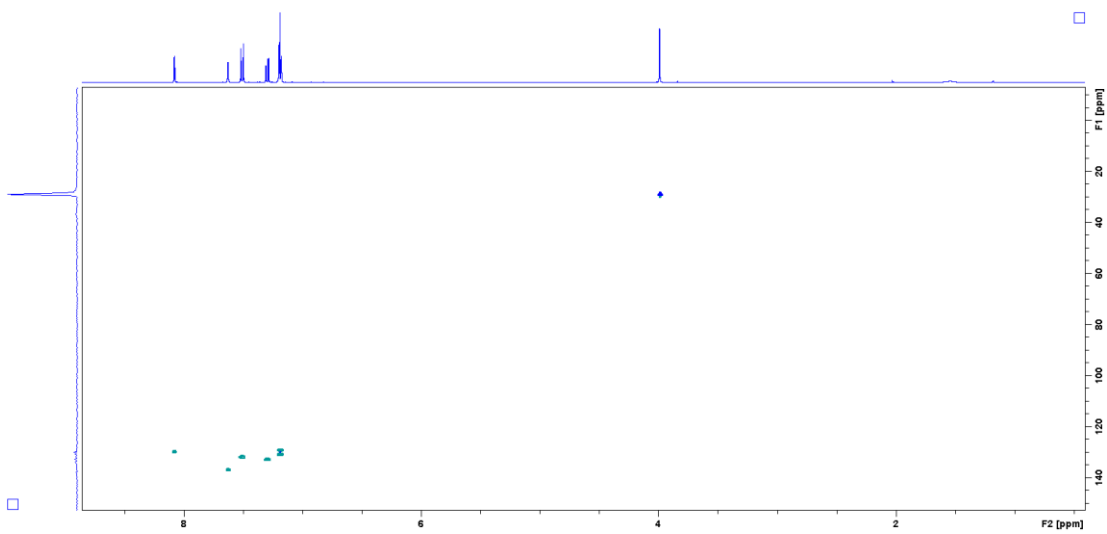


### A.8.1.3 COSY

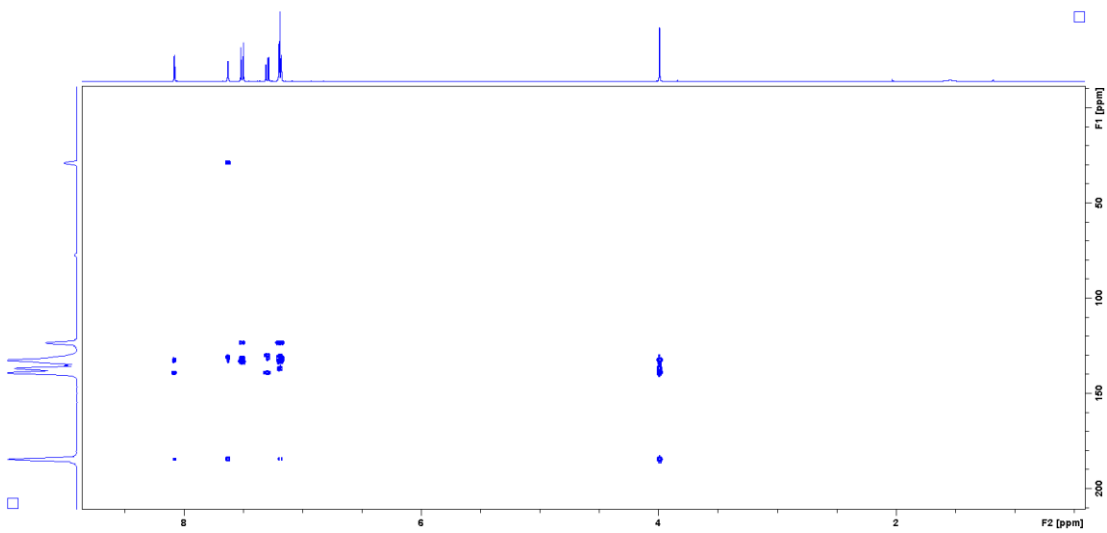




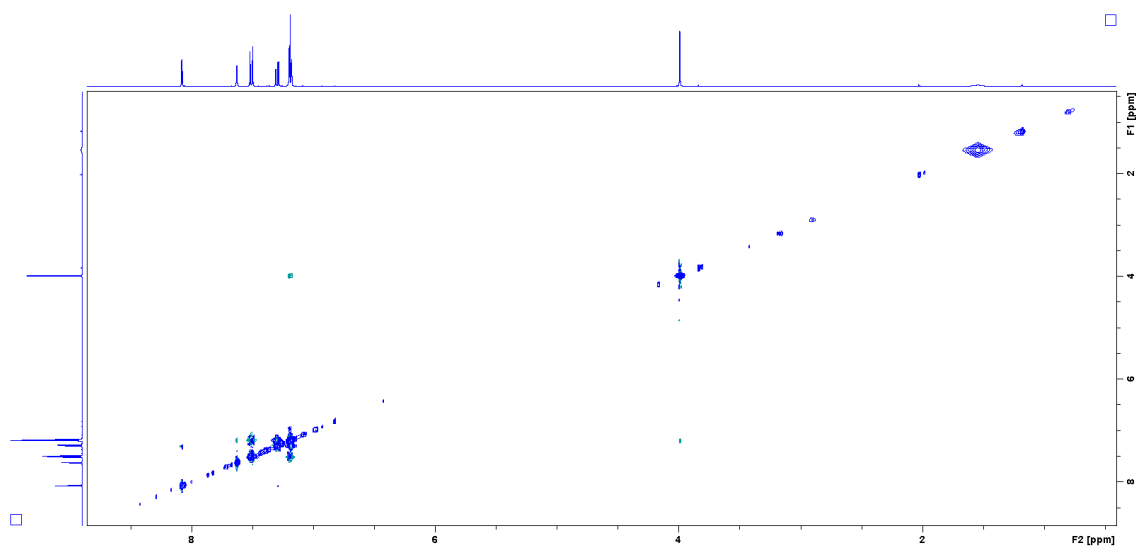
#### A.8.1.4 HSQC



#### A.8.1.5 HMBC



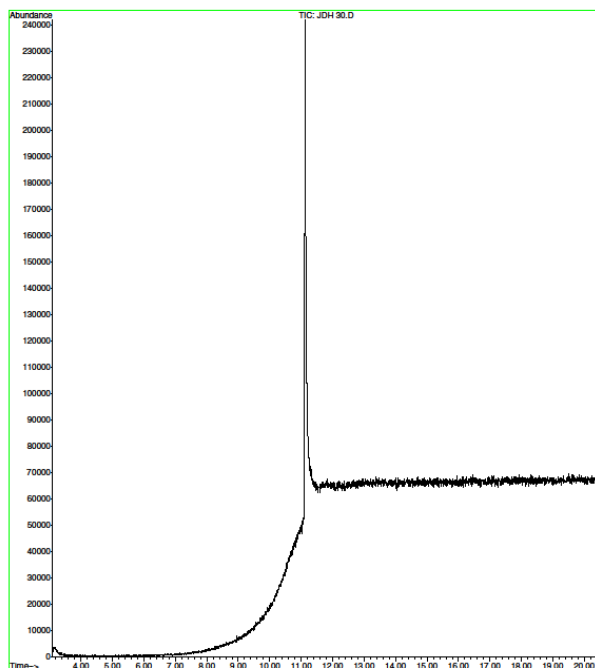
### A.8.1.6 NOESY



### A.8.2 GCMS

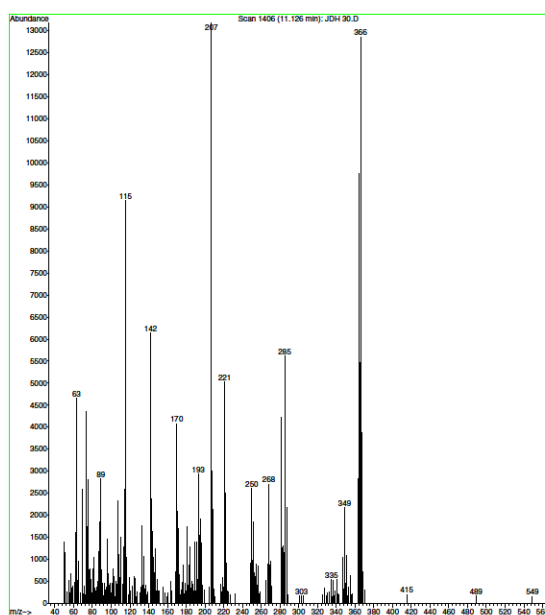
#### A.8.2.1 CHROMATOGRAM

File : E:\DATA\JDR 30.D  
Operator :  
Acquired : 8 May 2019 19:16 using AcqMethod EIGHTPAUTO.M  
Instrument : GC MS 1  
Sample Name: JDR 30  
Misc Info :  
Vial Number: 32

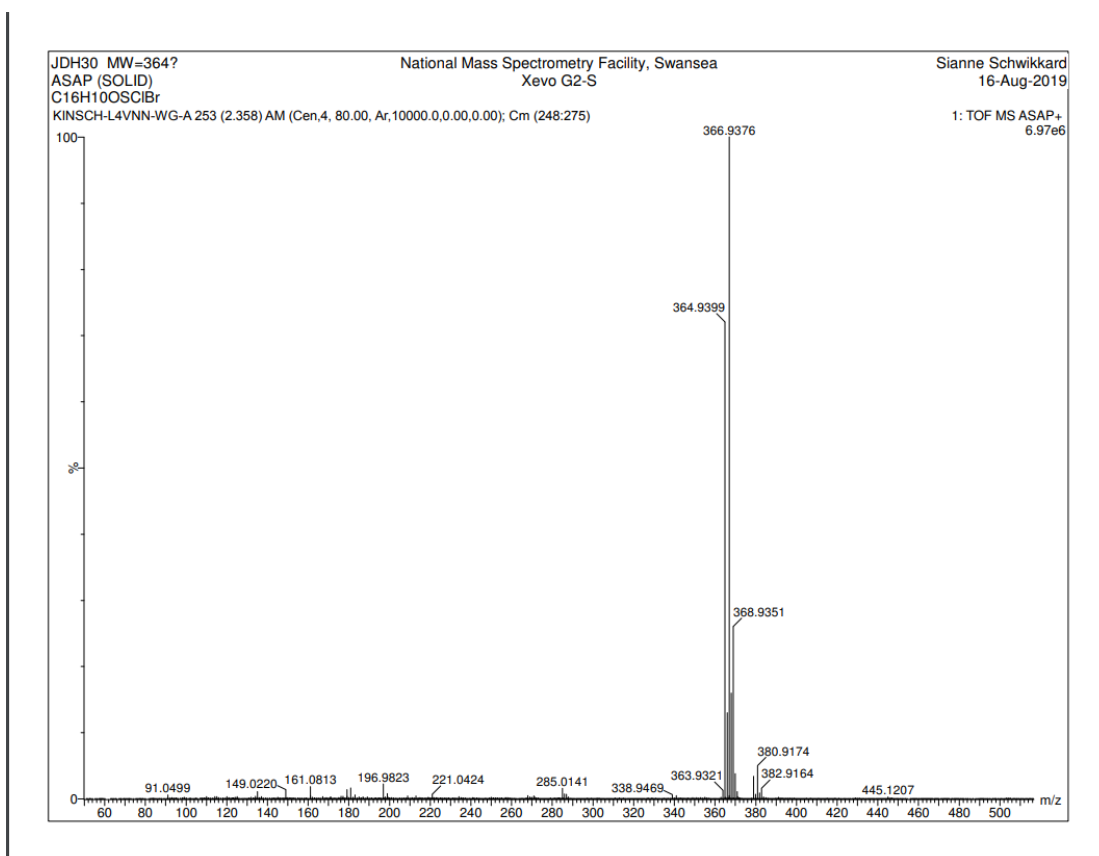


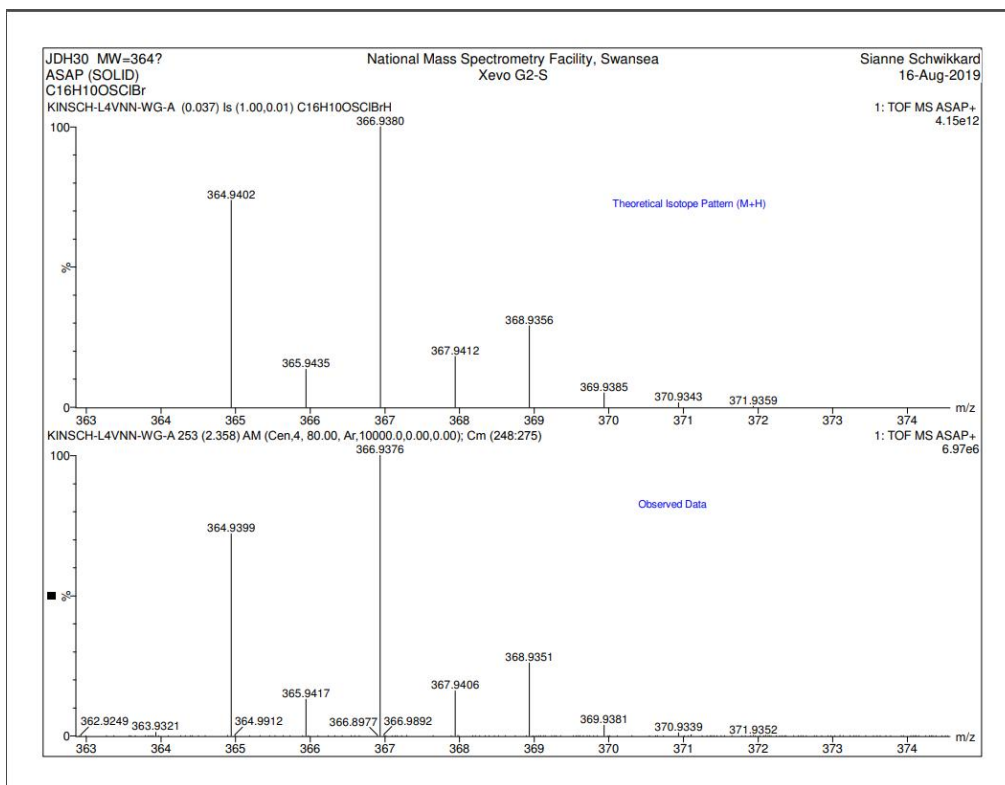
### A.8.2.2 MASS SPEC

File : E:\DATA\JDH 30.D  
Operator :  
Acquired : 8 May 2019 19:16 using AcqMethod HIGHTEMPAUTO.M  
Instrument : GC MS 3  
Sample Name : JDH 30  
Misc Info :  
Vial Number : 32

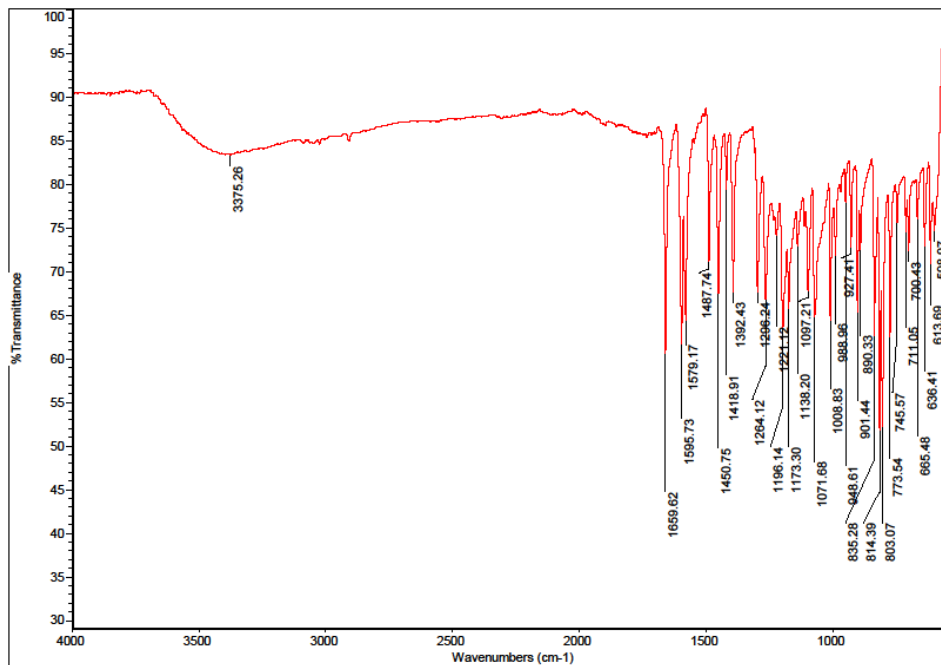


### A.8.3 HIGH RES MASS SPEC





#### A.8.4 IR DATA

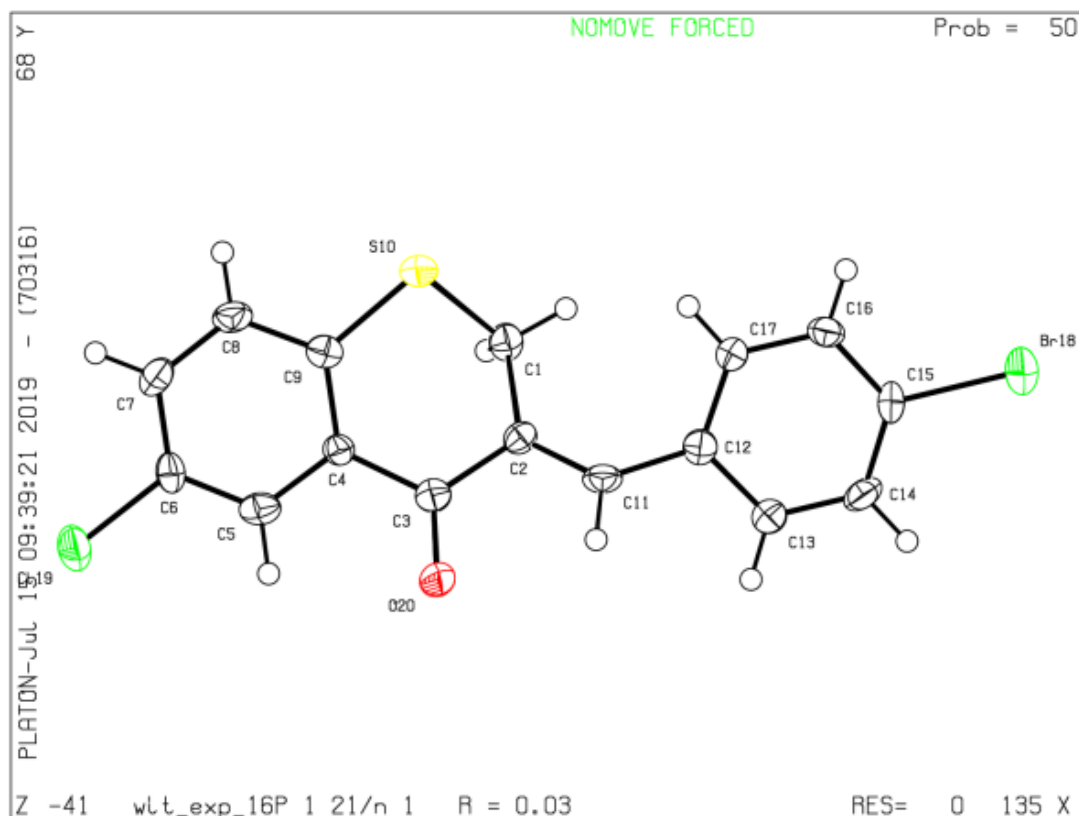


### A.8.5 XRD data

Bond precision: C-C = 0.0068 Å Wavelength=1.54184  
 Cell: a=4.0046(3) b=28.4381(16) c=12.1295(8)  
 alpha=90 beta=90.342(5) gamma=90  
 Temperature: 217 K

|                | Calculated        | Reported          |
|----------------|-------------------|-------------------|
| Volume         | 1381.32(16)       | 1381.32(16)       |
| Space group    | P 21/n            | P 1 21/n 1        |
| Hall group     | -P 2yn            | -P 2yn            |
| Moiety formula | C16 H10 Br Cl O S | C16 H10 Br Cl O S |
| Sum formula    | C16 H10 Br Cl O S | C16 H10 Br Cl O S |
| Mr             | 365.65            | 365.66            |
| Dx, g cm-3     | 1.758             | 1.758             |
| Z              | 4                 | 4                 |
| Mu (mm-1)      | 7.170             | 7.170             |
| F000           | 728.0             | 728.0             |
| F000'          | 729.44            |                   |
| h,k,lmax       | 4,28,12           | 3,28,11           |
| Nref           | 1480              | 1331              |
| Tmin,Tmax      |                   | 0.729,1.000       |
| Tmin'          |                   |                   |

Correction method= # Reported T Limits: Tmin=0.729 Tmax=1.000  
 AbsCorr = MULTI-SCAN  
 Data completeness= 0.899 Theta(max)= 51.240  
 R(reflections)= 0.0346( 1195) wR2(reflections)= 0.0933( 1331)  
 S = 1.069 Npar= 181



## A.8.5 BIOLOGICAL DATA

### A.8.5.1 CYTOTOXICITY (HeLa)

#### A.8.5.1.1 CYTOTOXICITY PER CONCENTRATION

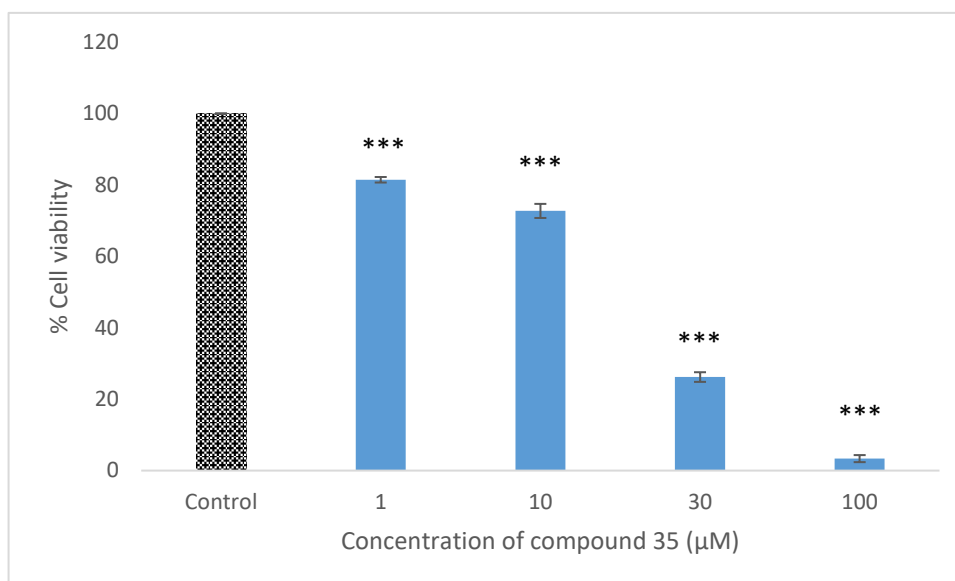
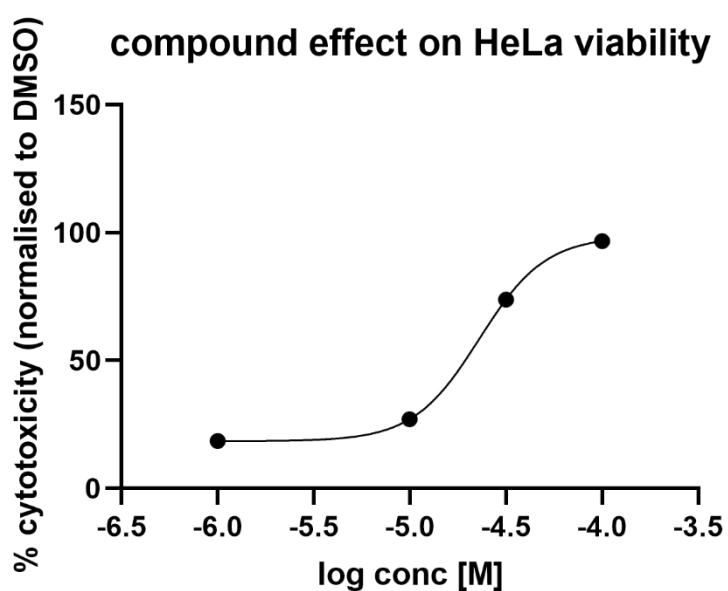


**Figure A.8.5.1.1.** Viability of HeLa cells exposed to different concentrations of compound 35 after 24 h incubation period. Cytotoxicity was determined via neutral red assay. The data is expressed as the percentage of inhibition compared with negative control in which the cell viability was assumed 100 % (means  $\pm$  SD, N =3). All concentrations tested showed significant cytotoxic effect compared to negative control (one way ANOVA with Dunnett's *posthoc* test, \*\*\*P<0.001)

#### A.8.5.1.2 IC<sub>50</sub>



## A.8.5.2 ANTI-PROLIFERATIVE DATA

### A.8.5.2.1 ANTI-PROLIFERATION PER CONCENTRATION (HREC)

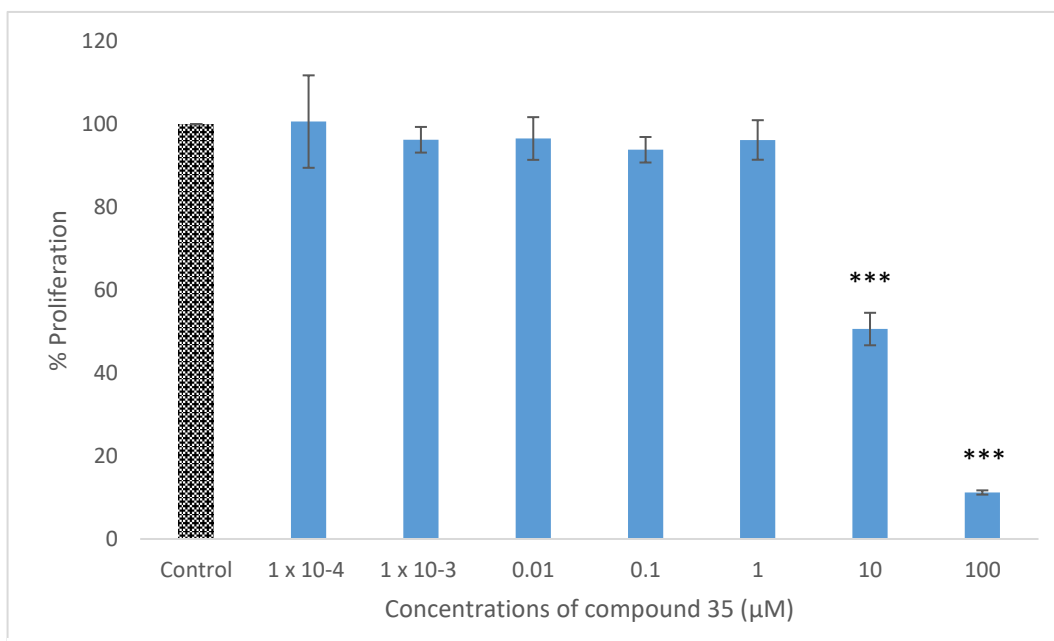
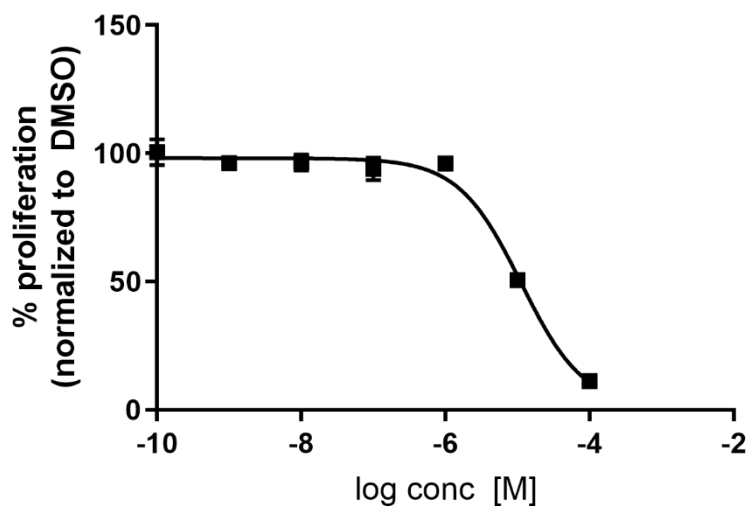


**Figure A.8.5.2.1.** Cell proliferation of HREC cells exposed to different concentrations of compound 35 after 24 hr incubation period. Cell proliferation was determined via the alamarBlue assay. The data is expressed as the percent proliferation compared with negative control in which the cell proliferation was assumed 100% (means  $\pm$  SD, N =3). Concentrations of 10  $\mu$ M and 100  $\mu$ M showed significant anti-proliferative effects compared to negative control (one way ANOVA with Dunnett's *posthoc* test, \*\*\*P <0.001).

### A.8.5.2.2 GI<sub>50</sub> (HREC)

#### compound effect on HREC proliferation



### A.8.5.2.3 ANTI-PROLIFERATION PER CONCENTRATION (ARPE-19)

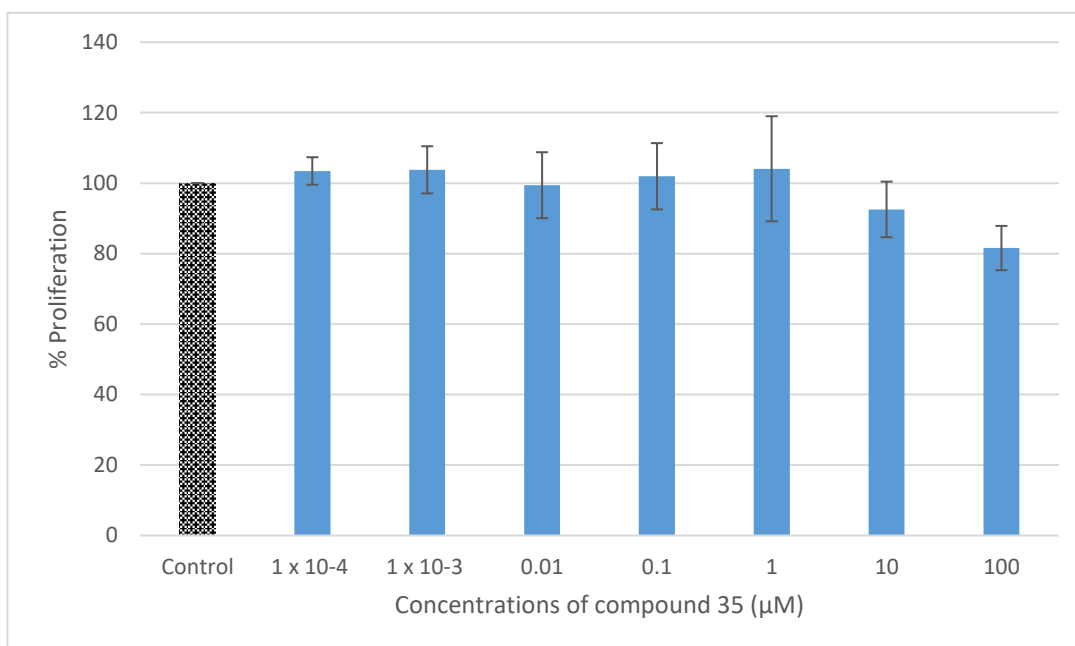
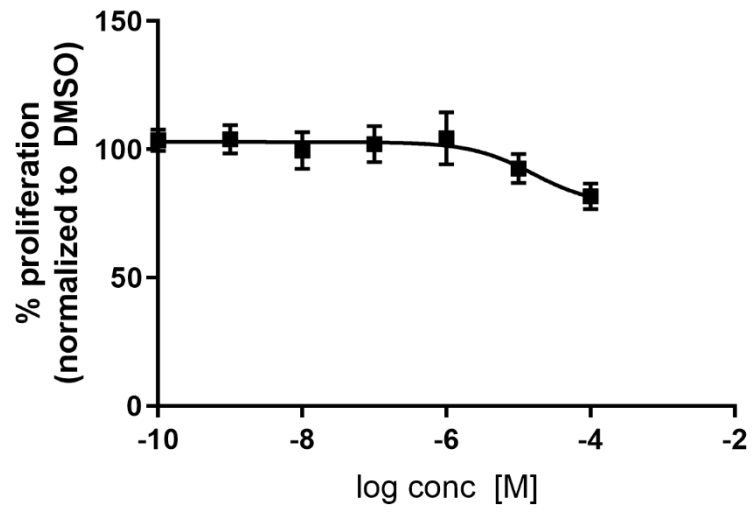


**Figure A.8.5.2.3.** Cell proliferation of ARPE-19 cells exposed to different concentrations of compound 35 after 24 hr incubation period. Cell proliferation was determined via the alamarBlue assay. The data is expressed as the percent proliferation compared with negative control in which the cell proliferation was assumed 100% (means  $\pm$  SD, N =3). No Concentrations showed significant anti-proliferative effects compared to negative control (one way ANOVA with Dunnett's *posthoc* test).



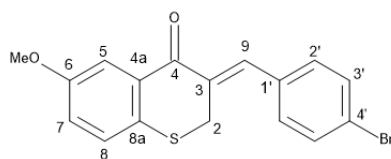
A.8.5.2.4 GI<sub>50</sub> (ARPE-19)

compound effect on ARPE-19 proliferation



## A.9 Compound 36

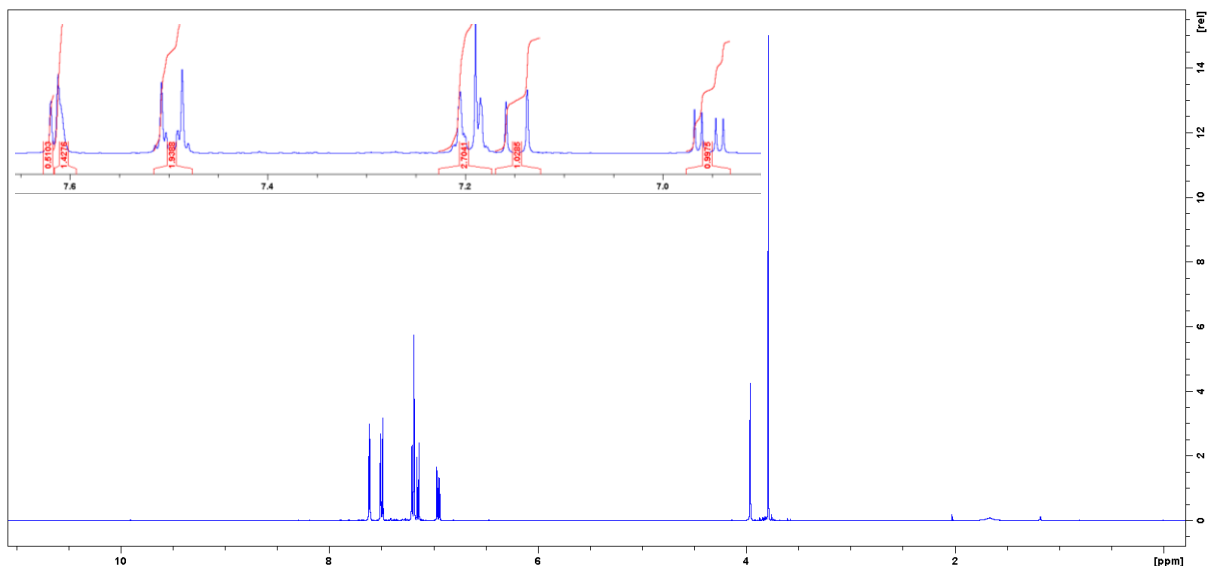
### (3Z)-3-[(4-bromophenyl)methylidene]-6-methoxy-2,3-dihydro-4H-1-benzothiopyran-4-one (36)



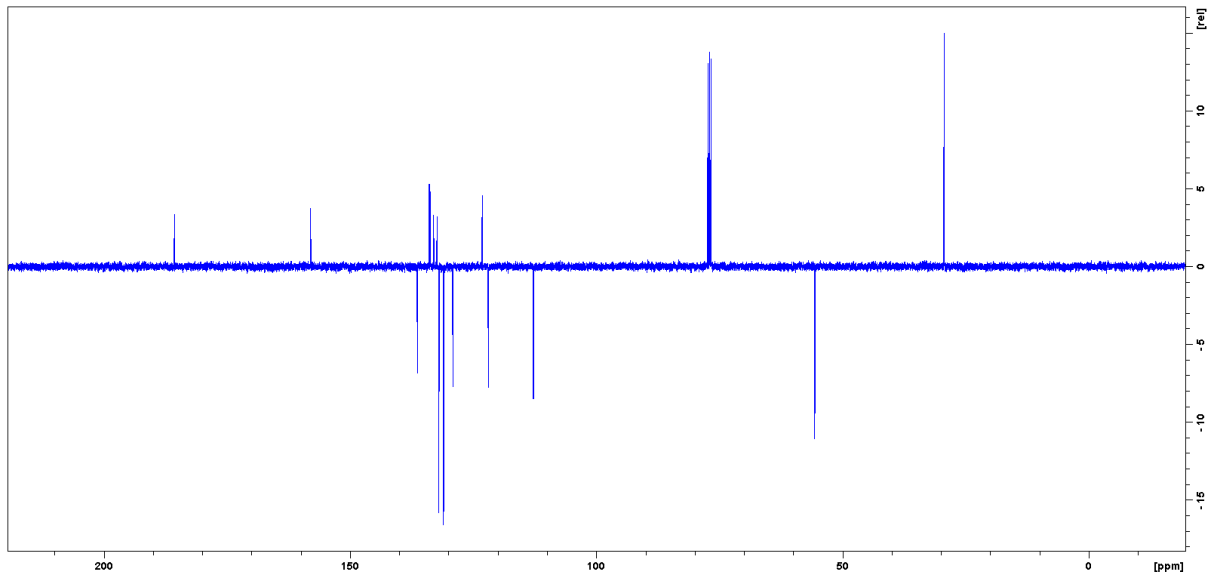
Light yellow solid, 260 mg, 44.4 %, 146.5 - 147.1 °C, IR  $\nu_{\max}$  (cm<sup>-1</sup>): 2934 (Ar-H), 1650 (C=O), 1583 (Aliphatic C=C), 1471 (Aromatic C=C), 1026 (C-O), 824 (C-Br), 654 (C-S), <sup>1</sup>H-NMR (400 MHz, CDCl<sub>3</sub>):  $\delta$  = 7.62 (1H, d, J = 3.0 Hz, H-5), 7.60 (1H, brs,  $w_{1/2}$  = 2.70 Hz, H-9), 7.49 (2H, d, J = 8.2 Hz, H-3'), 7.19 (2H, d, J = 8.2 Hz, H-2'), 7.14 (1H, d, J = 8.8 Hz, H-8), 6.95 (1H, dd, J = 3.0 Hz, 8.8 Hz, H-7), 3.96 (2H, d, J = 1.0 Hz, H-2), 3.79 (3H, s, OCH<sub>3</sub>); <sup>13</sup>C-NMR (100 MHz, CDCl<sub>3</sub>):  $\delta$  = 185.6 (C-4), 158.1 (C-6), 136.3 (C-9), 133.9 (C-4'), 133.7 (C-4a), 133.1 (C-8a), 132.4 (C-3), 132.0 (C-3'), 131.3 (C-8a), 129.1 (C-8), 123.2 (C-1'), 122.2 (C-7), 112.8 (C-5), 55.9 (OCH<sub>3</sub>), 29.4 (C-2), R<sub>f</sub> = 0.75 (1:1 EtOAc:hexane). HRESMS (ASAP)  $m/z$  360.9896 [M]<sup>+</sup> (calcd [C<sub>17</sub>H<sub>14</sub>O<sub>2</sub>SBr], 360.9898).

## A.9.1 NMR

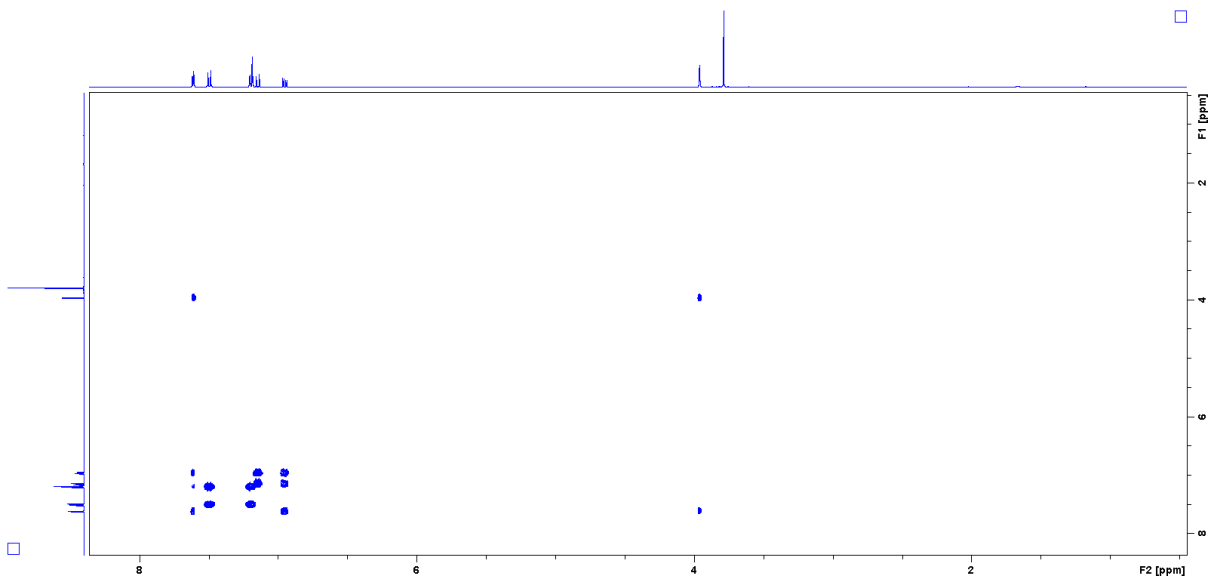
### A.9.1.1 <sup>1</sup>H-NMR



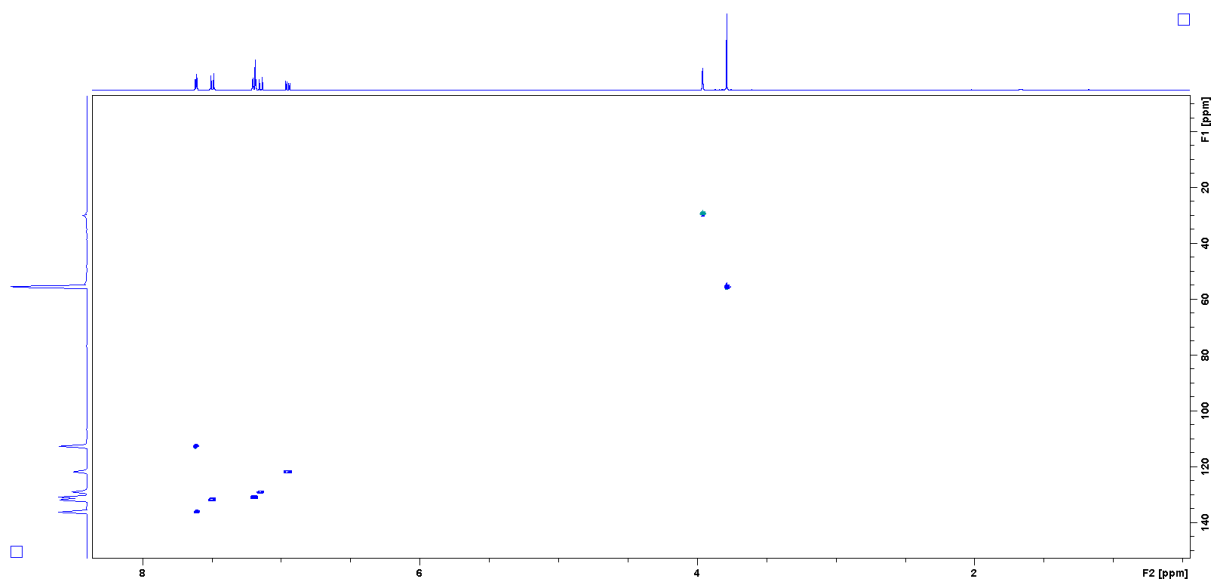
### A.9.1.2 $^{13}\text{C}$ -NMR



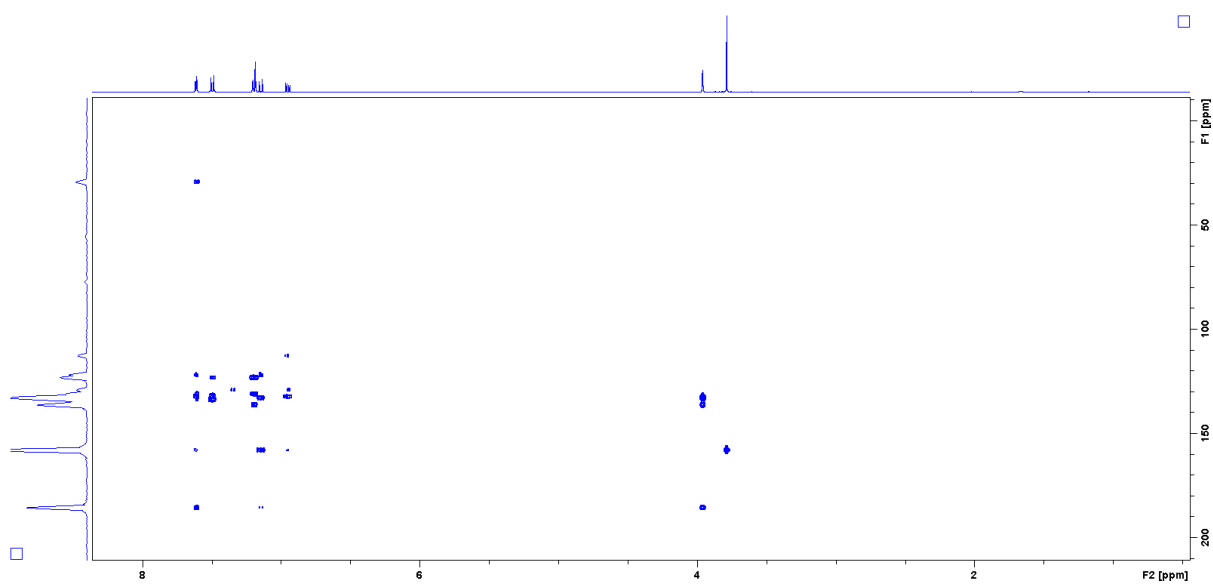
### A.9.1.3 COSY



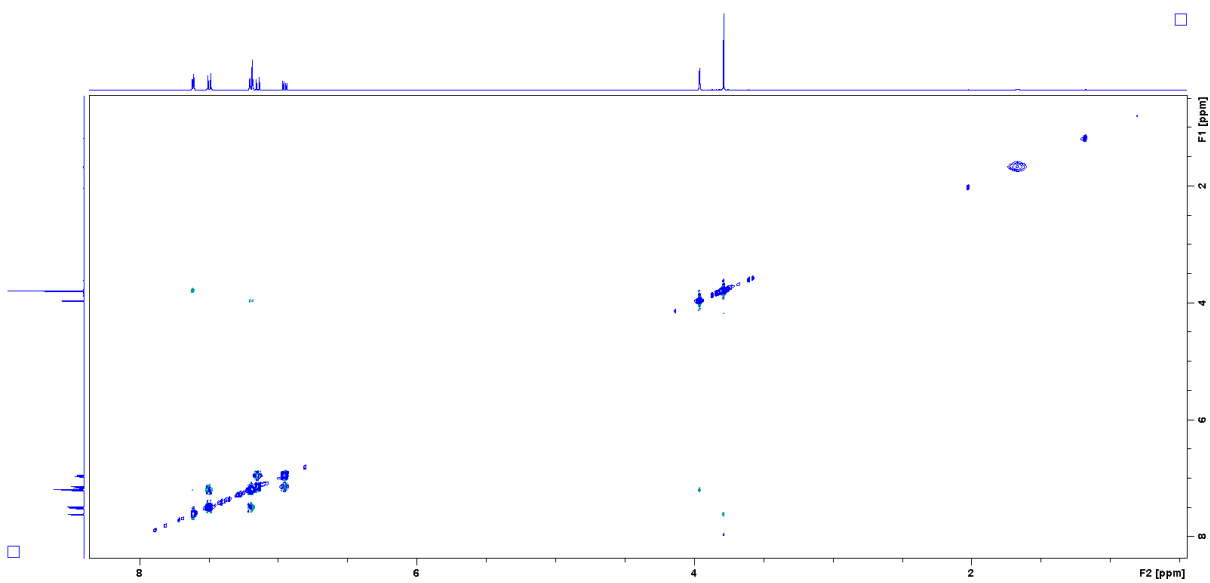
#### A.9.1.4 HSQC



#### A.9.1.5 HMBC



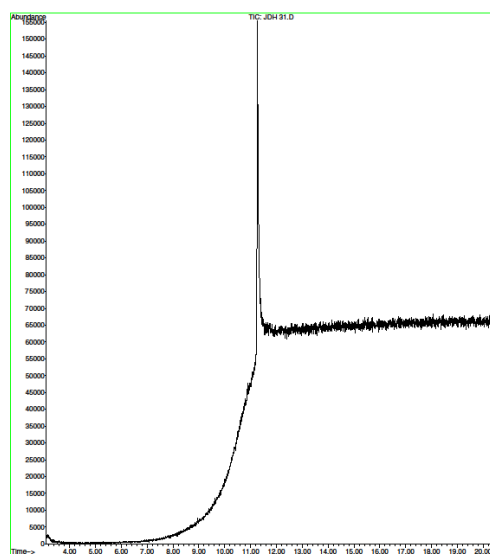
### A.9.1.6 NOESY



### A.9.2 GCMS

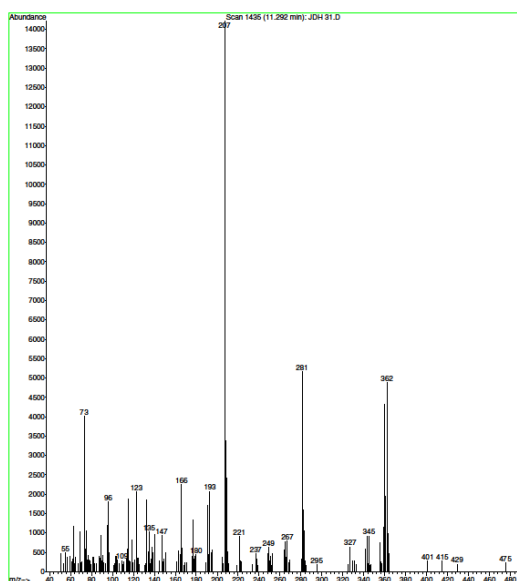
#### A.9.2.1 CHROMATOGRAM

File : E:\DATA\J08 31.D  
Operator :  
Acquired : 8 May 2019 19:40 using AcqMethod HIGHTEMPAUTO.M  
Instrument : GC MS 1  
Sample Name : J08 31  
Misc Info :  
Vial Number: 33

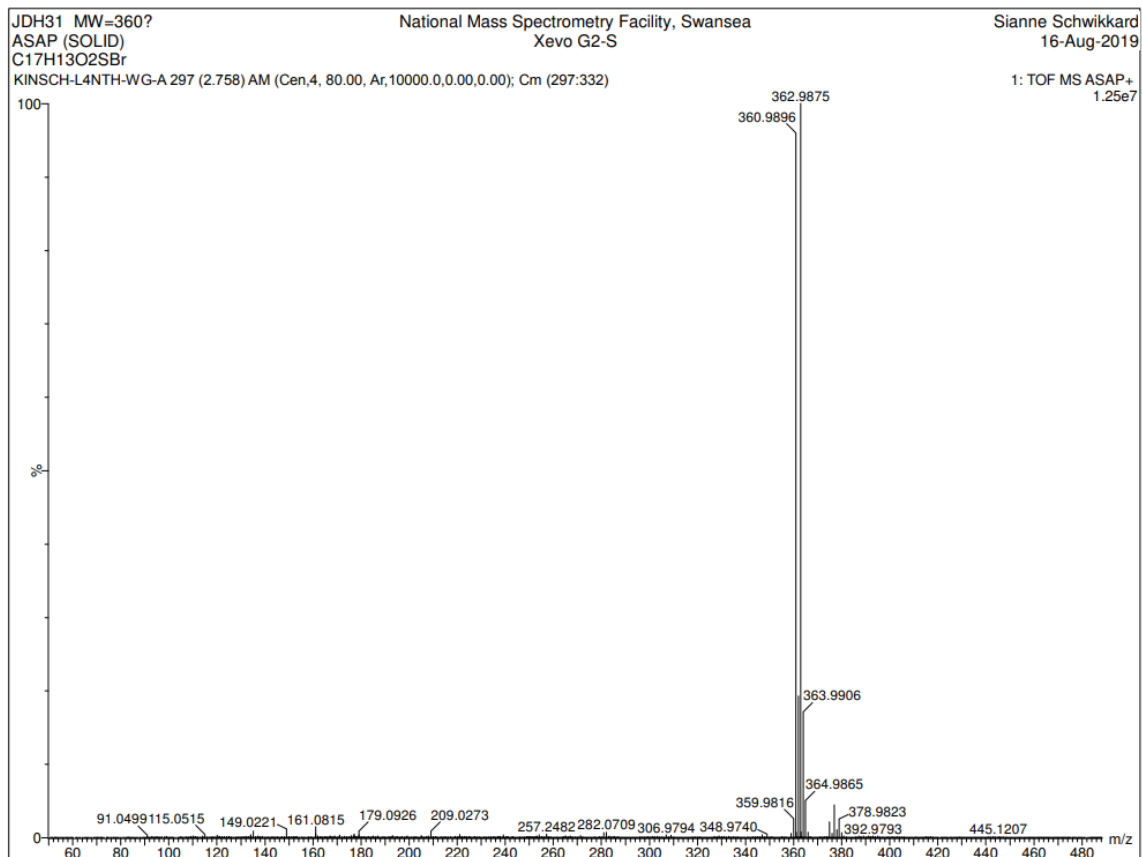


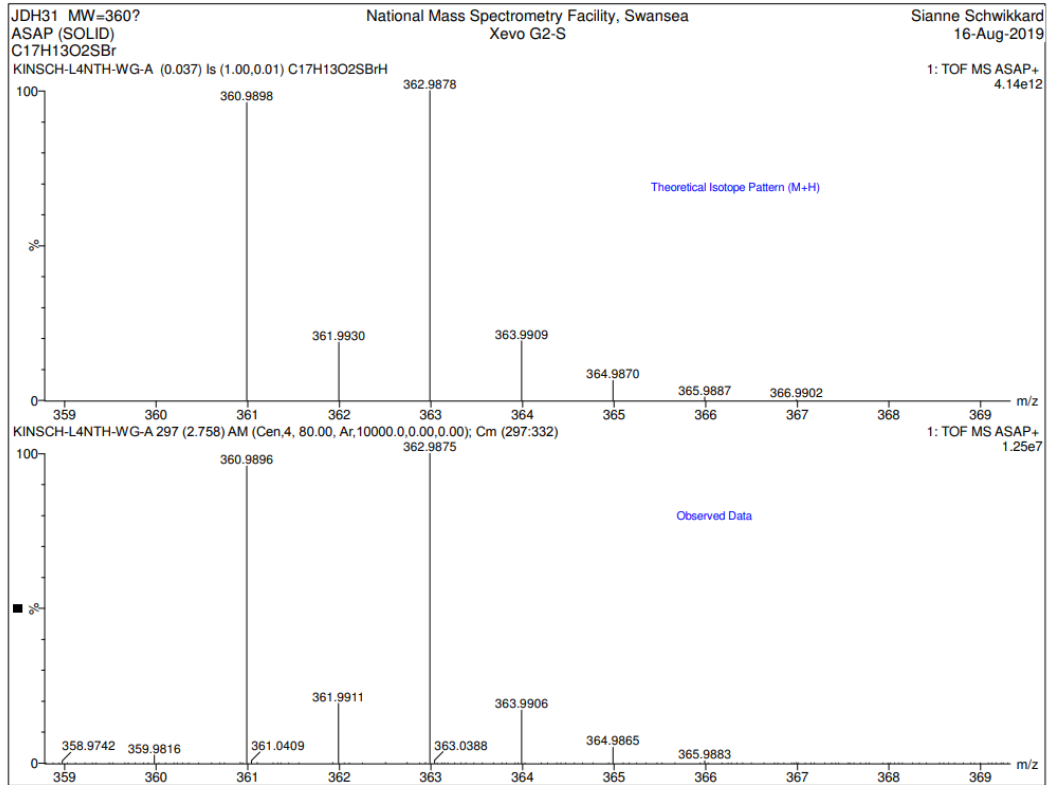
### A.9.2.2 MASS SPEC

File : E:\DATA\JDH 31.D  
Operator :  
Acquired : 8 May 2019 19:40 using AcqMethod HIGHTEMPAUTO.M  
Instrument : GC MS 1  
Sample Name: JDH 31  
Misc Info :  
Vial Number: 33



### A.9.3 HIGH RES MASS SPEC





## A.9.5 BIOLOGICAL DATA

### A.9.5.1 CYTOTOXICITY (HeLa)

#### A.9.5.1.1 CYTOTOXICITY PER CONCENTRATION

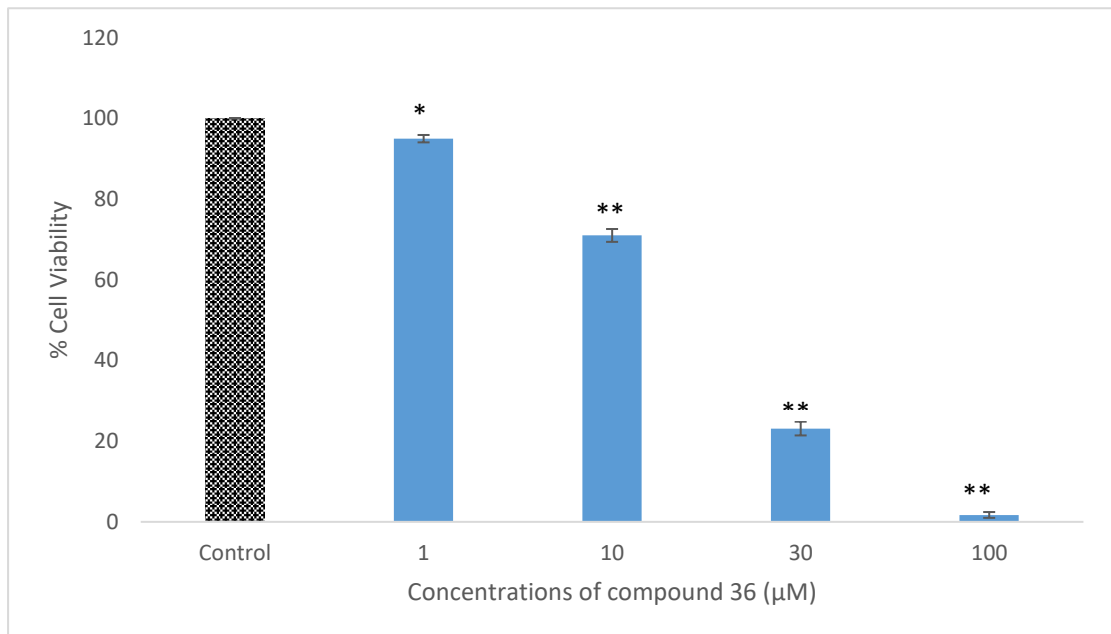
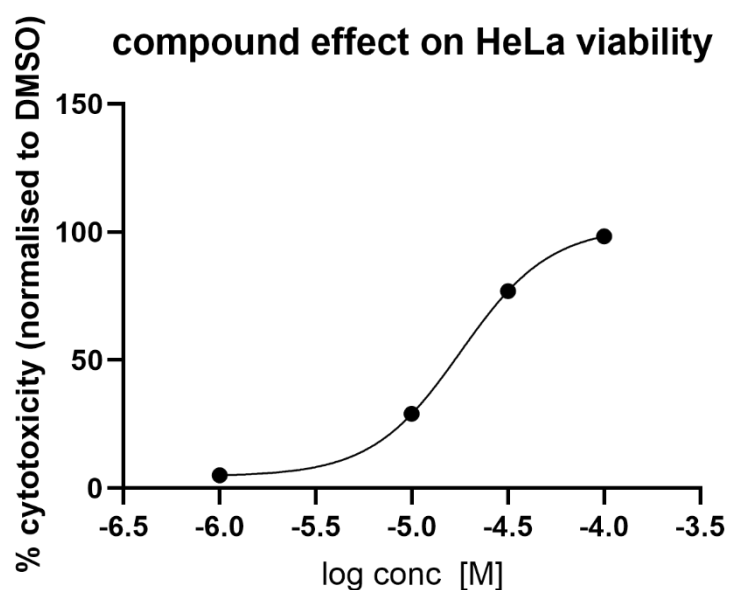


**Figure A.9.5.1.1.** Viability of HeLa cells exposed to different concentrations of compound 36 after 24 h incubation period. Cytotoxicity was determined via neutral red assay. The data is expressed as the percentage of inhibition compared with negative control in which the cell viability was assumed 100 % (means  $\pm$  SD, N =3). All concentrations tested showed significant cytotoxic effect compared to negative control (one way ANOVA with Dunnet's *posthoc* test, \*P <0.05, \*\*\*P<0.001)

#### A.9.5.1.2 IC<sub>50</sub>



#### A.9.5.2 ANTI-PROLIFERATIVE DATA

##### A.9.5.2.1 ANTI-PROLIFERATION PER CONCENTRATION (HREC)

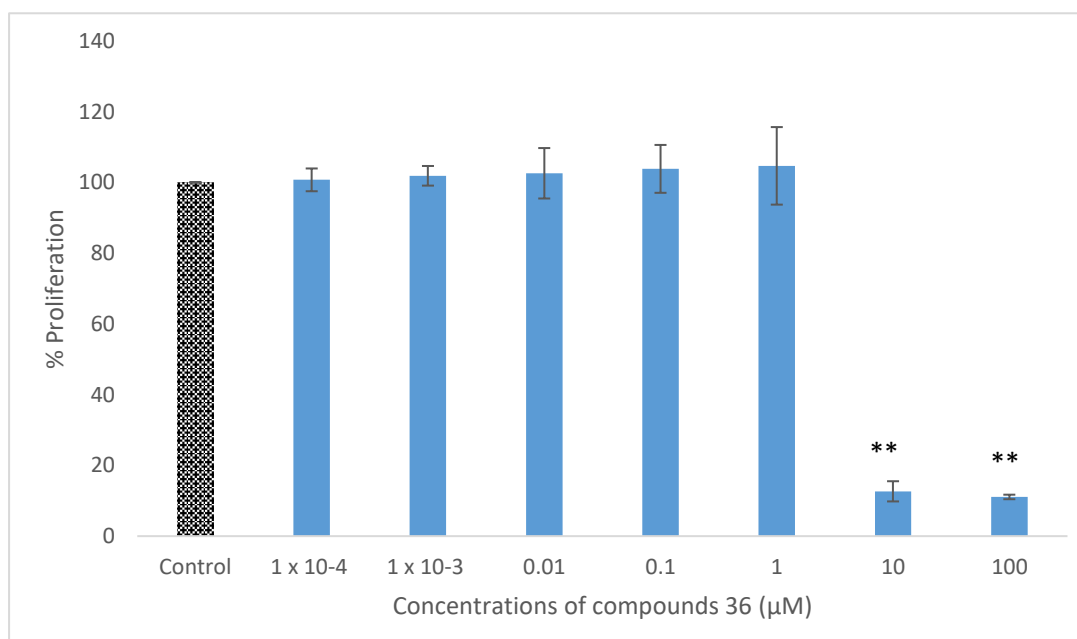
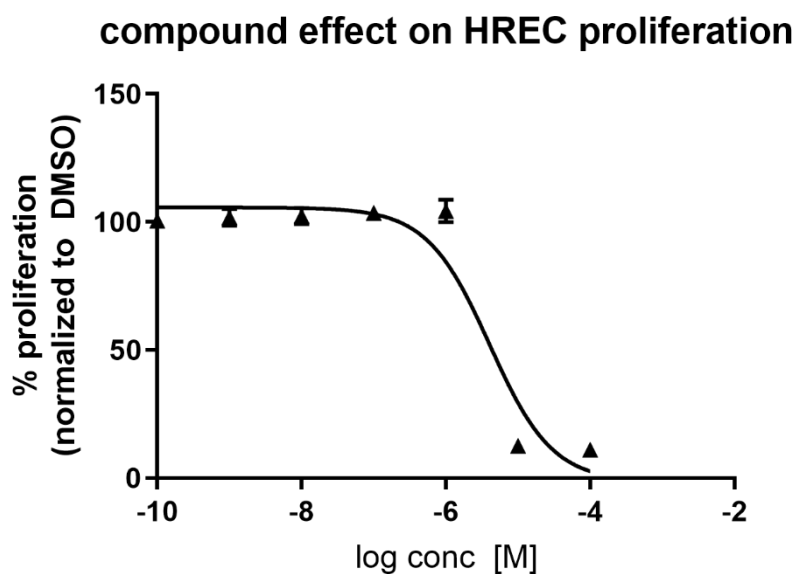


**Figure A.9.5.2.1.** Cell proliferation of HREC cells exposed to different concentrations of compound 36 after 24 hr incubation period. Cell proliferation was determined via the alamarBlue assay. The data is expressed as the percent proliferation compared with negative control in which the cell proliferation was assumed 100% (means  $\pm$  SD, N =3). Concentrations of 10  $\mu$ M and 100  $\mu$ M showed significant anti-proliferative effects compared to negative control (one way ANOVA with Dunnett's *posthoc* test, \*\*\*P <0.001).



#### A.9.5.2.2 GI<sub>50</sub> (HREC)



#### A.9.5.2.3 ANTI-PROLIFERATION PER CONCENTRATION (ARPE-19)

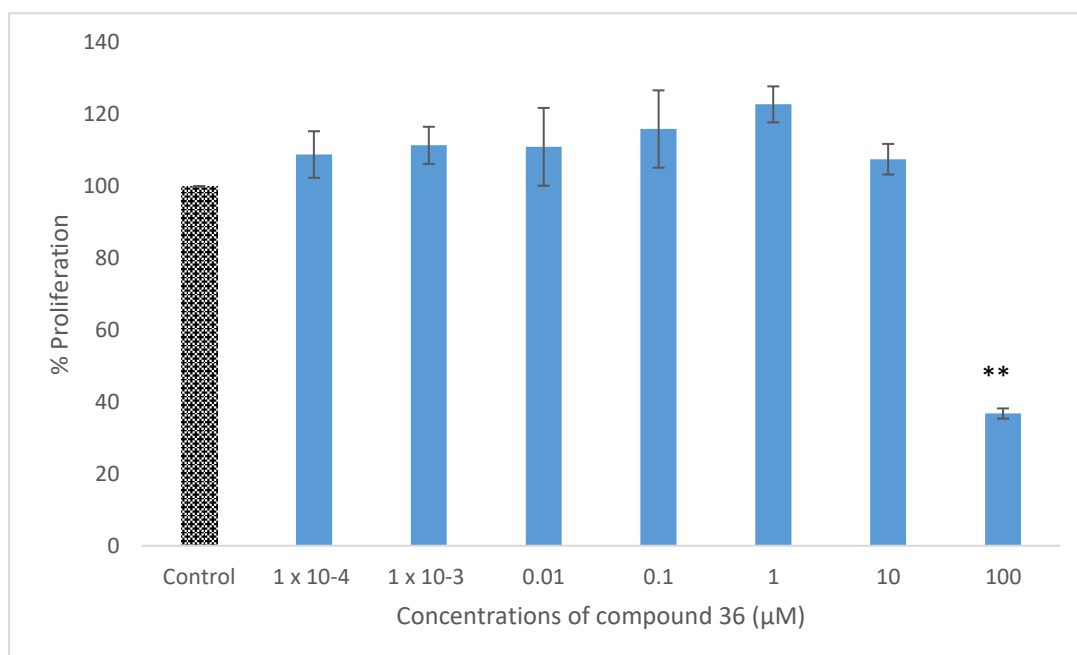
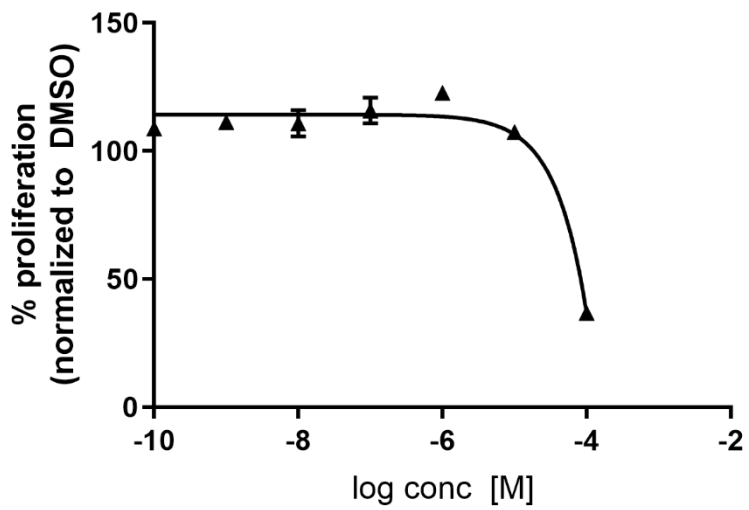


**Figure A.9.5.2.3.** Cell proliferation of ARPE-19 cells exposed to different concentrations of compound 36 after 24 hr incubation period. Cell proliferation was determined via the alamarBlue assay. The data is expressed as the percent proliferation compared with negative control in which the cell proliferation was assumed 100% (means  $\pm$  SD, N =3). Concentration 100  $\mu$ M showed significant anti-proliferative effects compared to negative control (one way ANOVA with Dunnett's *posthoc* test, \*\*\*P <0.001).

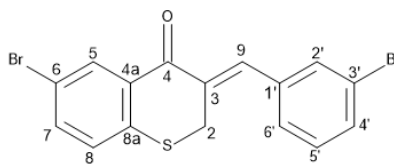
A.9.5.2.4 GI50 (ARPE-19)

compound effect on ARPE-19 proliferation



## A.10 Compound 37

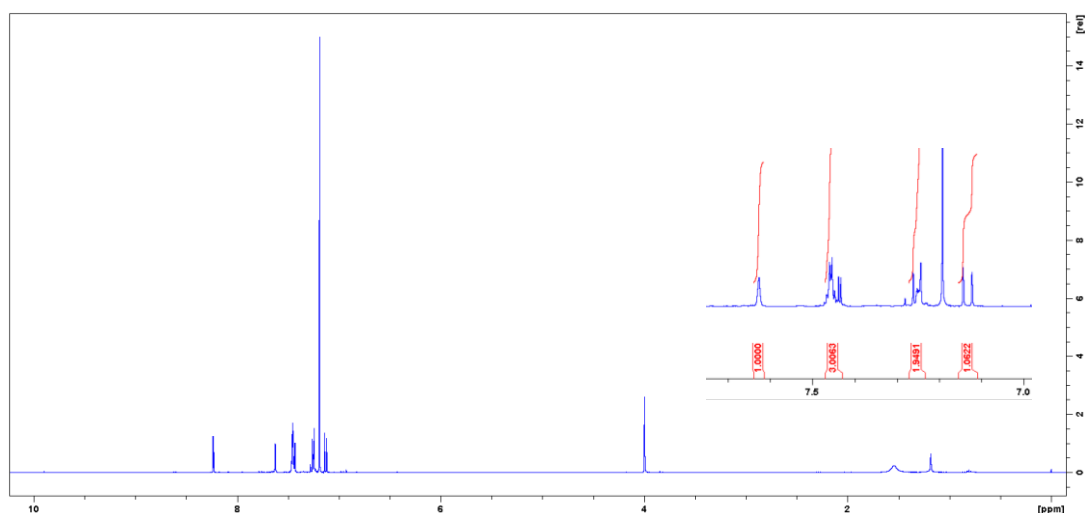
(3Z)-6-bromo-3-[(3-bromophenyl)methylidene]-2,3-dihydro-4H-1-benzothiopyran-4-one (37)



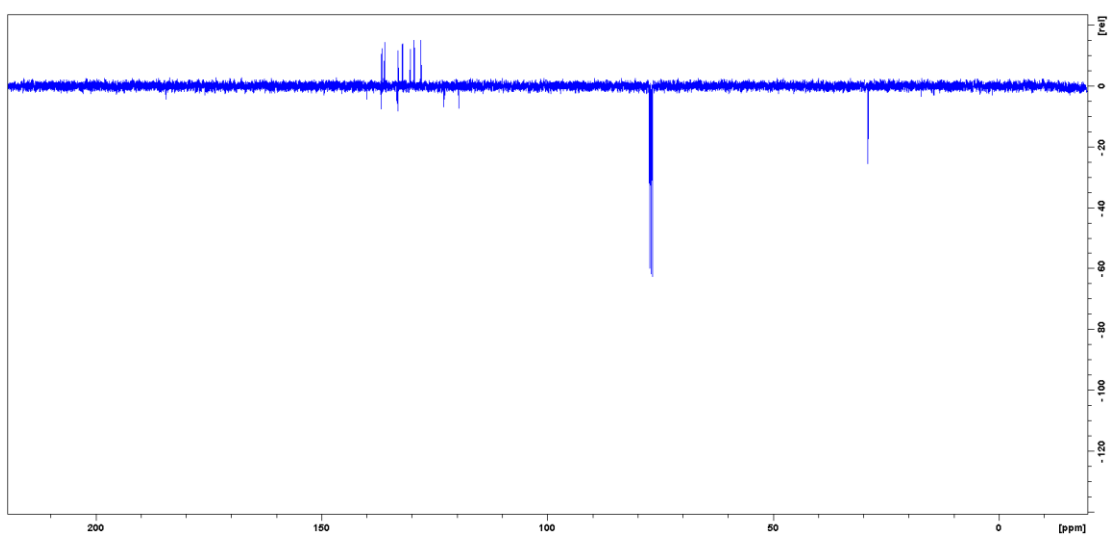
Light yellow solid, 61 mg, 10.3 %, 192.5 - 193.0 °C, IR  $\nu_{\max}$  ( $\text{cm}^{-1}$ ): 2907 (Ar-H), 1662 (C=O), 1600 (Aliphatic C=C), 1571 (Aromatic C=C), 805 (C-Br), 646 (C-S).  $^1\text{H-NMR}$  (400 MHz,  $\text{CDCl}_3$ ):  $\delta$  = 8.23 (1H, d,  $J$  = 2.1 Hz, H-5), 7.62 (1H, brs,  $w_{1/2}$  = 2.7 Hz, H-9), 7.45 (1H, d,  $J$  = 1.8 Hz, H-2'), 7.45 (1H, m, H-6'), 7.44 (1H, dd,  $J$  = 2.1, 8.6 Hz, H-7), 7.25 (1H, m, \*H-4'), 7.25 (1H, m, \*H-5'), 7.13 (1H, d,  $J$  = 8.6 Hz, H-8), 3.99 (2H, d,  $J$  = 1.2 Hz, H-2);  $^{13}\text{C-NMR}$  (100 MHz,  $\text{CDCl}_3$ ):  $\delta$  = 184.6 (C-4), 139.8 (C-8a), 136.8 (C-9), 136.4 (C-3), 135.8 (C-5'), 133.6 (C-4a), 133.0 (C-5), 132.2 (C-2'), 132.0 (C-7), 130.1 (C-4'), 129.55 (C-8), 127.9 (C-6'), 122.9 (C-3'), 119.6 (C-6), 28.9 (C-2),  $R_f$  = 0.74 (1:1 EtOAc:hexane). HRESMS (ASAP)  $m/z$  408.8896  $[\text{M}]^+$  (calcd  $[\text{C}_{16}\text{H}_{11}\text{OSBr}]$ , 408.8897). \* denotes interchangeable protons

### A.10.1 NMR

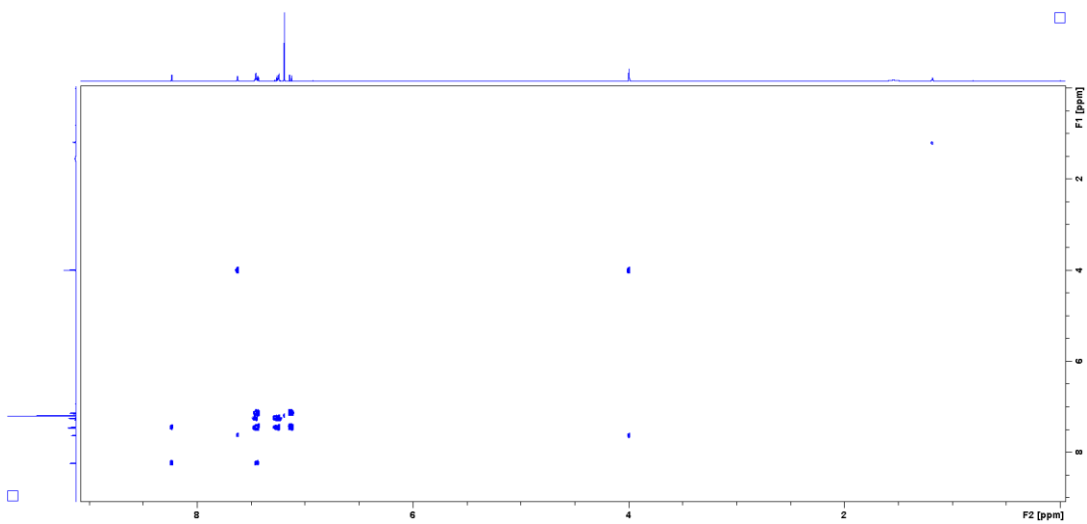
#### A.10.1.1 $^1\text{H-NMR}$



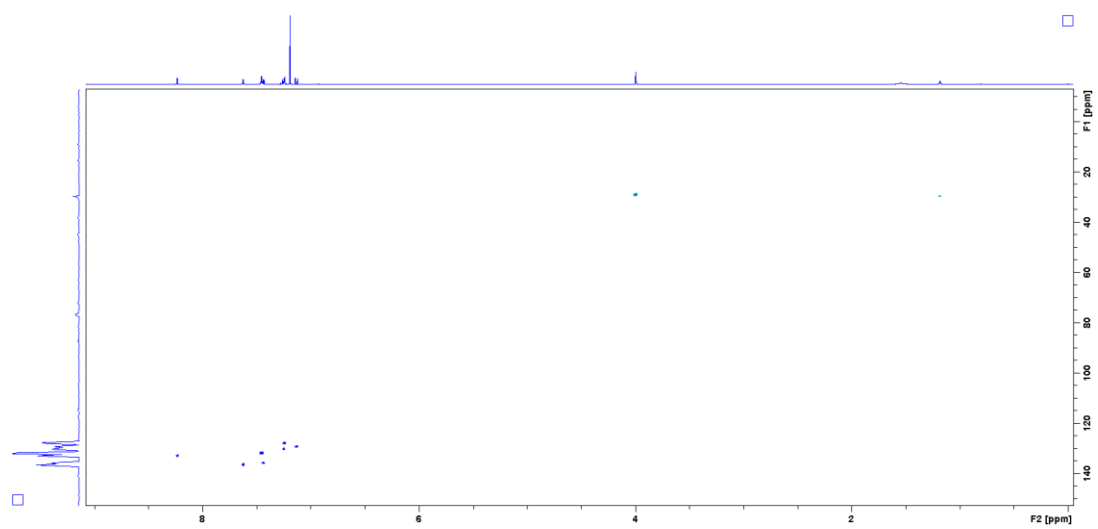
### A.10.1.2 $^{13}\text{C}$ -NMR



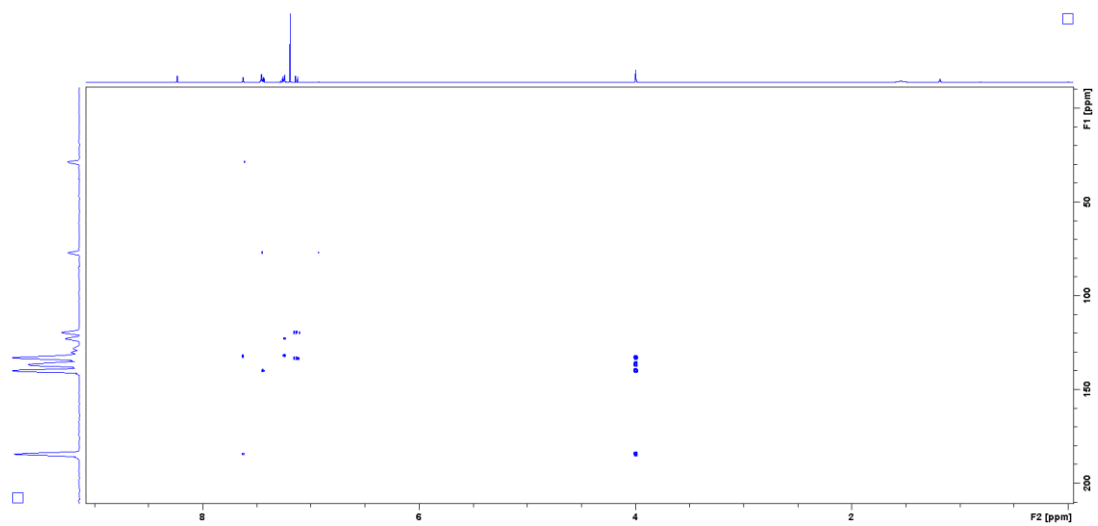
### A.10.1.3 COSY



#### A.10.1.4 HSQC



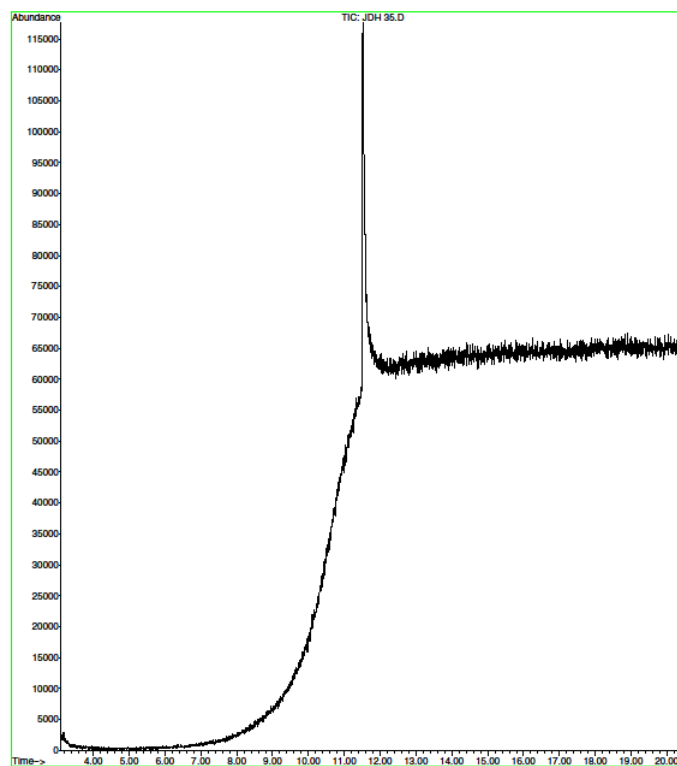
#### A.10.1.5 HMBC



## A.10.2 GCMS

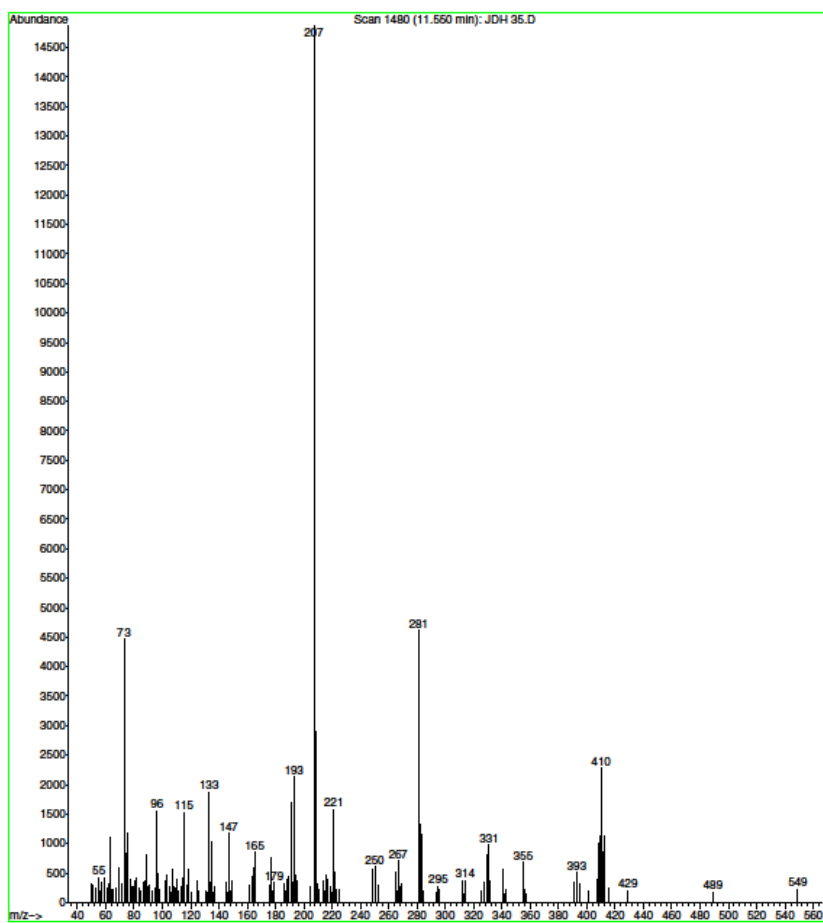
### A.10.2.1 CHROMATOGRAM

File : E:\DATA\JDH 35.D  
Operator :  
Acquired : 8 May 2019 20:05 using AcqMethod HIGHTEMPAUTO.M  
Instrument : GC MS 1  
Sample Name: JDH 35  
Misc Info :  
Vial Number: 34

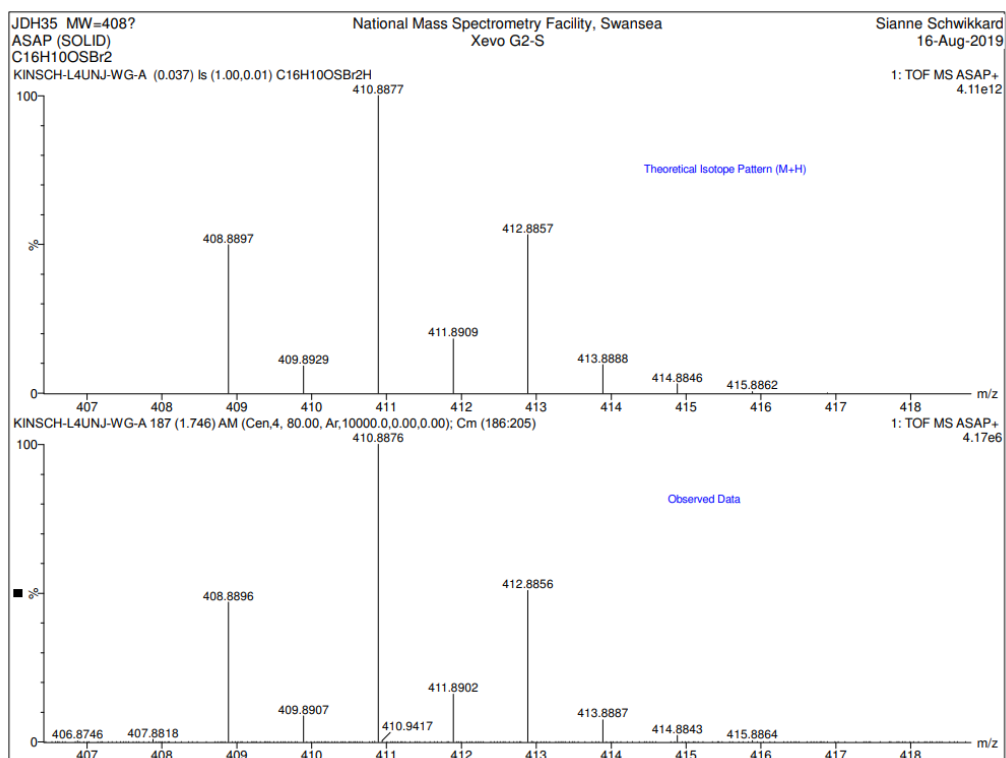
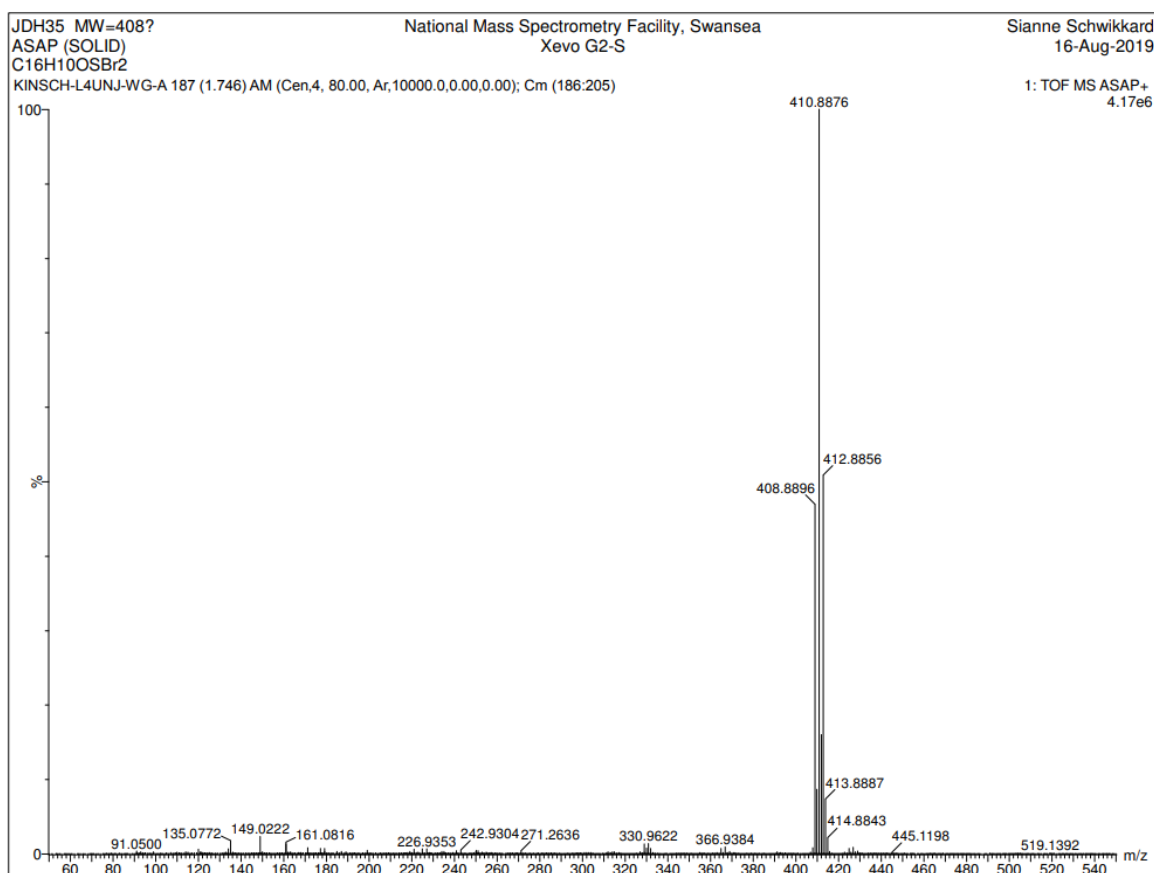


### A.10.2.2 MASS SPEC

File : E:\DATA\JDH 35.D  
Operator :  
Acquired : 8 May 2019 20:05 using AcqMethod HIGHTEMPAUTO.M  
Instrument : GC MS 1  
Sample Name : JDH 35  
Misc info :  
Vial Number: 34

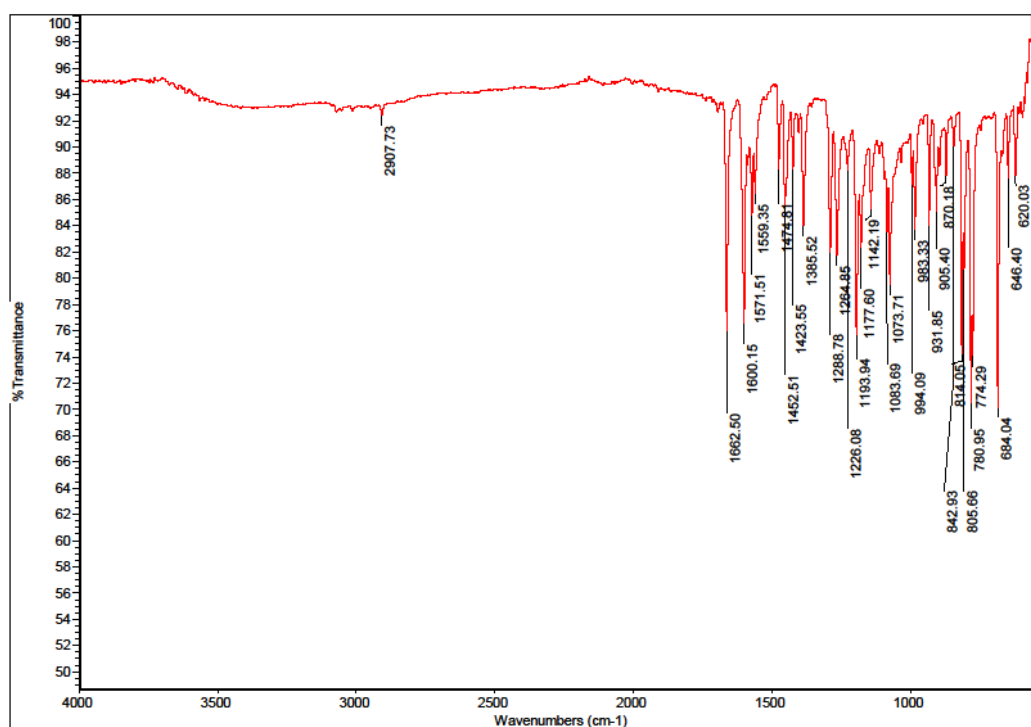


### A.10.3 HIGH RES MASS SPEC





## A.10.4 IR DATA



## A.10.5 BIOLOGICAL DATA

### A.10.5.1 CYTOTOXICITY (HeLa)

#### A.10.5.1.1 CYTOTOXICITY PER CONCENTRATION

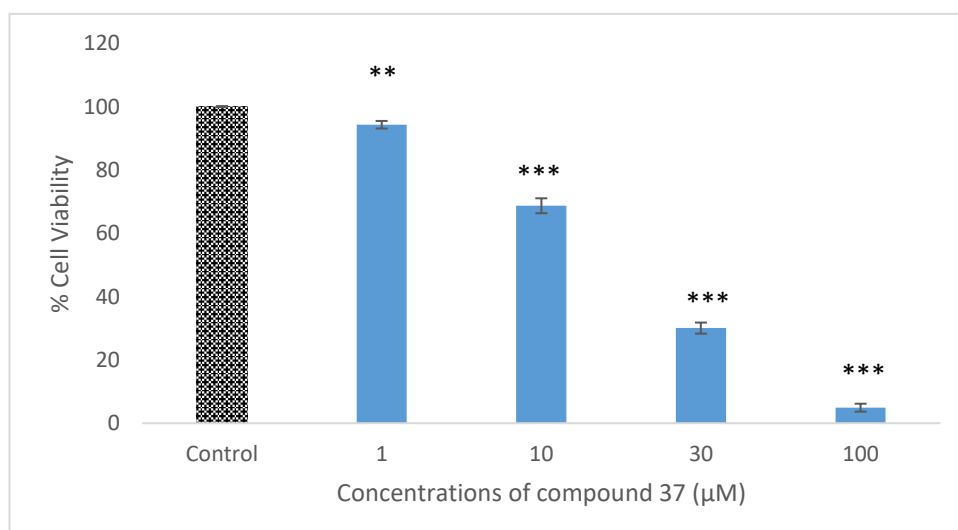
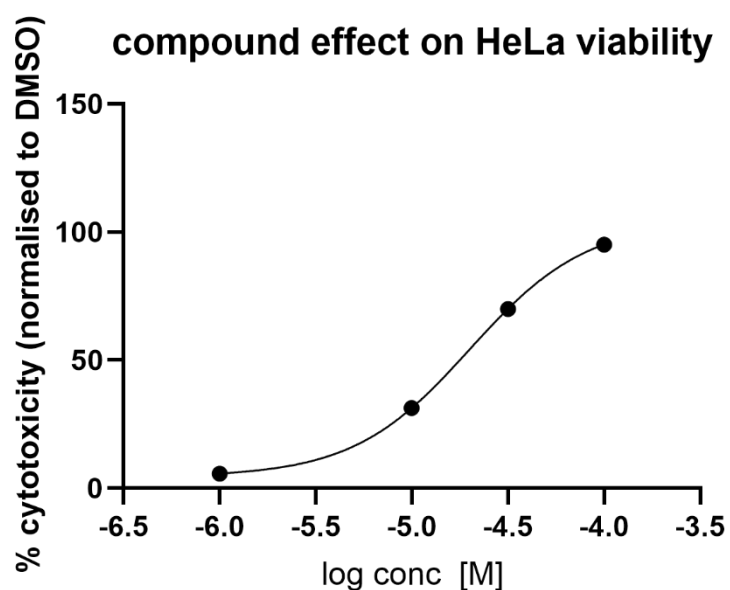


**Figure A.10.5.1.1.** Viability of HeLa cells exposed to different concentrations of compound 37 after 24 h incubation period. Cytotoxicity was determined via neutral red assay. The data is expressed as the percentage of inhibition compared with negative control in which the cell viability was assumed 100 % (means  $\pm$  SD, N=3). All concentrations tested showed significant cytotoxic effect compared to negative control (one way ANOVA with Dunnett's *posthoc* test, \*\*P <0.01, \*\*\*P <0.001)

#### A.10.5.1.2 IC<sub>50</sub>



#### A.10.5.2 ANTI-PROLIFERATIVE DATA

##### A.10.5.2.1 ANTI-PROLIFERATION PER CONCENTRATION (HREC)

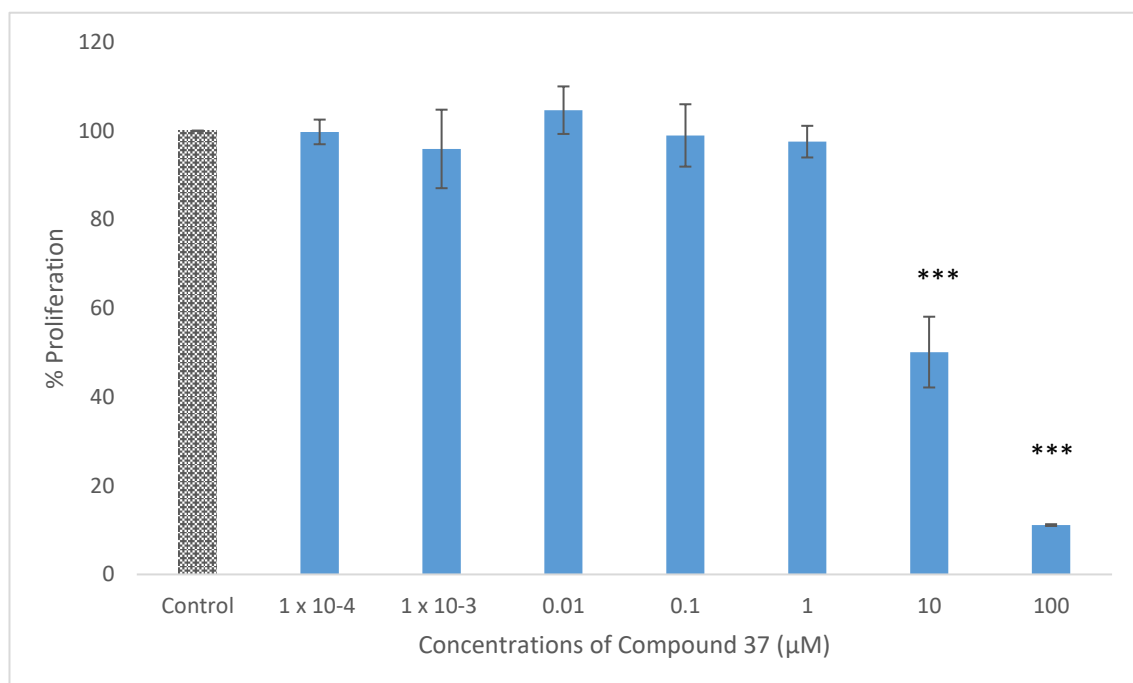
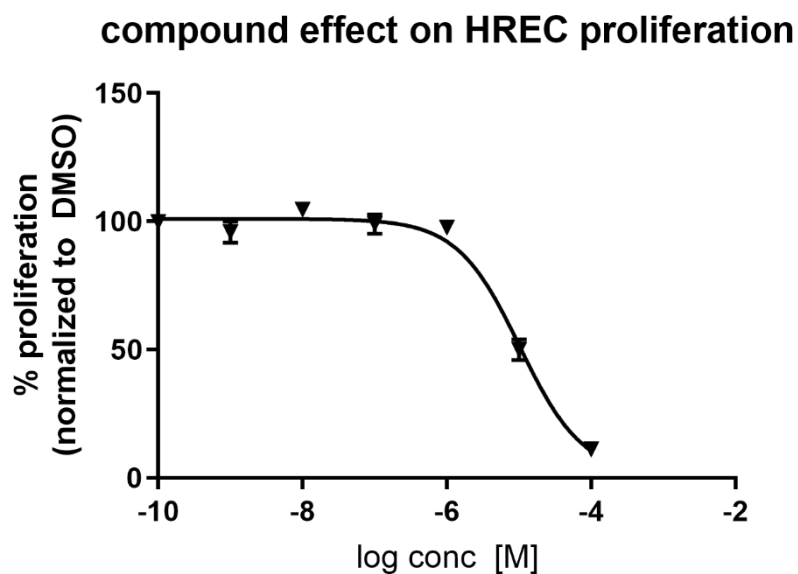


**Figure A.10.5.2.1** Cell proliferation of HREC cells exposed to different concentrations of compound 37 after 24 hr incubation period. Cell proliferation was determined via the alamarBlue assay. The data is expressed as the percent proliferation compared with negative control in which the cell proliferation was assumed 100% (means  $\pm$  SD, N =3).

Concentrations of 10  $\mu$ M and 100  $\mu$ M showed significant anti-proliferative effects compared to negative control (one way ANOVA with Dunnett's *posthoc* test, \*\*\*P <0.001).

#### A.10.5.2.2 GI<sub>50</sub> (HREC)



#### A.10.5.2.3 ANTI-PROLIFERATION PER CONCENTRATION (ARPE-19)

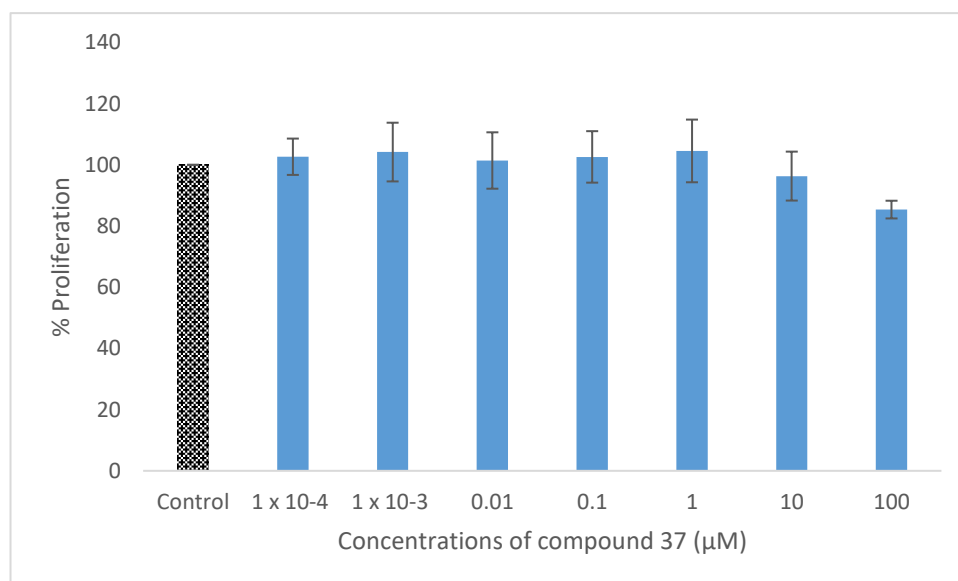
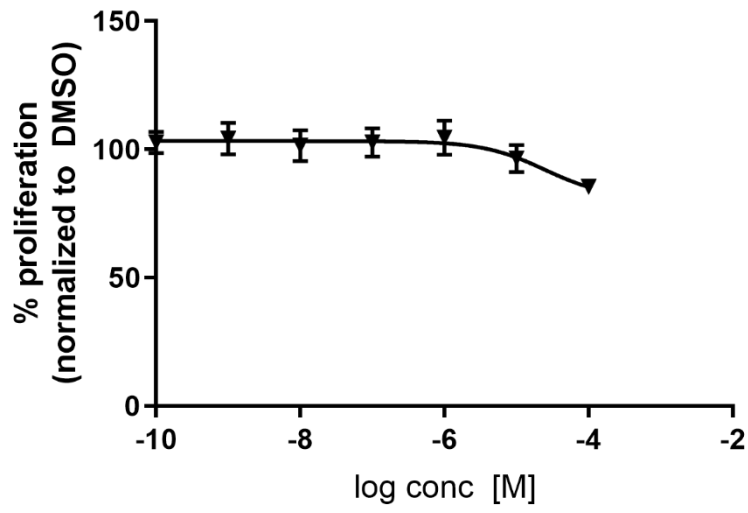


**Figure A.10.5.2.3.** Cell proliferation of ARPE-19 cells exposed to different concentrations of compound 37 after 24 hr incubation period. Cell proliferation was determined via the alamarBlue assay. The data is expressed as the percent proliferation compared with negative control in which the cell proliferation was assumed 100% (means  $\pm$  SD, N =3). No Concentrations showed significant anti-proliferative effects compared to negative control (one way ANOVA with Dunnett's *posthoc* test).

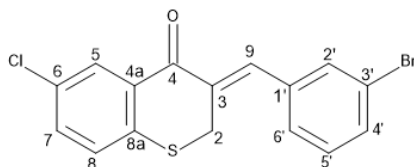
A.10.5.2.4 GI<sub>50</sub> (ARPE-19)

compound effect on ARPE-19 proliferation



## A.11 Compound 38

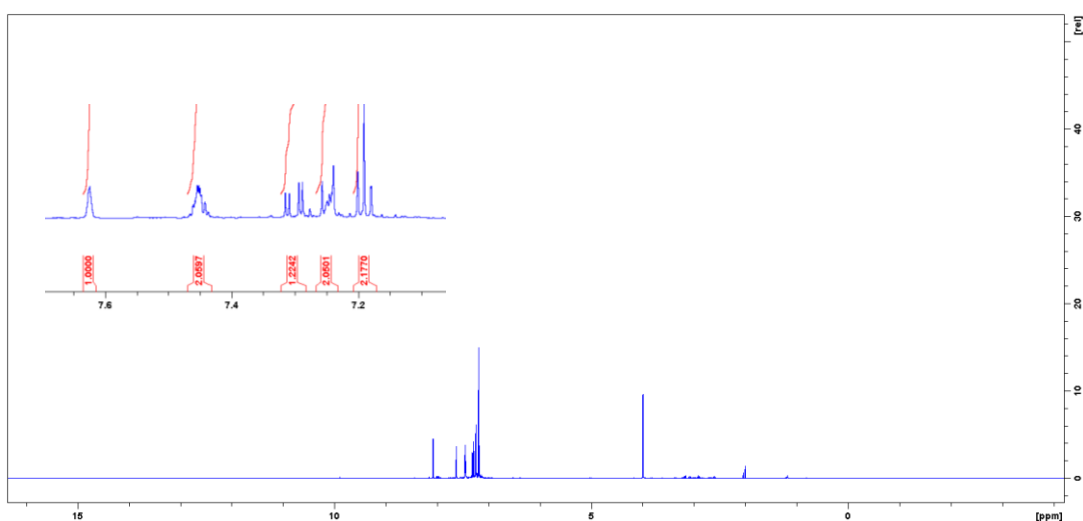
(3Z)-3-[(3-bromophenyl)methylidene]-6-chloro-2,3-dihydro-4H-1-benzothiopyran-4-one (38)



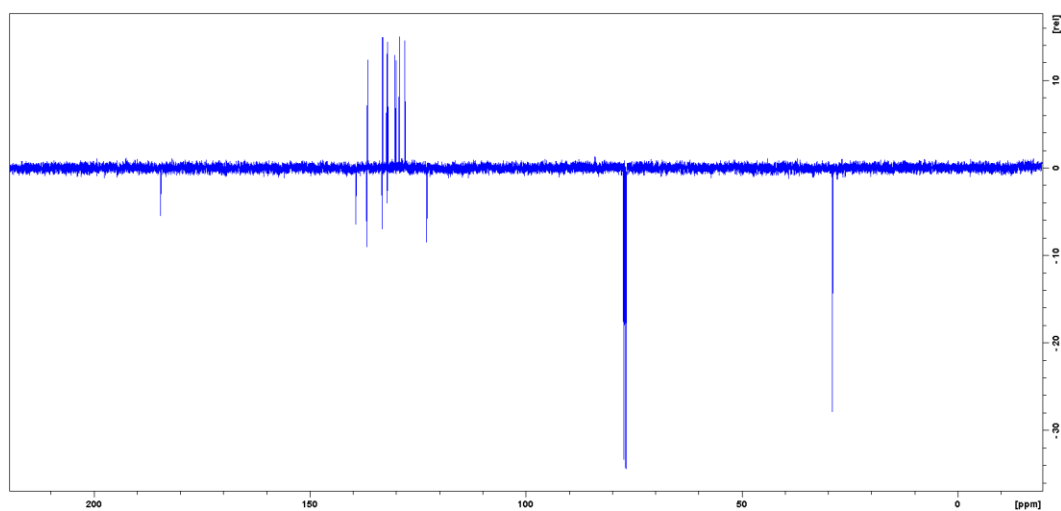
Light yellow solid, 217 mg, 36.6 %, 169.5 - 169.9 °C, IR  $\nu_{\max}$  (cm<sup>-1</sup>): 2908 (Ar-H), 1662 (C=O), 1599 (Aliphatic C=C), 1577 (Aromatic C=C), 814 (C-Cl), 782 (C-Br), 646 (C-S). <sup>1</sup>H-NMR (400 MHz, CDCl<sub>3</sub>):  $\delta$  = 8.07 (1H, d, J = 2.4 Hz, H-5), 7.62 (1H, brs w<sub>1/2</sub> = 2.5 Hz, H-9), 7.45 (1H, m, H-2'), 7.45 (1H, m, H-6'), 7.29 (1H, dd, J = 2.4, 8.5 Hz, H-7), 7.24 (1H, m, H-4'), 7.24 (1H, m, H-5'), 7.19 (1H, d, J = 8.5 Hz, H-8), 3.99 (2H, d, J = 1.1 Hz, H-2); <sup>13</sup>C-NMR (100 MHz, CDCl<sub>3</sub>):  $\delta$  = 184.4 (C-4), 139.8 (C-8a), 136.8 (C-1'), 136.7 (C-9), 133.2 (C-4a), 133.2 (C-3), 133.1 (C-7), \*132.4 (C-5'), 132.1 (C-6), \*132.0 (C-4'), 130.1 (C-5), \*130.0 (C-2'), 129.2 (C-8), \*127.9 (C-6'), 122.9 (C-3'), 29.8 (C-2), R<sub>f</sub> = 0.74 (1:1 EtOAc:hexane). HRESMS (ASAP)  $m/z$  364.9400 [M]<sup>+</sup> (calcd [C<sub>16</sub>H<sub>11</sub>OSeClBr], 364.9403). \* Denotes interchangeable carbons.

### A.11.1 NMR

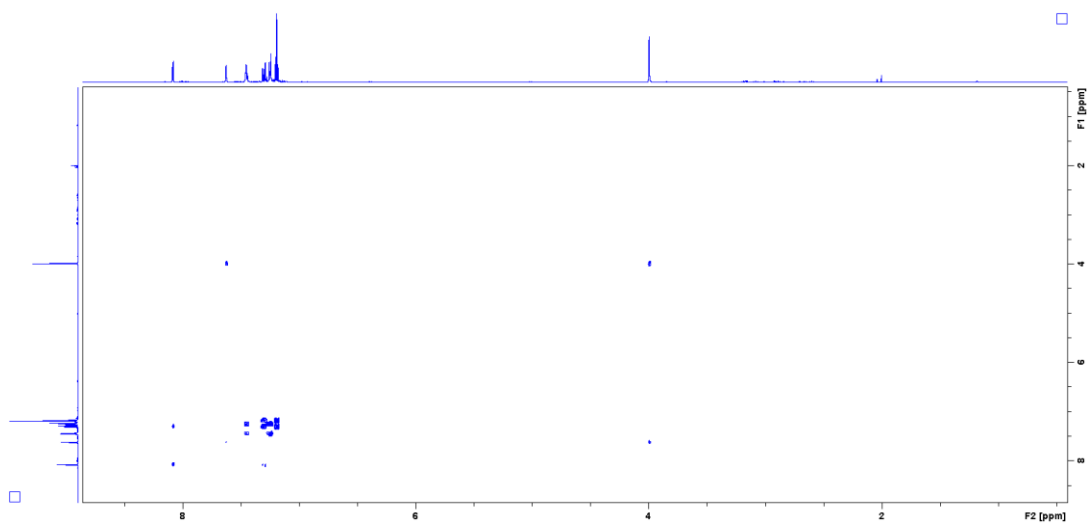
#### A.11.1.1 <sup>1</sup>H-NMR



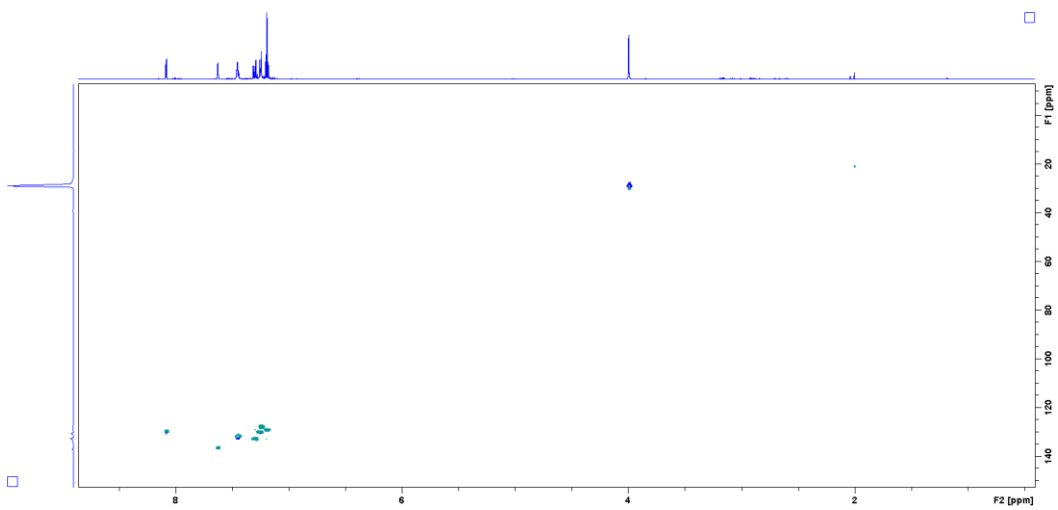
### A.11.1.2 $^{13}\text{C}$ -NMR



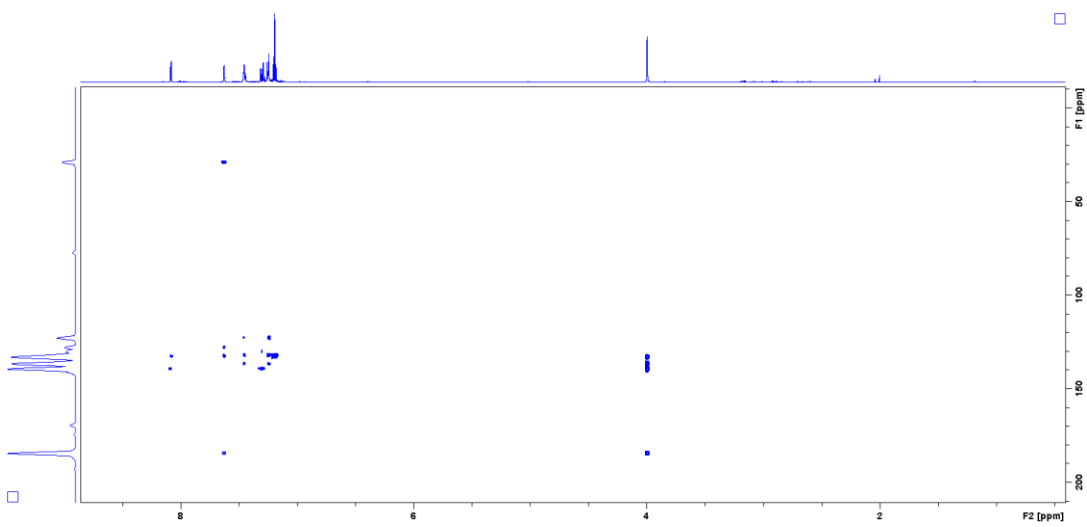
### A.11.1.3 COSY



#### A.11.1.4 HSQC



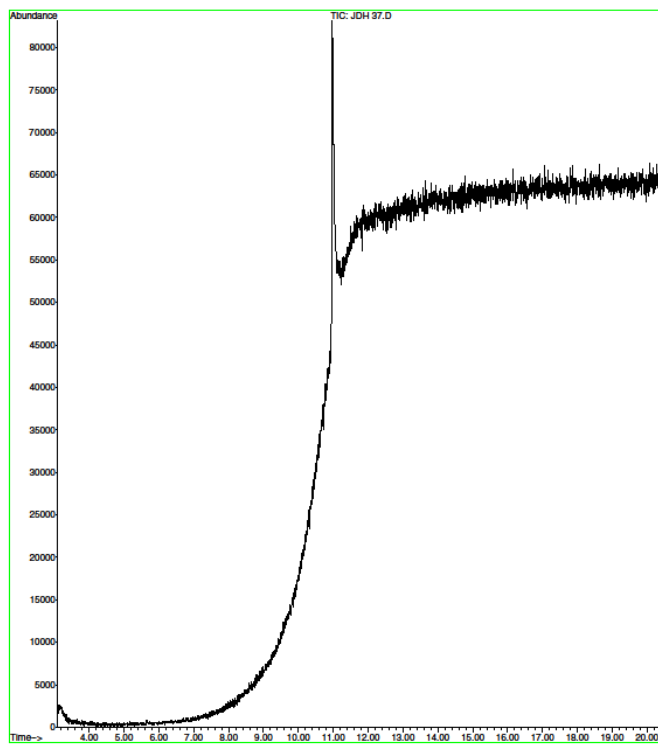
#### A.11.1.5 HMBC



## A.11.2 GCMS

### A.11.2.1 CHROMATOGRAM

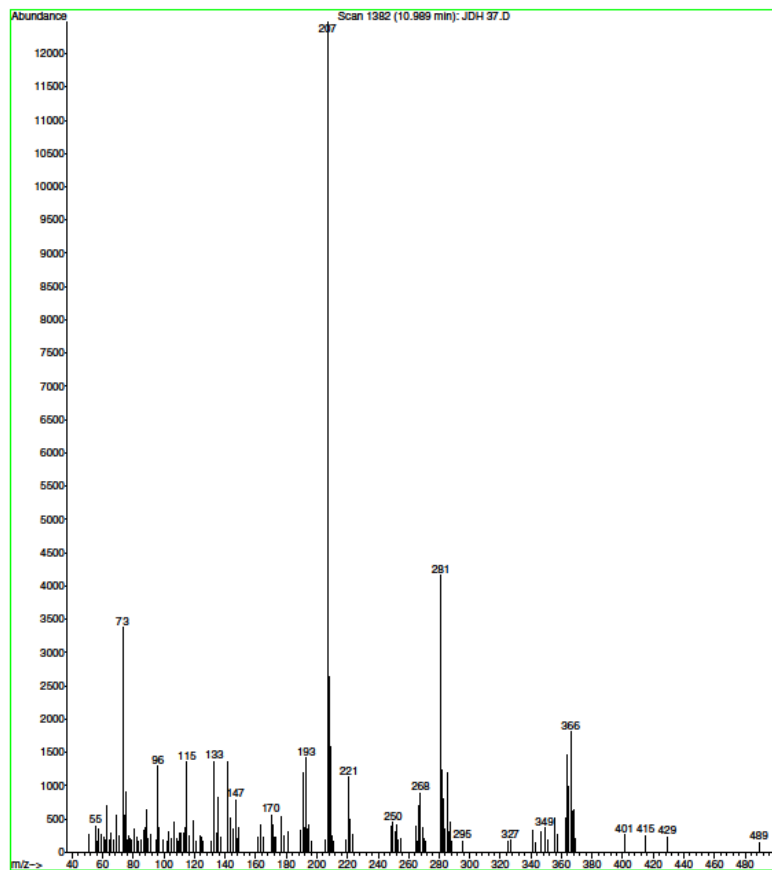
File : E:\DATA\JDH 37.D  
Operator :  
Acquired : 8 May 2019 20:29 using AcqMethod HIGHTEMPAUTO.M  
Instrument : GC MS 1  
Sample Name: JDH 37  
Misc Info :  
Vial Number: 35



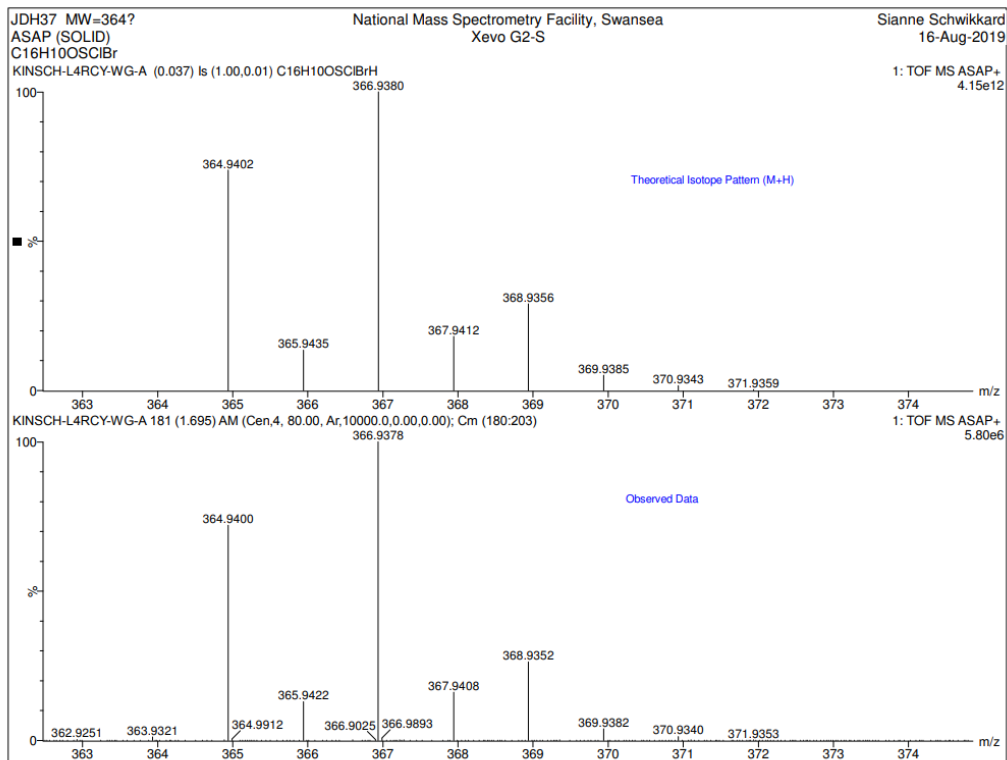
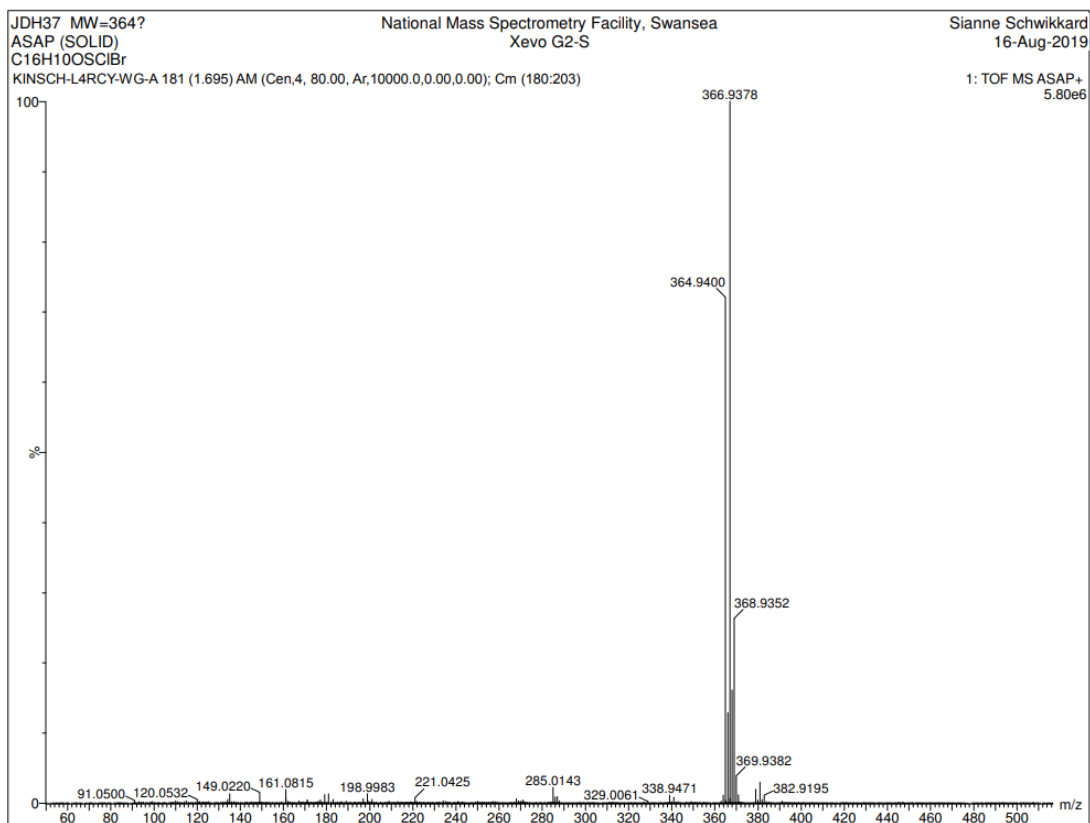


### A.11.2.2 MASS SPEC

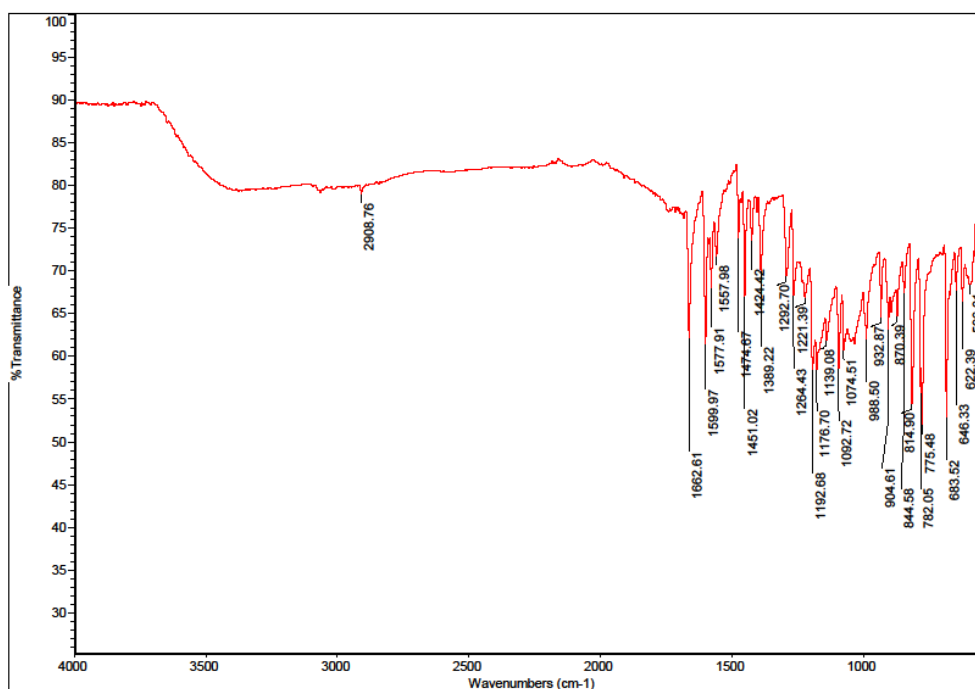
File : E:\DATA\JDH 37.D  
Operator :  
Acquired : 8 May 2019 20:29 using AcqMethod HIGHTEMPAUTO.M  
Instrument : GC MS 1  
Sample Name: JDH 37  
Misc Info :  
Vial Number: 35



### A.11.3 HIGH RES MASS SPEC



#### A.11.4 IR DATA



#### A.11.5 BIOLOGICAL DATA

##### A.11.5.1 CYTOTOXICITY (HeLa)

##### A.11.5.1.1 CYTOTOXICITY PER CONCENTRATION

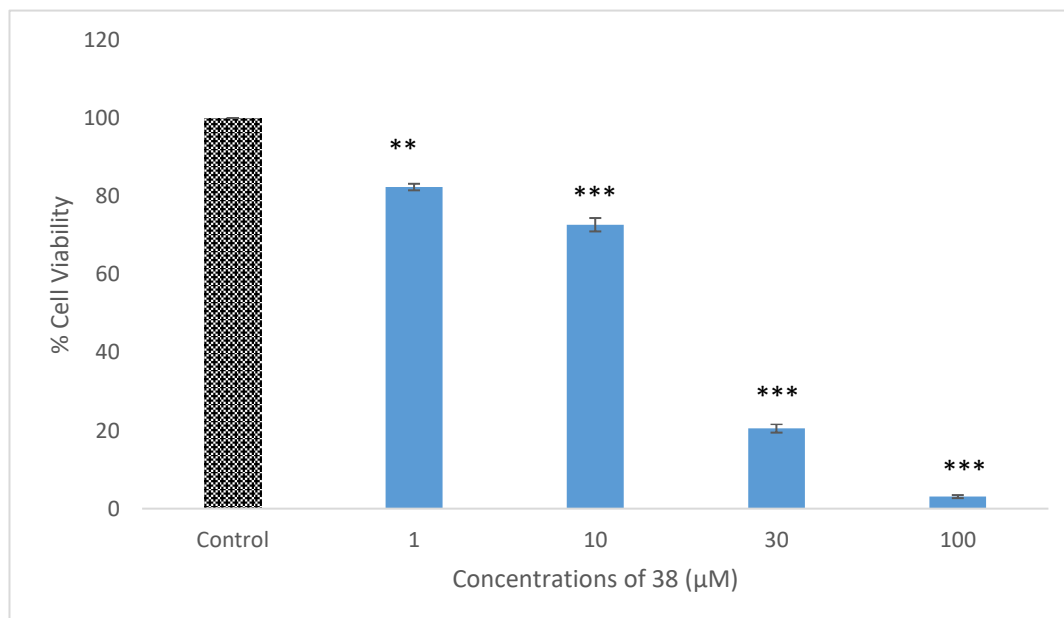
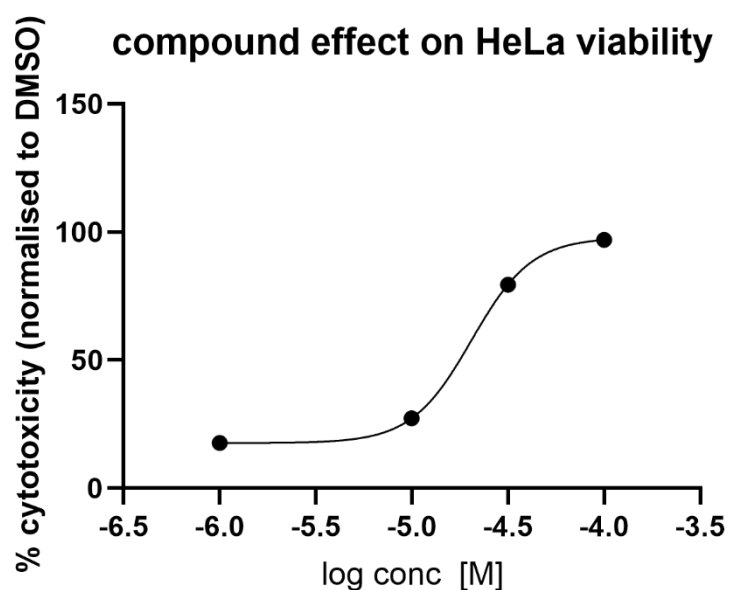


**Figure A.11.5.1.1.** Viability of HeLa cells exposed to different concentrations of compound 38 after 24 h incubation period. Cytotoxicity was determined via neutral red assay. The data is expressed as the percentage of inhibition compared with negative control in which the cell viability was assumed 100 % (means  $\pm$  SD, N =3). All concentrations tested showed significant cytotoxic effect compared to negative control (one way ANOVA with Dunnett's *posthoc* test, \*\*\*P <0.001)

#### A.11.5.1.2 IC<sub>50</sub>



#### A.11.5.2 ANTI-PROLIFERATIVE DATA

##### A.11.5.2.1 ANTI-PROLIFERATION PER CONCENTRATION (HREC)

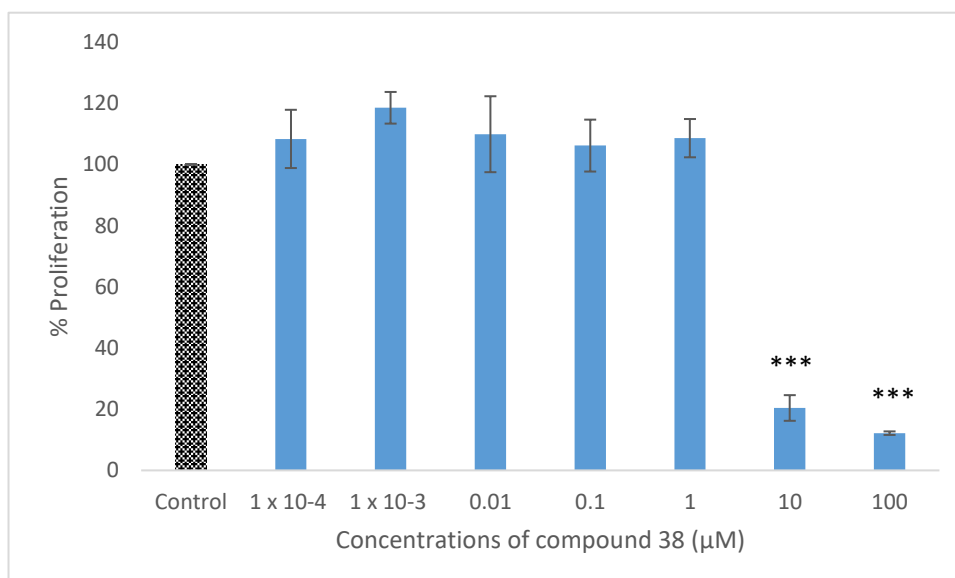
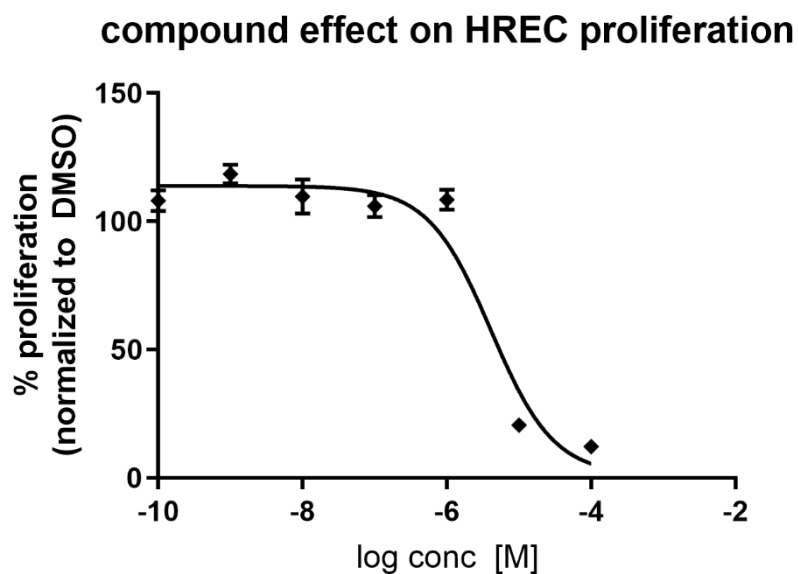


**Figure A.11.5.2.1.** Cell proliferation of HREC cells exposed to different concentrations of compound 38 after 24 hr incubation period. Cell proliferation was determined via the alamarBlue assay. The data is expressed as the percent proliferation compared with negative control in which the cell proliferation was assumed 100% (means  $\pm$  SD, N =3). Concentrations of 10  $\mu$ M and 100  $\mu$ M showed significant anti-proliferative effects compared to negative control (one way ANOVA with Dunnett's *posthoc* test, \*\*\*P <0.001).

#### A.11.5.2.2 GI<sub>50</sub> (HREC)



#### A.11.5.2.3 ANTI-PROLIFERATION PER CONCENTRATION (ARPE-19)

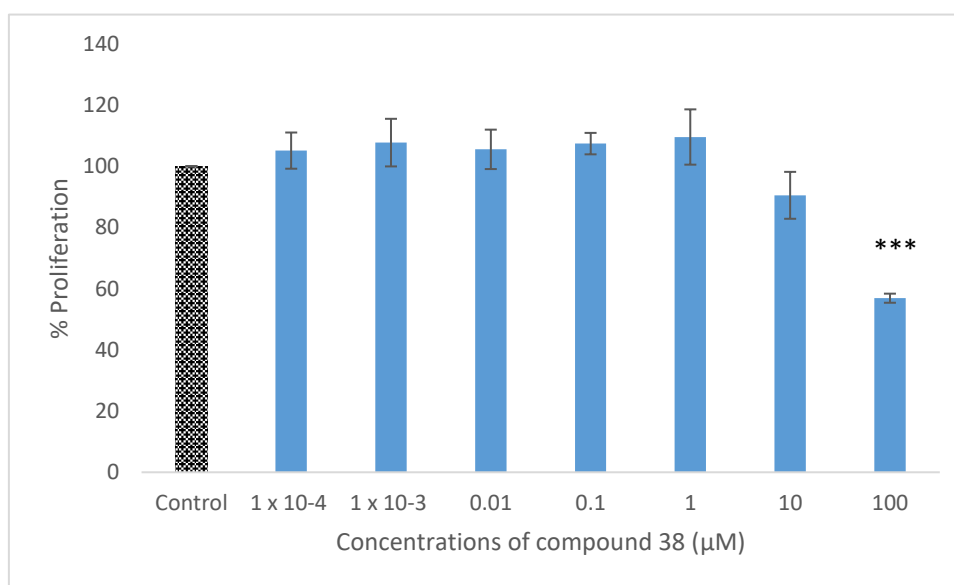
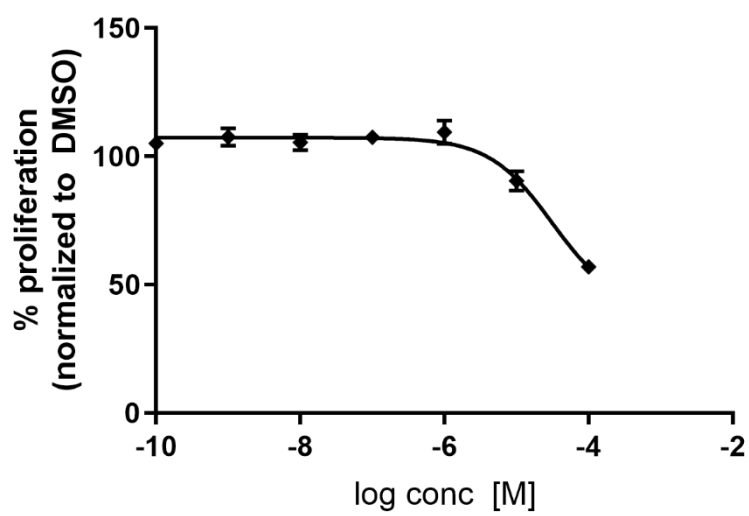


**Figure A.7.5.2.3.** Cell proliferation of ARPE-19 cells exposed to different concentrations of compound 38 after 24 hr incubation period. Cell proliferation was determined via the alamarBlue assay. The data is expressed as the percent proliferation compared with negative control in which the cell proliferation was assumed 100% (means  $\pm$  SD, N =3). Concentration 100  $\mu$ M showed significant anti-proliferative effects compared to negative control (one way ANOVA with Dunnett's posthoc test, \*\*\*P <0.001).

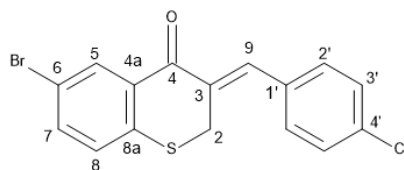
A.11.5.2.4 GI<sub>50</sub> (ARPE-19)

compound effect on ARPE-19 proliferation



## A.12 Compound 39

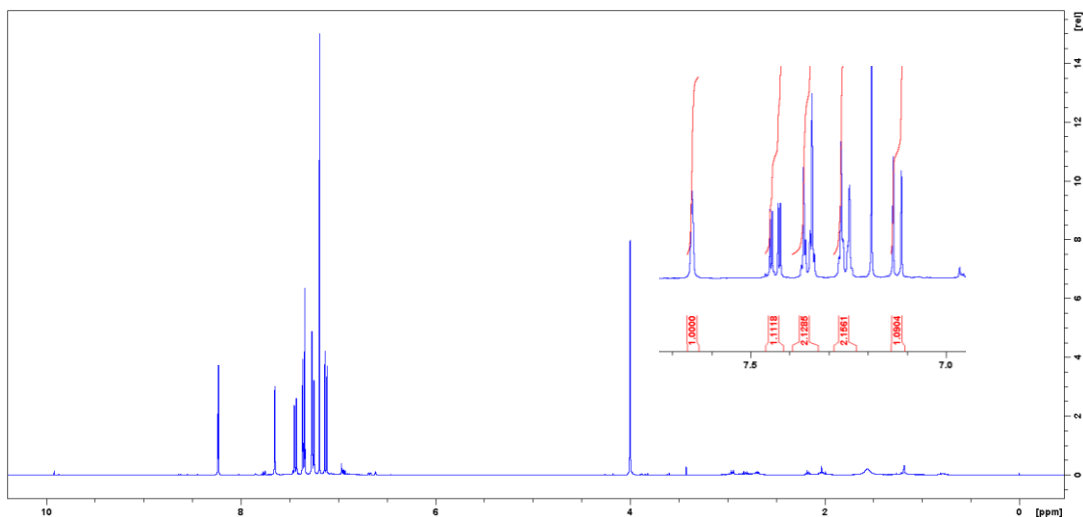
(3Z)-6-bromo-3-[(4-chlorophenyl)methylidene]-2,3-dihydro-4H-1-benzothiopyran-4-one (39)



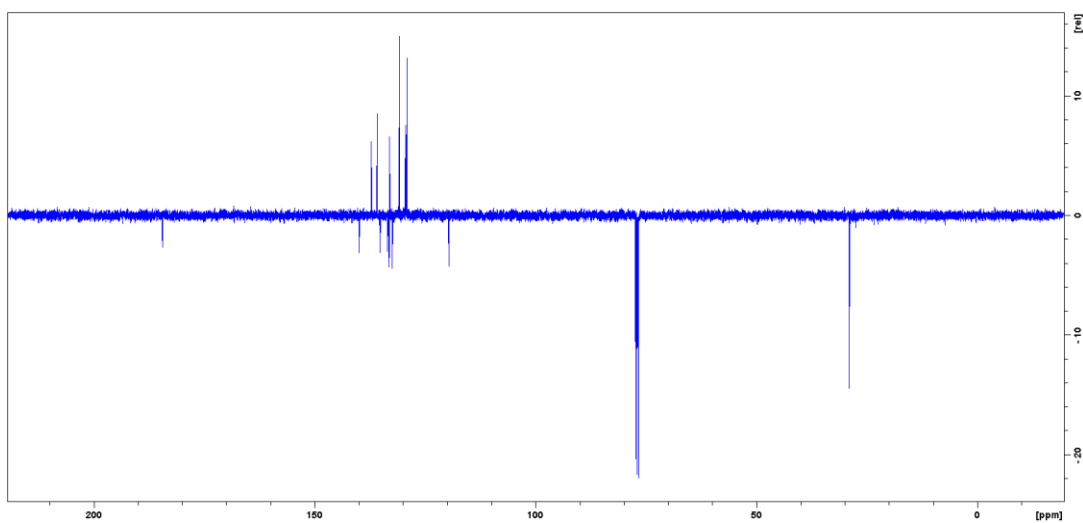
Light yellow solid, 692 mg, 13.1 %, 157.8 - 158.0 °C, IR  $\nu_{\max}$  (cm<sup>-1</sup>): 2909 (Ar-H), 1662 (C=O), 1648 (Aliphatic C=C), 1600 (Aromatic C=C), 815 (C-Cl), 772 (C-Br), 646 (C-S), <sup>1</sup>H-NMR (400 MHz, CDCl<sub>3</sub>):  $\delta$  = 8.23 (1H, d, J = 2.2 Hz, H-5), 7.65 (1H, brs, W<sub>1/2</sub> = 2.5 Hz, H-9), 7.44 (1H, dd, J = 2.2 Hz, 8.5 Hz, H-7), 7.35 (2H, s, J = 8.4 Hz, H-2'), 7.25 (2H, d, J = 8.4 Hz, H-3'), 7.13 (1H, d, J = 8.5 Hz, H-8), 3.99 (2H, d, J = 1.1 Hz, H-2); <sup>13</sup>C-NMR (100 MHz, CDCl<sub>3</sub>):  $\delta$  = 184.3 (C-4), 139.9 (C-8a), 137.2 (C-9), 136.0 (C-7), 135.2 (C-4'), 133.5 (C-4a), 133.1 (C-3), 133.0 (C-5), 132.5 (C-1'), 130.9 (C-3'), 129.5 (C-8), 129.2 (C-2'), 119.6 (C-6), 29.1 (C-2), R<sub>f</sub> = 0.80 (1:1 EtOAc:hexane). HRESMS (ASAP)  $m/z$  364.9398 [M]<sup>+</sup> (calcd [C<sub>16</sub>H<sub>11</sub>OSClBr], 364.9403).

### A.12.1 NMR

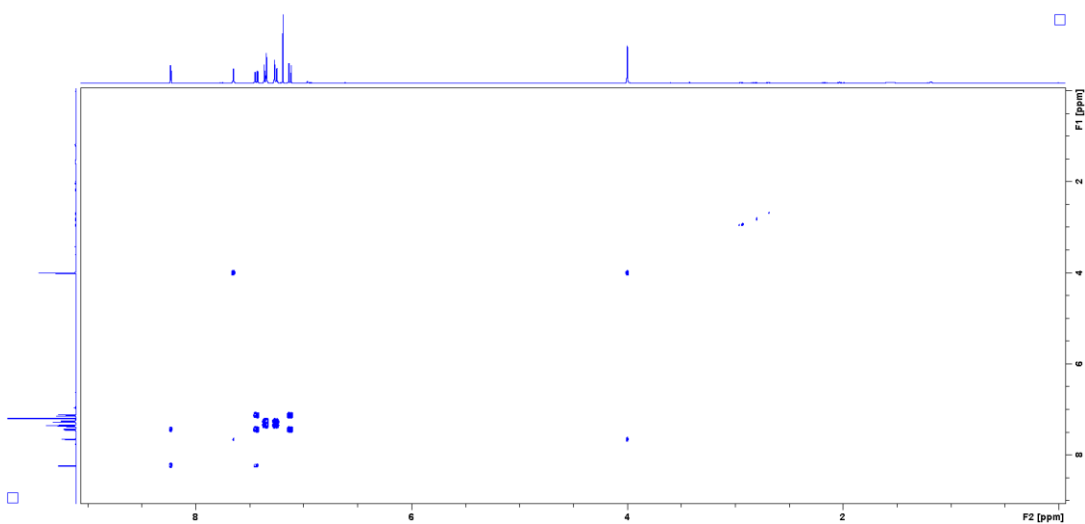
#### A.12.1.1 <sup>1</sup>H-NMR



### A.12.1.2 $^{13}\text{C}$ -NMR

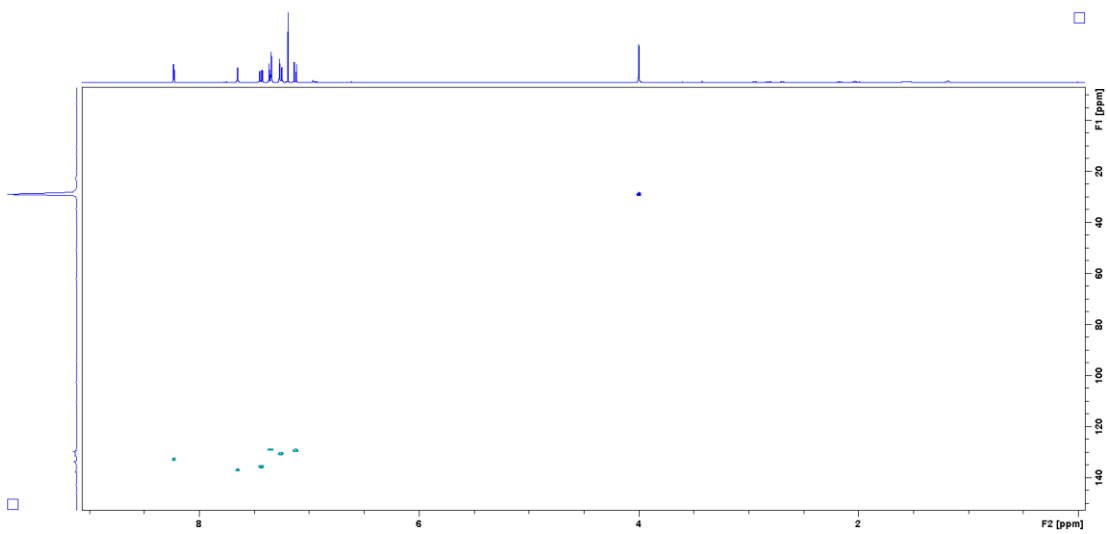


### A.12.1.3 COSY

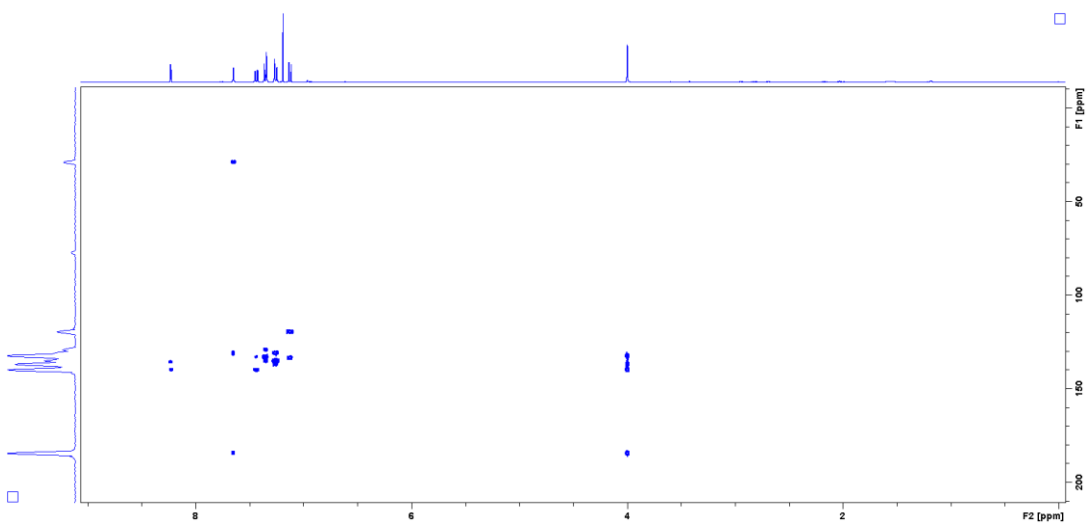




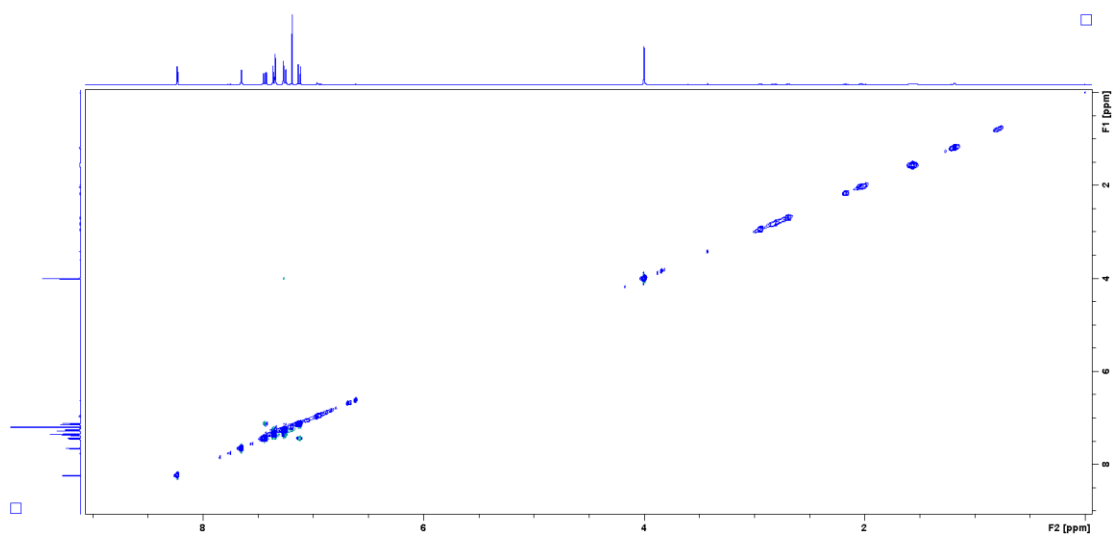
#### A.12.1.4 HSQC



#### A.12.1.5 HMBC



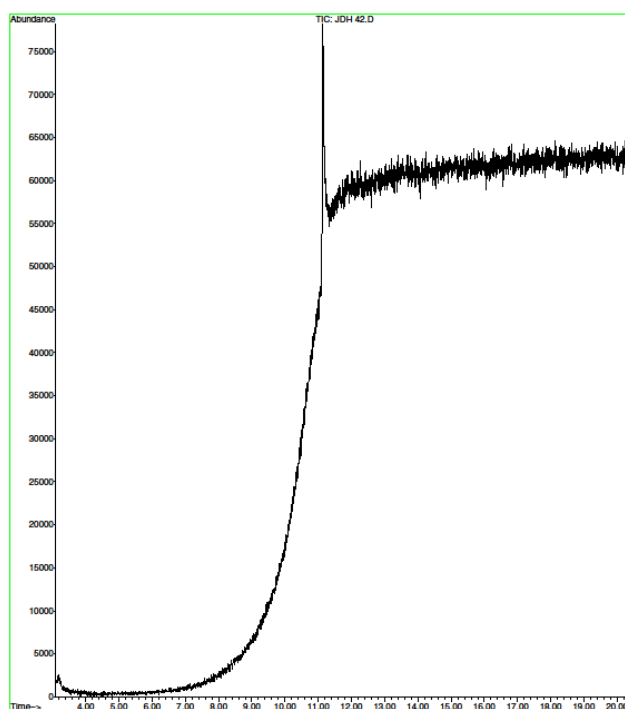
### A.12.1.6 NOESY



### A.12.2 GCMS

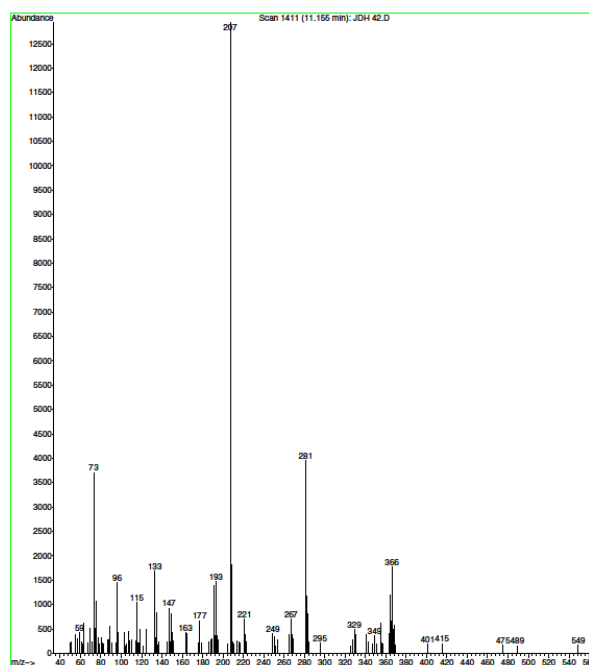
#### A.12.2.1 CHROMATOGRAM

File : E:\DATA\JDH 42.D  
Operator :  
Acquired : 8 May 2019 20:53 using AcqMethod HIGHTEMPAUTO.M  
Instrument : GC MS 1  
Sample Name: JDH 42  
Misc Info :  
Vial Number: 36

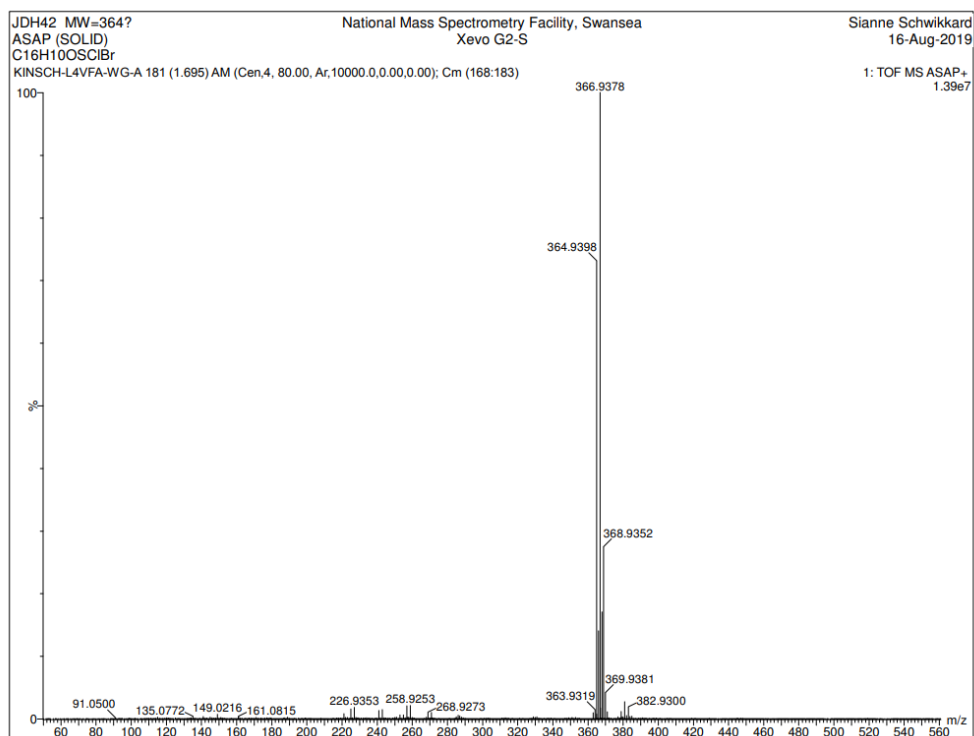


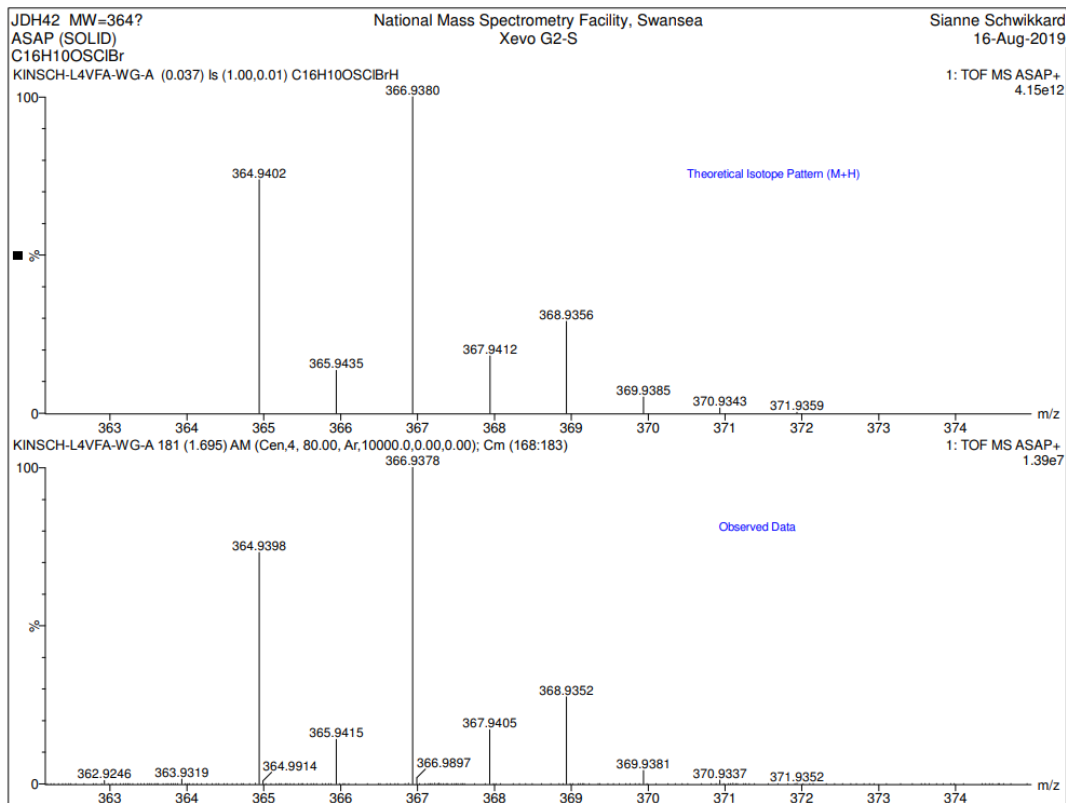
### A.12.2.2 MASS SPEC

File : E:\DATA\JDH 42.D  
Operator :  
Acquired : 8 May 2019 20:53 using AcqMethod HIGHTEMPAUTO.M  
Instrument : GC MS 1  
Sample Name: JDH 42  
Misc Info :  
Vial Number: 36

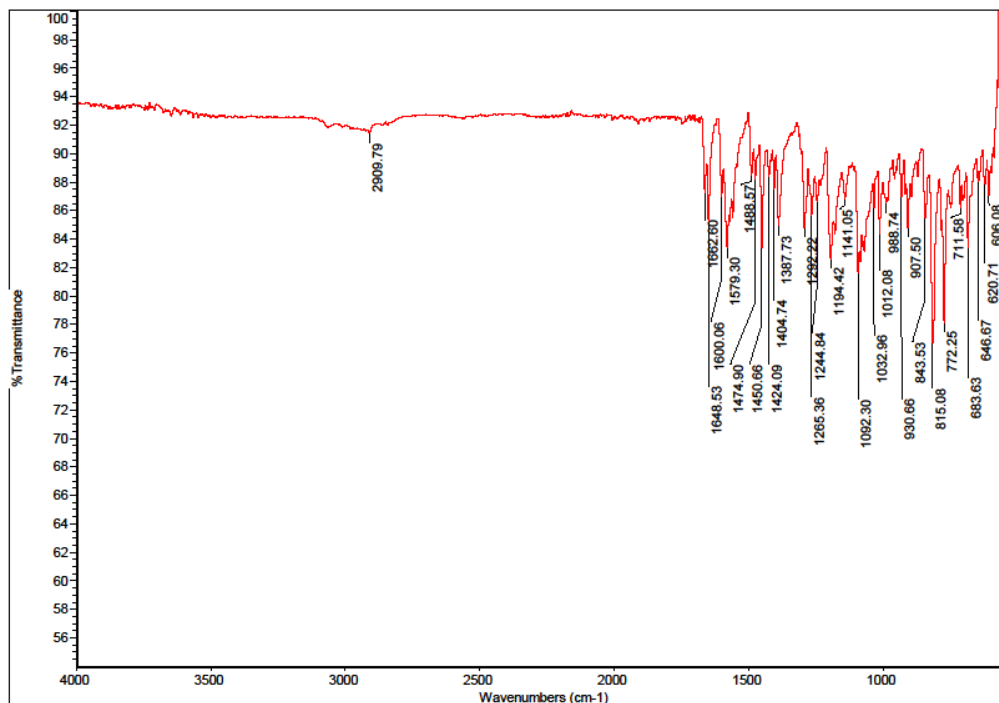


### A.12.3 HIGH RES MASS SPEC





#### A.12.4 IR DATA



## A.12.5 BIOLOGICAL DATA

### A.12.5.1 CYTOTOXICITY (HeLa)

#### A.12.5.1.1 CYTOTOXICITY PER CONCENTRATION

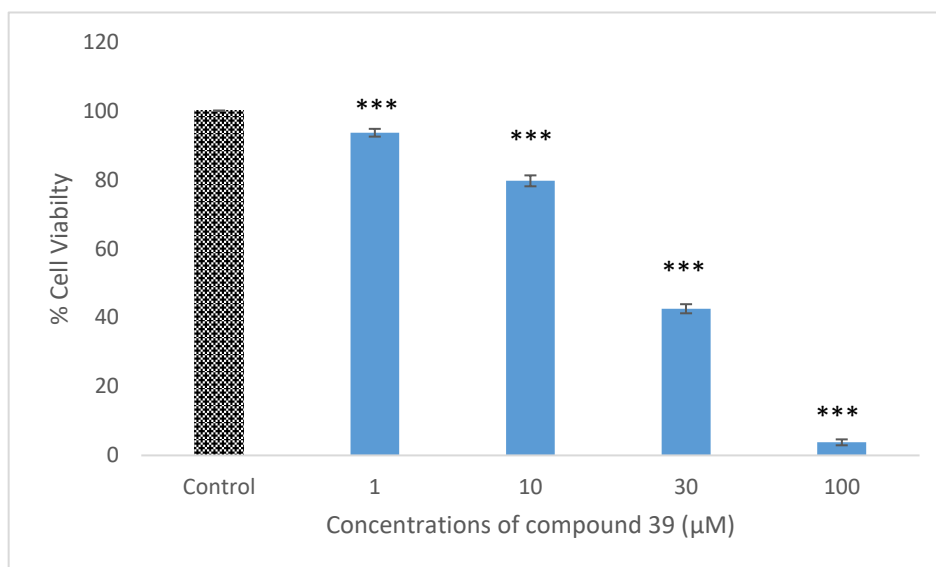
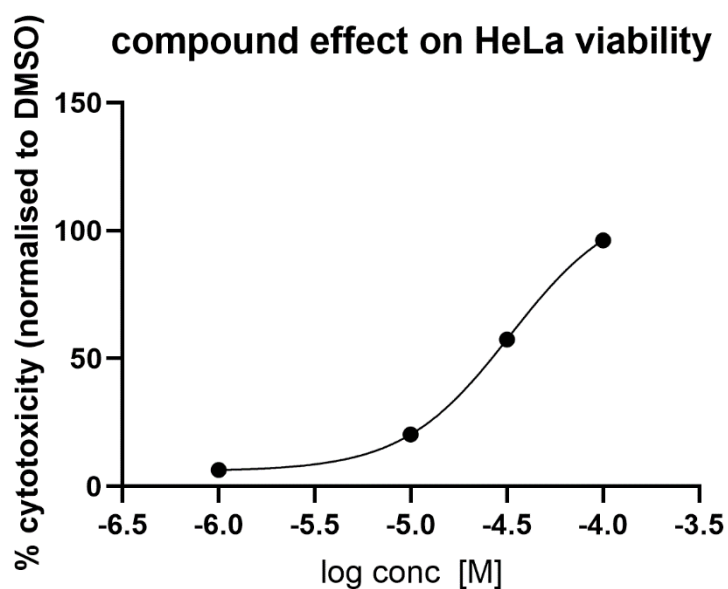


**Figure A.12.5.1.1.** Viability of HeLa cells exposed to different concentrations of compound 39 after 24 h incubation period. Cytotoxicity was determined via neutral red assay. The data is expressed as the percentage of inhibition compared with negative control in which the cell viability was assumed 100 % (means  $\pm$  SD, N =3). All concentrations tested showed significant cytotoxic effect compared to negative control (one way ANOVA with Dunnett's *posthoc* test, \*\*\*P <0.001)

#### A.12.5.1.2 IC<sub>50</sub>



## A.12.5.2 ANTI-PROLIFERATIVE DATA

### A.12.5.2.1 ANTI-PROLIFERATION PER CONCENTRATION (HREC)

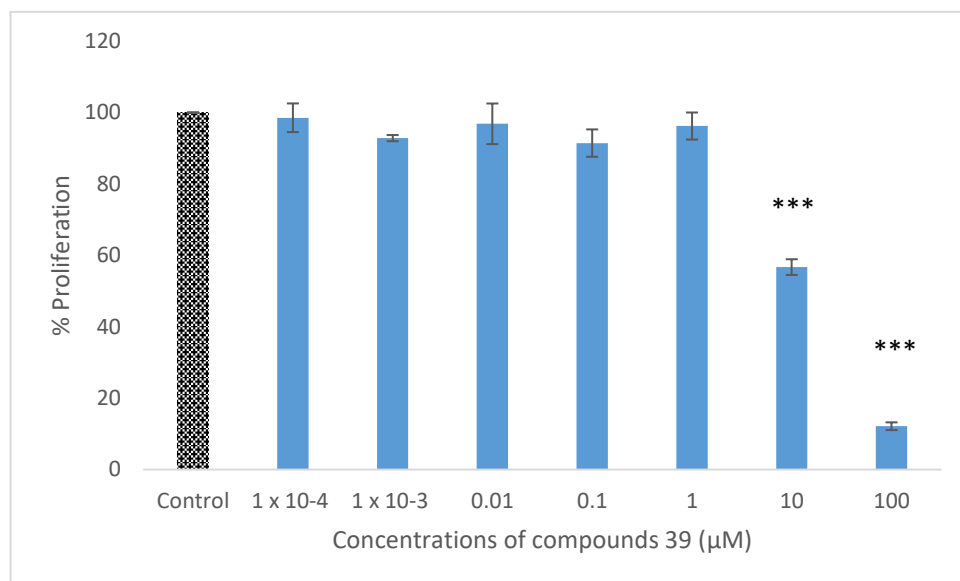
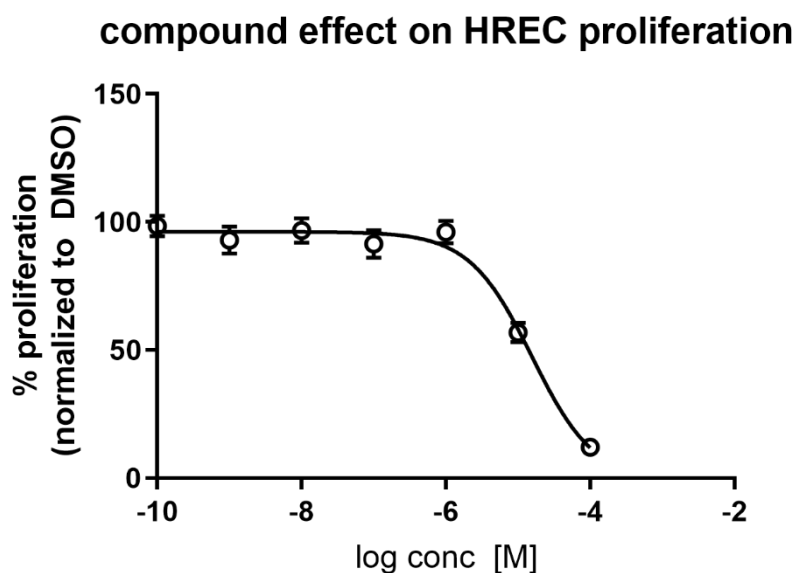


**Figure A.12.5.2.1.** Cell proliferation of HREC cells exposed to different concentrations of compound 39 after 24 hr incubation period. Cell proliferation was determined via the alamarBlue assay. The data is expressed as the percent proliferation compared with negative control in which the cell proliferation was assumed 100% (means  $\pm$  SD, N =3). Concentrations of 10  $\mu$ M and 100  $\mu$ M showed significant anti-proliferative effects compared to negative control (one way ANOVA with Dunnett's *posthoc* test, \*\*\*P <0.001).

### A.12.5.2.2 GI<sub>50</sub> (HREC)



### A.12.5.2.3 ANTI-PROLIFERATION PER CONCENTRATION (ARPE-19)

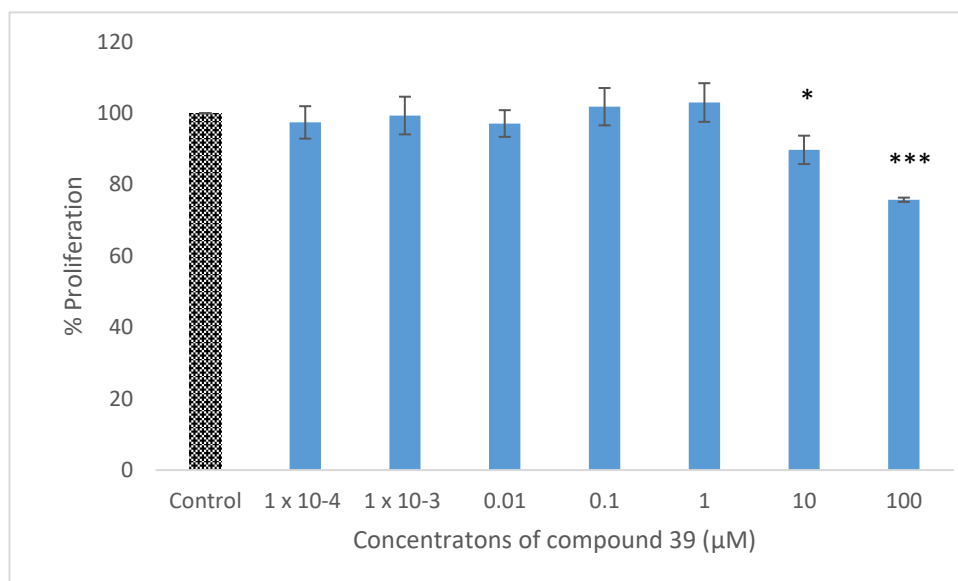
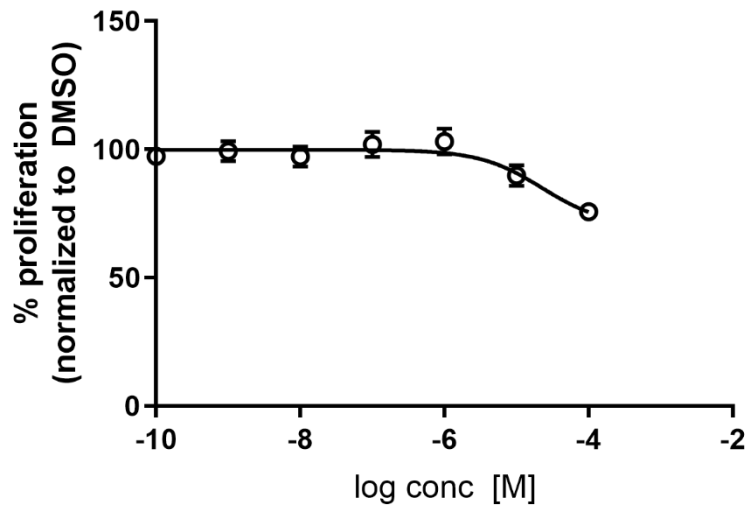


**Figure A.12.5.2.3.** Cell proliferation of ARPE-19 cells exposed to different concentrations of compound 39 after 24 hr incubation period. Cell proliferation was determined via the alamarBlue assay. The data is expressed as the percent proliferation compared with negative control in which the cell proliferation was assumed 100% (means  $\pm$  SD, N =3). Concentrations 10  $\mu$ M and 100  $\mu$ M showed significant anti-proliferative effects compared to negative control (one way ANOVA with Dunnett's posthoc test, \*P<0.05, \*\*\*P <0.001).

A.12.5.2.4 GI<sub>50</sub> (ARPE-19)

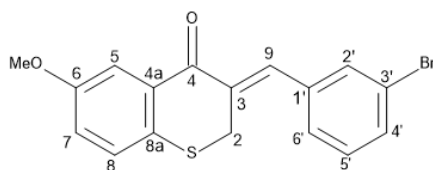
compound effect on ARPE-19 proliferation





### A.13 Compound 40

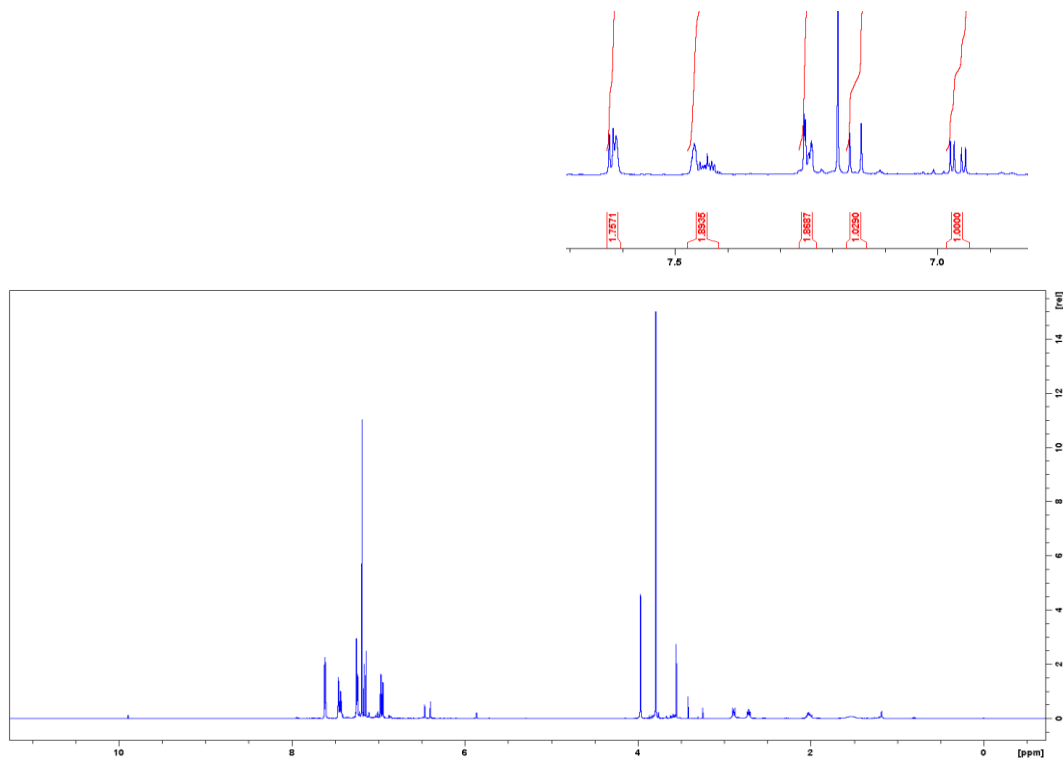
(3Z)-3-[(3-bromophenyl)methylidene]-6-methoxy-2,3-dihydro-4H-1-benzothiopyran-4-one (40)



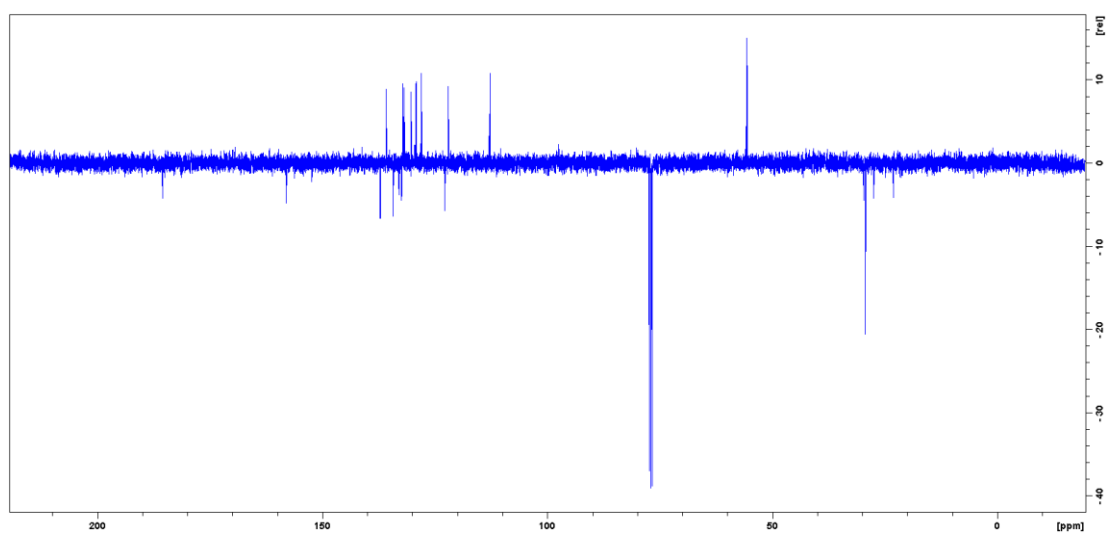
Yellow solid, 104 mg, 17.8 %, 106.5 - 107.0 °C, IR  $\nu_{\max}$  (cm<sup>-1</sup>): 2910 (Ar-H), 1660 (C=O), 1592 (Aliphatic C=C), 1558 (Aromatic C=C), 1031 (C-O), 775 (C-Br), 662 (C-S). <sup>1</sup>H-NMR (400 MHz, CDCl<sub>3</sub>):  $\delta$  = 7.62 (1H, d, J = 2.90 Hz, H-5), 7.61 (1H, s, H-9), 7.45 (1H, m, H-2'), 7.45 (1H, m, H-6'), 7.24 (1H, m, H-4'), 7.24 (1H, m, H-5'), 7.15 (1H, d, J = 8.70 Hz, H-8), 6.96 (1H, dd, J = 2.9, 8.7 Hz, H-7), 3.97 (2H, d, J = 1.1 Hz, H-2), 3.79 (s, OCH<sub>3</sub>). <sup>13</sup>C-NMR (100 MHz, CDCl<sub>3</sub>):  $\delta$  = 185.7 (C-4), 158.4 (C-6), 137.2 (C-1'), 135.2 (C-9), 134.4 (C-3'), 133.0 (C-8a), 132.4 (C-3), 132.1 (C-6'), 131.8 (C-2'), 130.2 (C-4'), 129.5 (C-8), 127.9 (C-5'), 55.6 (OCH<sub>3</sub>), 29.3 (C-2). R<sub>f</sub> = 0.75 (1:1 EtOAc:hexane). HRESMS (ASAP)  $m/z$  360.9897 [M]<sup>+</sup> (calcd [C<sub>17</sub>H<sub>14</sub>O<sub>2</sub>SBr], 360.9898).

#### A.13.1 NMR

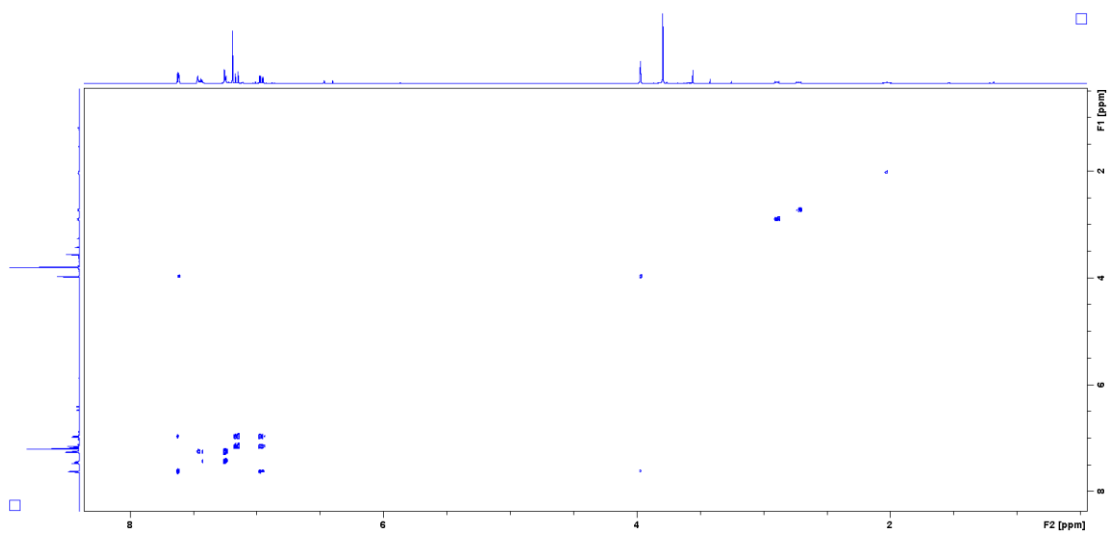
##### A.13.1.1 <sup>1</sup>H-NMR



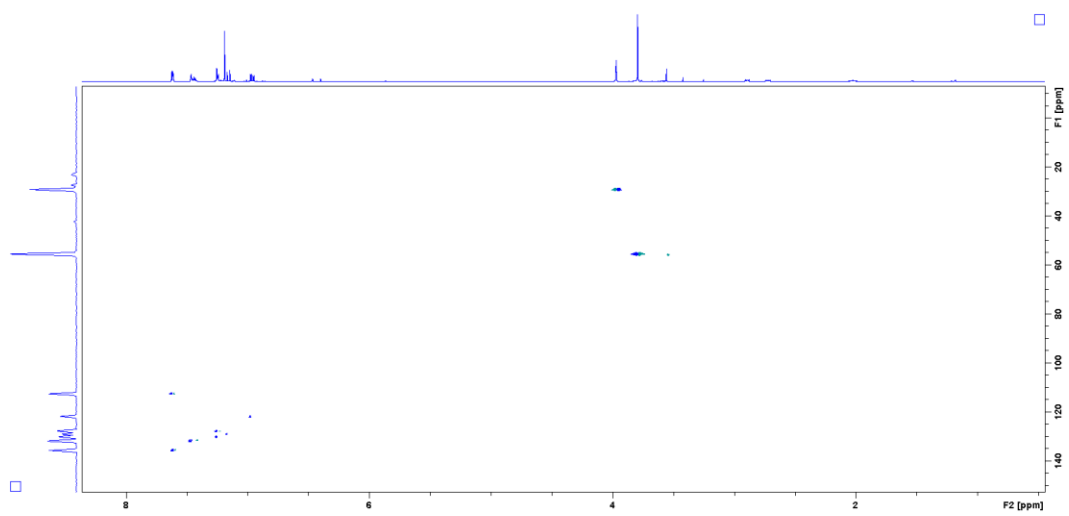
### A.13.1.2 $^{13}\text{C}$ -NMR



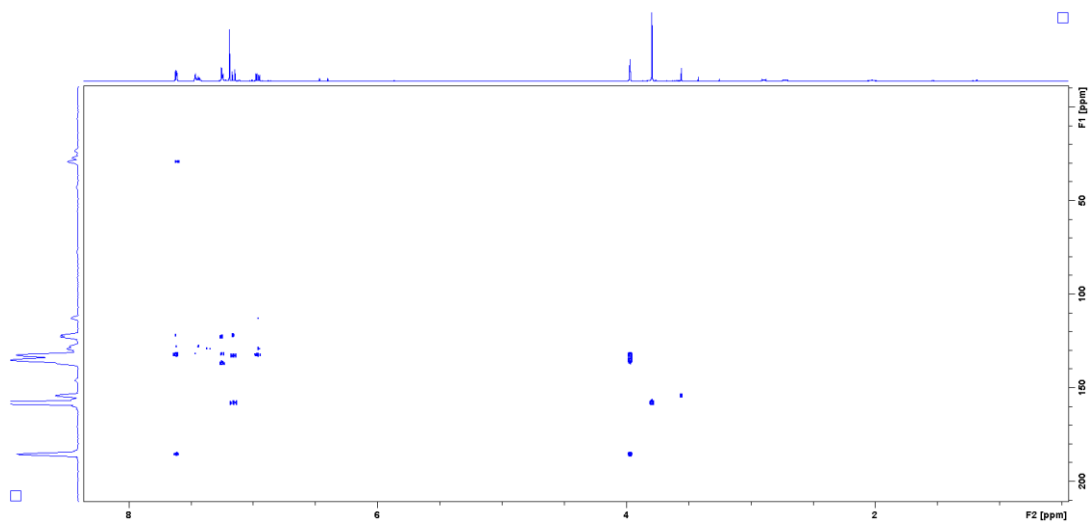
### A.13.1.3 COSY



### A.13.1.4 HSQC



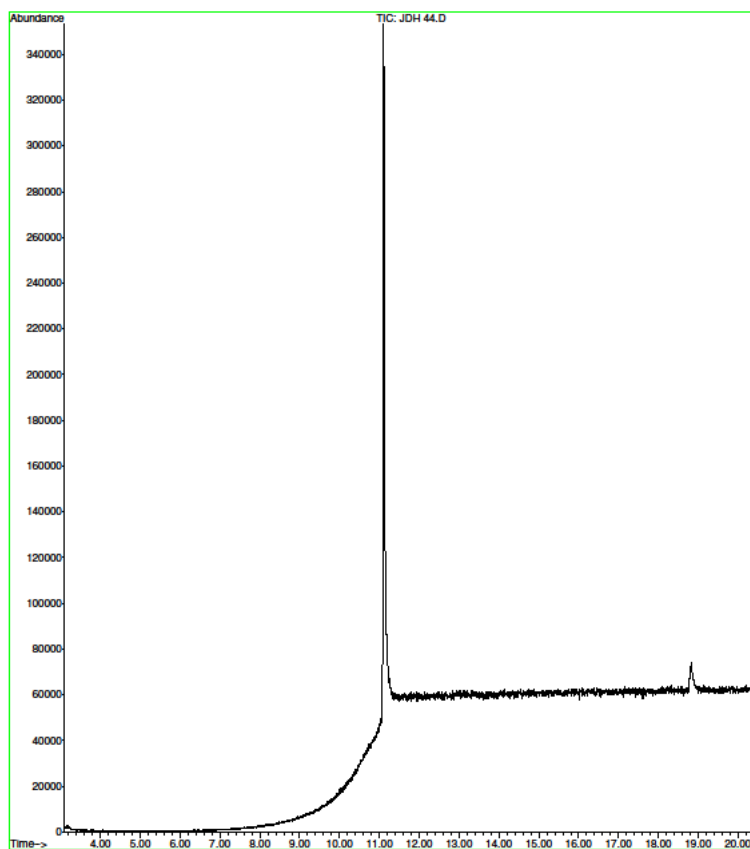
### A.13.1.5 HMBC



## A.13.2 GCMS

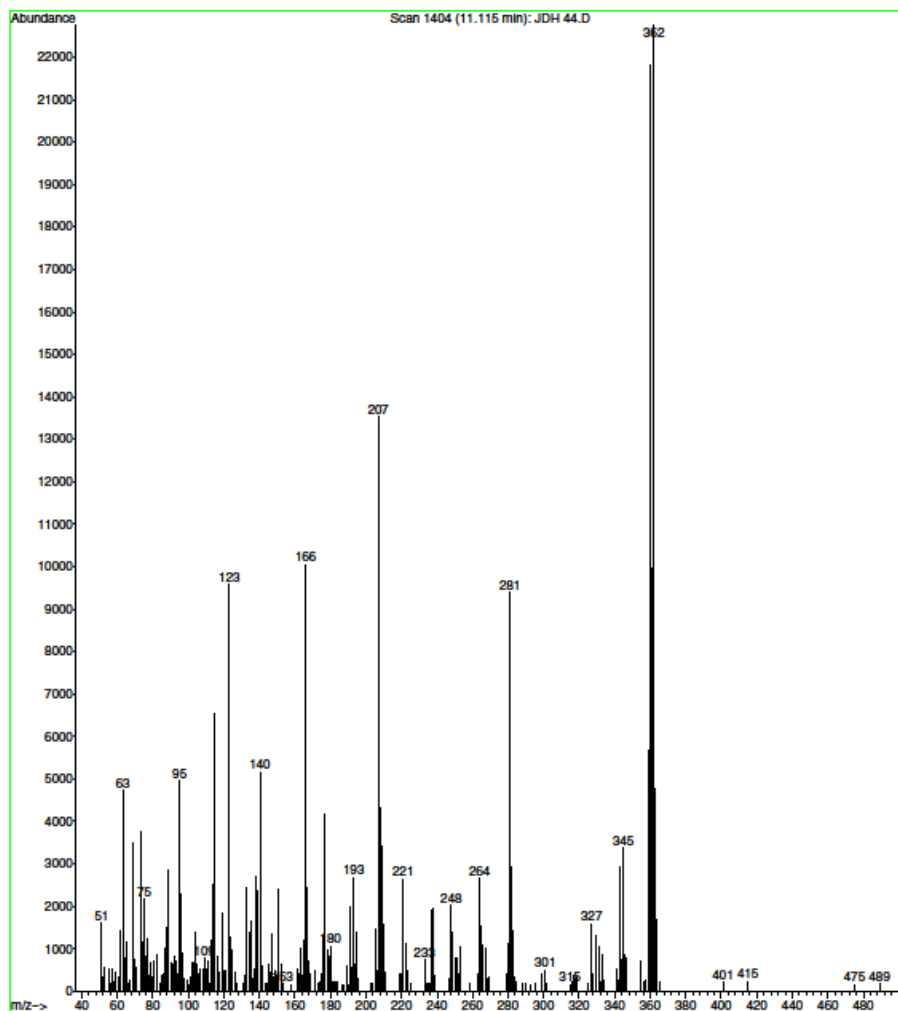
### A.13.2.1 CHROMATOGRAM

File : E:\DATA\JDH 44.D  
Operator :  
Acquired : 8 May 2019 21:18 using AcqMethod HIGHTEMPAUTO.M  
Instrument : GC MS 1  
Sample Name: JDH 44  
Misc Info :  
Vial Number: 37

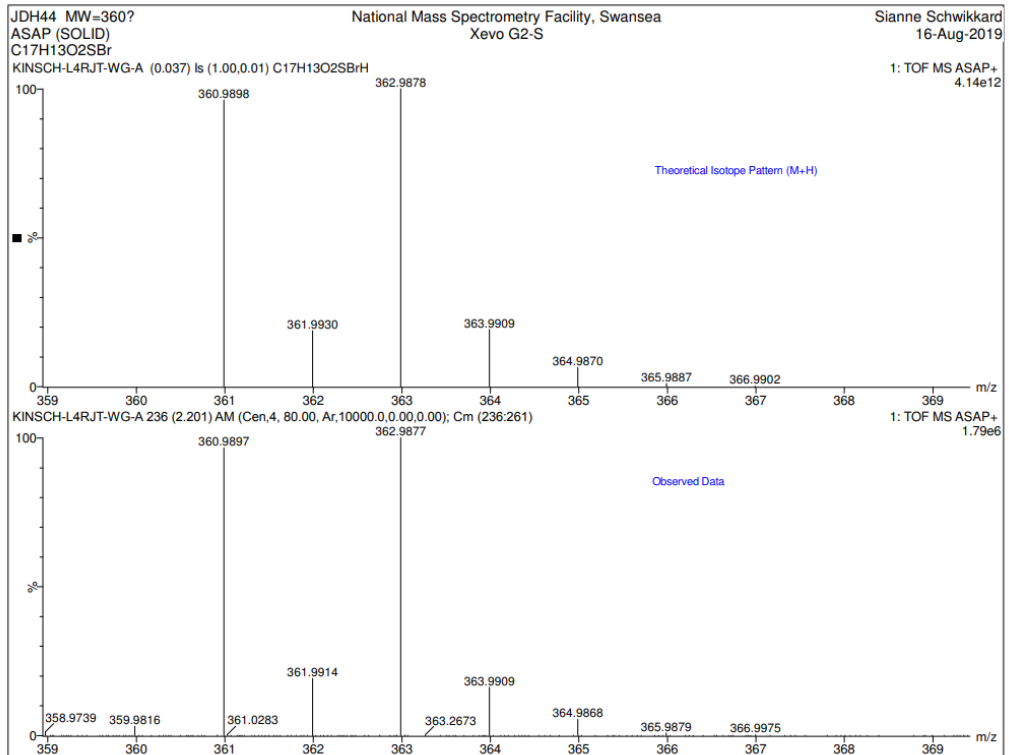
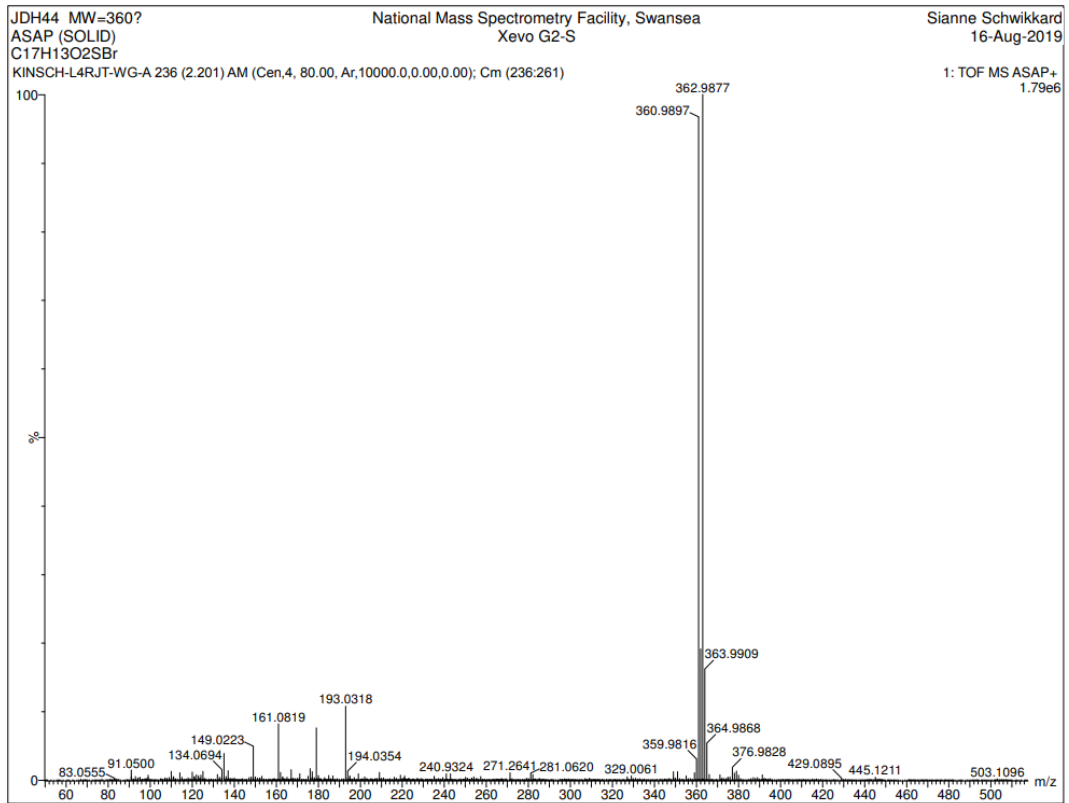


### A.13.2.2 MASS SPEC

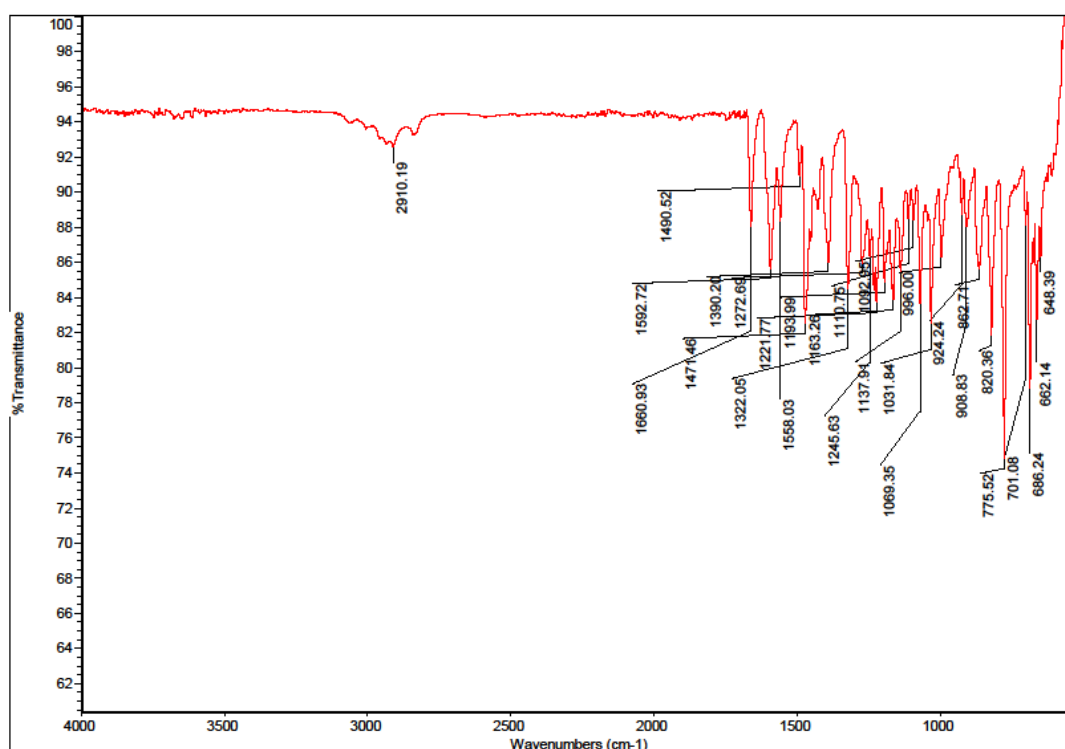
File :E:\DATA\JDH 44.D  
Operator :  
Acquired : 8 May 2019 21:18 using AcqMethod HIGHTEMPAUTO.M  
Instrument : GC MS 1  
Sample Name: JDH 44  
Misc Info :  
Vial Number: 37



### A.13.3 HIGH RES MASS SPEC



### A.13.4 IR DATA



### A.13.5 BIOLOGICAL DATA

#### A.13.5.1 CYTOTOXICITY (HeLa)

##### A.13.5.1.1 CYTOTOXICITY PER CONCENTRATION

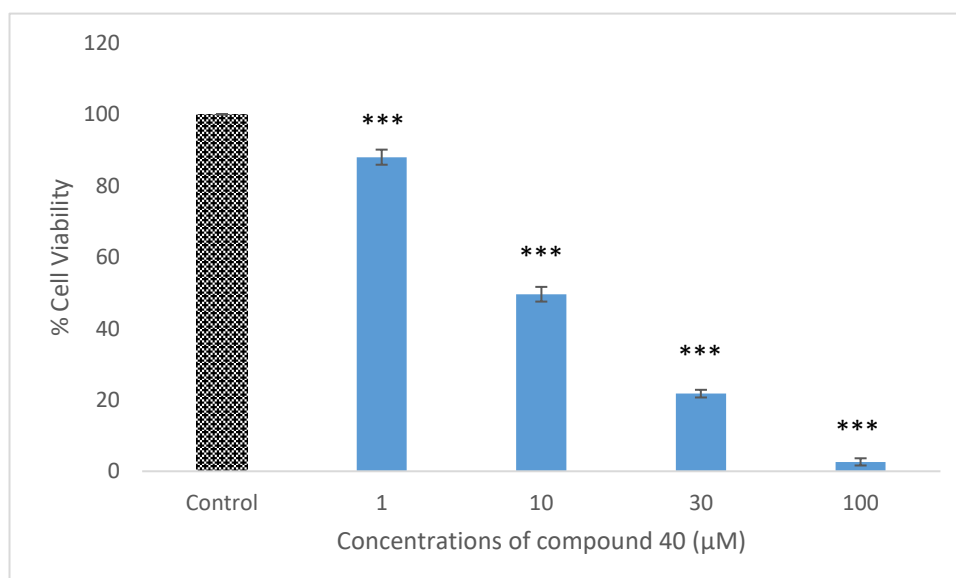
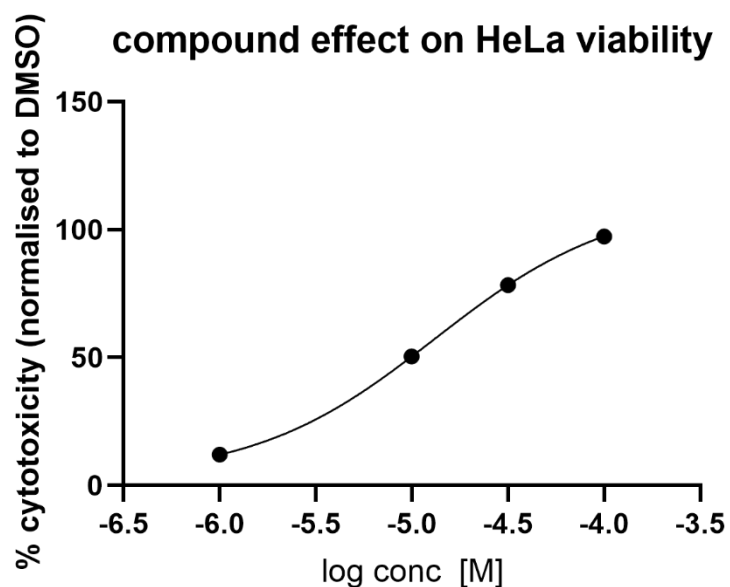


**Figure A.13.5.1.1.** Viability of HeLa cells exposed to different concentrations of compound 40 after 24 h incubation period. Cytotoxicity was determined via neutral red assay. The data is expressed as the percentage of inhibition compared with negative control in which the cell viability was assumed 100 % (means  $\pm$  SD, N =3). All concentrations tested showed significant cytotoxic effect compared to negative control (one way ANOVA with Dunnett's *posthoc* test, \*\*\*P <0.001)

### A.13.5.1.2 IC<sub>50</sub>



### A.13.5.2 ANTI-PROLIFERATIVE DATA

#### A.13.5.2.1 ANTI-PROLIFERATION PER CONCENTRATION (HREC)

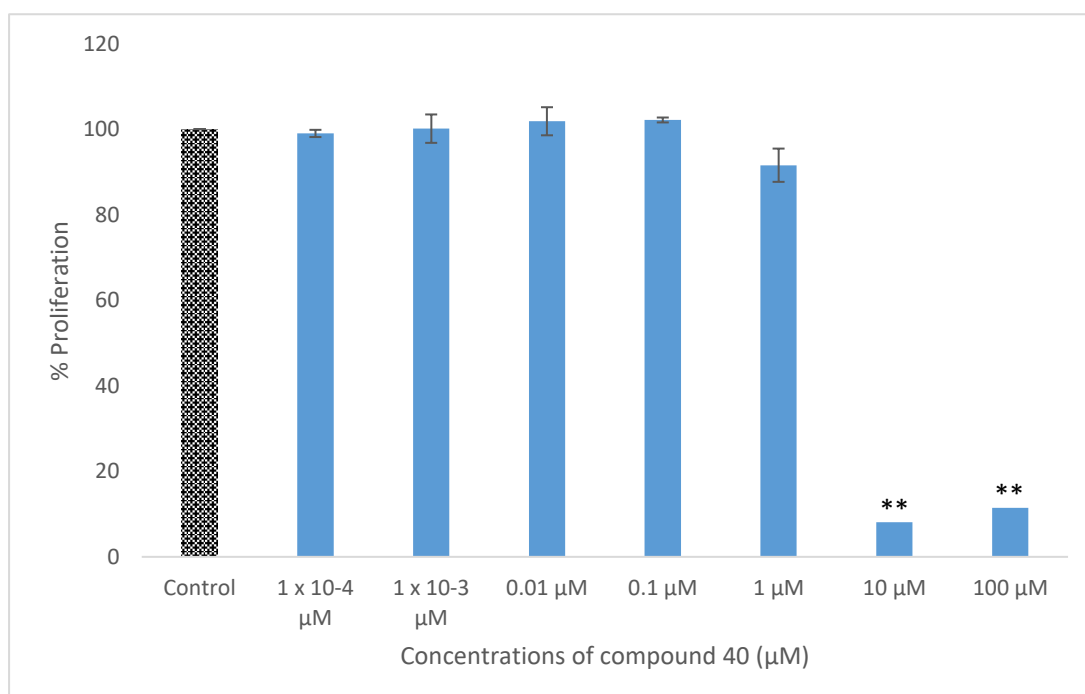
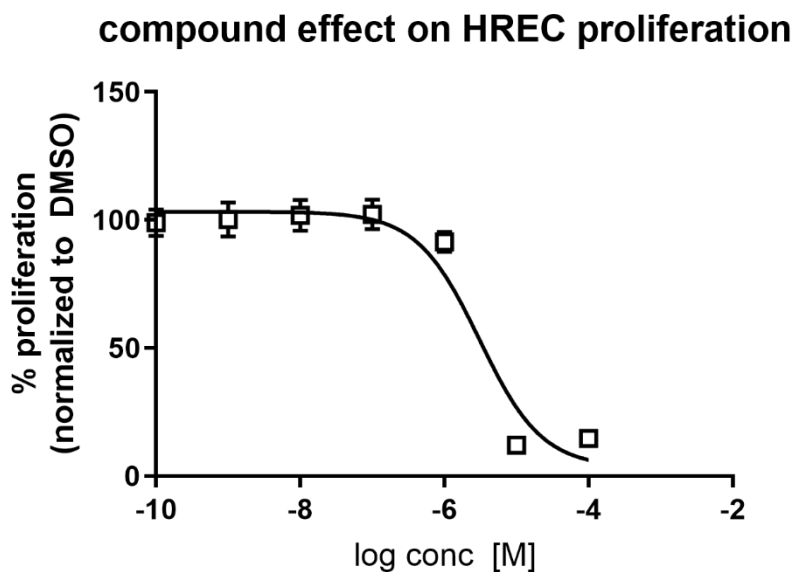


**Figure A.13.5.2.1.** Cell proliferation of HREC cells exposed to different concentrations of compound 40 after 24 hr incubation period. Cell proliferation was determined via the alamarBlue assay. The data is expressed as the percent proliferation compared with negative control in which the cell proliferation was assumed 100% (means  $\pm$  SD, N =3). Concentrations of 10  $\mu$ M and 100  $\mu$ M showed significant anti-proliferative effects compared to negative control (one way ANOVA with Dunnett's *posthoc* test, \*P <0.001).



#### A.13.5.2.2 GI<sub>50</sub> (HREC)



#### A.13.5.2.3 ANTI-PROLIFERATION PER CONCENTRATION (ARPE-19)

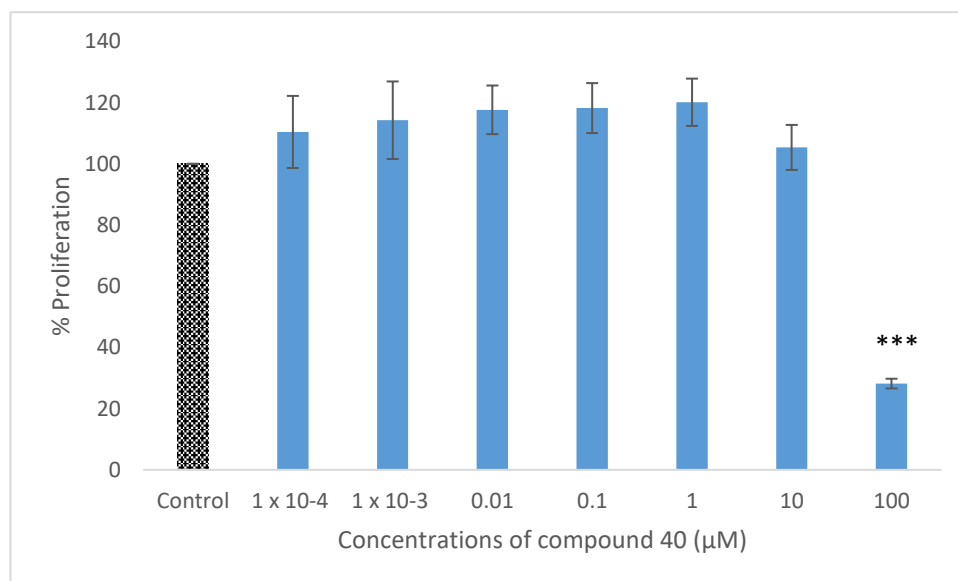
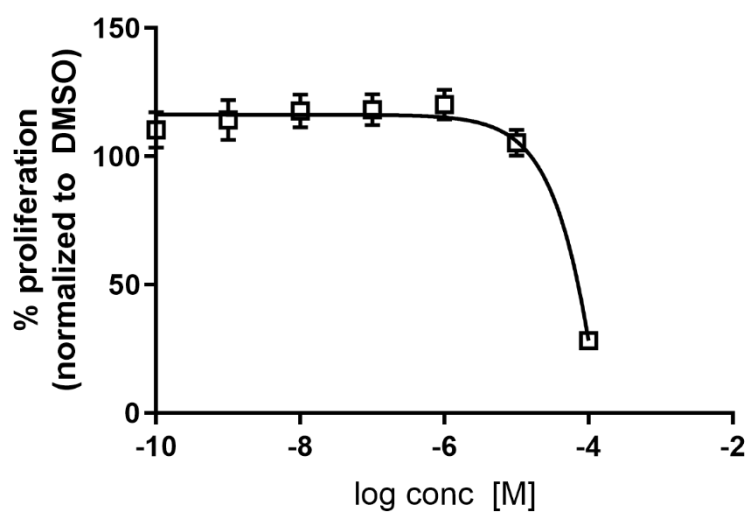


**Figure A.13.5.2.3.** Cell proliferation of ARPE-19 cells exposed to different concentrations of compound 40 after 24 hr incubation period. Cell proliferation was determined via the alamarBlue assay. The data is expressed as the percent proliferation compared with negative control in which the cell proliferation was assumed 100% (means  $\pm$  SD, N=3). Concentration 100  $\mu$ M showed significant anti-proliferative effects compared to negative control (one way ANOVA with Dunnett's posthoc test, \*\*\*P < 0.001).

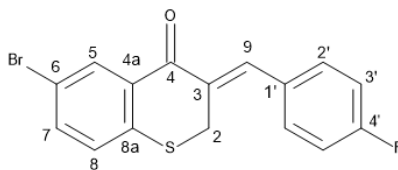
A.13.5.2.4 GI<sub>50</sub> (ARPE-19)

compound effect on ARPE-19 proliferation



## A.14Compound 41

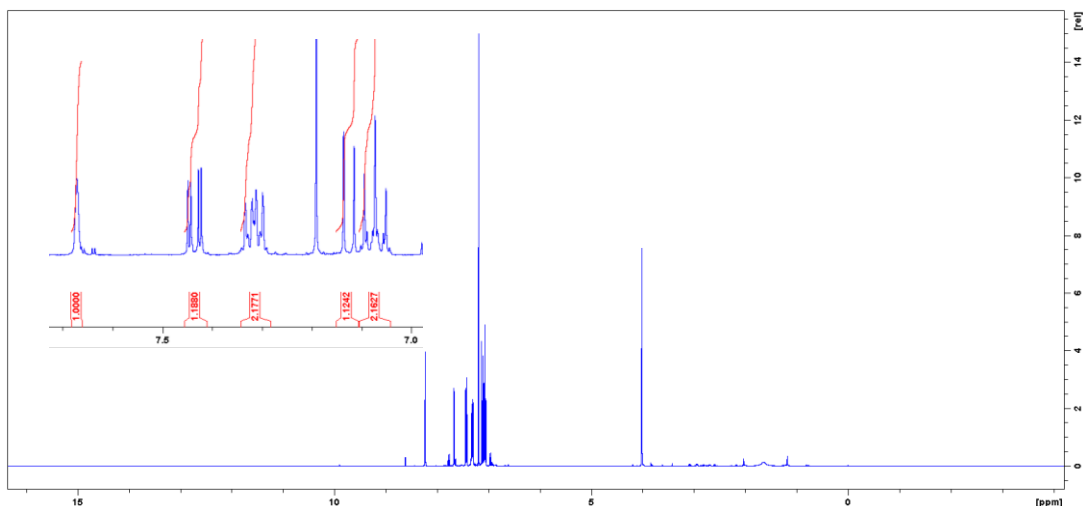
(3Z)-6-bromo-3-[(4-fluorophenyl)methylidene]-2,3-dihydro-4H-1-benzothiopyran-4-one (41)



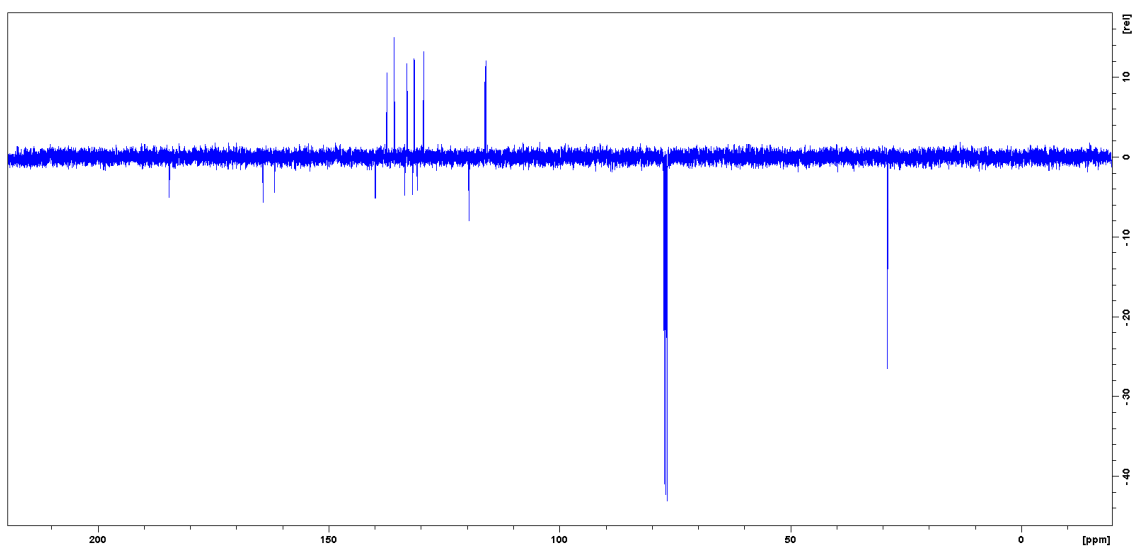
Light grey solid, 162 mg, 28.2 %, 136.8 - 137.4 °C, IR  $\nu_{\max}$  ( $\text{cm}^{-1}$ ): 3055 (Ar-H), 1662 (C=O), 1598 (Aliphatic C=C), 1583 (Aromatic C=C), 904 (C-F), 784 (C-Br), 684 (C-S),  $^1\text{H-NMR}$  (400 MHz,  $\text{CDCl}_3$ ):  $\delta$  = 8.32 (1H, d,  $J$  = 2.3 Hz, H-5), 7.77 (1H, brs  $w_{1/2}$  , H-9), 7.43 (1H, dd,  $J$  = 2.3 Hz, 8.5 Hz, H-7), 7.41 (2H, dd,  $J$  =5.3 Hz, 9.0 Hz, H-2'), 7.22 (1H, d, 8.5 Hz, H-8), 7.14 (2H, t,  $J$  = 8.5 Hz, H-3'), 4.10 (2H, d,  $J$  = 1.1 Hz, H-2);  $^{13}\text{C-NMR}$  (100 MHz,  $\text{CDCl}_3$ ):  $\delta$  = 184.6 (C-4), 164.2 (d,  $J$  = 244.9 Hz, C-4'), 119.6 (C-6), 137.4 (C-9), 135.8 (C-7), 131.8 (C-1'), 133.2 (C-5), 133.5 (C-4a), 131.4 (C-2'), 130.9 (C-3), 129.4 (C-8), 139.9(C-8a), 116.2 (d,  $J$  = 21.8 Hz, C-3'), 29.1 (C-2),  $R_f$  = 0.80 (1:1 EtOAc:hexane). HRESMS (ASAP)  $m/z$  348.9695  $[\text{M}]^+$  (calcd  $[\text{C}_{16}\text{H}_{11}\text{OSBrF}]$ , 348.9698).

### A.14.1 NMR

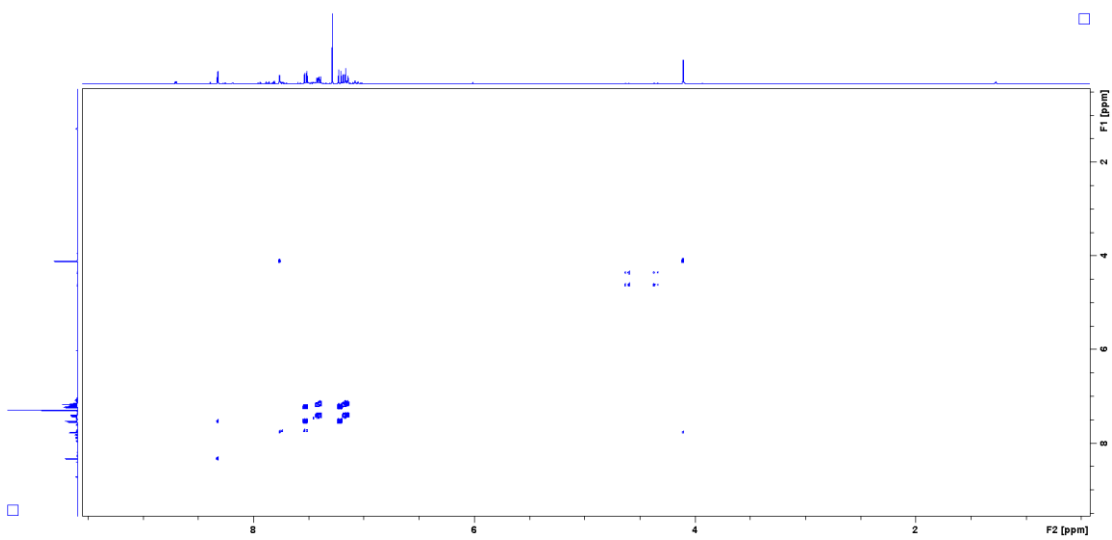
#### A.14.1.1 $^1\text{H-NMR}$



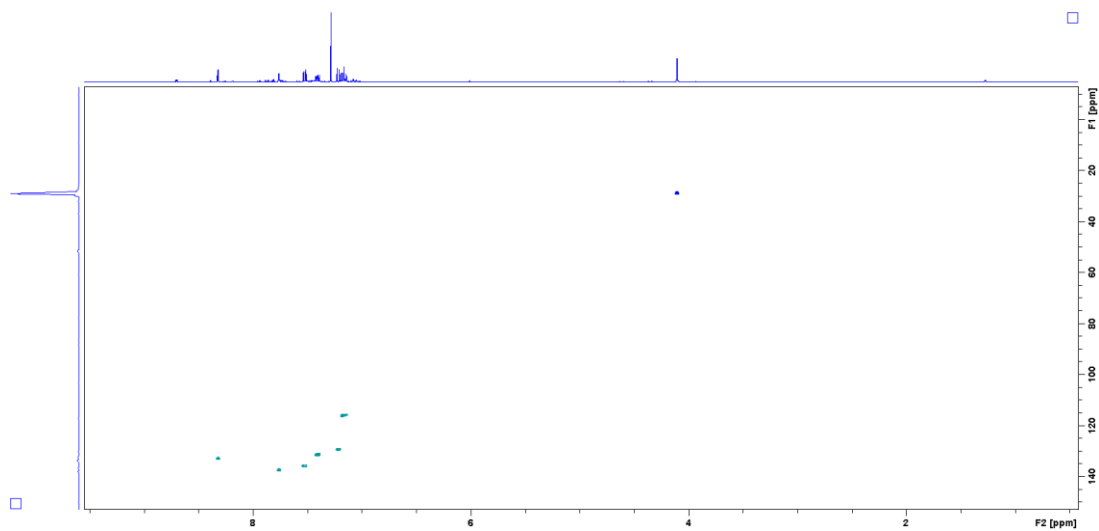
### A.14.1.2 $^{13}\text{C}$ -NMR



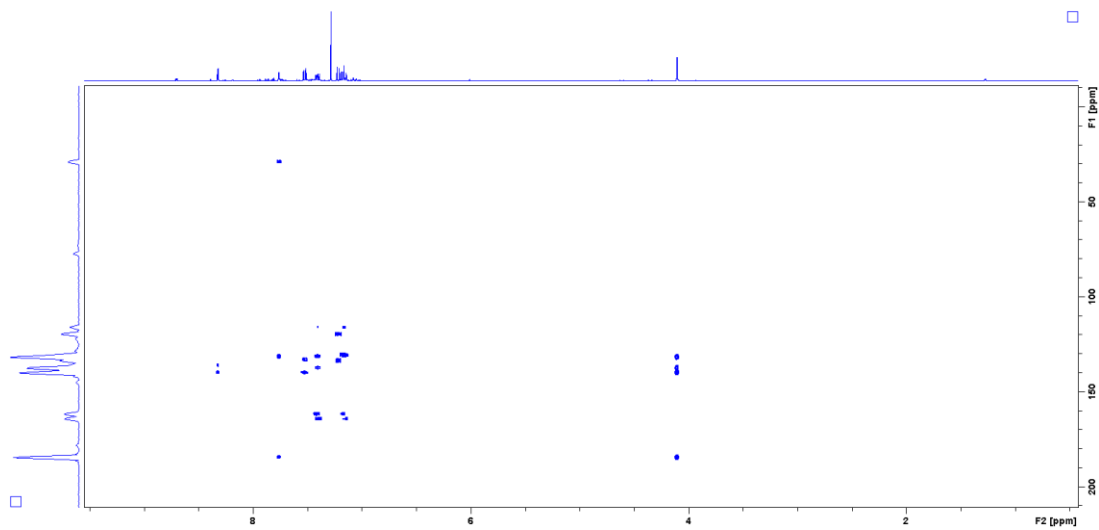
### A.14.1.3 COSY



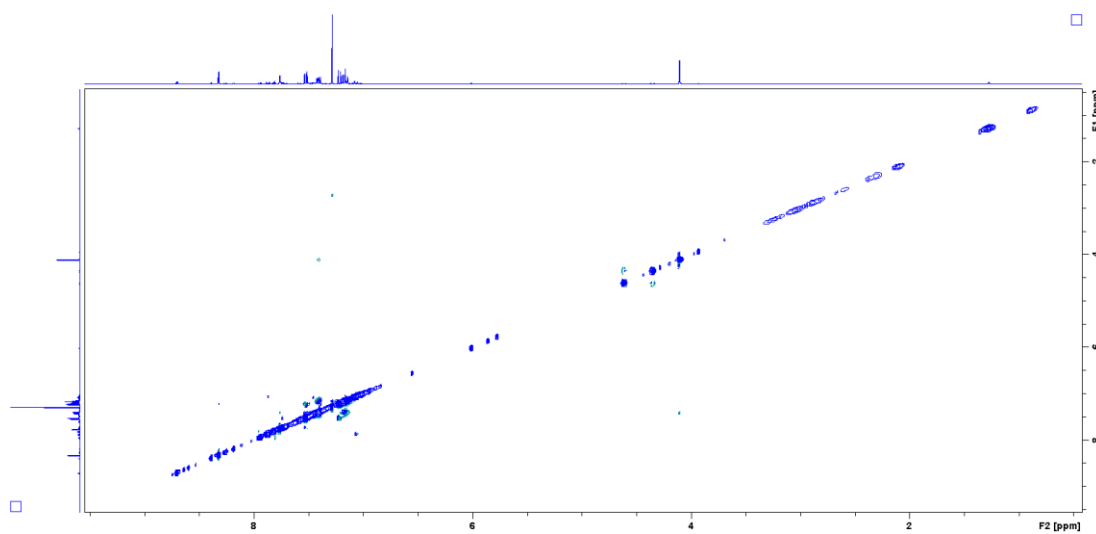
#### A.14.1.4 HSQC



#### A.14.1.5 HMBC



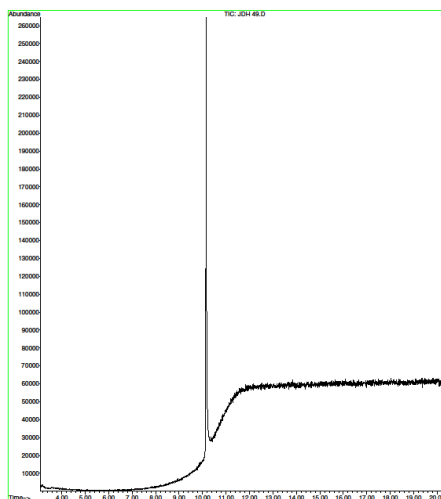
### A.14.1.6 NOESY



### A.14.2 GCMS

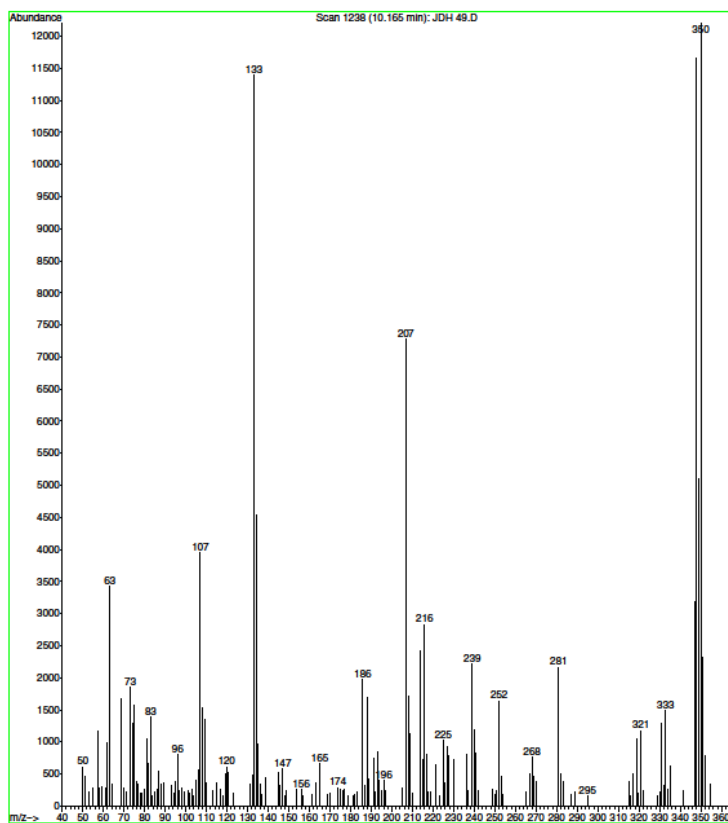
#### A.14.2.1 CHROMATOGRAM

File : E:\DATA\008 49.D  
Operator :  
Acquire : 8 May 2019 21:42 using AcqMethod RIGHTMSAUTO.M  
Instrument : GC MS  
Sample Name : 008 49  
Misc Info :  
Vial Number: 38

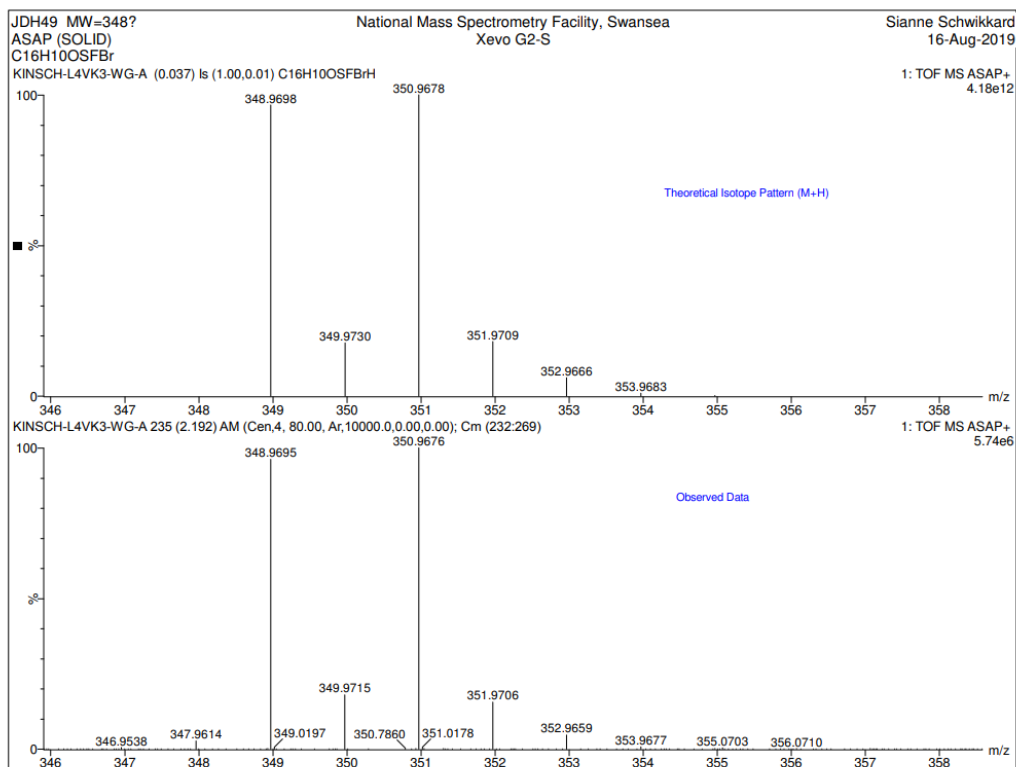
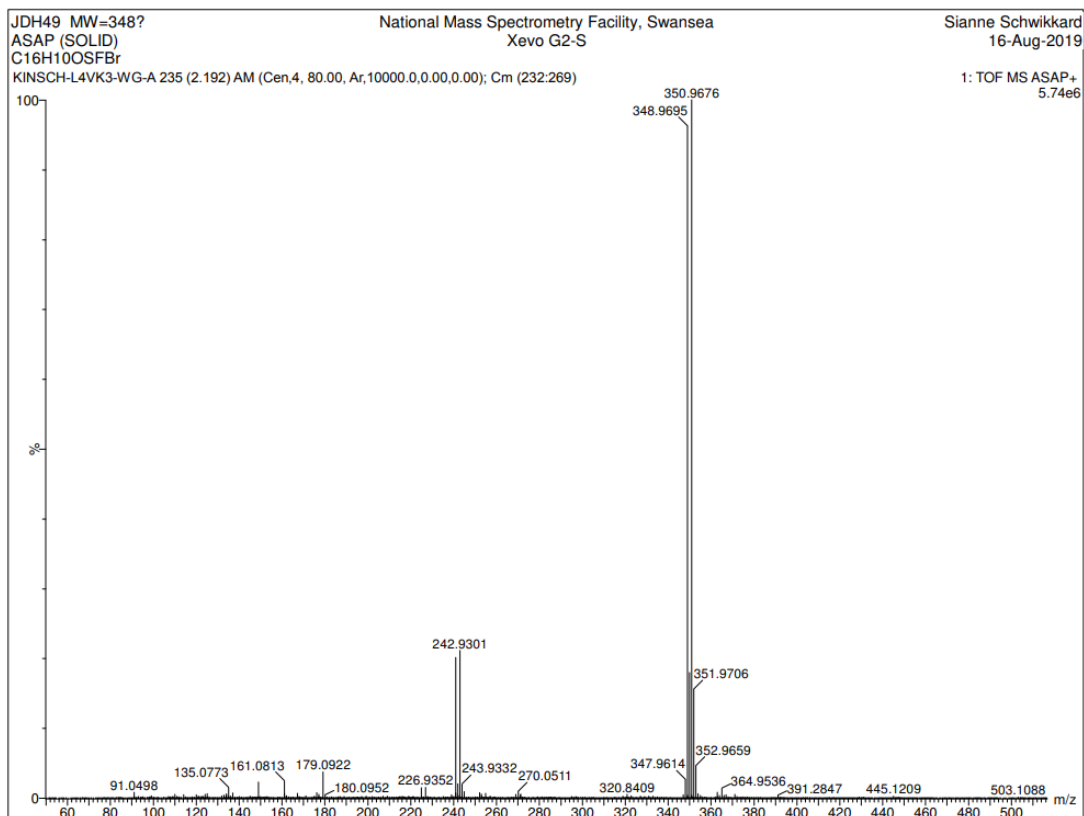


### A.14.2.2 MASS SPEC

File : E:\DATA\JDH 49.D  
Operator :  
Acquired : 8 May 2019 21:42 using AcqMethod HIGHTEMPAUTO.M  
Instrument : GC MS 1  
Sample Name: JDH 49  
Misc Info :  
Vial Number: 38

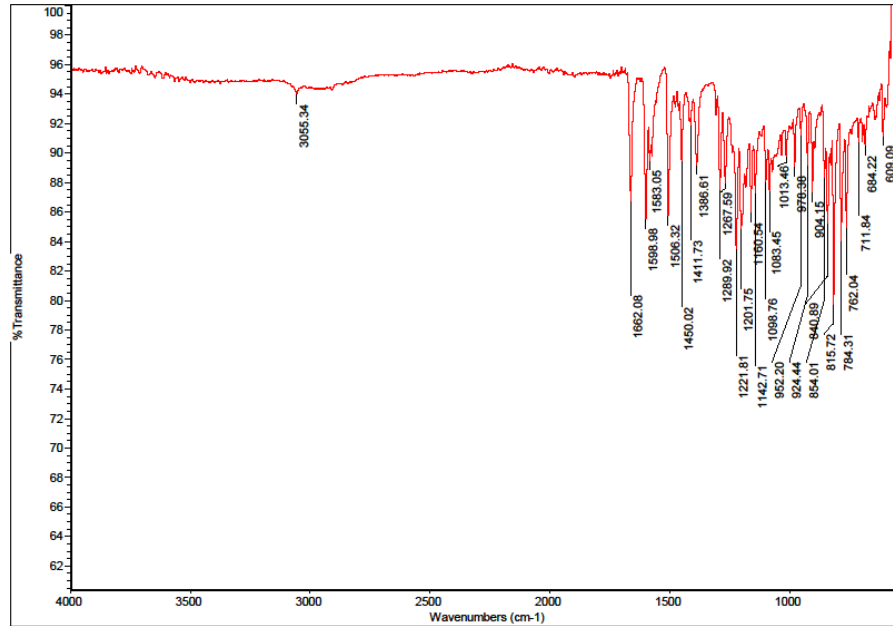


### A.14.3 HIGH RES MASS SPEC



### A.14.4 IR DATA





#### A.14.5 BIOLOGICAL DATA

##### A.14.5.1 CYTOTOXICITY (HeLa)

##### A.14.5.1.1 CYTOTOXICITY PER CONCENTRATION

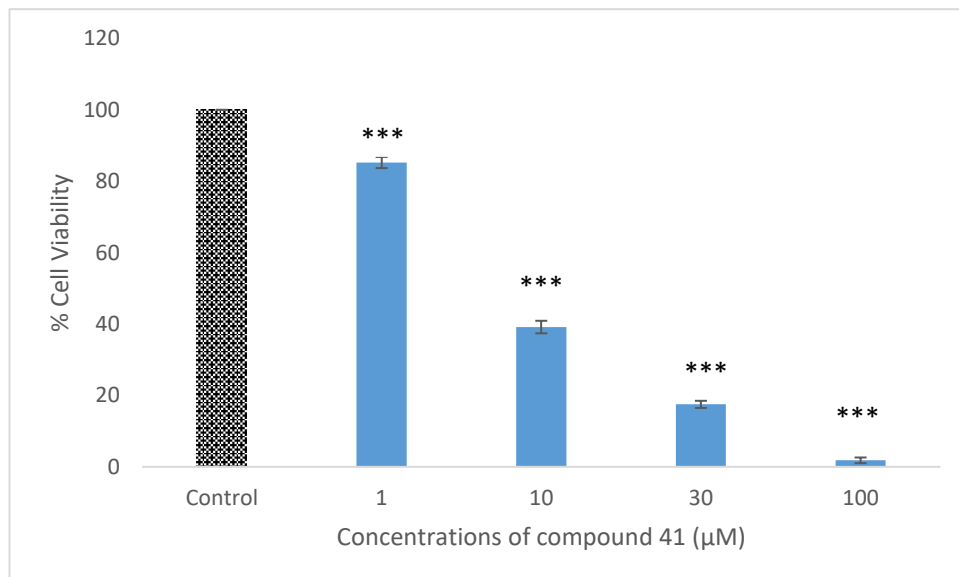
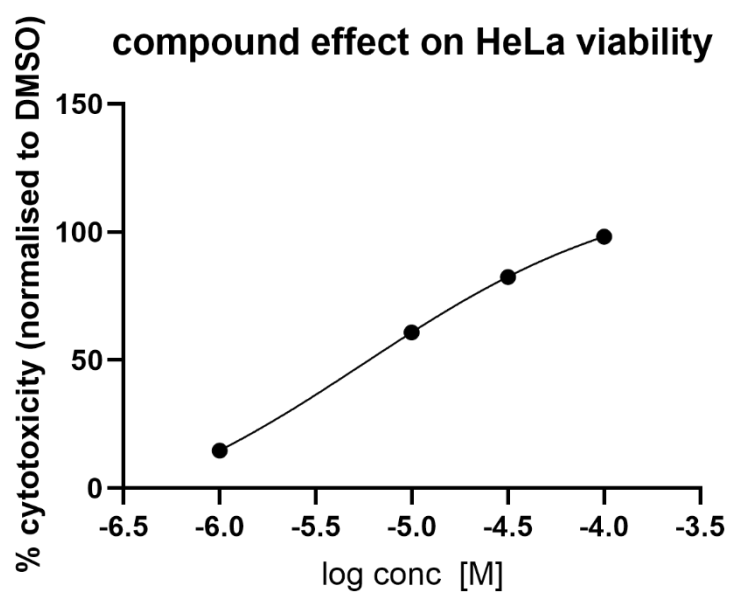


**Figure A.14.5.1.11.** Viability of HeLa cells exposed to different concentrations of compound 41 after 24 h incubation period. Cytotoxicity was determined via neutral red assay. The data is expressed as the percentage of inhibition compared with negative control in which the cell viability was assumed 100 % (means  $\pm$  SD, N =3). All concentrations tested showed significant cytotoxic effect compared to negative control (one way ANOVA with Dunnett's *posthoc* test, \*\*\*P <0.001)

#### A.14.5.1.2 IC<sub>50</sub>



#### A.14.1.2 ANTI-PROLIFERATIVE DATA

##### A.14.5.2.1 ANTI-PROLIFERATION PER CONCENTRATION (HREC)

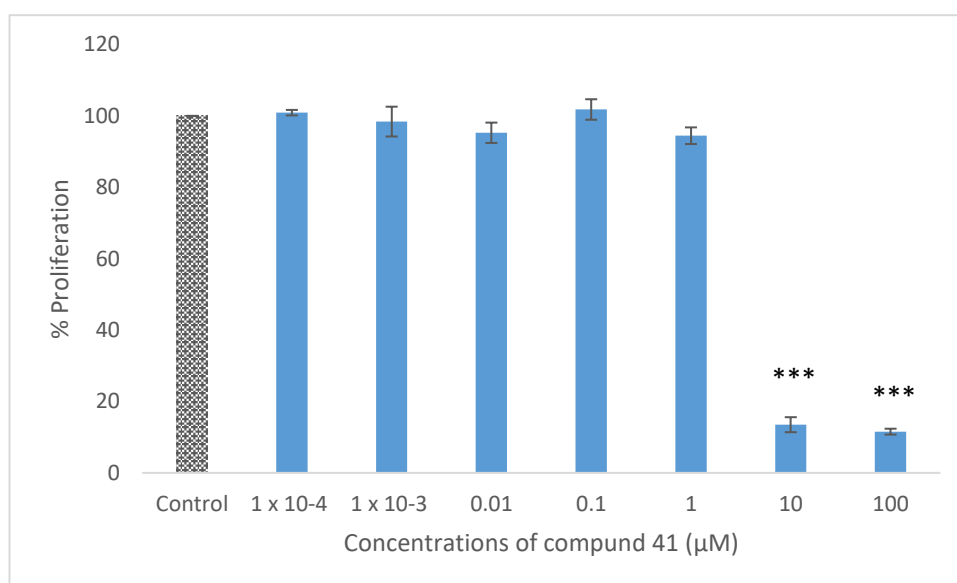
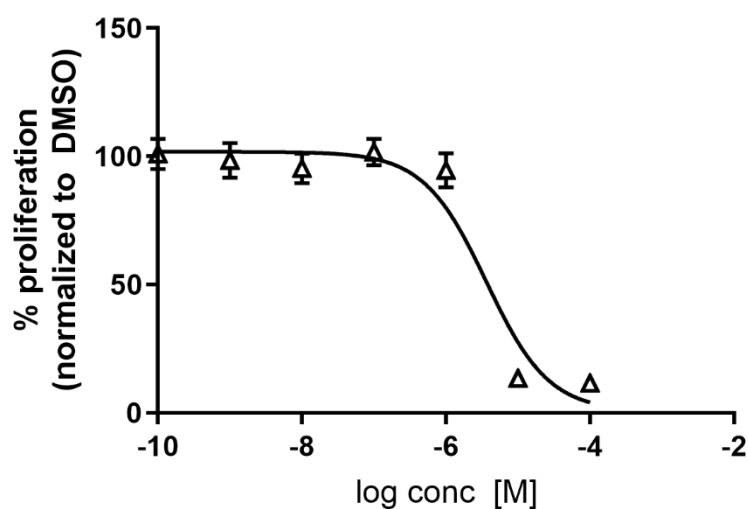


**Figure A.14.5.2.1.** Cell proliferation of HREC cells exposed to different concentrations of compound 41 after 24 hr incubation period. Cell proliferation was determined via the alamarBlue assay. The data is expressed as the percent proliferation compared with negative control in which the cell proliferation was assumed 100% (means  $\pm$  SD, N =3). Concentrations of 10  $\mu$ M and 100  $\mu$ M showed significant anti-proliferative effects compared to negative control (one way ANOVA with Dunnett's *posthoc* test, \*\*\*P <0.001).

#### A.14.5.2.2 GI<sub>50</sub> (HREC)

### compound effect on HREC proliferation



#### A.14.5.2.3 ANTI-PROLIFERATION PER CONCENTRATION (ARPE-19)

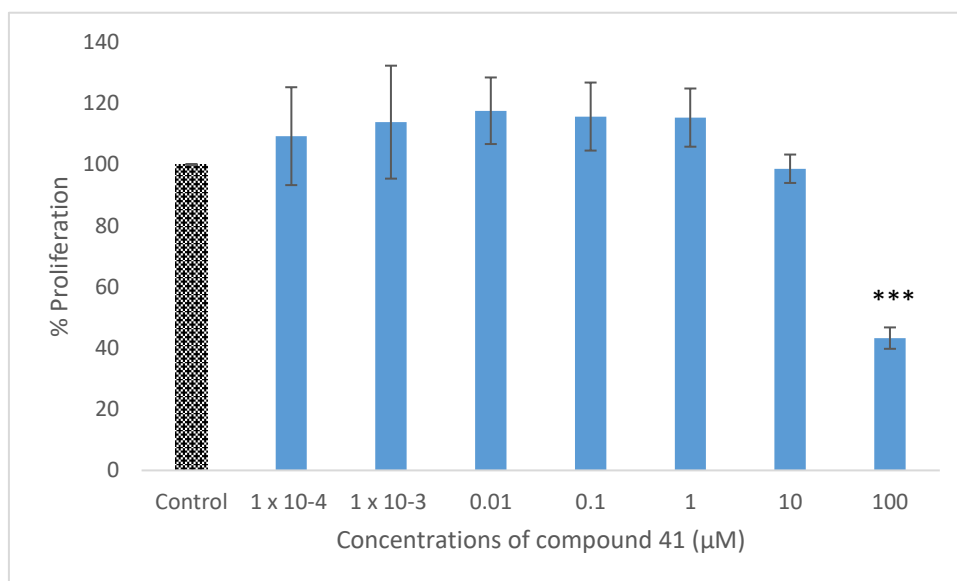
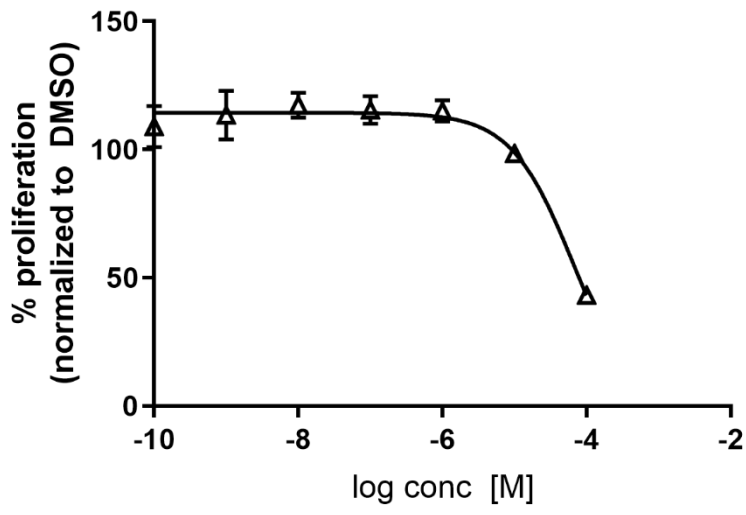


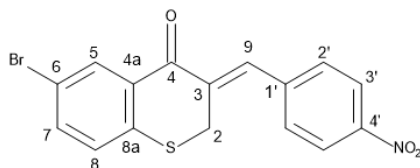
**Figure A.14.5.2.3.** Cell proliferation of ARPE-19 cells exposed to different concentrations of compound 41 after 24 hr incubation period. Cell proliferation was determined via the alamarBlue assay. The data is expressed as the percent proliferation compared with negative control in which the cell proliferation was assumed 100% (means  $\pm$  SD, N =3). Concentration 100  $\mu$ M showed significant anti-proliferative effects compared to negative control (one way ANOVA with Dunnett's posthoc test, \*\*\*P <0.001).

A.14.5.2.4 GI<sub>50</sub> (ARPE-19)



## A.15 Compound 42

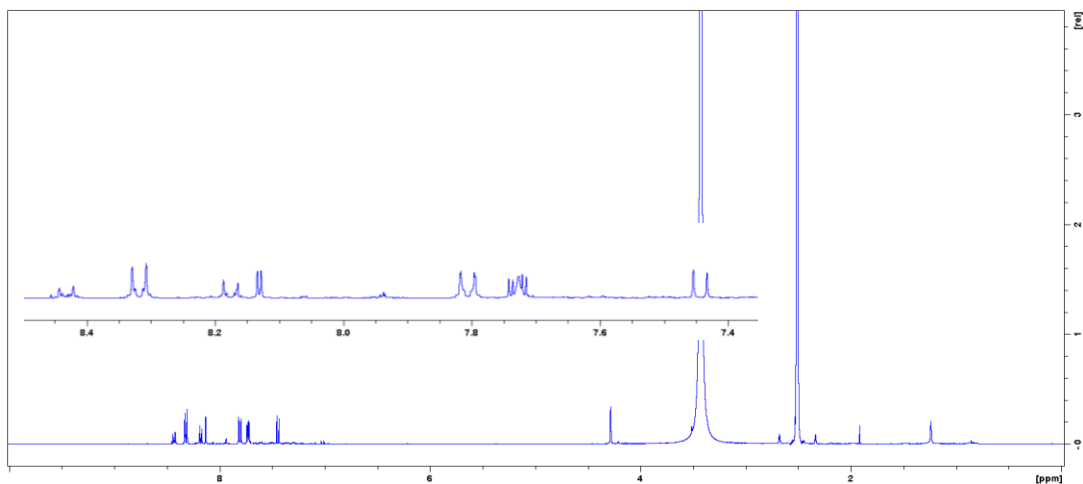
(3Z)-6-bromo-3-[(4-nitrophenyl)methylidene]-2,3-dihydro-4H-1-benzothiopyran-4-one (42)



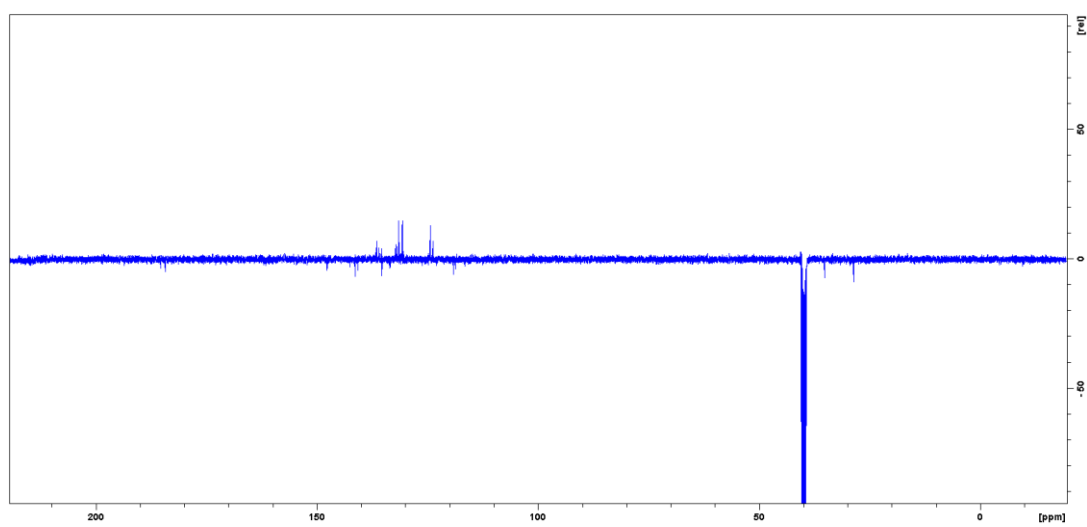
Yellow solid, 221 mg, 35.5 %, 229.3 - 229.9 °C, IR  $\nu_{\max}$  ( $\text{cm}^{-1}$ ): 3080 (Ar-H), 1663 (C=O), 1614 (Aliphatic C=C), 1594 (Aromatic C=C), 1511, 1340 ( $\text{NO}_2$ ), 1289 (C-N), 777 (C-Br), 635 (C-S)  $^1\text{H-NMR}$  (400 MHz, DMSO- $d_6$ ):  $\delta$  = 8.32 (2H, d,  $J$  = 8.7 Hz, H-2'), 8.13 (1H, d,  $J$  = 2.4 Hz, H-5), 7.81 (1H, d,  $J$  = 8.7 Hz, H-3'), 7.73 (1H, dd,  $J$  = 2.4, 8.4 Hz, H-7), 7.72 (1H, brs,  $w_{1/2}$  = 1.8 Hz, H-9), 7.44 (1H, d,  $J$  = 8.4 Hz, H-8), 4.27 (2H, s, H-2),  $^{13}\text{C-NMR}$  (100 MHz, DMSO- $d_6$ ):  $\delta$  = 184.5 (C-4), 147.7 (C-4'), 141.4 (C-3'), 140.8 (C-1'), 136.5 (C-7), 135.5 (C-8a), 135.3 (C-9), 133.5 (C-4a), 132.1 (C-5), 131.1 (C-3'), 130.5 (C-8), 123.9 (C-2'), 118.7 (C-6), 28.5 (C-2)  $R_f$  = 0.78 (1:1 EtOAc:hexane). HRESMS (ASAP)  $m/z$  375.9640  $[\text{M}]^+$  (calcd  $[\text{C}_{16}\text{H}_{11}\text{NO}_3\text{SBr}]$ , 375.9643).

### A.15.1 NMR

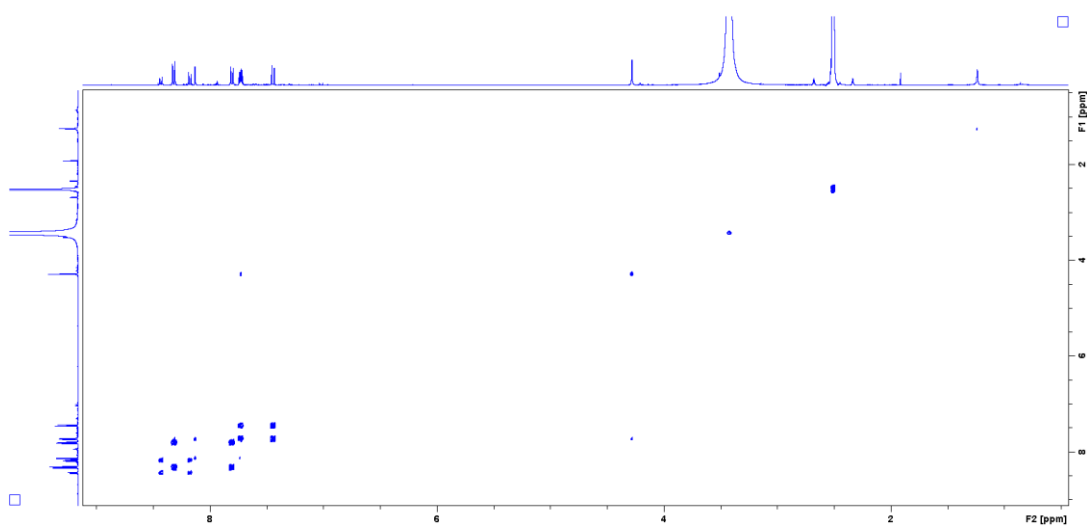
#### A.15.1.1 $^1\text{H-NMR}$



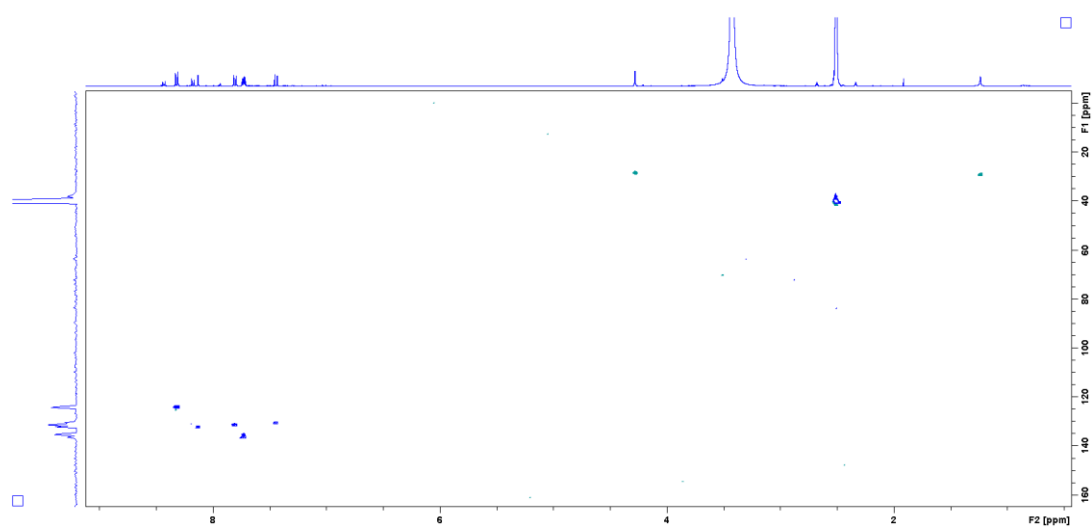
### A.15.1.2 $^{13}\text{C}$ -NMR



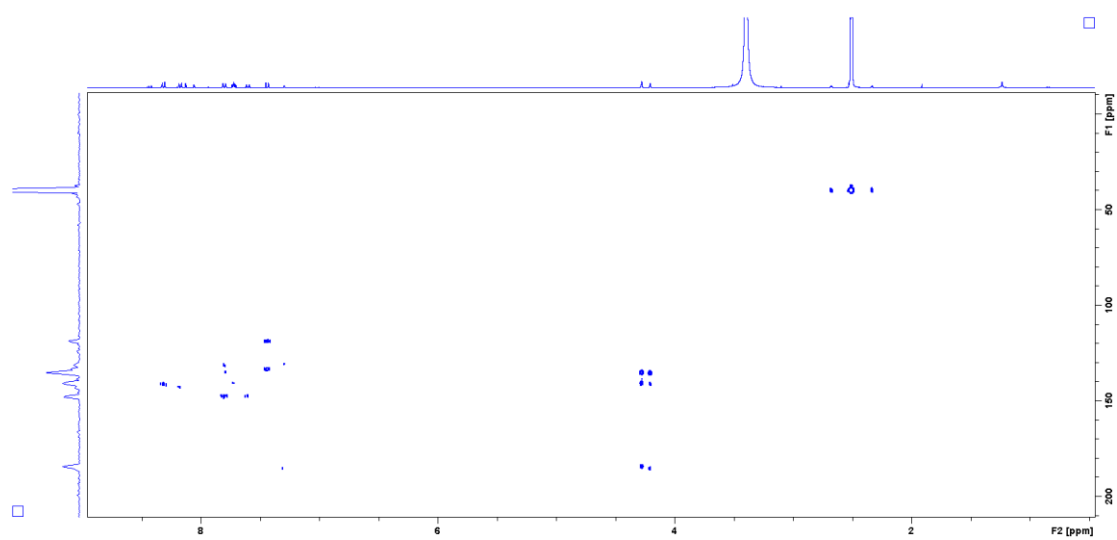
### A.15.1.3 COSY



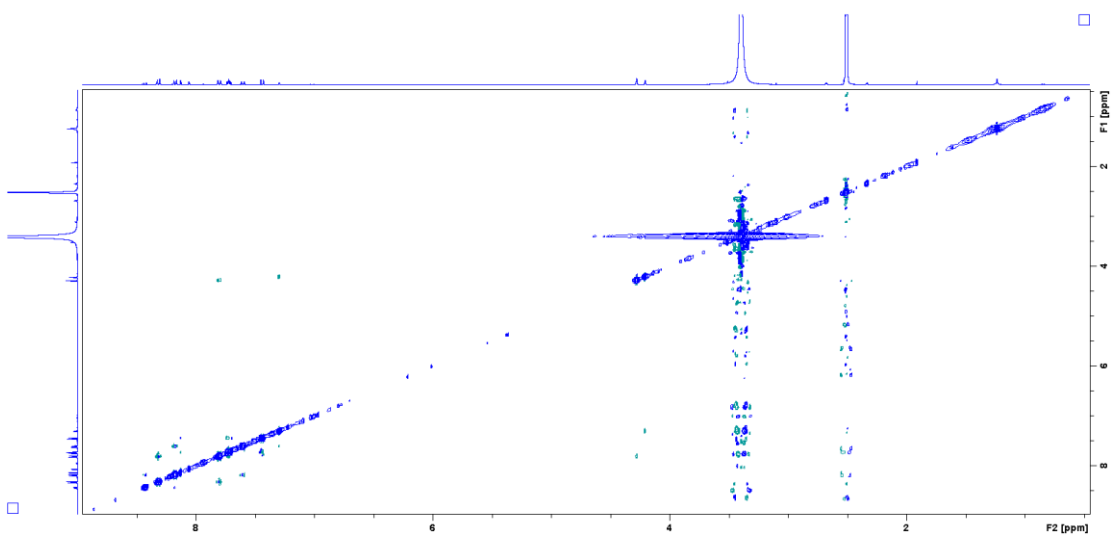
#### A.15.1.4 HSQC



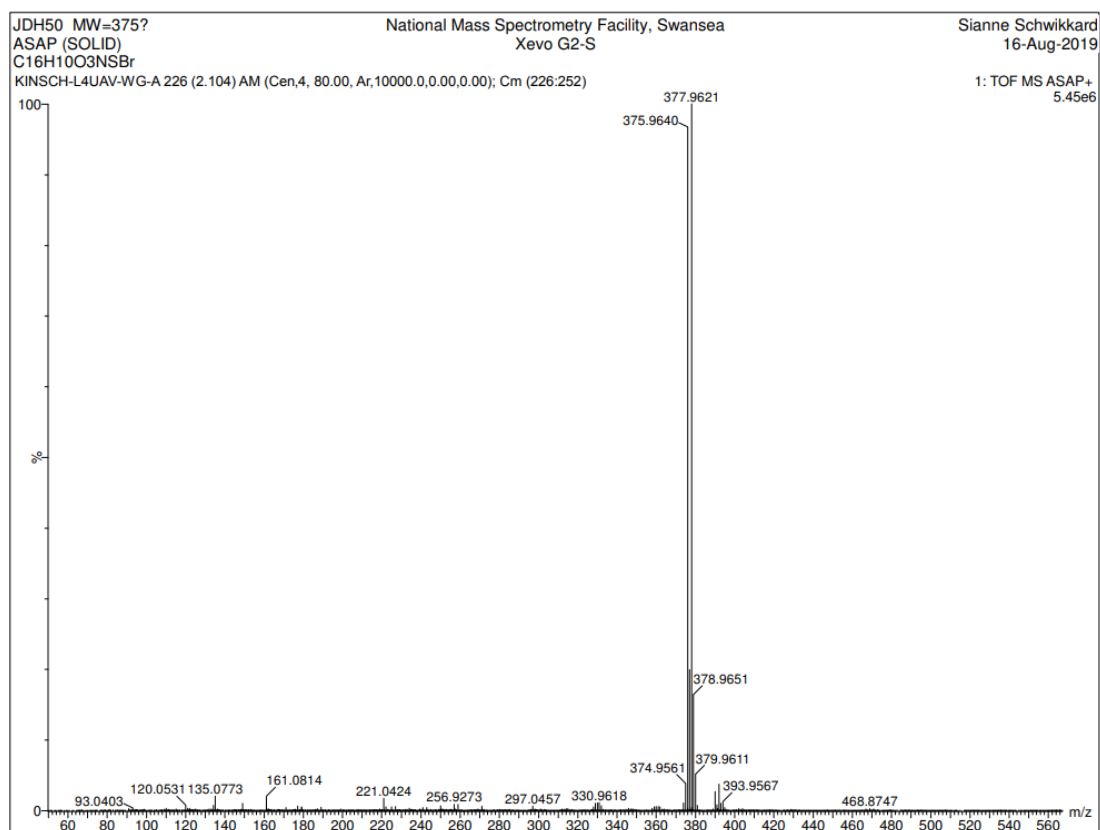
#### A.15.1.5 HMBC



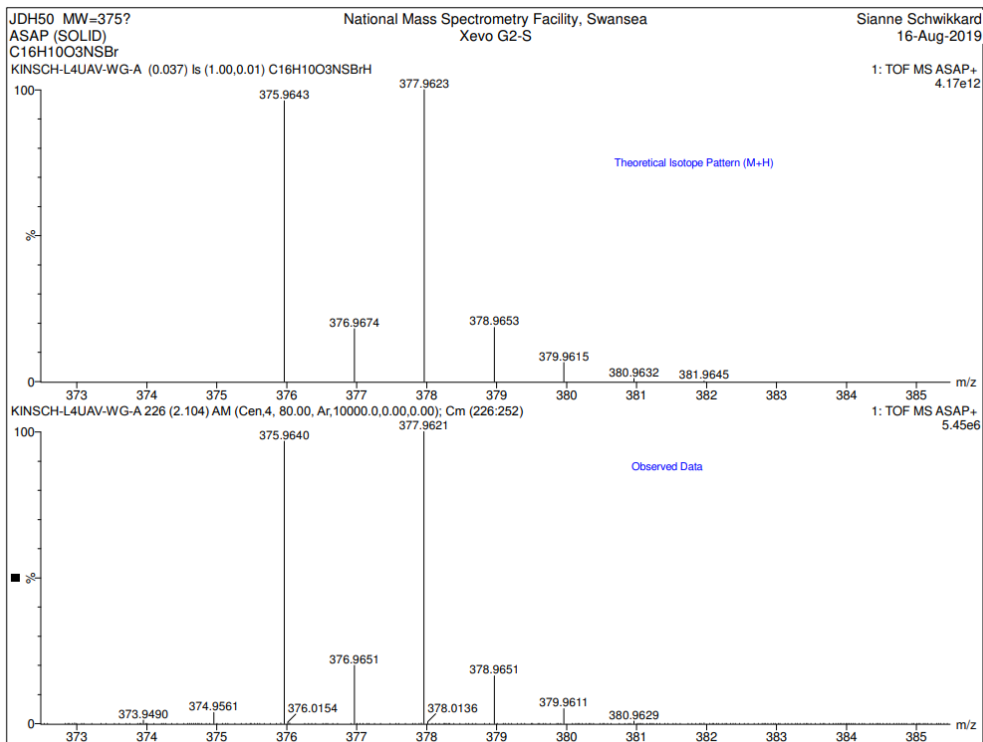
### A.15.1.6 NOESY



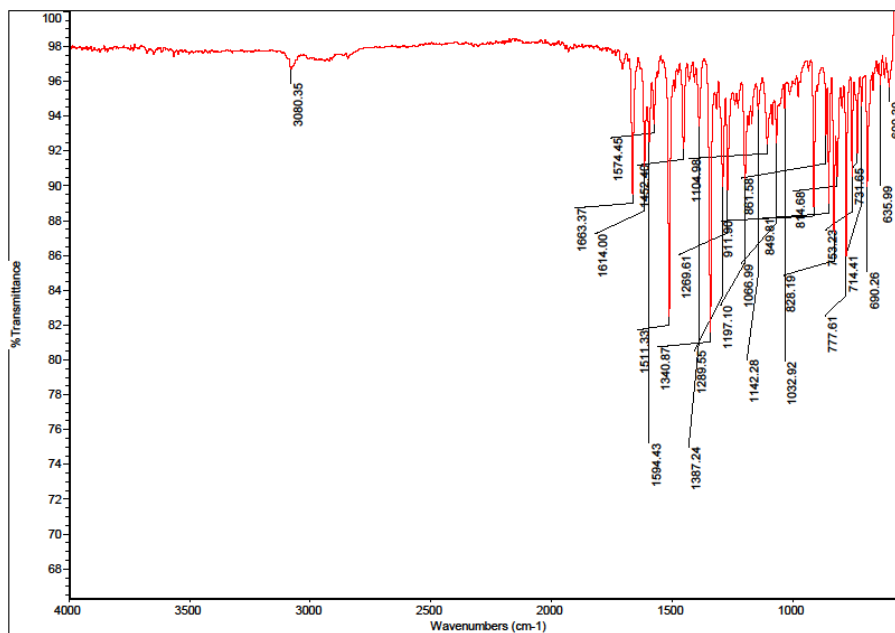
### A.15.3 HIGH RES MASS SPEC







#### A.15.4 IR DATA



## A.15.5 BIOLOGICAL DATA

### A.15.5.1 CYTOTOXICITY (HeLa)

#### A.15.5.1.1 CYTOTOXICITY PER CONCENTRATION

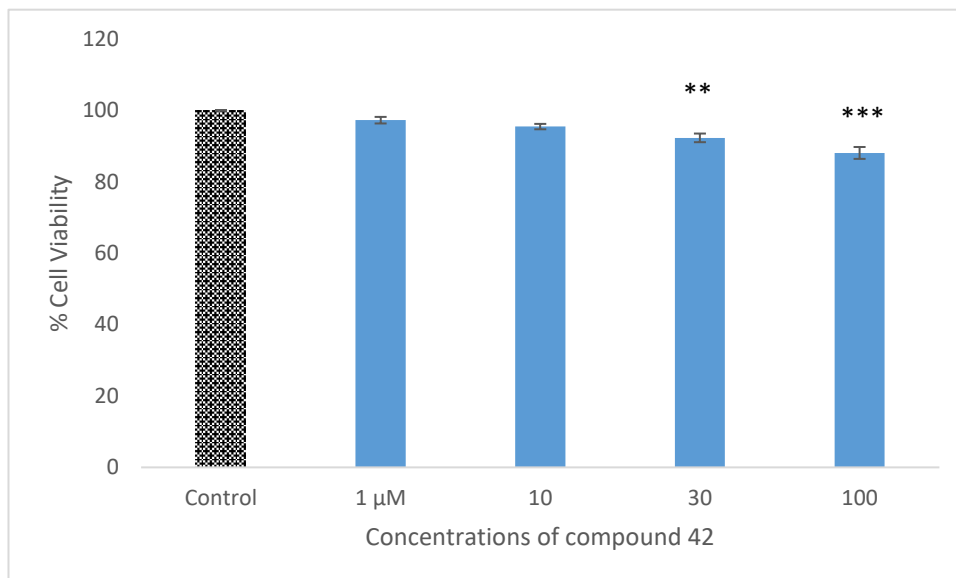
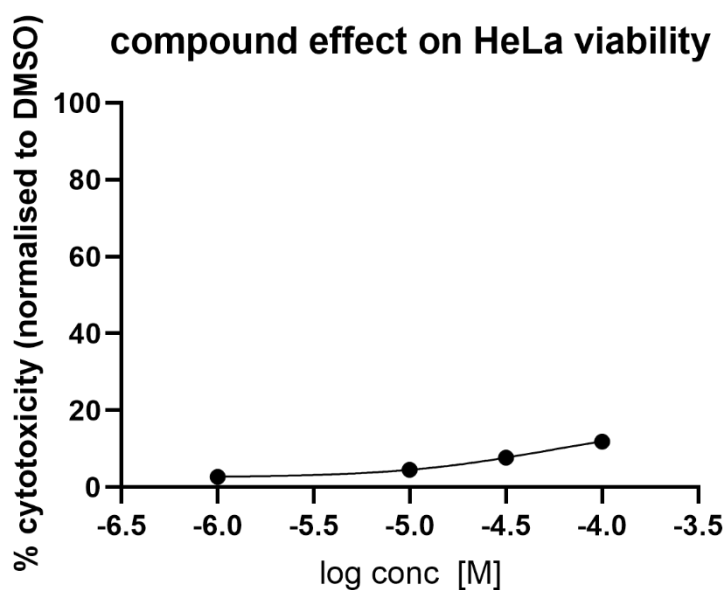


**Figure A.15.5.1.1.** Viability of HeLa cells exposed to different concentrations of compound 42 after 24 h incubation period. Cytotoxicity was determined via neutral red assay. The data is expressed as the percentage of inhibition compared with negative control in which the cell viability was assumed 100 % (means  $\pm$  SD, N =3). Concentrations of 30  $\mu\text{M}$  and 100  $\mu\text{M}$  showed significant cytotoxic effect compared to negative control (one way ANOVA with Dunnett's *posthoc* test, \*\* $P < 0.01$ , \*\*\* $P < 0.001$ ).

#### A.15.5.1.2 IC<sub>50</sub>



### A.15.5.2 ANTI-PROLIFERATIVE DATA

#### A.15.5.2.1 ANTI-PROLIFERATION PER CONCENTRATION (HREC)

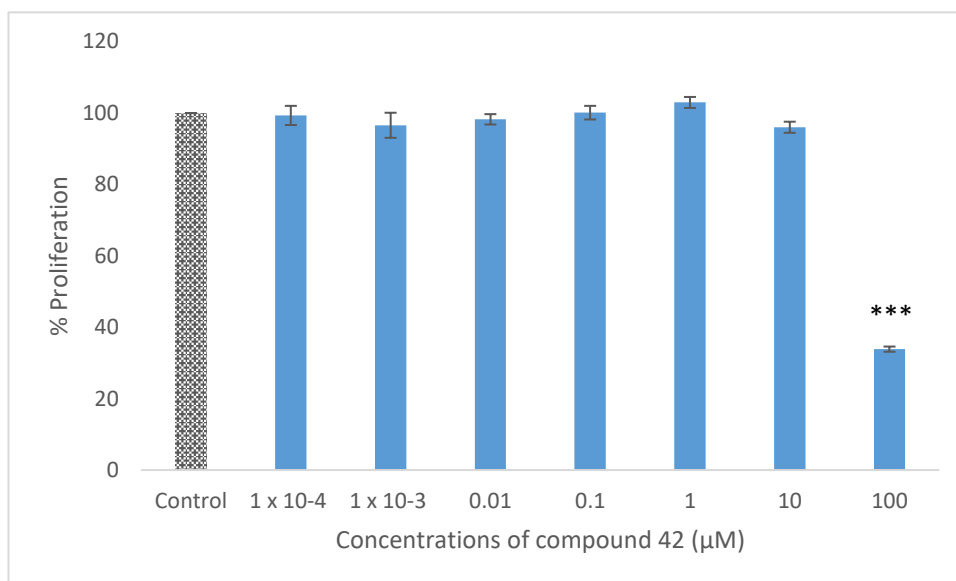
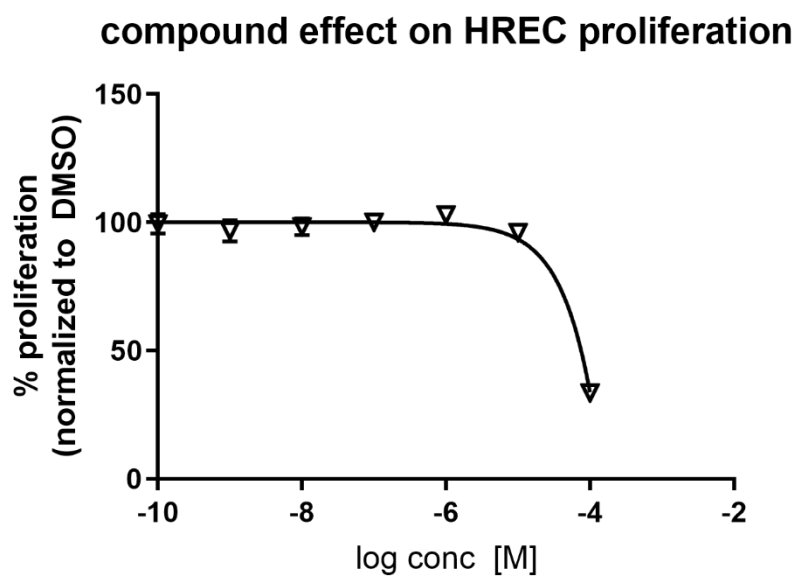


**Figure A.15.5.2.1.** Cell proliferation of HREC cells exposed to different concentrations of compound 42 after 24 hr incubation period. Cell proliferation was determined via the alamarBlue assay. The data is expressed as the percent proliferation compared with negative control in which the cell proliferation was assumed 100% (means  $\pm$  SD, N =3). Concentration of 100  $\mu$ M showed significant anti-proliferative effects compared to negative control (one way ANOVA with Dunnett's *posthoc* test, \*\*\*P <0.001).

#### A.15.5.2.2 GI<sub>50</sub> (HREC)



### A.15.5.2.3 ANTI-PROLIFERATION PER CONCENTRATION (ARPE-19)

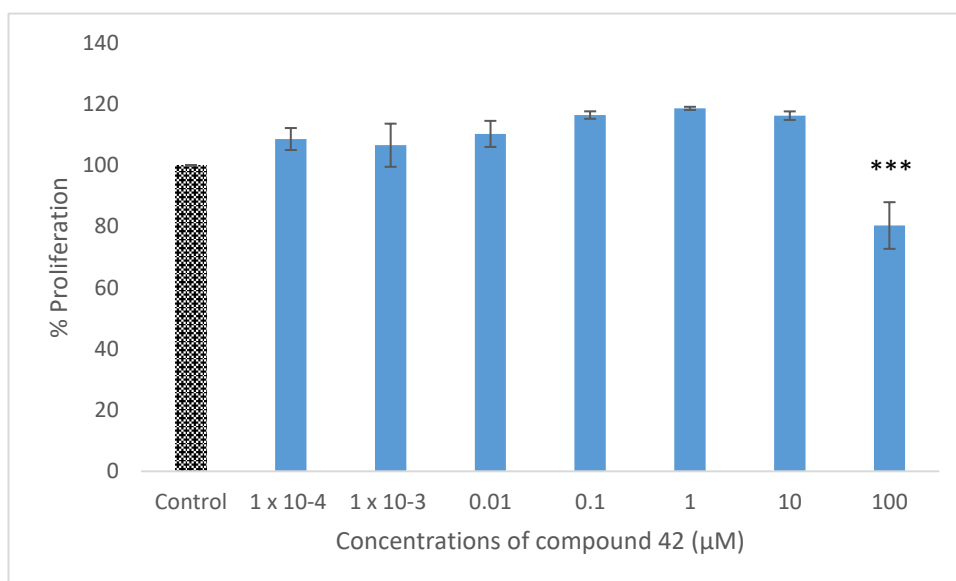
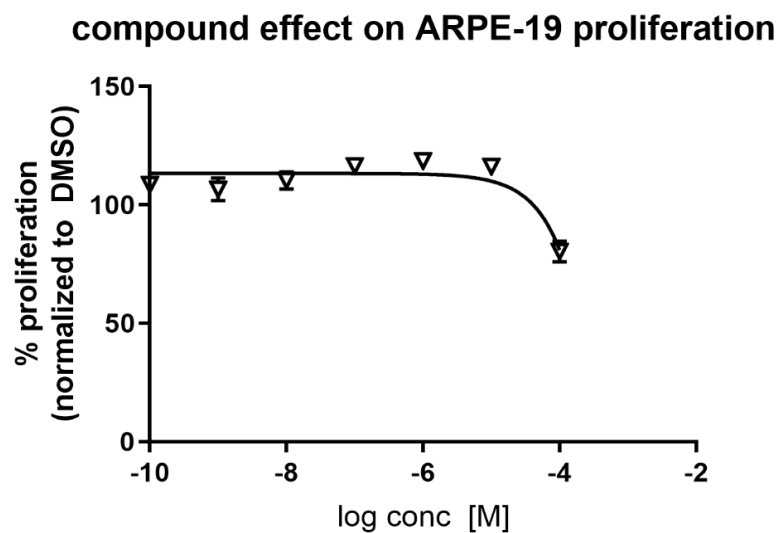


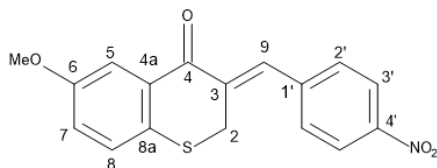
**Figure A.15.5.2.3.** Cell proliferation of ARPE-19 cells exposed to different concentrations of compound 42 after 24 hr incubation period. Cell proliferation was determined via the alamarBlue assay. The data is expressed as the percent proliferation compared with negative control in which the cell proliferation was assumed 100% (means  $\pm$  SD, N =3). Concentration 100  $\mu$ M showed significant anti-proliferative effects compared to negative control (one way ANOVA with Dunnett's posthoc test, \*\*\*P <0.001).

### A.15.5.2.4 GI<sub>50</sub> (ARPE-19)



## A.16 Compound 43

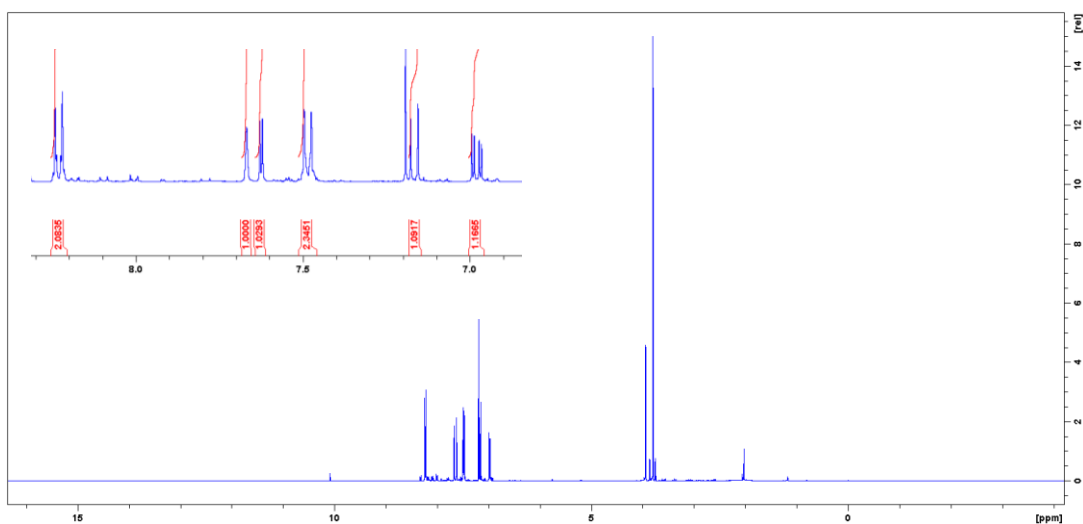
(3*Z*)-6-methoxy-3-[(4-nitrophenyl)methylidene]-2,3-dihydro-4*H*-1-benzothiopyran-4-one (43)



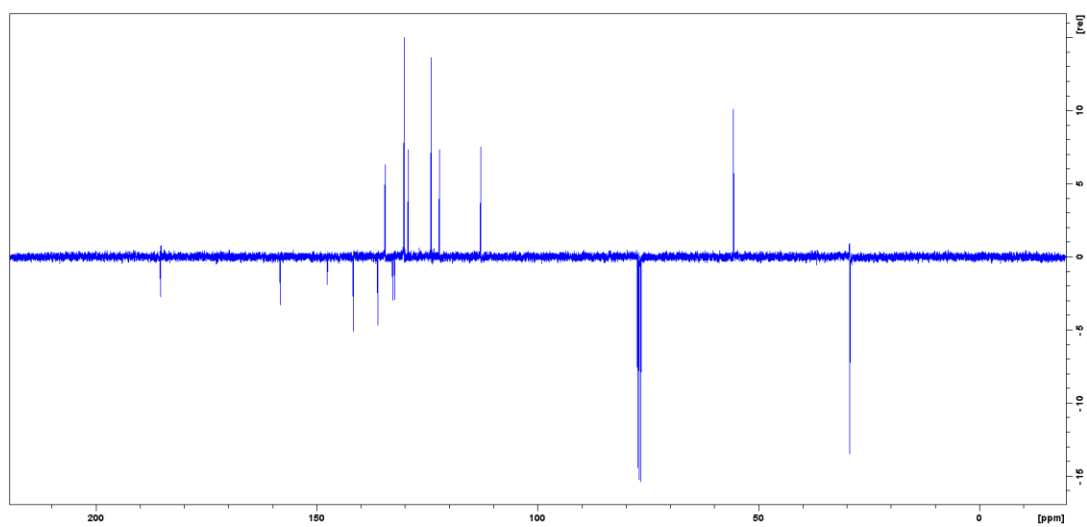
Yellow solid, 682 mg, 94.7 %, 176.3 - 176.7 °C, IR  $\nu_{\max}$  (cm<sup>-1</sup>): 3012 (Ar-H), 1663 (C=O), 1589 (Aliphatic C=C), 1512 (Aromatic C=C), 1475, 1341 (NO<sub>2</sub>), 1105 (C-O), 654 (C-S), <sup>1</sup>H-NMR (400 MHz, CDCl<sub>3</sub>):  $\delta$  = 8.23 (2H, d, *J* = 8.8 Hz, H-2'), 7.67 (1H, brs, *w*<sub>1/2</sub> = 3.2 Hz, H-9), 7.62 (1H, d, *J* = 3.0 Hz, H-5), 7.48 (2H, s, *J* = 8.6 Hz, H-3'), 7.16 (1H, d, 8.8 Hz, H-8), 6.98 (1H, dd, *J* = 3.0 Hz, 8.8 Hz, H-7), 3.94 (2H, d, *J* = 1.1 Hz, H-2), 3.79 (3H, s, OCH<sub>3</sub>); <sup>13</sup>C-NMR (100 MHz, CDCl<sub>3</sub>):  $\delta$  = 185.3 (C-4), 132.8 (C-4a), 147.7 (C-4'), 141.7 (C-1'), 136.3 (C-3), 134.6 (C-9), 136.1 (C-8a), 158.2 (C-6), 130.3 (C-3'), 129.4 (C-8), 124.0 (C-2'), 122.3 (C-7), 112.8 (C-5), 55.7 (OCH<sub>3</sub>), 29.3 (C-2), *R*<sub>f</sub> = 0.73 (1:1 EtOAc:hexane). HRESMS (ASAP) *m/z* 328.0644 [M]<sup>+</sup> (calcd [C<sub>17</sub>H<sub>14</sub>NO<sub>4</sub>S], 328.0644).

### A.16.1 NMR

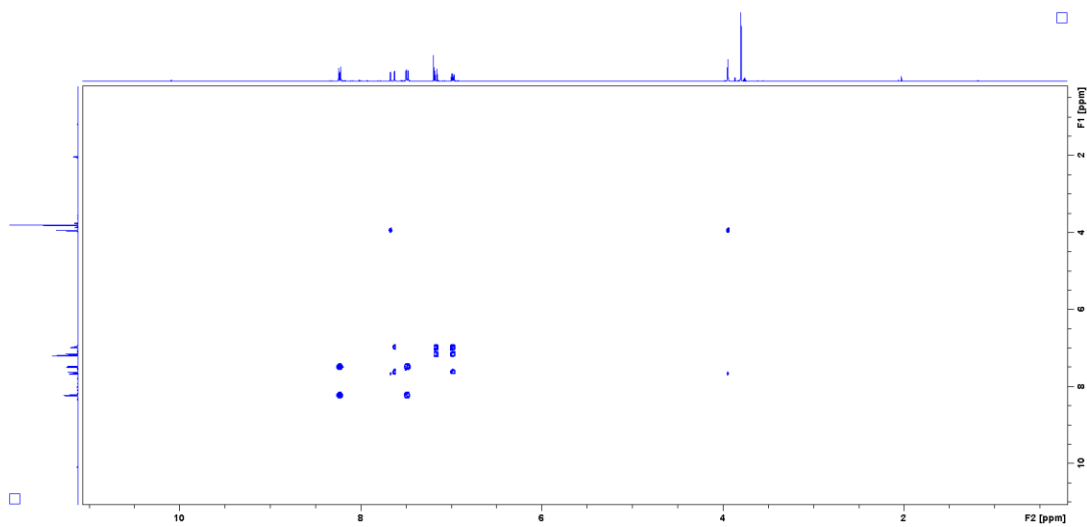
#### A.16.1.1 <sup>1</sup>H-NMR



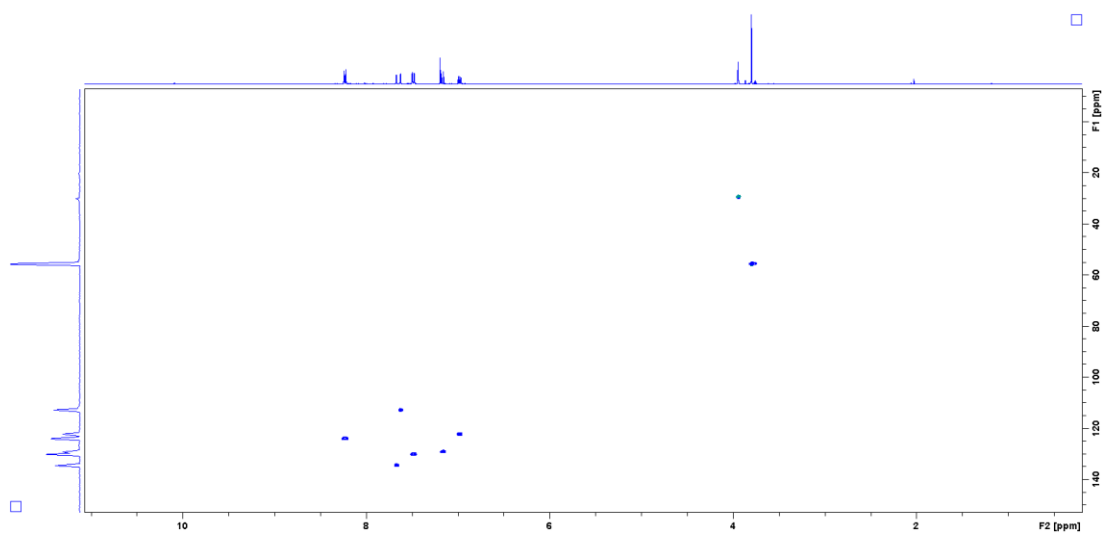
### A.16.1.2 $^{13}\text{C}$ -NMR



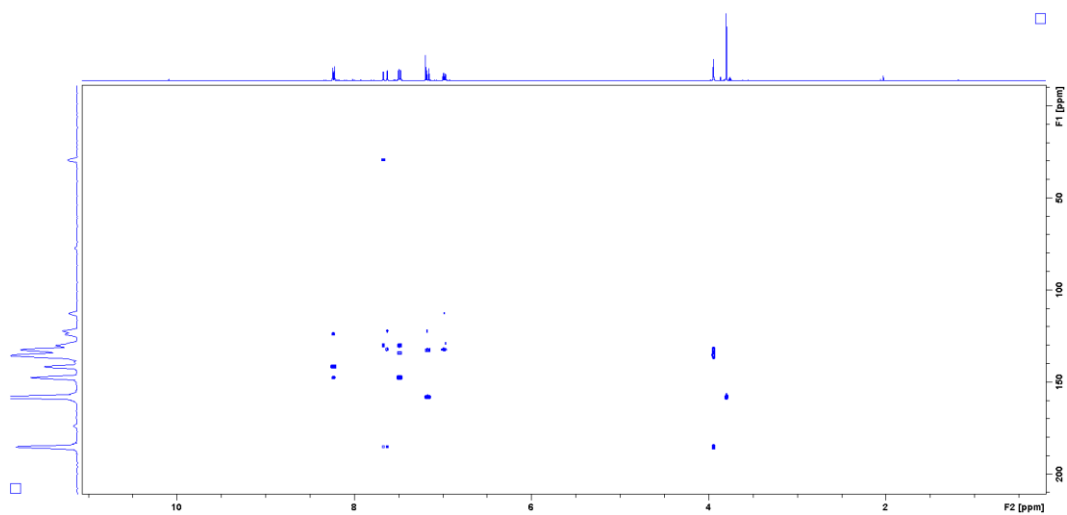
### A.16.1.3 COSY



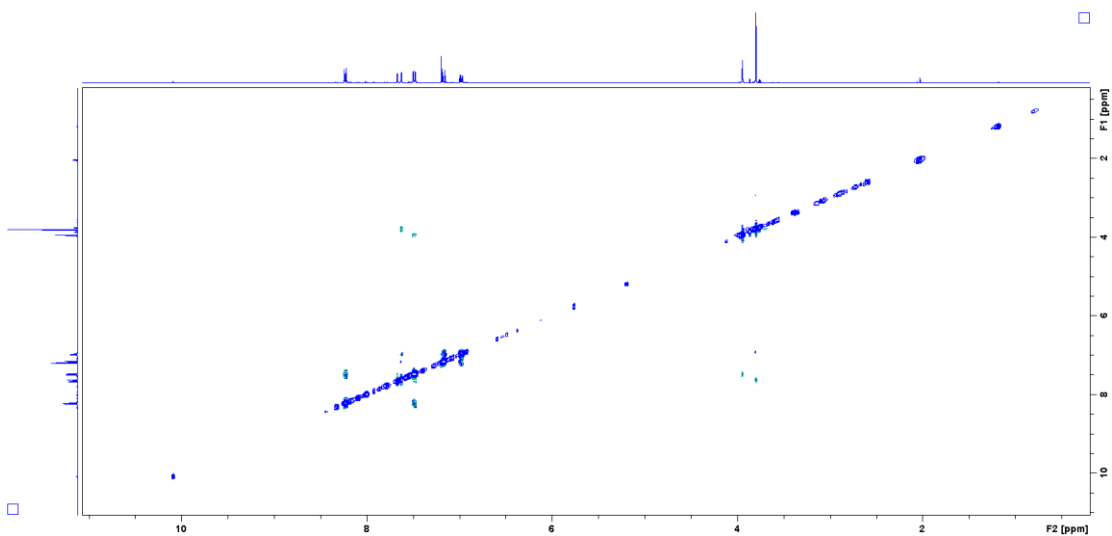
### A.16.1.4 HSQC



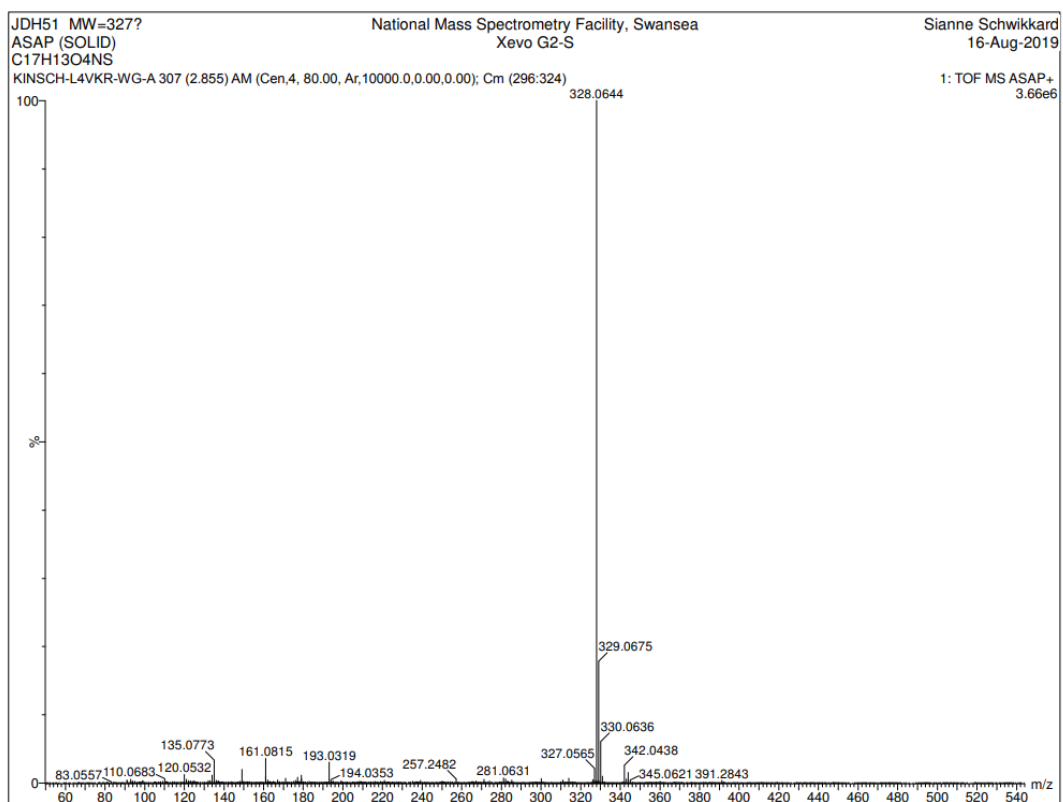
### A.16.1.5 HMBC



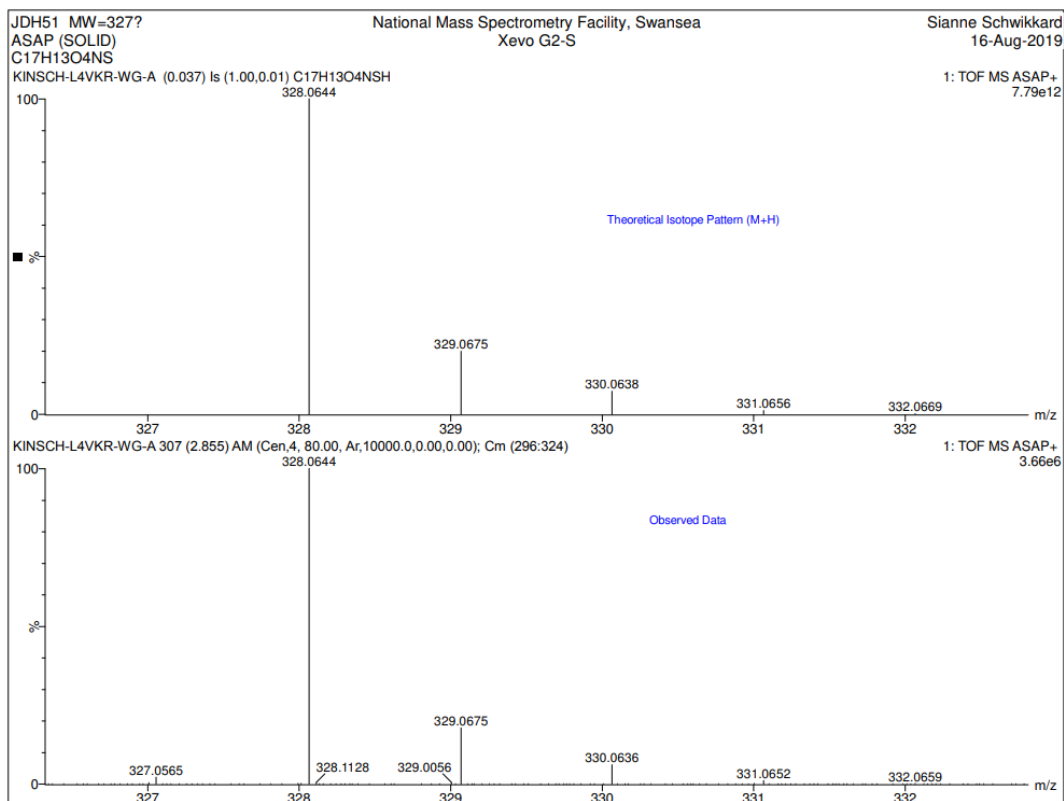
### A.16.1.6 NOESY



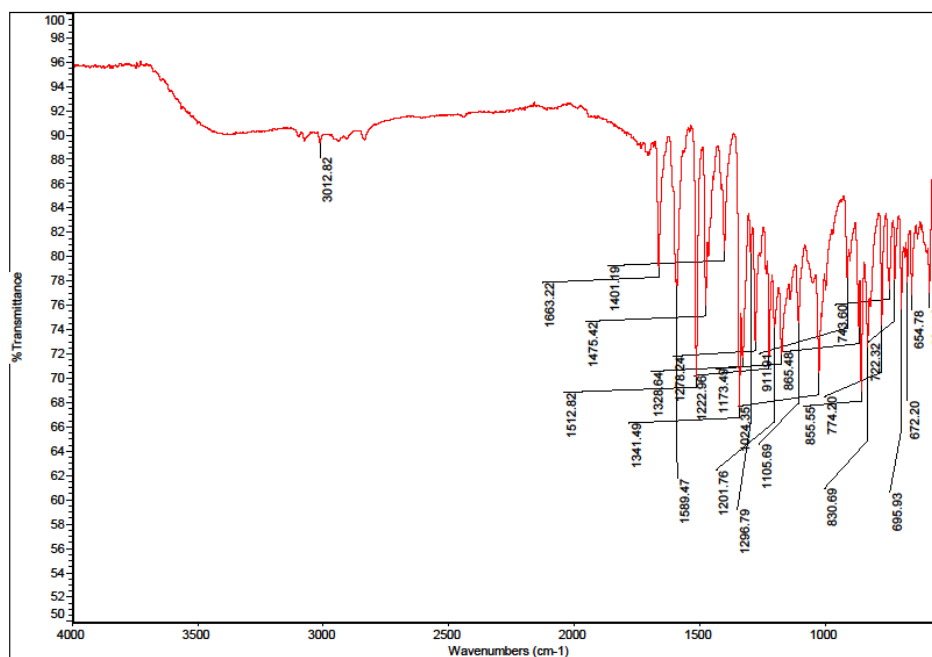
### A.16.3 HIGH RES MASS SPEC







#### A.16.4 IR DATA



## A.16.5 BIOLOGICAL DATA

### A.16.5.1 CYTOTOXICITY (HeLa)

#### A.16.5.1.1 CYTOTOXICITY PER CONCENTRATION

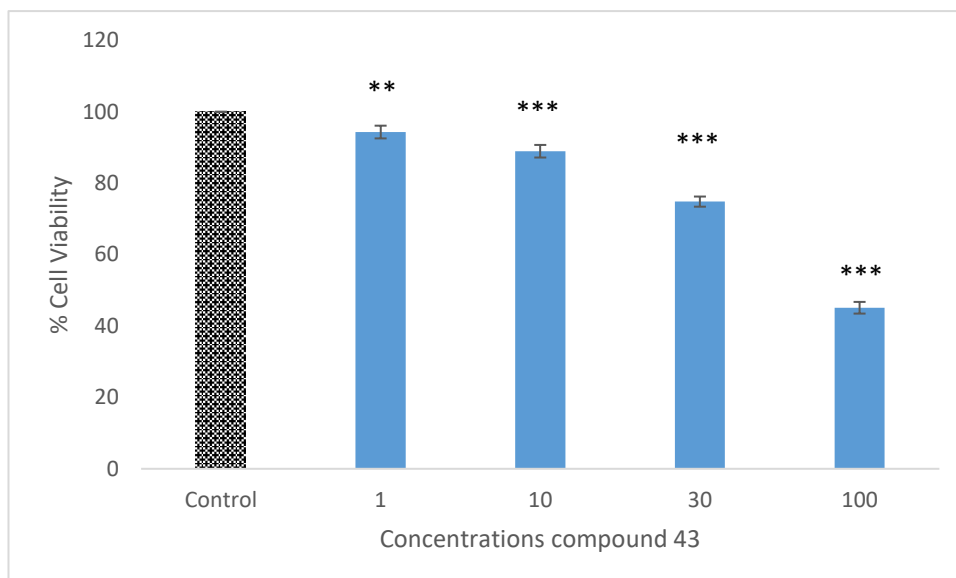
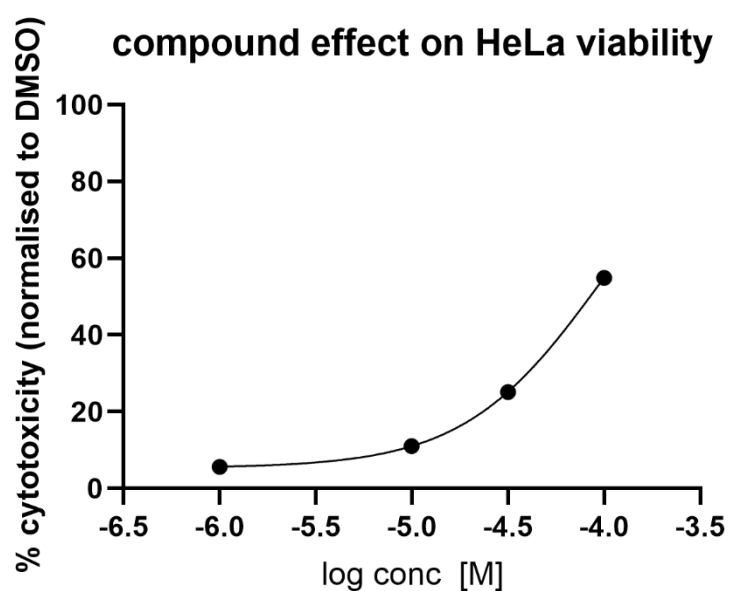


**Figure A.16.5.1.1.** Viability of HeLa cells exposed to different concentrations of compound 43 after 24 h incubation period. Cytotoxicity was determined via neutral red assay. The data is expressed as the percentage of inhibition compared with negative control in which the cell viability was assumed 100 % (means  $\pm$  SD, N =3). All concentrations tested showed significant cytotoxic effect compared to negative control (one way ANOVA with Dunnett's *posthoc* test, \*\*P <0.01, \*\*\*P<0.001).

#### A.16.5.1.2 IC<sub>50</sub>



## A.16.5.2 ANTI-PROLIFERATIVE DATA

### A.16.5.2.1 ANTI-PROLIFERATION PER CONCENTRATION (HREC)

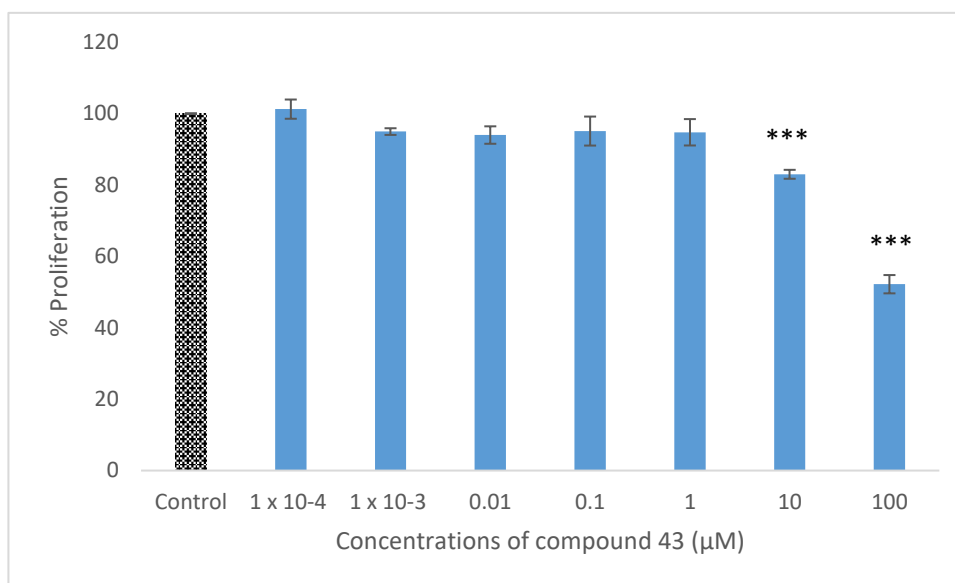
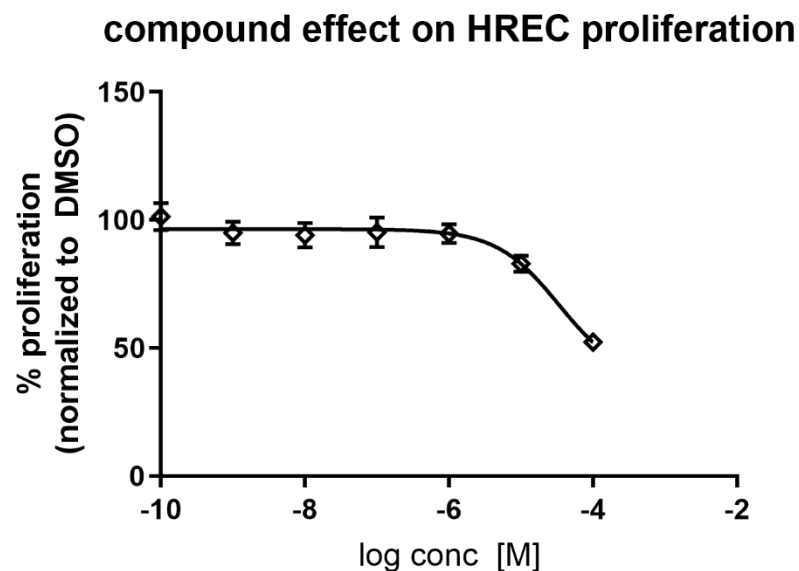


**Figure A.16.5.2.1.** Cell proliferation of HREC cells exposed to different concentrations of compound 43 after 24 hr incubation period. Cell proliferation was determined via the alamarBlue assay. The data is expressed as the percent proliferation compared with negative control in which the cell proliferation was assumed 100% (means  $\pm$  SD, N=3). Concentrations of 10  $\mu\text{M}$  and 100  $\mu\text{M}$  showed significant anti-proliferative effects compared to negative control (one way ANOVA with Dunnett's *posthoc* test, \*\*\*P < 0.001).

### A.16.5.2.2 GI<sub>50</sub> (HREC)



#### A.16.5.2.3 ANTI-PROLIFERATION PER CONCENTRATION (ARPE-19)

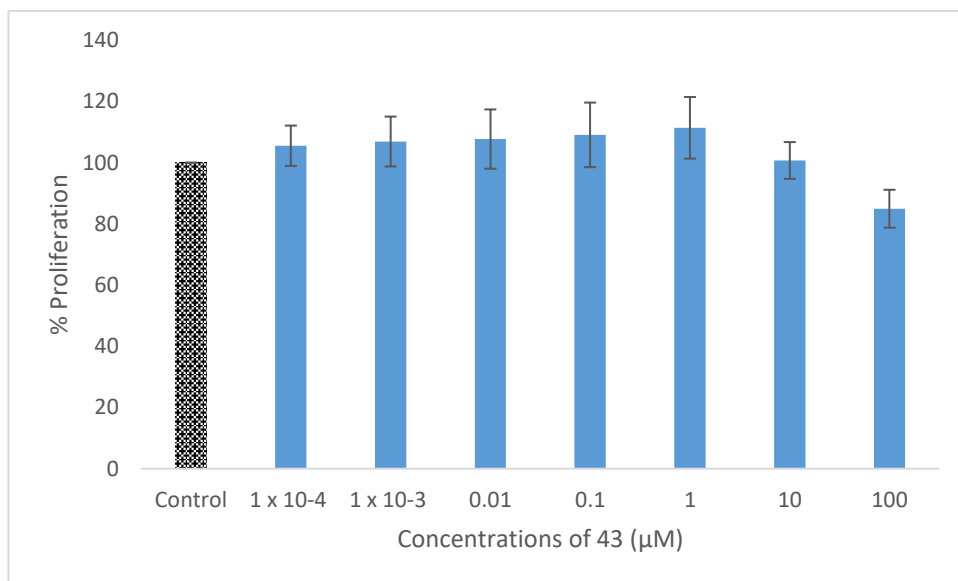


**Figure A.16.5.2.3.** Cell proliferation of ARPE-19 cells exposed to different concentrations of compound 43 after 24 hr incubation period. Cell proliferation was determined via the alamarBlue assay. The data is expressed as the percent proliferation compared with negative control in which the cell proliferation was assumed 100% (means  $\pm$  SD, N =3). No Concentrations showed significant anti-proliferative effects compared to negative control (one way ANOVA with Dunnett's posthoc test).

#### A.16.5.2.4 GI<sub>50</sub> (ARPE-19)

